REPORT NO.
EERC 73-2
June 1973

EARTHQUAKE ENGINEERING RESEARCH CENTER

ANALYSIS OF THE SLIDES IN THE SAN FERNANDO DAMS DURING THE EARTHQUAKE OF FEB. 9, 1971

by

H. BOLTON SEED
K. L. LEE
I. M. IDRISS
F. MAKDISI

Report to:

State of California Department of Water Resources
Los Angeles Department of Water and Power
National Science Foundation

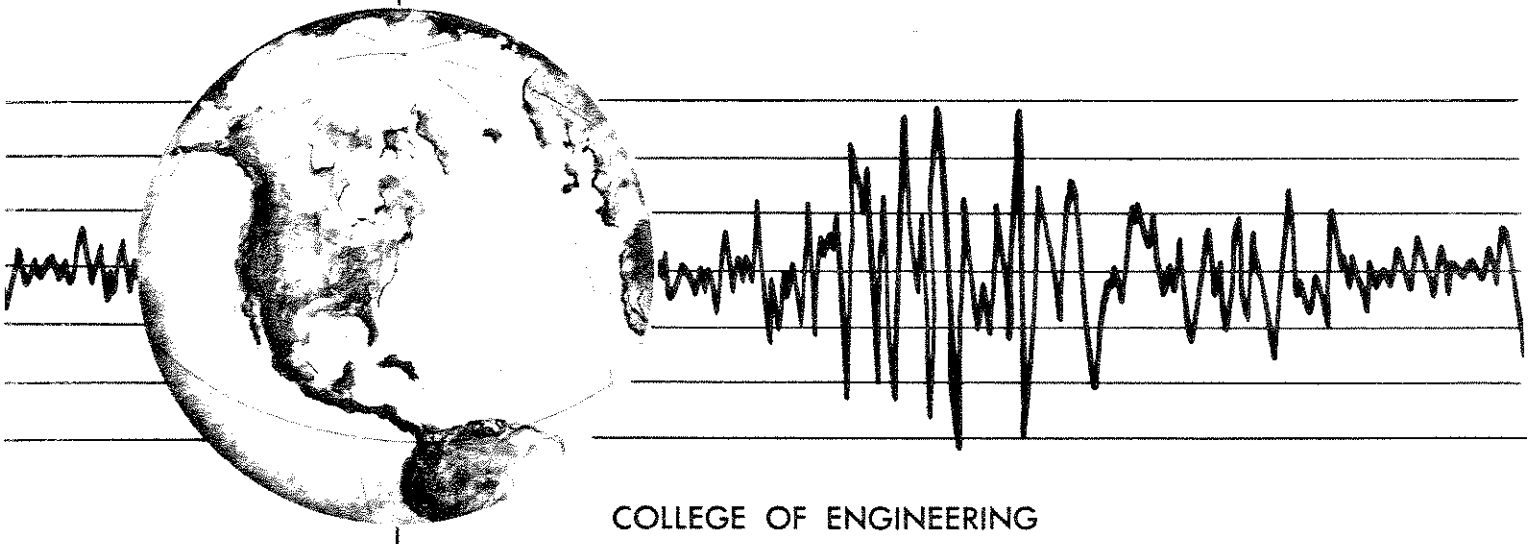

COLLEGE OF ENGINEERING

UNIVERSITY OF CALIFORNIA · Berkeley, California

EARTHQUAKE ENGINEERING RESEARCH CENTER

ANALYSIS OF THE SLIDES IN THE SAN FERNANDO DAMS DURING THE EARTHQUAKE OF FEB. 9, 1971

by

H. Bolton Seed
K. L. Lee
I. M. Idriss
F. I. Makdisi

Report to:
State of California Department of Water Resources
Los Angeles Department of Water and Power
National Science Foundation

Report No. EERC 73-2

June 1973

College of Engineering
University of California
Berkeley, California

Acknowledgements

The investigation described in this report was sponsored cooperatively by the State of California Department of Water Resources (Division of Safety of Dams), the Los Angeles Department of Water and Power and the National Science Foundation.

The Department of Water and Power was responsible for field work at the damsites including borings and sampling, trench sections, field density determinations and associated laboratory tests.

The Department of Water Resources provided drilling personnel and equipment, performed the field seismic surveys, supervised the boring and sampling operations and performed all standard laboratory tests and a small amount of dynamic testing on the samples at its Bryte laboratories near Sacramento.

The National Science Foundation, through research grants to the University of California at Berkeley and Los Angeles, supported the analytical studies, the dynamic laboratory testing and the overall evaluation of the results obtained. The cyclic load tests on undisturbed samples were performed in the Soil Mechanics Laboratory at UCLA. All analyses and evaluation studies were performed at the University of California at Berkeley.

The entire investigation was directed by H. B. Seed and Kenneth L. Lee.

For the Department of Water and Power, important contributions to the field investigations were made by D. Georgeson, R. Triay and J. M. Wool.

In the Division of Safety of Dams, major contributions to the investigation were made by C. J. Cortright, P. M. Schwartz, J. W. Keysor,

W. D. Hammond, R. E. Stephenson, A. A. Coluzzi, W. W. Peak, W. D. Pedersen, J. M. Parsons and G. Heyes, R. F. Laird, J. S. Nelson, W. W. Hogate, and J. Miller.

The cyclic load laboratory tests at UCLA were performed by J. Fitton, B. D. Adams and A. Albaisa.

Analytical studies at Berkeley were performed by I. M. Idriss, F. I. Makdisi and G. Lefebvre.

The contributions of the sponsoring agencies and of all the engineers involved are gratefully acknowledged. The entire investigation has been characterized by a degree of thoughtful cooperation on the part of all parties concerned which can rarely have been exceeded in a study of this magnitude. No agency or individual involved has spared any effort to obtain the information or data required for successful completion of the objectives of the study and difficult tasks have often been undertaken with a willingness which has greatly enhanced, as well as facilitated, the conduct of the investigation.

Special appreciation is due to C. J. Thiel of the National Science Foundation, C. J. Cortright of the Division of Safety of Dams and R. V. Phillips of the L. A. Department of Water and Power, without whose foresight the detailed study reported in the following pages might never have been possible.

H. Bolton Seed

Kenneth L. Lee

TABLE OF CONTENTS

		Page No.
Part I	- Introduction	1
Part II	- History of Dams and Conditions Prior to the Earthquake	4
Part III	- Effects of the Earthquake on the Dams	17
Part IV	- Field and Laboratory Investigations - Upper San Fernando Dam	31
Part V	- Field and Laboratory Investigations - Lower San Fernando Dam	63
Part VI	- Reconstruction of Mechanics of Sliding for Lower San Fernando Dam	85
Part VII	- Pseudo Static Analyses of Stability of Embankments	88
Part VIII	- Dynamic Analyses of the Stability of the Lower Dam During the San Fernando Earthquake	95
Part IX	- Dynamic Analyses of the Stability of the Upper Dam During the San Fernando Earthquake	116
Part X	- Dynamic Analyses of Lower San Fernando Dam for Other Earthquakes	125
Part XI	- Dynamic Analyses of Lower San Fernando Dam for other Conditions	130
Part XII	- Stability of Other Hydraulic Fill Dams in the San Fernando Earthquake	134
Part XIII	- Conclusions	137
Part XIV	- References	148

ANALYSIS OF THE SLIDES IN THE SAN FERNANDO DAMS DURING THE EARTHQUAKE OF FEB. 9, 1971

Part I - Introduction

One of the major effects of the San Fernando earthquake of February 9, 1971 was a major slide in the upstream slope of the Lower San Fernando Dam. This embankment dam, about 140 ft high at its maximum section, provided a reservoir capacity of about 20,000 acre-ft and at the time of the earthquake the water level in the reservoir was about 35 ft below the crest. The slide movements resulting from the earthquake shaking involved both the upstream slope and the upper part of the downstream slope, leaving about 5 ft of freeboard and obviously in a very precarious position. The upper part of the remaining embankment contained several large longitudinal cracks and the upstream face of the slide scarp was almost vertical. It seemed likely that further sliding might occur, especially if the embankment was subjected to a severe after-shock. Accordingly an order was immediately issued to evacuate some 80,000 people living downstream of the dam until the reservoir could be drawn down to a safe elevation. This was accomplished in a period of 4 days. However the margin by which a major disaster was averted was uncomfortably small.

Somewhat less serious but of major importance in its own right, was the downstream slide movement in the Upper San Fernando Dam, about 80 ft high and forming a reservoir of about 1850 acre-feet. The two dams form the major part of the Van Norman Lake complex, the total complex involving one additional dam for water storage, some smaller dikes forming storm diversion structures, debris collection basins and several miles of channels and artificially improved reservoir side slopes. It is the terminal

storage area for two aqueducts and the major water distribution center for the city of Los Angeles. The normal water flow through the Van Norman complex in the last half of 1970 was 650 cfs, which is about 80 percent of the city's total water supply. An aerial photograph of the Van Norman Lake complex is shown in Fig. I-1.

The downstream movement of the Upper Dam led to some cracking of the embankment, opening up of joints in the outlet conduit through the embankment and formation of a sink-hole along the line of the conduit due to erosion through those joints. However although the crest moved downstream about 5 ft and settled about 3 ft there was no breach resulting in loss of water from the reservoir. If this had not been the case and water from the Upper Van Norman Lake had been released, overtopping of the Lower Dam would have ensued.

The near-catastrophe resulting from the earthquake-induced slides in the Upper and Lower San Fernando Dams immediately raised a number of questions concerning the adequacy of earth dam design criteria to protect the public against failures resulting from earthquake shaking. Both of the affected dams were old structures constructed in the period 1915 to 1925, and both were hydraulic fill construction. However the safety of the Lower Dam had been evaluated using current design procedures and seismic criteria as recently as 1966 and it had been considered to be adequately resistant to earthquake effects. Accordingly the performance of the dams raised the following major questions:

(1) Were the slide movements initiated primarily in the embankment soils or in the foundation soils?

(2) What was the mechanics of sliding? Were the slides the result of soil liquefaction or were they the result of the

more conventional sliding block type of movement?

(3) Could the slides have been anticipated using available analytical or design procedures?

(4) Are new criteria required for evaluating the safety of earth dams to earthquake effects?

In order to provide answers to these questions a major study of the slide movements was initiated by the State of California Department of Water Resources, Division of Safety of Dams and the Los Angeles Department of Water and Power with the research support of the National Science Foundation. The results of the study are presented in the following pages.

Part II - History of Dams and Conditions Prior to the Earthquake

Early Construction Procedures

Both of the San Fernando Dams were constructed to provide terminal storage reservoir capacity for the Los Angeles Aqueduct, at sufficient elevation for gravity distribution into the city. The Lower Dam was constructed first, beginning in 1912, followed by the Upper Dam beginning in 1921. These were the 5th and 6th earth dams to be constructed as part of the Los Angeles aqueduct system. While specific construction details are lacking, especially for the Upper Dam, the existing records indicate that the method of construction was similar to that used on the earlier dams.

The final report on the construction of the Los Angeles Aqueduct (Kelly, 1916) which was written just after the first stage of the Lower Dam had been completed and the reservoir partly filled, provides much useful and interesting information concerning the construction techniques of that time. For background reference a summary of some of the construction details of the dams along the Los Angeles Aqueduct is presented in Table II-1. Both hydraulic fill and rolled fill construction procedures were used. The unit cost for hydraulic fill was about 15 to 18 cents per cu yd as compared to 25 to 30 cents per cu yd for dry wagon-hauled material. Apart from the cost advantage, the report indicates that in the opinion of the designers, the hydraulic fill technique produced a soundly engineered earth dam.

The hydraulic process began at the borrow area where ordinary 4 inch canvas fire hoses conveyed water at 80 to 100 psi to 2 inch nozzles. These were mounted on iron tripods and the water jet directed at the vertical bank of the borrow pit. Where possible, the loosened material was conveyed by

Table II-1

Some Construction Details on the Earth Dams of the Los Angeles Aqueduct

Name of Dam (Spillway Elevation)	Distance from Lower San Fernando miles	Reservoir Capacity-acre ft	Max. Height ft	Total Cost	Type of Construction (vol.-cu yds)	Unit Cost $/cu yd
North Haiwee Dyke (3760)	170	58,520	34	$50,000	Hydraulic Fill (141,000) Wagon hauled, hydraulic sluiced (26,000)	0.15 0.25 to 0.30
South Haiwee Dam (3760)			81		Hydraulic Fill (599,000)	0.25
Fairmont Dam (3036)	35	7,510	121	$60,000	Wagon hauled and rolled Wagon hauled and hydraulic sluiced (Total 695,000 c.y.)	
Dry Canyon Dam (1505)	15	1,140	66	$81,000	Hydraulic Fill (140,000) Wagon hauled and rolled (95,000)	0.18 0.26
Upper San Fernando	1.8	1,850	82	$280,000	Wagon hauled hydraulic sluice (500,000) Wagon hauled and rolled (50,000)	
Lower San Fernando	0	20,500	142	$1,326,000	Hydraulic Fill (2.7×10^6) Rolled (various methods) (0.6×10^6)	

Most construction in period 1908-1915. At a total cost of $23,000,000 including 230 miles of aqueduct, syphons, trestles, etc. Upper San Fernando Dam constructed 1921-22. Lower San Fernando Dam modified 1924, 1929, 1940. Dry Canyon Dam taken out of service 1966 pending extensive reconstruction.

gravity along wooden troughs at 4 to 6 percent grade to the dam. This procedure appears to have been used for much of the construction at the Lower Dam. Old scars in the abutments and on an island in the reservoir, as well as some old wooden posts formerly used to support the conveying troughs are still visible. The wooden posts are in the reservoir area and have been submerged for the past 60 years.

Where sufficient gravity head was not available the material was transported by a series of mud pumps and pipes capable of passing gravel and small stones as well as the finer soils. This fluid mixture of water and soil was discharged along the beach forming the outside edges of the dam. The coarser material settled out rapidly near the point of discharge while the finer materials flowed into the quiet waters of the pond and settled out later.

A dry fill dyke was usually placed at the outer edges of the dam to contain the ponded hydraulically-placed material. Also, when water was scarce large portions of the entire embankment would be placed as "dry" fill. The material would be hauled from the borrow area, deposited on the fill, spread in lifts using teams and Fresno scrapers, sprinkled with water and compacted by routing the hauling equipment over the area. This procedure seems to have been used to construct dikes at the outer edges of the Lower Dam, and to construct the later uppermost portions of both the Lower and the Upper Dams.

Another method of construction sometimes used when water was scarce was the "semi-hydraulic" procedure. The fill material would be excavated from the borrow area by teams and Fresno scrapers or steam shovels and hauled to the dam, dumped into the pond and dispersed by monitors operating from barges floating in the center pool. It is believed that most of the Upper Dam was constructed in this manner although no detailed early records

or photographs seem to be available. However, this semi-hydraulic fill procedure was also used for the South Haiwee Dam. The detailed description of the construction of this dam (Kelly, 1916) gives an insight into how the Upper Dam was probably constructed. The major difference was that at the South Haiwee Dam the fill was excavated by a 2-1/2 yard steam shovel from a borrow area 1000 ft from the damsite and hauled to the damsite by three trains, each consisting of seven, 4 cu yd capacity cars, whereas at the Upper San Fernando Dam the fill was probably hauled by teams and wagons. Quoting from Kelly, page 123:

> "The waters of Haiwee Creek were carried three miles and those of Hogback Creek were brought five miles in riveted steel pipe, and were discharged into the pool between the two toes of the dam. In this pool two steel hulls were floated, 20 feet long, 10 feet wide, and 2-1/2 feet deep. On the first one that was built, a 6-inch Krogh centrifugal pump, directly connected with a 30 horse power motor, was mounted. The pump discharged the water from the pool through a 2-inch nozzle against the dump made by the trains. Energy was furnished the motor through an insulated cable carried on a reel on the hull. The reel permitted the shifting of the position of the pontoon. The jet discharged against the dump, washing the material down towards the pool, the finer particles proceeding towards the center of the pool and the coarser material staying on the outer edges.
>
> "It was originally the intention to build the dam by a hydraulic process, pumping the materials into the fill direct, but the water supply was found to be insufficient during the summer months to permit this method of work, and the material

available at proper elevations contained too many boulders."

Although standard hydraulic fill construction was used for the lower part of the Lower San Fernando Dam and the semi-hydraulic fill process was used for most of the fill at the Upper Dam, the results of recent drilling, sampling and trenching at both dams indicate no major difference in the type or quality of finished product obtained by either of the two methods.

It is clear from the old records that the engineers of that time felt that the use of hydraulic fill procedures for the construction of earth dams was not only economical but would also lead to perfectly safe structures. The 1916 final report (Kelly, 1916), after describing the process in some detail states:

> "...The reason for building these dams by various hydraulic processes was that it gave the desired arrangement of the fine clay material in the center of the dam and the sand and gravel near the outer slopes, resulting in an impervious core with outside drainage, and compacting of the mass by settlement..."
>
> "The cost of handling earth with water is cheaper than loading wagons with power shovels and transporting to the dam, even with the necessary pumping and small volume of water....
>
> "This method of work is a western development and when properly built, these dams are a success. Where failures have occurred elsewhere, it has been due to discharging the silt into the central portions of the dam, or to undue rushing of the work which may cause slips in the outer faces."

A photograph illustrating the construction techniques at the Lower San Fernando Dam is presented in Fig. II-1. The semi-hydraulic fill process used at the Upper Dam is illustrated on Fig. II-2; this photograph was taken during construction of the South Haiwee Dam by the same process.

Geology and Foundation Conditions

The embankment of the Lower San Fernando Dam in the channel section and the lower portions of the abutments rests on Recent alluvium consisting of stiff clay with lenses of sand and gravel. This alluvium attains a maximum thickness of about 35 ft beneath the dam.

Underlying the alluvium and forming the upper parts of the abutments for the dam are shales and siltstones and sandstones. The east or left abutment consists primarily of shales and siltstones of Upper Miocine age, the upper 30 to 50 ft being weathered to varying degrees and containing numerous gypsum-filled seams along joints, fractures and bedding planes. Solution of this gypsum by reservoir waters throughout the years is believed to have been responsible for excessive seepage through the left abutment. Extensive grouting of the abutment in 1964 significantly ameliorated this condition.

Forming the right abutment and underlying the westerly part of the foundation alluvium is a massive friable sandstone of the Pico Formation (Middle Pliocene).

Exploration subsequent to the earthquake in an old borrow area on the west abutment revealed several faults about 100 ft downstream from the axis of the dam. These faults cut the overlying alluvium and showed vertical offsets of 2 to 5 ft. They were not traceable laterally, but possibly extend under the dam. There is no indication that any movement occurred on any of these faults during the Feb. 9th earthquake.

FIG. I-1 AERIAL VIEW OF VAN NORMAN LAKE COMPLEX TAKEN AFTER EARTHQUAKE.
(Photograph by Department of Water Resources)

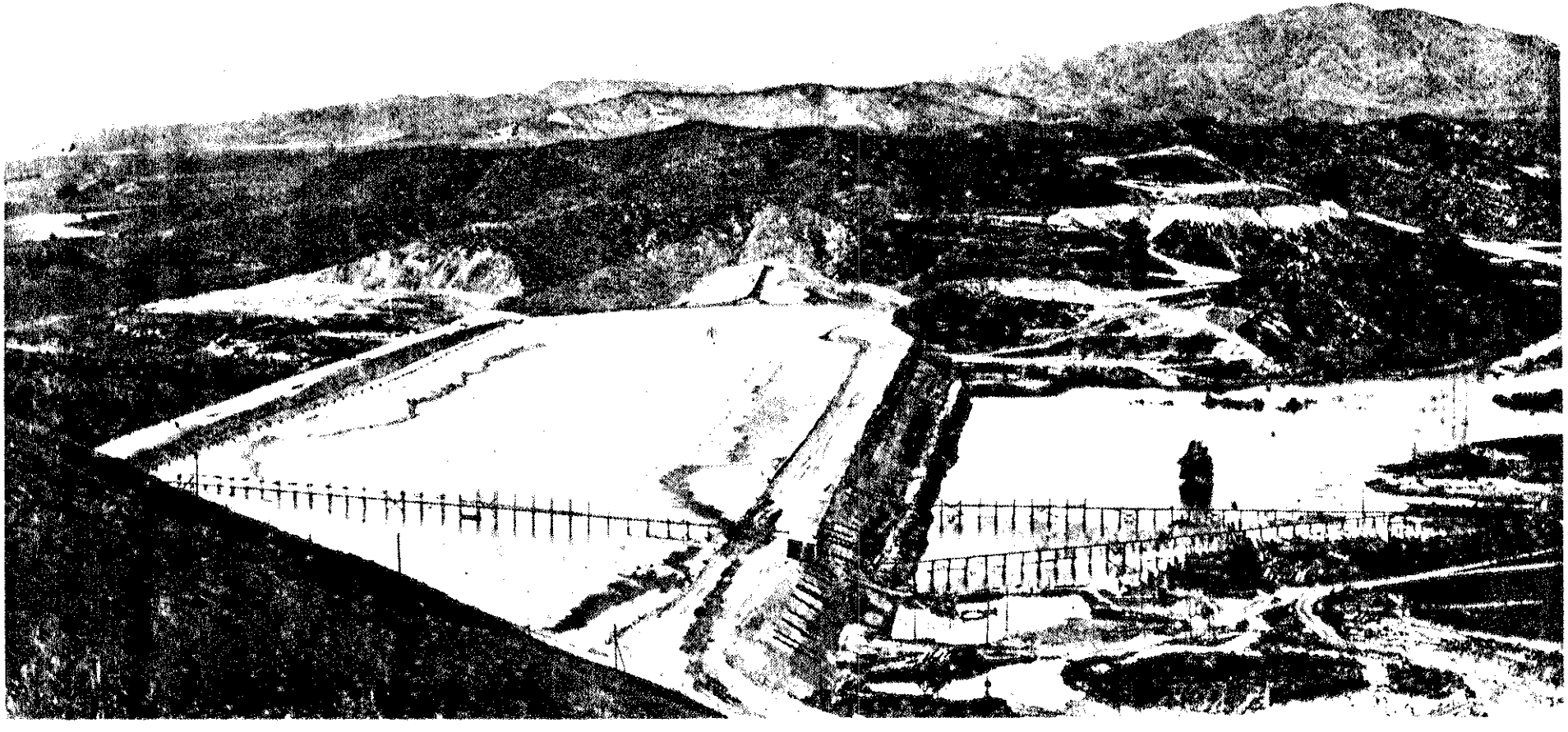

Fig. II-1 CONSTRUCTION OF LOWER SAN FERNANDO DAM.

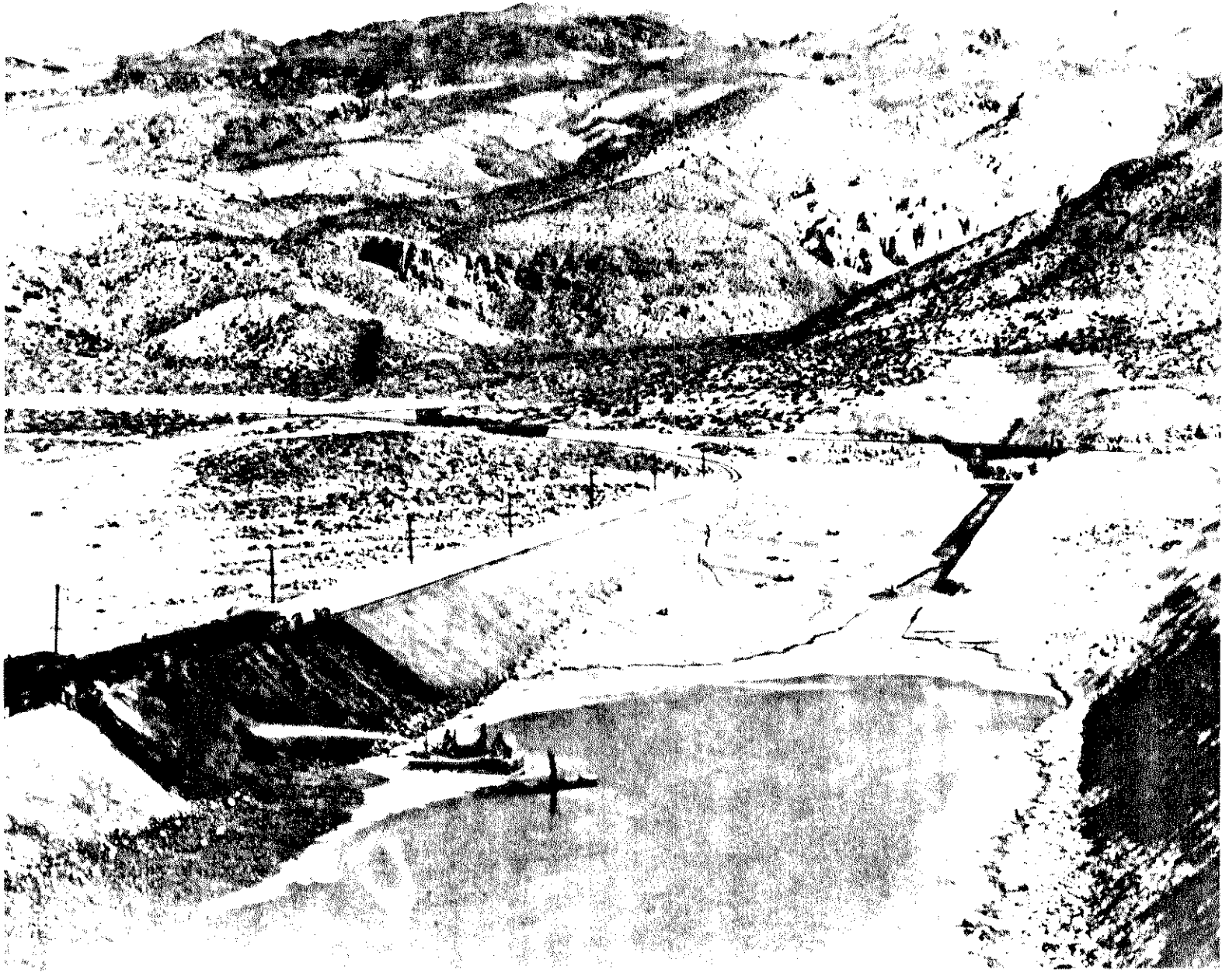

Fig. II–2 CONSTRUCTION PROCEDURE FOR UPPER SAN FERNANDO DAM.

The embankment of the Upper Dam is founded on deposits of Recent alluvium, consisting of stiff clays and clayey gravels about 50 to 60 ft in thickness. Underlying the alluvium and forming the abutments of the dam are poorly cemented conglomeritic sandstone and coarse-grained sandstone of the Saugus Formation (Lower Pleistocene).

Construction of the Lower San Fernando Dam

Construction of the Lower San Fernando Dam began in 1912. The foundation alluvium was not stripped off prior to placing the embankment fill. However there are reported to be three cutoff trenches through this alluvium which extend down into the bedrock, and which were backfilled with hydraulicked material or puddled clay. One of these trenches containing plastic clay was encountered in one of the recent exploratory drill holes. An adjacent drill hole some 30 ft upstream encountered only alluvium at the same elevations between the hydraulic fill and the bedrock.

Judging by the available early photographs, the embankment was constructed by first making a broad dike of wagon-dumped and rolled fill at both the upstream and downstream edges. The large central area between the dikes was filled by hydraulicked material. Unfortunately the lateral and vertical extent of these dry fill dikes is unknown.

Between the years 1912 and 1915 the embankment was constructed to about Elevation 1080 at the axis and 1090 at the upstream and downstream edges (streambed at axis was approximately at Elevation 995) using material hydraulicked from the floor of the reservoir. Records indicate that the borrow area was then shifted and hydraulic construction was continued using ground-up shale from a borrow area on the hillside at the left end of the dam, until the dam was built to Elevation 1097 at the axis. Since

the hydraulic fill process requires beaches and a slope toward the axis from both faces, it is probable that the top of the hydraulic fill section at the edges could be as high as Elevation 1105. In 1916-17 the hydraulic fill section was capped by a rolled earthfill composed of shales from the east abutment. This fill was placed to about Elevation 1118 for a narrow width at the upstream side and 1108 across the remainder of the dam. In 1920 additional fill was placed to bring the upstream edge to Elevation 1125 (L. A. Department of Water and Power Report, 1929).

In 1924 the embankment was again raised. This time, rolled fill was placed to about Elevation 1133 along the upstream side and 1118 on the downstream side. The material used was a combination of heavy clay and gravel from a hill at the right end of the dam.

In 1929-30 the dam was raised for the last time, to Elevation 1144.6. A trench was excavated through all the previously placed rolled fill zones and into the hydraulic fill. All shale materials encountered were removed and the new fill placed against what was reported to be a very plastic material. The shale material excavated from the core trench was mixed with gravelly material from borrow pits at the right end and upstream side of the dam and placed in a downstream toe addition. This is called a rock blanket in some of the reports but summary notes recorded in the Field Report on Addition to Lower San Fernando Dam (L. A. Department of Water and Power, 1929-30) indicated it was not rock. This addition was placed on a 3:1 slope to Elevation 1074.

In 1940 a final major modification was made with the construction of a rolled earth downstream toe addition terminating in a 20-foot-wide berm at Elevation 1096. This addition has a 4-1/2:1 slope except that it steepens to 3-1/2:1 at the right end.

Thus the dam can best be described as essentially a hydraulic fill embankment capped by a potpourri of wagon-dumped and rolled fills, founded on alluvium with three cutoff trenches to bedrock, and with a 20-foot downstream berm at Elevation 1096; it had an upstream slope of 2-1/2:1, downstream slopes of 2-1/2:1 and 4-1/2:1, a height of 142 feet, a crest width of 20 feet, and a length of 2080 feet. It was faced upstream with lightly reinforced concrete and had a 3-foot-high concrete parapet wall at the upstream edge of the crest. Altogether, about 3.3 million cubic yards of embankment were used in construction to impound 20,500 acre-feet of water.

Work done in 1929-30 was during the period of emergence of better moisture control and use of better compaction equipment. Light sheepsfoot tampers, either mounted on drums and pulled by crawler tractors or on rims mounted on the rear wheels of Fordson tractors, were used for compaction. The drum-mounted feet were reported to exert a pressure of about 71 psi on the soil. Efforts were also made to place the soil in controlled lifts and to add water by sprinkling. The additional fill added in 1940 was a well-controlled and well-compacted embankment.

A cross-section through the completed dam is presented in Fig. II-3.

Two concrete outlet towers were constructed as intakes for the service outlets from the reservoir. Tower No. 2, near the right end of the dam, was founded at Elevation 1072 and was 74 feet high. It had three rows of 36-inch-diameter gated ports and a 36-inch-diameter gated sluice-way near the bottom at Elevation 1078. The tower had a constant outside diameter of 20 feet with inside diameters of 13, 15, and 17 feet stepped at each third point. The outlet from Tower No. 2 was a 6-foot inside diameter cast-in-place reinforced-concrete pipe running through the base of the dam with invert near the tower at Elevation 1078.

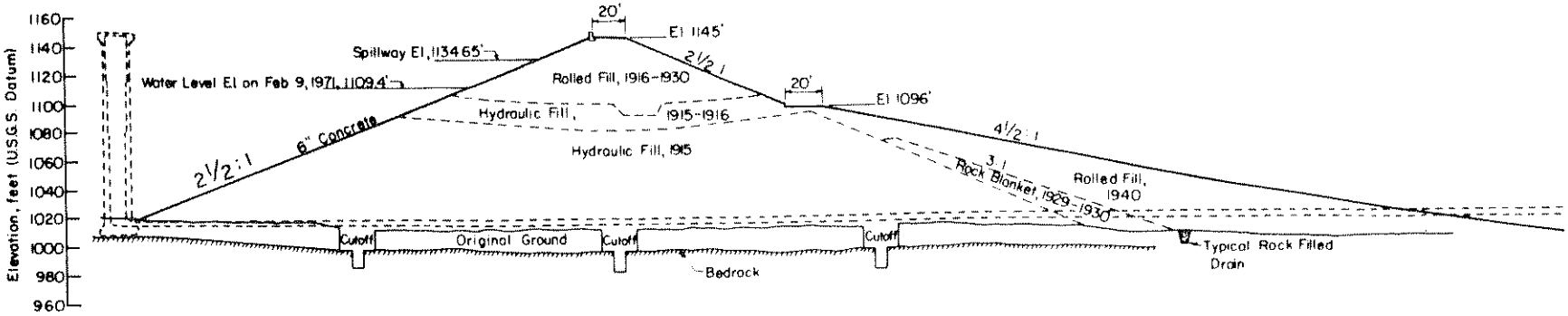

Fig. II–3 CROSS–SECTION THROUGH LOWER SAN FERNANDO DAM.
(After L.A. Dept. of Water and Power)

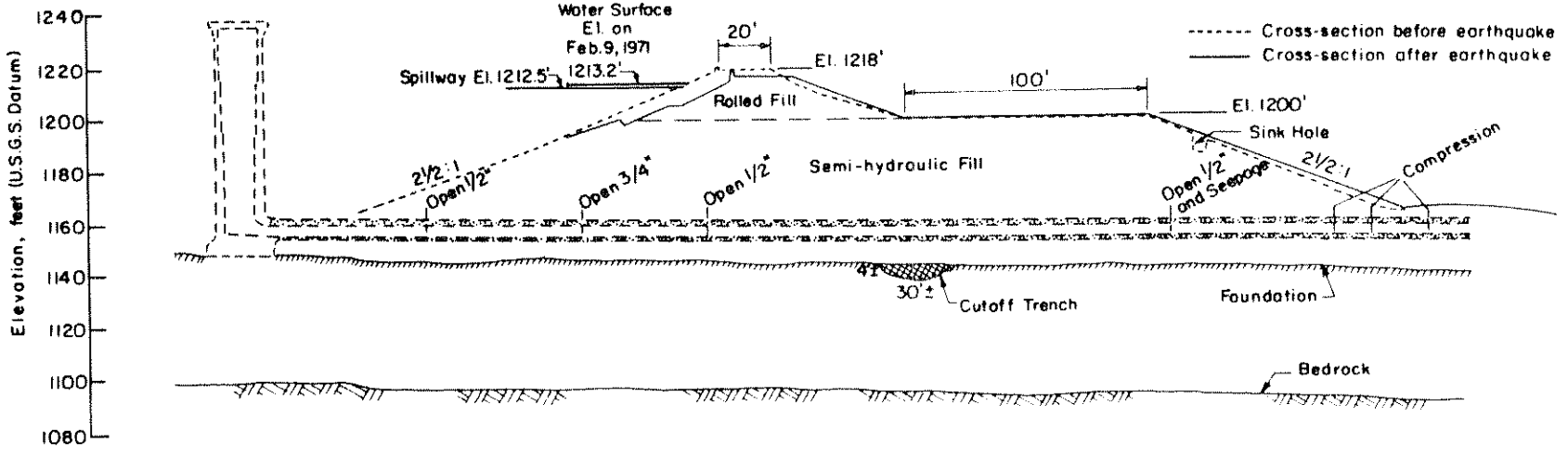

Fig. II–4 CROSS–SECTION THROUGH UPPER SAN FERNANDO DAM.
(After L.A. Dept. of Water and Power)

Tower No. 1 was constructed near Station 13+00 of the dam; it was founded on rock at Elevation 1007, and was about 140 feet high. It had a nearly constant outside diameter of 20 feet except that the lower 20-foot section is slightly larger. The inside diameter was stepped from 16-1/2 to 15 to 13-1/2 to 12 feet, approximately at quarter points. The outlet from Tower No. 1 was a reinforced-concrete conduit cast in place with an inside diameter of 8.5 feet for about 400 feet, reducing to 8.1 feet for about 400 feet. A 62-inch inside diameter steel cylinder reinforced-concrete pipe with lead-filled joints was inserted into the downstream half of the outlet in 1940 and the annular space filled with concrete. This pipe in turn connected to a 54-inch riveted-steel pipe which provided conveyance to the City distribution system.

Surveillance of the Lower Van Norman Reservoir included measuring the movement and settlement of the dam through monuments located initially on the parapet wall and later in the embankment at the dam crest. Observation wells were located on the upstream and downstream slopes of the dam to measure the phreatic line within the embankment of the dam at various locations. Drains were provided in the foundation of the dam and the seepage collected by these drains was measured and recorded. A Wilmot seismoscope and a Teledyne peak recording accelerograph were located on the crest near the center of the dam, and another Wilmot seismoscope was located at the left end of the dam on the abutment. There were three tiltmeters located at the crest, on the Elevation 1096 berm, and at the toe of the dam. All surveillance data were reviewed periodically in reviewing the safety of the dam.

The dam was operated for many years with the reservoir peaking at its full design elevation of 1134.6 (some 140 ft above the old stream bed).

However, in 1966, following various engineering studies and reviews, the maximum operating reservoir level was reduced by 9.6 ft to elevation 1125.

Construction of the Upper San Fernando Dam

Like the Lower Dam, the Upper San Fernando Dam was also constructed directly on the alluvial soil.

Available cross sections of the dam show a cutoff trench extending to a depth of 4 feet into alluvium for a width of 30 feet. This was probably intended only to cut off rodent holes and vegetation.

The main body of the dam was constructed by the semi-hydraulic fill method using a similar procedure to that described previously for the South Haiwee Dam, the material being hauled from the borrow area to the edges of the embankment by wagons, dumped into the pond and dispersed by monitors working from floating barges as illustrated in Fig. II-2. The semi-hydraulic fill portion was constructed to about Elevation 1200 in 1921 by using about 500,000 cubic yards of material obtained from the valley floor. Although it was originally planned to be constructed to Elevation 1238 in 1922, the dam was instead raised to Elevation 1218 by placing some 50,000 cubic yards of compacted dry fill on the upstream side. The dry-fill material was obtained from side hill borrow, spread in thin layers, sprinkled and wagon-rolled. The completed section of the dam has a 2.5:1 concrete-paved upstream slope, a crest 20 feet wide, and a downstream slope of 2.5:1 with a 100-foot berm at Elevation 1200. Originally, the reservoir capacity was 1977 acre-feet but the storage capacity was reduced to 1848 acre-feet by siltation during the 1938 flood and later by the construction of the dikes along the western side of the reservoir. These dikes provide flood-control protection and divert the local upstream runoff and debris from the reservoir.

A cross-section through the embankment is shown in Fig. II-4.

An outlet tower stands just upstream of the toe of the embankment at about the midpoint of the dam. The tower is founded on alluvium at about Elevation 1149 and rises about 90 feet to Elevation 1239. It is similar to the towers at the lower reservoir having a constant outside diameter of 20 feet and stepped internal diameters estimated to be 16, 14, 12, and 10 feet. The tower connects to an 8-foot-diameter concrete cast-in-place outlet conduit. This conduit has a 62-inch inside diameter concrete lined and coated steel cylinder pipe with lead-filled joints inserted through it with the annular space between the two filled with concrete for the upstream 160 feet.

In 1968 a second outlet was constructed by concrete encasement of a 99-inch welded-steel pipe through the right abutment at an inlet elevation of 1185. In addition to these outlets it has been standard procedure to operate the reservoir to spill water into the lower reservoir through the overflow spillway at the left end of the dam.

Movement and settlement data were obtained from the parapet wall and from monuments embedded in the embankment at the center of the dam crest. Observation wells on the downstream slope and berm indicated the condition of the phreatic line within the embankment. Drains constructed at the abutment contacts and toe of the dam provided data on seepage losses. In addition, a basin drain was constructed in 1965 to remove any water that accumulated under the dumped backfill in the area below the dam. Surveillance measurements on all instrumentation were made at regular intervals.

Seismic Stability Investigations Prior to the Earthquake

In a general review of the seismic stability of earth dams throughout California, conducted in 1966, the earthquake resistance of the Lower San Fernando Dam was investigated by means of a conventional analysis procedure using a seismic coefficient of 0.15. This value was recommended by a consulting board appointed by the Los Angeles Department of Water and Power, based on the known and expected seismicity of the region.

The strengths of the soils comprising the embankment were determined by means of drained direct shear and triaxial compression tests on undisturbed samples. The rate of loading in these tests may have been too fast for full drainage to occur, but the data were interpreted conservatively to provide strength parameters for analysis purposes.

Stability computations were made using the conventional method of slices for the combined effects of (1) an earthquake represented by a seismic coefficient of 0.15 and (2) a partial drawdown of the reservoir level from El. 1125 to El. 1100. These computations showed a minimum factor of safety of 1.01.

Based on the results of these studies, it was concluded that since the method of analysis was based on conservative strength values and force applications in keeping with conventional practice, the dam was safe against any anticipated ground motion if the water level was not allowed to exceed El. 1125. The reservoir was operated with this restriction during the following years, as illustrated by the water levels in the reservoir for 1970-71, shown in Fig. II-5.

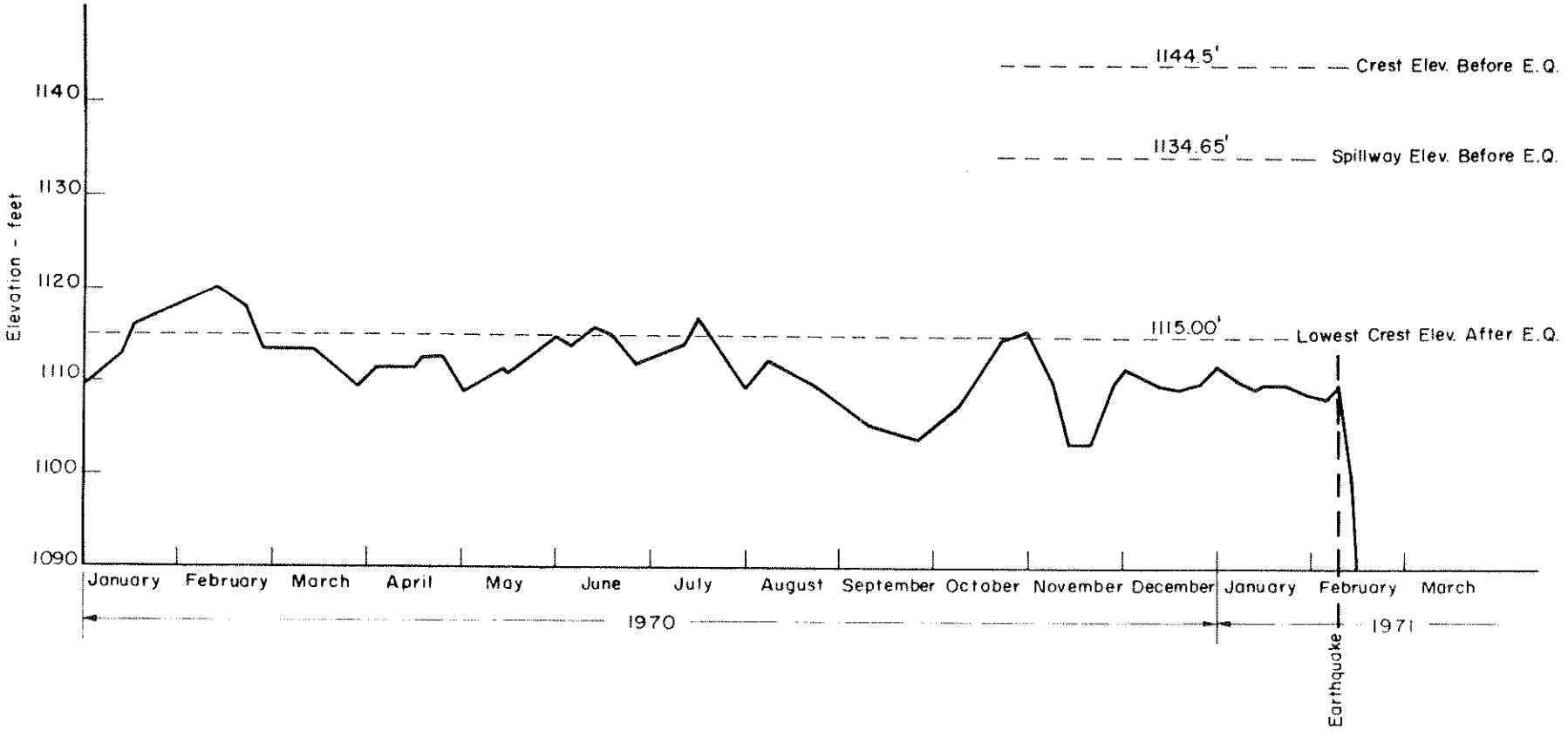

FIG. II-5 WATER LEVELS IN RESERVOIR OF LOWER SAN FERNANDO DAM DURING 1970-71.

Part III - Effects of the Earthquake on the Dams

Earthquake

Since detailed information on the seismological, geological, engineering and political aspects of the San Fernando earthquake are readily available elsewhere, only those aspects of the earthquake which pertain to the performance of the San Fernando Dams are reviewed briefly in the following pages.

An aerial photograph showing the relative location of the dams to the epicenter and the surface fault scarps produced by the earthquake is shown on Fig. III-1. The dams are located approximately 8-1/2 miles southwest of the epicenter, and near the extreme western extension of the observed surface fault breaks.

The earthquake occurred at 6:00 AM local time and has been assigned a Richter Magnitude of 6.6. The focal depth was about 8 miles. The earthquake was accompanied by thrust faulting in which the north block moved relatively up and over the south block at an angle of about 45 degrees leaving the surface scarp shown on Fig. III-1. In some areas near the eastern end of this scarp the relative upward movement amounted to more than 4 feet. The magnitude of these movements diminished and the visible surface breaks became discontinuous toward the western end of the scarp. However as indicated on Fig. III-1, features resembling a fault break were traced to the eastern edge of the Lower Van Norman reservoir. Some small fresh cracks parallel to steeply dipping bedding planes which lined up with the other observed surface fault scarps were faintly observed on a small island in the lower reservoir.

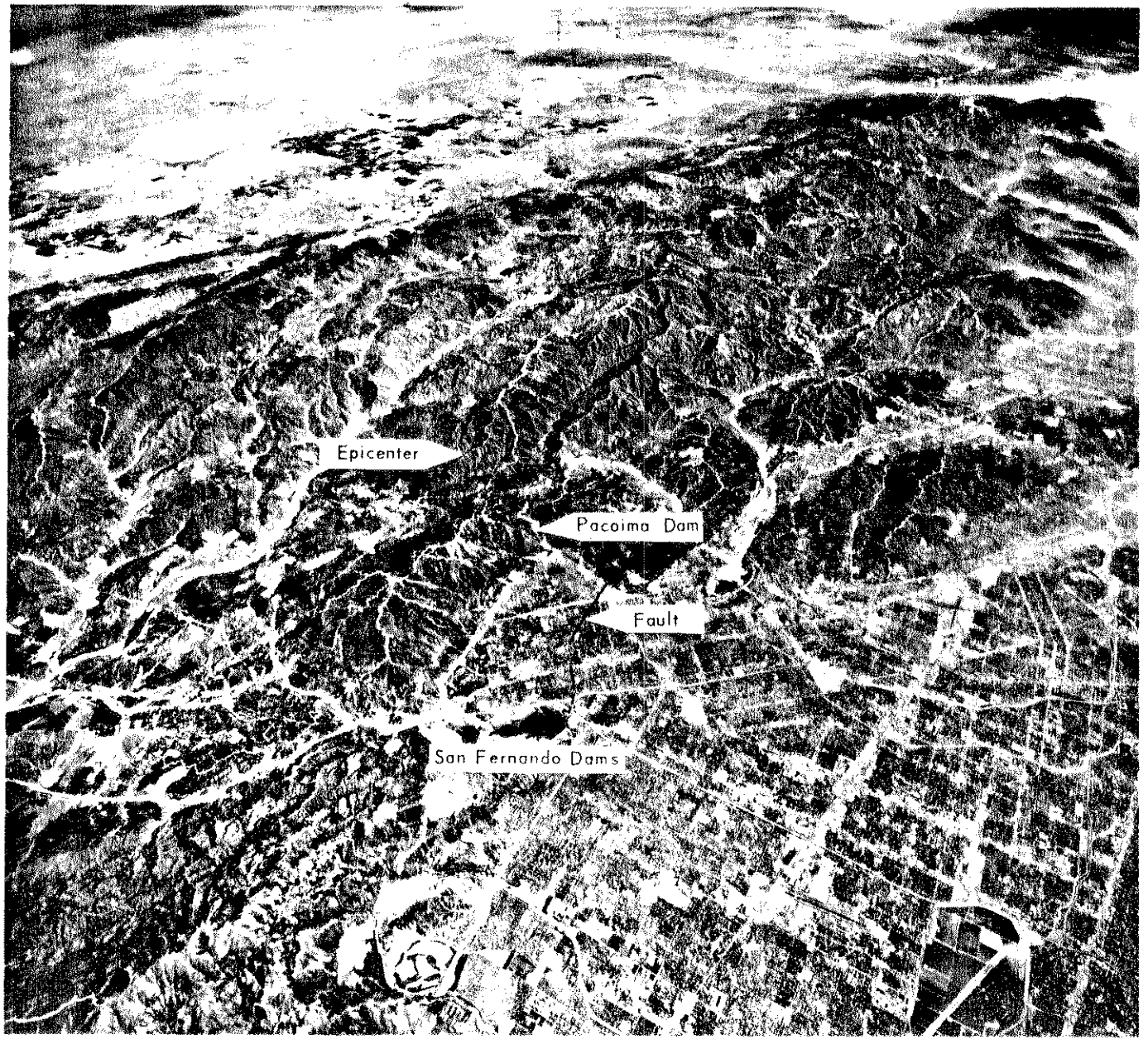

FIG. III-1 LOCATION OF SAN FERNANDO DAMS IN RELATION TO EPICENTER AND SURFACE FAULTS.
(Photographed by U.S. Geological Survey)

The strong motion shaking produced by this earthquake was recorded at a number of locations within the area of high intensity shaking. One of the most interesting records was that obtained at a station some 55 ft above the left abutment of the 365 ft high Pacoima Dam, located about 5 miles south of the epicenter. The two horizontal components of ground motion at this station showed maximum accelerations of about 1.25g and the vertical component a maximum acceleration of 0.72g. However it has been suggested by some investigators that the high acceleration peaks in this record may have been due to the peculiar topographic conditions of the recording station and that substantially smaller accelerations would have been recorded near the base of the dam. An argument in favor of this is the lack of damage to the caretaker's house located in the valley a few hundred feet from the dam, (the house did not even lose its chimney during the earthquake). However even allowing for the amplifying effects of the local topography, it seems likely that the maximum acceleration in the vicinity of the Pacoima Dam was about 0.75g.

A second set of instrumental records of special interest in the study of the San Fernando Dams were those obtained on two seismoscopes, one located on the east abutment of the Lower Dam and one on the crest of the Lower Dam. The location of these instruments relative to the dam immediately after the earthquake is shown on Fig. III-2. The instrument located on the crest of the dam was carried into the reservoir by the slide, and became submerged below the surface of the reservoir water. Fortunately, it was not damaged, and after the water had subsided, the instrument was recovered.

Photographs of the traces made by the seismoscopes on the abutment and crest of the Lower Dam are shown on Fig. III-3. It may be seen that

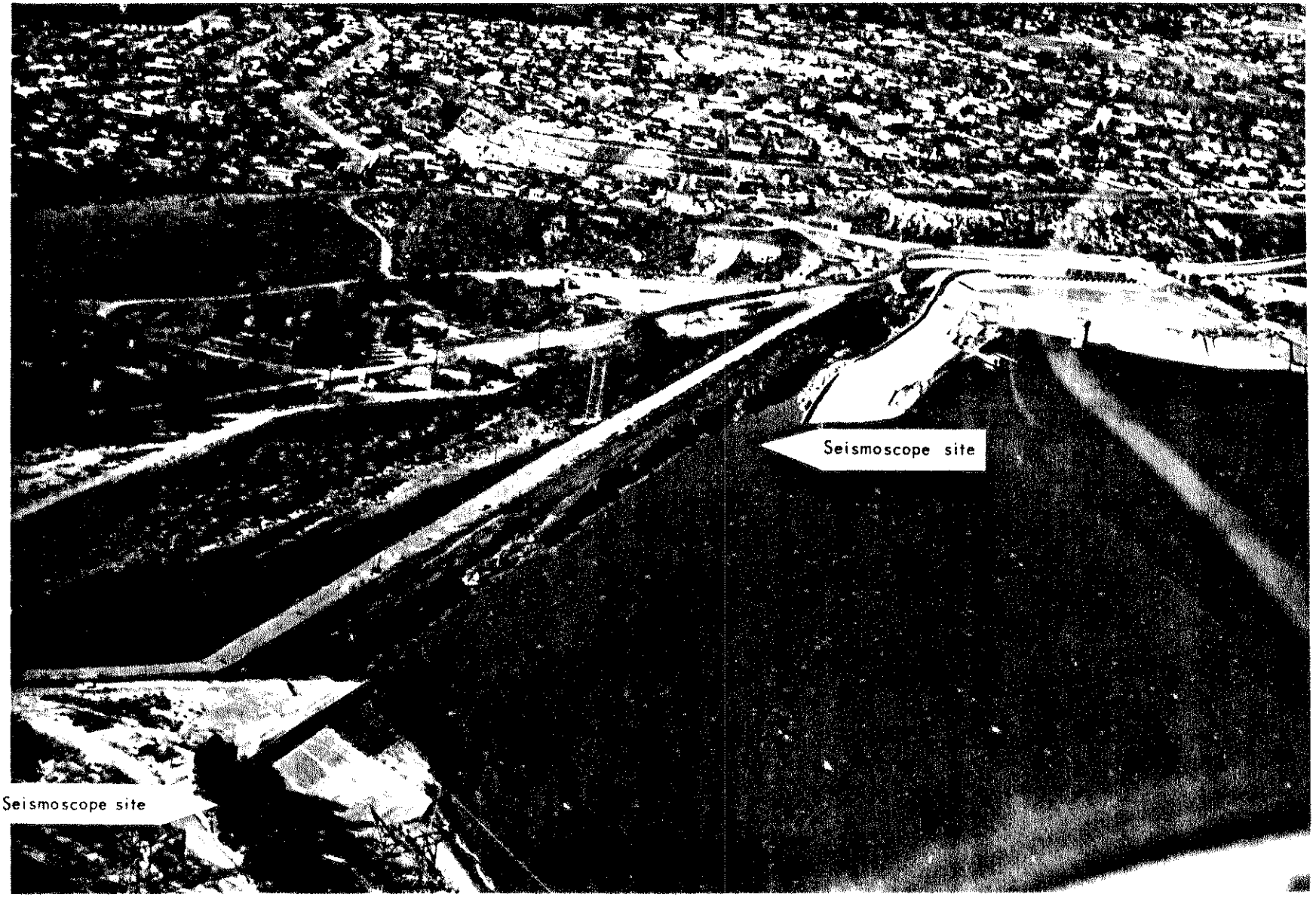

FIG. III–2 AERIAL VIEW OF LOWER SAN FERNANDO DAM AFTER EARTHQUAKE OF FEBRUARY 9, 1971. ARROWS INDICATE SEISMOSCOPE SITES. THE CREST SITE WAS COMPLETELY SUBMERGED FOLLOWING THE EARTHQUAKE.

(Photograph by U.S. Geologic Survey)

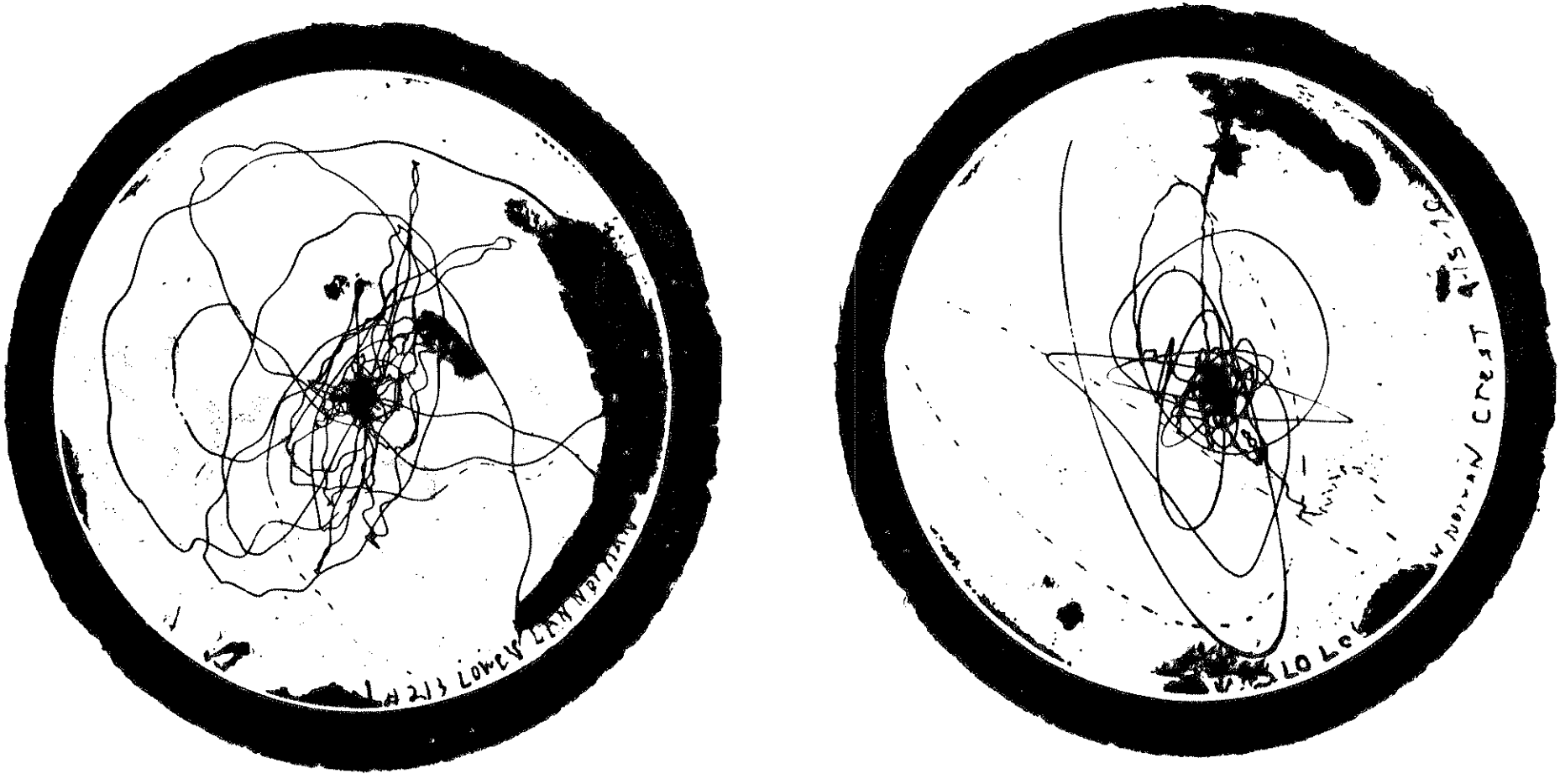

Abutment Record

Crest Record

FIG. III–3 SEISMOSCOPE RECORDS AT LOWER SAN FERNANDO DAM DURING EARTHQUAKE OF FEBRUARY 9, 1971

the motion at the rock abutment of the dam appears to have no preferred direction whereas the motion at the crest appears to be strongest in the transverse direction. However detailed study shows that the seismoscope on the crest recorded a duration of motion somewhat comparable to that recorded on the abutment, thus indicating that the slide probably did not occur until near or just after the end of the stronger earthquake motions.

Morrill (1972) has computed the maximum spectral displacement for these two records, as well as for the other seismoscope records obtained during the San Fernando earthquake. He also lists the instrument characteristics, including the natural period. Duke et al (1972) have computed the spectral acceleration of these seismoscope records and assigned the following values to the two records from the lower dam:

Abutment	≈0.48g
Crest	≈0.55g

They further found that for all sites where there were both seismoscopes and accelerometers, that with some scatter the maximum spectral acceleration obtained from the seismoscope record was about the same as the peak acceleration recorded on a strong motion accelerometer. Thus this data would indicate that the maximum acceleration in the rock foundation at the damsite was about 0.5g and that there was no significant amplification between the foundation and the crest of the dam.

A detailed study and an ingenious interpretation of the trace of the seismoscope record from the east abutment has been made by Scott (1972), who observed that some of the small regular waves on the trace were a peculiarity of the instrument and not of the earthquake. These waves provided a time scale to the record, from which it was possible to convert the trace on the seismoscope into a time history of acceleration.

Some uncertainties developed where the instrument reached its maximum travel and bounced against its support, and where, in several instances, the pen went off scale. The computed accelerogram determined by Scott contained one peak up to about 0.8g, but because of the uncertainties involved, Scott suggested that the peaks should probably be no greater than 0.55g to 0.6g.

Unfortunately, the seismoscope record from the crest of the Lower Dam has not yet been converted into an accelerogram.

A plot of the maximum accelerations recorded at rock sites at different distances from the epicentral region in the San Fernando earthquake is shown in Fig. III-4. In the light of these results a maximum acceleration of the order of 0.55 to 0.6g in the vicinity of the dams seems entirely reasonable.

Earthquake Effects on the Upper Dam

An aerial view of the Upper Dam taken some 12 days after the earthquake is shown on Fig. III-5. Severe longitudinal cracks are clearly evident running almost the full length of the dam on the upstream slope. At the time of the earthquake the water level in the reservoir was above these cracks so that they were only visible after the reservoir level had been drawn down. These cracks resulted from a general downstream movement and settlement of the top portion of the dam with respect to the foundation. Subsequent surveys showed that at the center line, the crest moved downstream about five feet and settled vertically about three feet (see Fig. II-4).

A close-up view from the ground along the crest of the dam showing the bowing of the parapet wall resulting from the downstream movements is shown on Fig. III-6 and a close-up view of the upstream cracks is

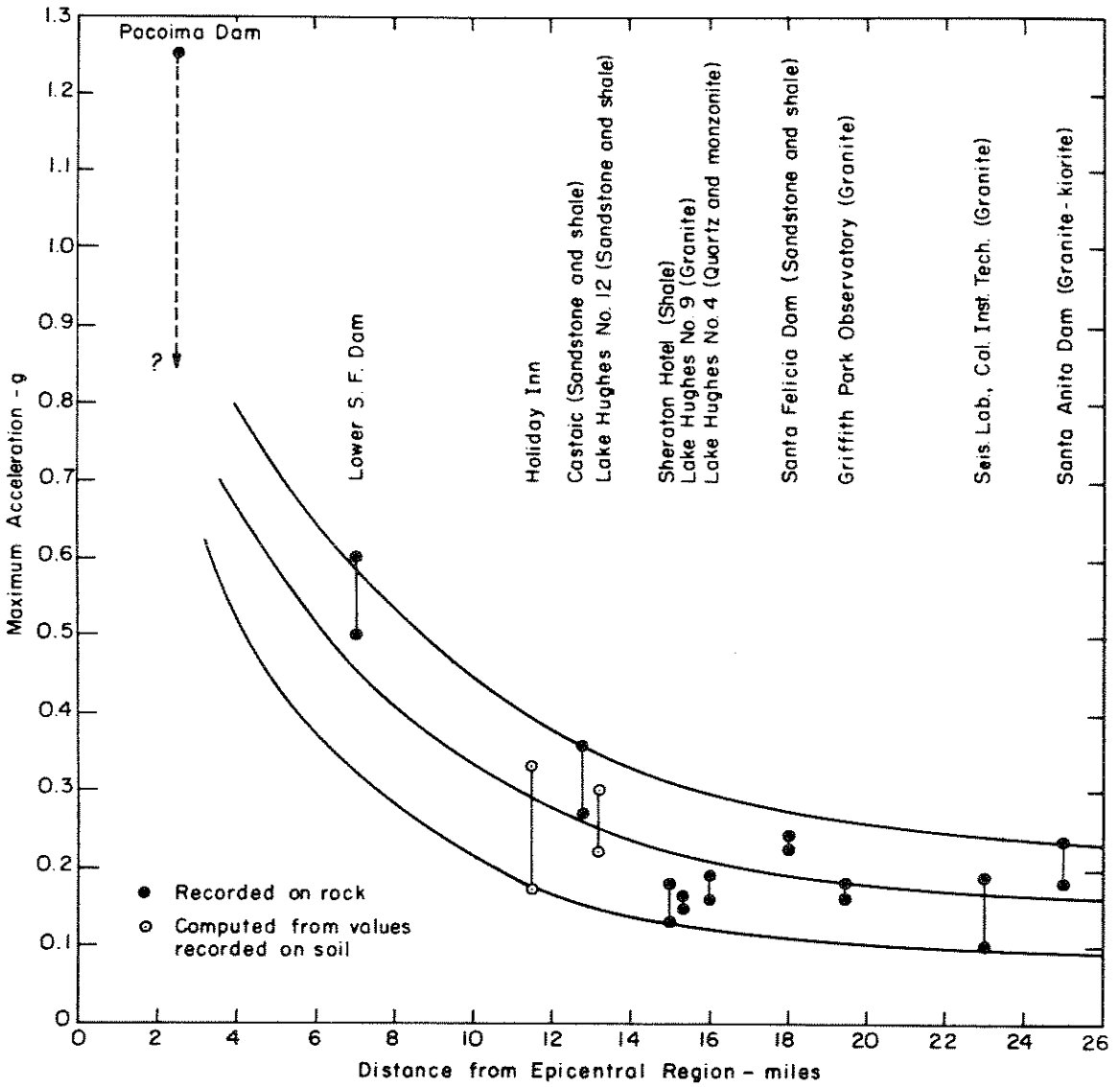

Fig. III–4 MAXIMUM ACCELERATIONS RECORDED ON ROCK IN SAN FERNANDO EARTHQUAKE, 1971.

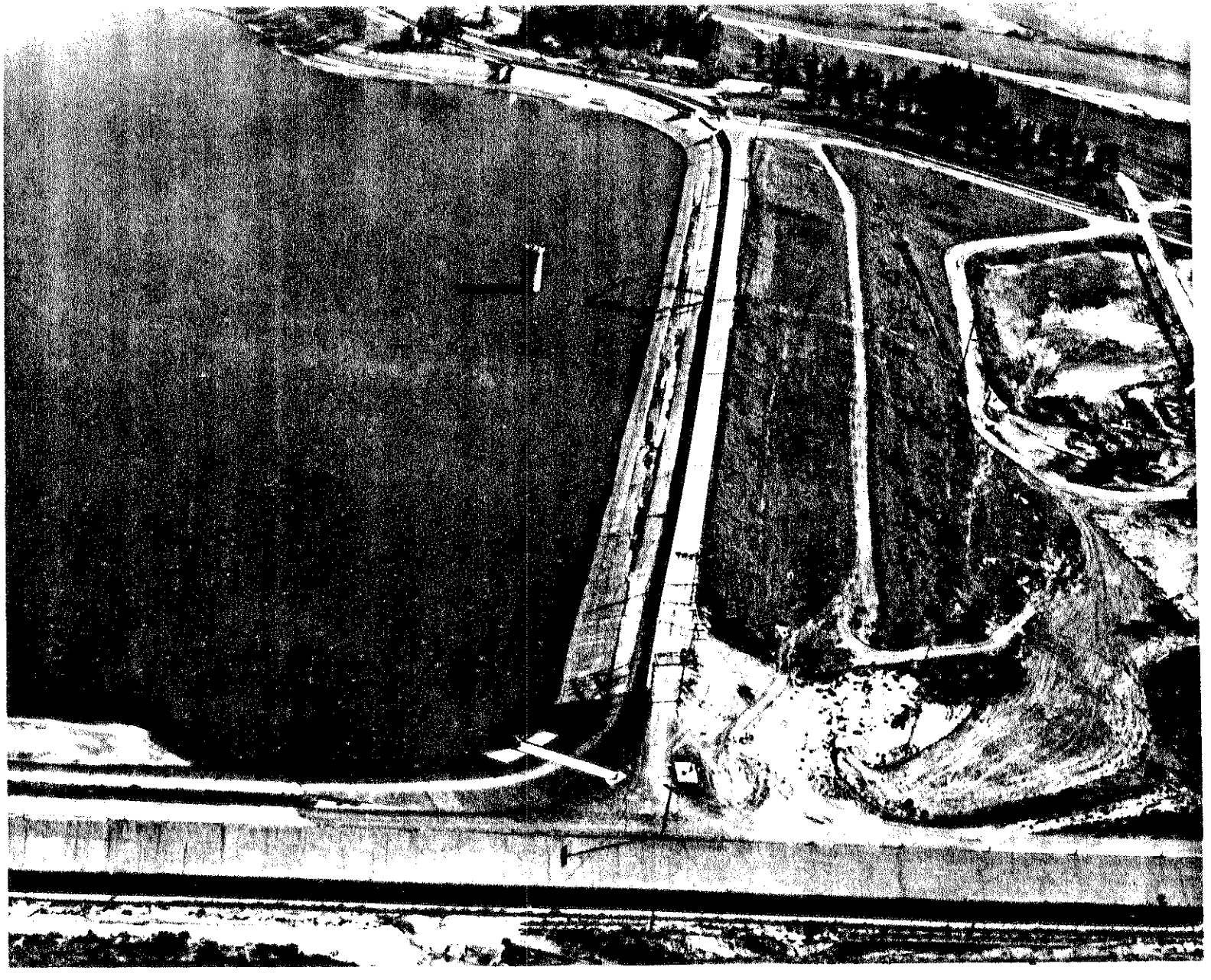

FIG. III-5 VIEW OF UPPER SAN FERNANDO DAM AFTER EARTHQUAKE.
(Photograph by Department of Water Resources, Feb. 21,1971)

FIG. III-6 DEFORMATION OF PARAPET WALL RESULTING FROM DOWNSTREAM MOVEMENT OF EMBANKMENT

FIG. III-7 SLIDE SCARPS ON UPSTREAM FACE OF EMBANKMENT

presented in Fig. III-7. These cracks appear to be multiple shear scarps at the outer edge of the fill.

At the downstream toe of the dam a two feet high pressure ridge developed and a three feet diameter concrete manhole near the east abutment was tilted and sheared noticeably in the downstream direction. Also a concrete post near the center line and at the toe was also tilted downstream due to the soil ploughing around it. These movements clearly show that the entire upper part of the dam participated in the movement downstream.

Shortly after the earthquake the interior of the outlet conduit was surveyed to determine the extent of damage. The results of this survey are shown on the cross section through the dam in Fig. II-4. In the central and upstream portion, there were several 1/2 to 3/4 inch cracks indicating extension movement in this zone. Near the toe of the dam there were compression failures in the conduit. The nature and direction of the movements at the conduit as indicated by these observations were generally the same as those observed from the surface. However, the magnitude of the cumulative movements at the conduit level was considerably less than the observed 5 ft. movement at the crest, indicating that the major movements either occurred within the fill above the conduit, or the fill slipped along the outside edge of the conduit. The first possibility is considered to be the most probable.

Other surface features indicating the nature of damage within the dam included a large sinkhole above the downstream portion of the outlet conduit. This extended to the surface, and is shown on Fig. III-8. The location is indicated on Fig. II-4, almost directly above an open crack in the conduit. It was apparently formed by seepage and erosion through the cracks in the conduit during or immediately following the earthquake.

A large vertical longitudinal crack shown in Fig. III-9 developed midway down the downstream slope of the upper rolled fill section of the dam. The location of this crack is also shown on Fig. II-4.

In the area below the downstream toe of the dam several sandboils were formed, one of which is shown in Fig. III-10. The soil in this area consisted of about 8 ft of loose silty sandy fill overlying alluvium. The origin, date and method of placing this fill is unknown.

In addition to the transverse movements described above, there was also some relative longitudinal movement of the embankment. A transverse compression crack in the paved roadway across the crest of the dam near the west abutment and damage to the concrete spillway wall at the east abutment indicated either some lateral spreading of the dam or some relative movements of one or both abutments in toward the center of the valley. The total amount of relative longitudinal movement appeared to be less than 2 ft, and it was therefore considerably less significant than the downstream movements.

Of special interest in studying the causes of the movements described above were the observations of water level in two piezometers which had been installed in the dam for surveillance purposes prior to the earthquake. The locations of these piezometers in the cross-section and the water level changes following the earthquake are shown in Fig. III-11. The effect of the shaking was to cause an immediate increase in pore water pressure in the embankment, which slowly dissipated with time following the earthquake. As may be seen from the figure the recorded changes in pore pressure ranged from 8.5 to 17 ft of water. However the increases for piezometers 1 and 2 near the center of the embankment were so large that water spilled over the tops of the well casings and the maximum values could not therefore be measured. Furthermore since the

FIG. III-8 SINK HOLE WHICH DEVELOPED ABOVE THE OUTLET CONDUIT ON THE DOWNSTREAM SLOPE OF THE UPPER DAM.

FIG. III-9 LONGITUDINAL CRACK WHICH DEVELOPED ALONG THE DOWNSTREAM SLOPE OF THE UPPER ROLLED FILL SECTION, UPPER SAN FERNANDO DAM.

FIG. III-10 SAND BOIL NEAR DOWNSTREAM TOE OF UPPER SAN FERNANDO DAM

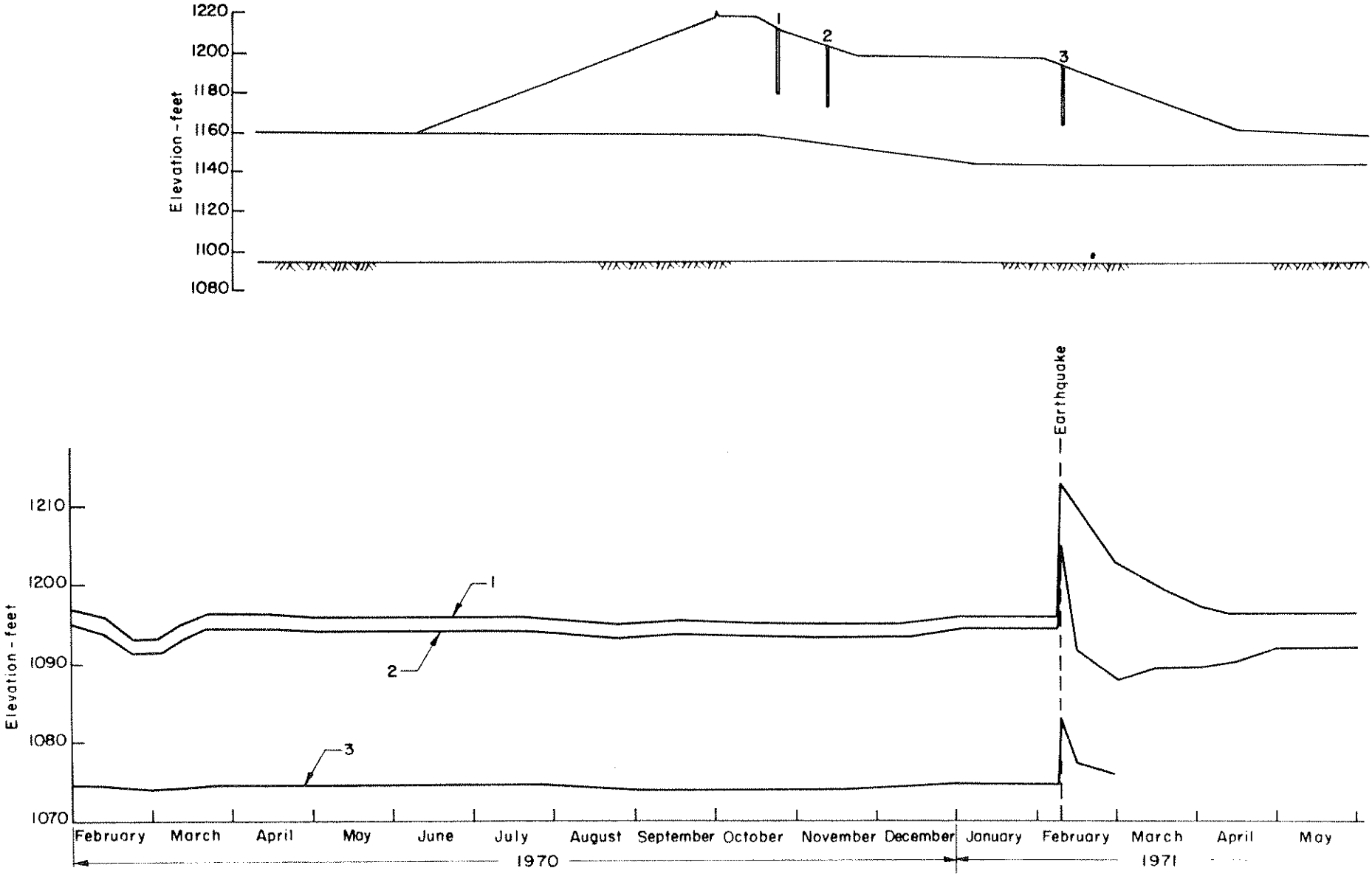

Fig. III-11 CHANGES IN WATER LEVEL IN PIEZOMETERS FOLLOWING THE EARTHQUAKE – UPPER SAN FERNANDO DAM.

first observations on these piezometers were made about 24 hours after the earthquake occurred, the actual increase in pore water pressure in piezometer 3 is likely to be substantially higher than that shown.

The field observations at the Upper Dam suggest that the movements were due to increases in pore water pressure and a corresponding weakening of the soil within a large portion of the dam. Near the top of the upstream face these movements appeared to be concentrated in 2 or 3 well-defined slip surfaces. However the relatively small amount of movement in the outlet conduit, plus the vertical longitudinal crack on the downstream slope suggest that the zone of movements within the dam extended vertically over a large portion of the embankment, and was not limited to a well defined slip surface at depth. The observed changes in piezometric levels together with the sandboils in the fill at the downstream toe of the dam and the sinkhole which developed in erodible soil within the embankment suggest that the movements could also have been associated with liquefaction of some zones within the dam. This possibility was further enhanced by a knowledge of the construction method which would have created a relatively loose embankment (Whitman, 1970) and the knowledge that this type of material would be particularly susceptible to loss of strength under seismic loading (Lee and Fitton, 1969; Seed and Idriss, 1971).

Earthquake Effects on the Lower Dam

An aerial photograph of the Lower Dam taken very soon after the earthquake and showing the slide scarp extending only a few feet above the water is shown in Fig. III-12. Also shown in the photograph are portions of the residential areas immediately downstream of the dam.

The earthquake occurred at 6:00 AM in the morning, just before daylight. The caretaker of the dam immediately walked to the crest from his home near the toe of the dam, arriving there within approximately 5 minutes. He found the reservoir to be perfectly quiet with no waves or sloshing action. Subsequent inspection around the shoreline gave no indication that there had been any abnormal waves or seiches resulting from the earthquake or the subsurface landslide.

A closer view of the dam taken the day of the earthquake is shown on Fig. III-13. At the lowest point on the embankment the water level in the reservoir was only about 5 ft below the sharp crest of the remaining near-vertical scarp. Numerous large longitudinal cracks had developed behind the scarp at lower elevations offering a potential for still further sliding that could reduce or eliminate the meager precarious freeboard which remained. Some of these cracks are shown in Fig. III-14.

Sandbags were immediately rushed to the site and used to build up and reinforce the lowest area. Also as a precautionary measure all of the 80,000 persons living within a 2 mile by 12 mile rectangular area below the dam were immediately evacuated and kept out of the area for a period of four days while the water level in the reservoir was lowered to a safe elevation.

Since mid-1966 the lower San Fernando Reservoir had been operated with the maximum water level restricted to Elevation 1125, about 10 ft below the spillway crest. At the time of the earthquake, the water surface elevation was at about Elevation 1109, some 25 ft below the spillway and about 35 ft below the crest of the dam. The reservoir was storing about 11,000 acre ft of water compared to its maximum design capacity of 20,500 acre ft. Water was flowing into the reservoir at about 474 cfs, and was flowing out through the two outlet towers at about 390 cfs.

FIG. III–12 AERIAL VIEW OF LOWER SAN FERNANDO DAM SOON AFTER EARTHQUAKE

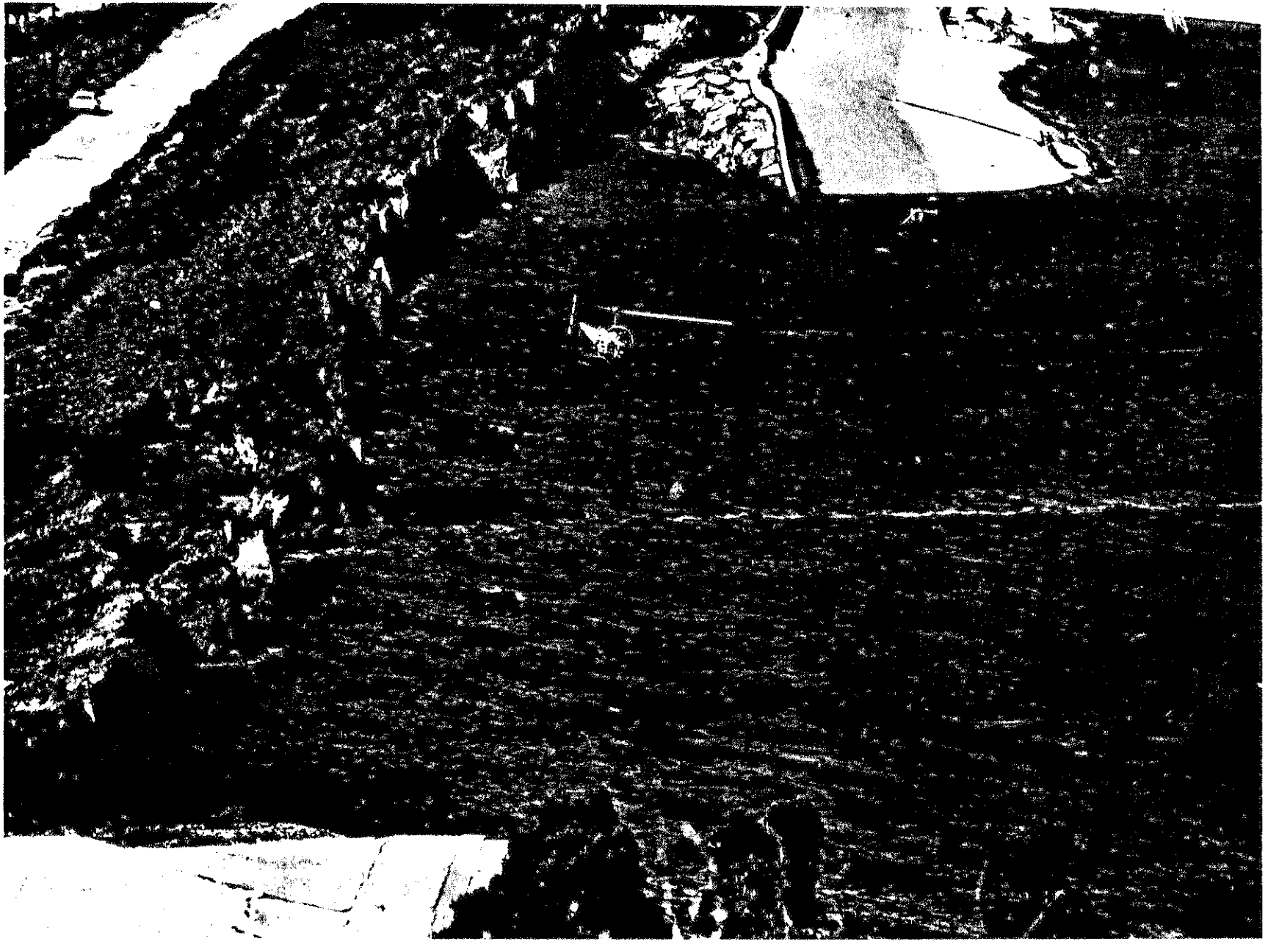

Fig. III–13 LOWER SAN FERNANDO DAM A FEW HOURS AFTER THE EARTHQUAKE.

FIG. III-14 LONGITUDINAL CRACKS IN REMAINING PORTION OF EMBANKMENT - LOWER SAN FERNANDO DAM

As soon as possible following the quake, all the inflow to the reservoir was turned off and the outflow was increased to the maximum possible rate. A view of the dam taken three days after the earthquake is shown on Fig. III-15. The outlet tower near the west abutment remained standing and was not damaged during the earthquake although the walkway leading from the crest of the dam to the tower was broken during the slide. However, the outlet tower located near the center of the dam had broken off during the earthquake and was not visible above the reservoir water level. The position of this tower prior to the earthquake is indicated in Fig. III-15. It was later determined that this tower was broken off about 20 ft above the base and had fallen over with the top in an upstream orientation. The broken section of the tower was covered by the slide material thereby restricting the flow through this outlet to approximately 100 cfs. However, within a short period of time the entrance to the tower had cleared sufficiently by erosion that the outlet was quite effective in removing water from the reservoir.

In addition to removal of water through the two outlet towers some water was also drawn off through three 12 inch blow off valves reaching into the unpaved channel downstream from the dam. The U. S. Army Corps of Engineers also provided additional capacity by installing pumps to the shoreline with a total capacity of about 70 cfs. During the period when all available outlets were being used the maximum outflow from the Lower Van Norman Reservoir was about 700 cfs. Most of this water was taken into the city's water supply system and other storage reservoirs.

During the first few days following the earthquake the water level in the reservoir dropped at an average rate of about 4 ft per day. After about four days the water level had been lowered sufficiently to eliminate

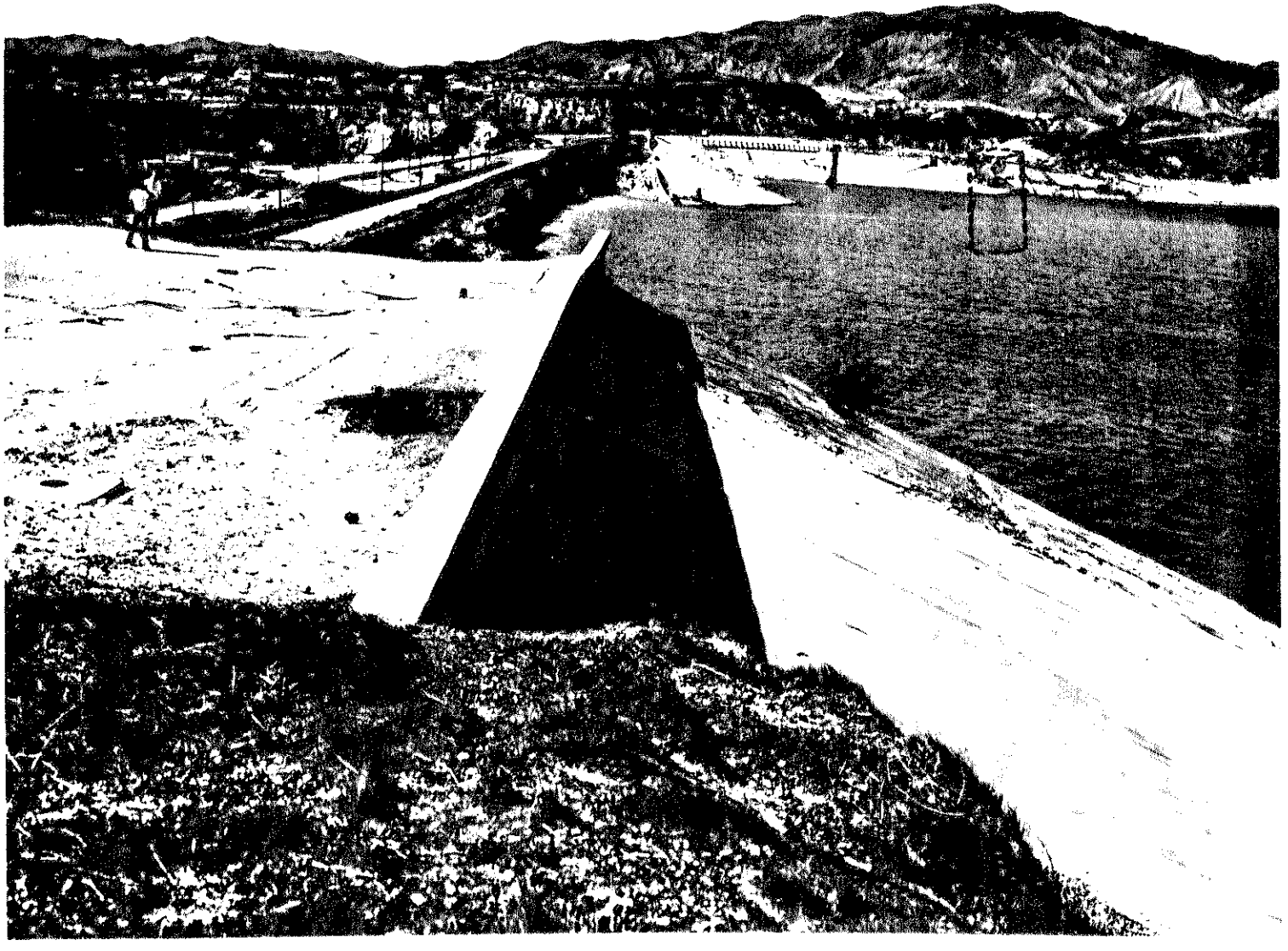

FIG. III–15 LOWER SAN FERNANDO DAM THREE DAYS AFTER THE EARTHQUAKE
(The approximate location of Outlet Tower No. 1 prior to the earthquake is indicated by the dotted outline)

the danger of a breech occuring in the remaining portion of the dam and the 80,000 residents living downstream were permitted to return to their homes.

Piezometers located in the downstream portion of the embankment which was not destroyed by the movements were read and other surveillance data were taken as quickly as possible following the earthquake. It was noted that seepage had increased for a short period and several seepage flows became turbid at first but then cleared within 36 hours after the earthquake. The water levels in the piezometers showed an initial rise but then later returned to normal and slowly decreased as the water level in the reservoir was lowered. The locations of two piezometers and the observed changes in water level in them during and following the earthquake are shown in Fig. III-16. It may be seen that the recorded water pressure increases for well 37 in the foundation soil near the downstream toe of the embankment and for well 64-J with a tip located near the downstream toe of the original embankment were approximately 5 and 3 ft respectively. The actual increases in water pressure even in these locations are likely to have exceeded these values since no readings were taken until about 6 hours after the shaking had stopped. Pore water pressure changes in the upstream shell of the embankment are likely to have been much greater.

As the reservoir drained the full extent of damage to the dam became increasingly apparent. A photograph of the dam taken some 13 days following the earthquake is shown on Fig. III-17. By this time the water level had been lowered some 31 ft. Much of the slide debris was then visible. The original upstream sloping face of the dam was paved with concrete and sloped at 2-1/2 horizontal to 1 vertical. As shown on Fig. III-17, this upstream slope had moved out horizontally into the reservoir, dropped

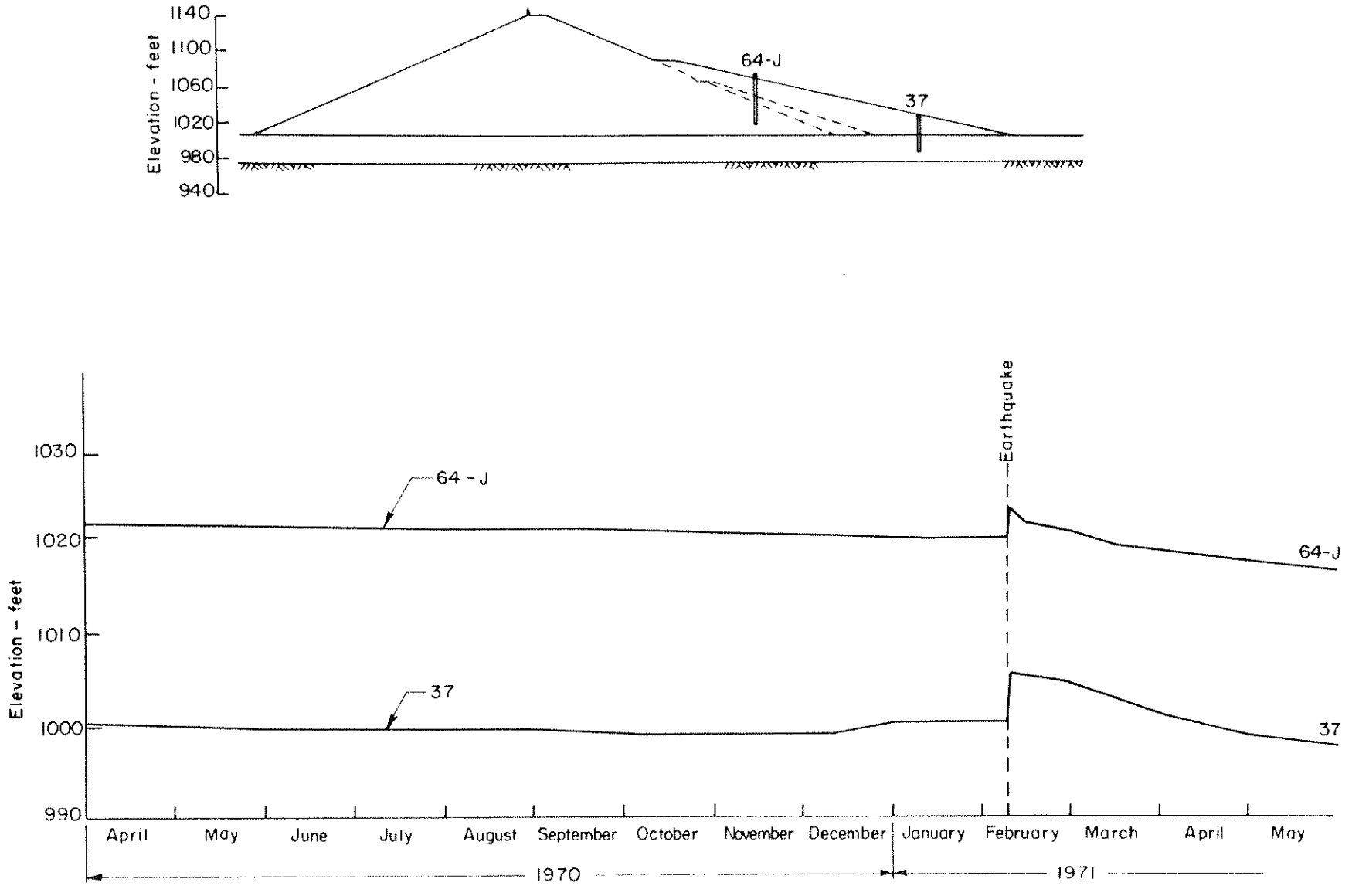

Fig. III-16 CHANGES IN WATER LEVEL IN PIEZOMETERS FOLLOWING THE EARTHQUAKE – LOWER SAN FERNANDO DAM.

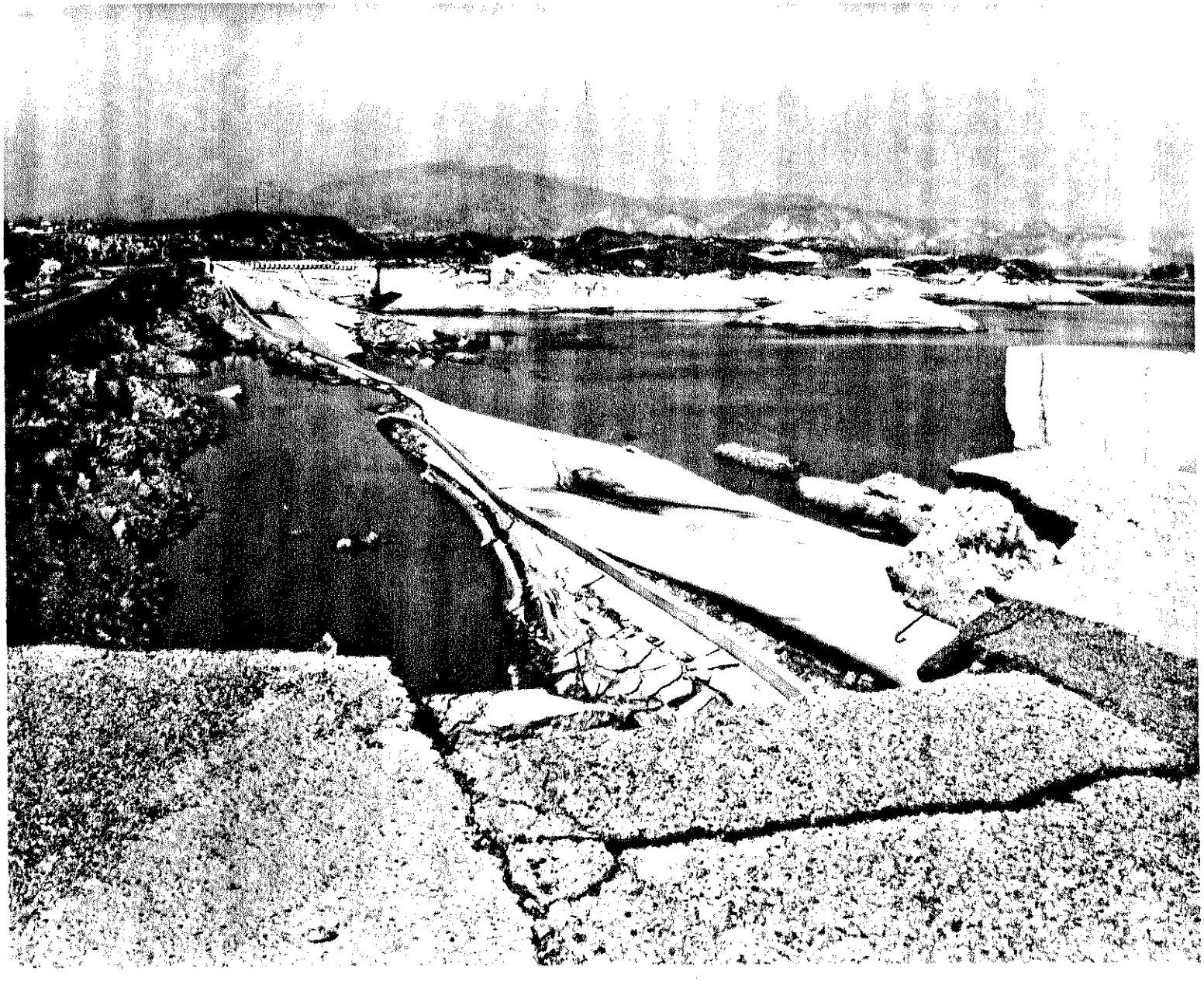

FIG. III–17 SLIDE DAMAGE TO LOWER SAN FERNANDO DAM.
(Photograph by Department of Water Resources, Feb. 22, 1971)

considerably in elevation, and was lying almost horizontally. The eastern outlet control tower was still not visible at that time. A close-up view of the damage near the west abutment is shown on Fig. III-18; the undamaged western outlet tower may be seen in the background. The surface of the slide debris consists of a series of scarps indicating relative movements along many surfaces in the embankment.

Finally after the water in the reservoir had been almost completely drawn down, the broken central tower became visible as shown on Fig. III-19. The tower had apparently tilted several degrees in the upstream direction about the foundation before it finally failed about 20 ft above the base.

An interesting curiosity was observed near the central tower after the water level had been almost completely drawn down. As with the western tower shown on Fig. III-18, a walkway had been constructed to connect the crest of the dam with the top of the tower. This walkway was supported at about mid-span by a column bent founded on the upstream slope of the dam. The photograph on Fig. III-18 shows the condition of this western walkway and its mid-span support following the earthquake. At the center tower the sliding was more severe. The tower collapsed and the walkway collapsed also.

A sketch showing the arrangement of the central walkway with respect to the dam and the tower before the earthquake is shown in the upper portion of Fig. III-20. The center support bent was founded on piles composed of railroad rails driven into the hydraulic fill of the upstream slope. A sketch showing the relative position of this pile-supported bent following the earthquake is shown in the lower part of Fig. III-20. The entire bent had moved out horizontally into the reservoir

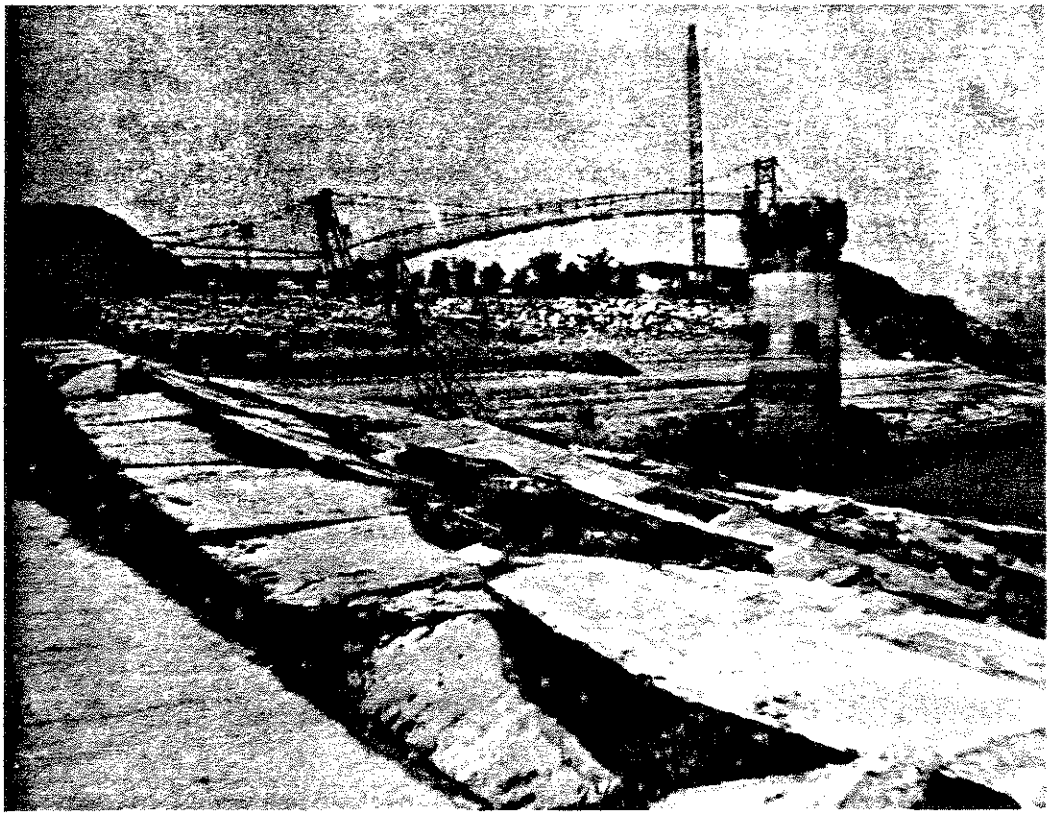

FIG. III – 18 SLIDE DAMAGE NEAR WEST ABUTMENT – LOWER SAN FERNANDO DAM

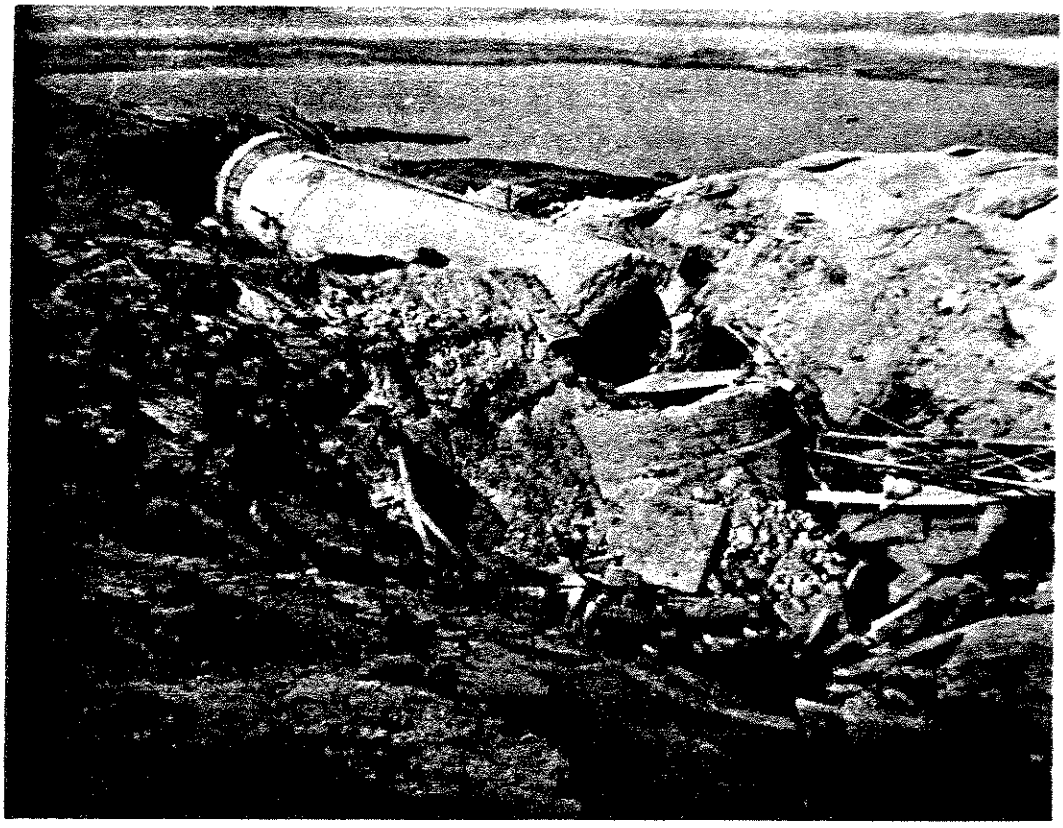

FIG. III–19 CENTRAL OUTLET TOWER – LOWER SAN FERNANDO DAM

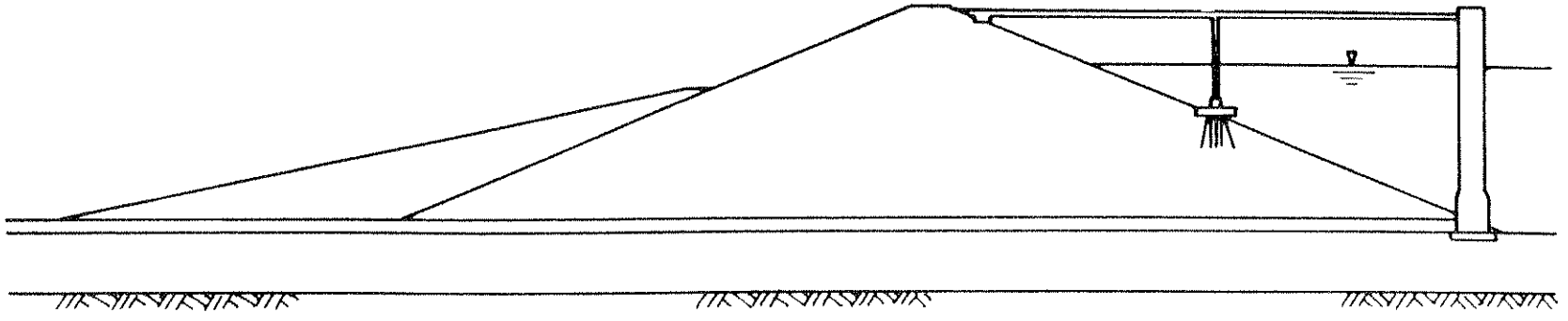

(a) Before Earthquake

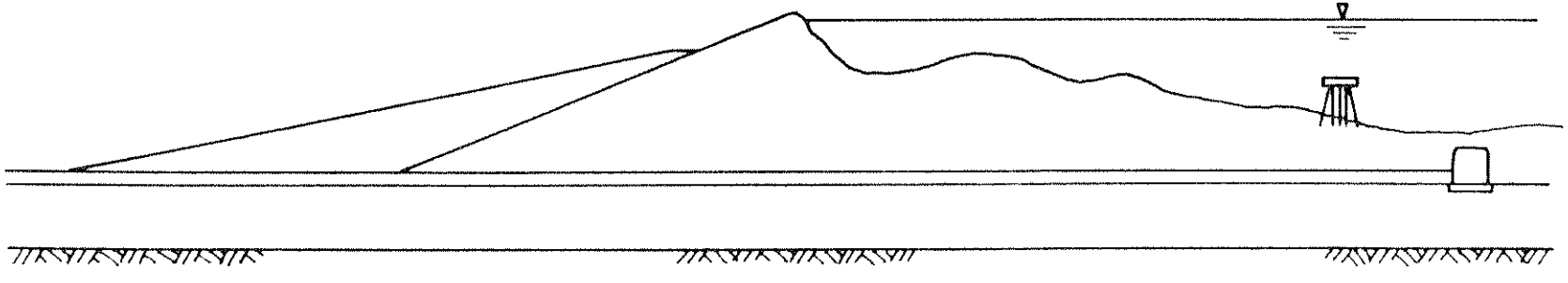

(b) After Earthquake

Fig. III-20 SCHEMATIC CROSS-SECTIONS NEAR CENTRAL OUTLET TOWER.

about 70 ft from its original position and dropped about 6 ft in elevation. A large quantity of material had apparently moved around the piles without causing any significant disturbance to them.

A photograph of this pile supported footing after the water level had been drawn down is shown on Fig. III-21. The pile cap was left standing some 30 ft above the surface of the slide debris into which the vertically-standing piles remained embedded only a few feet. It is clear that the major movements in the slide were located below the tips of these piles otherwise they must have been severely distorted during the slide. Whether some of the material surrounding the piles liquefied during the earthquake or was eroded as the water flowed down through the broken outlet tower following the earthquake will probably never be known. In either case the behavior of this pile supported foundation demonstrates the non-rotational form of the slide movement and indicates an upper limit of the position of the slide zone within the upstream part of the embankment.

Another close-up view of the slide debris from about the middle of the dam facing east, after the water level had been almost completely drawn down is shown on Fig. III-22. The surface characteristics of the slide show a series of steps indicating multiple shear zones within the fill. Although the overall movement was towards the left of the photograph many individual slide scarps slope down toward the right and, like the pile foundations shown on Fig. III-21, indicate that large blocks of material moved more or less intact a considerable distance out into the reservoir area. Thus the final topography of the slide debris had the same general form of blocks, grabens and wedges that characterized landslides during the 1964 Alaska earthquake, and which were shown to be a result of deep seated liquefaction (Seed and Wilson, 1967).

Finally after the water had been completely removed from the reservoir it was possible to inspect other portions of the slide near the toe of the debris. Sand boils such as those shown on Fig. III-23 were found in some of the depressions or grabens in the lower portions of the slide. A view of the extreme toe of the slide is shown on Fig. III-24. The lighter colored material on which the two men are standing is the toe of the main embankment soil. It is a fine silty sand which appears to have flowed out over the darker colored silts which had collected in the bottom of the reservoir during the sixty years of operation. The toe of the slide did not take the form of a pressure ridge which is typical of the more conventional type of landslide.

The field observations of the performance of the Lower Dam during the earthquake suggested that the slide was due to liquefaction of soil within the hydraulic fill portion of the embankment. Evidence of this was provided by:

(1) The seismoscope record from the crest of the dam indicated that the slide developed after the earthquake had continued for some time and not during one of the early seismic peaks.

(2) The topography of the landslide debris observed after the water level had been drawn down was typical of the topography of the Turnagain Heights landslide during the 1964 Alaska earthquake, and of other landslides which are believed to have developed as a result of liquefaction well below the surface during earthquakes. These peculiar topographic features include grabens, multiple shear surfaces many of which slope backwards into the debris, and blocks of material which moved more or less intact during the landslide.

FIG. III – 21 PILE–SUPPORTED FOOTING FOR BRIDGE TO CENTRAL OUTLET TOWER – LOWER SAN FERNANDO DAM

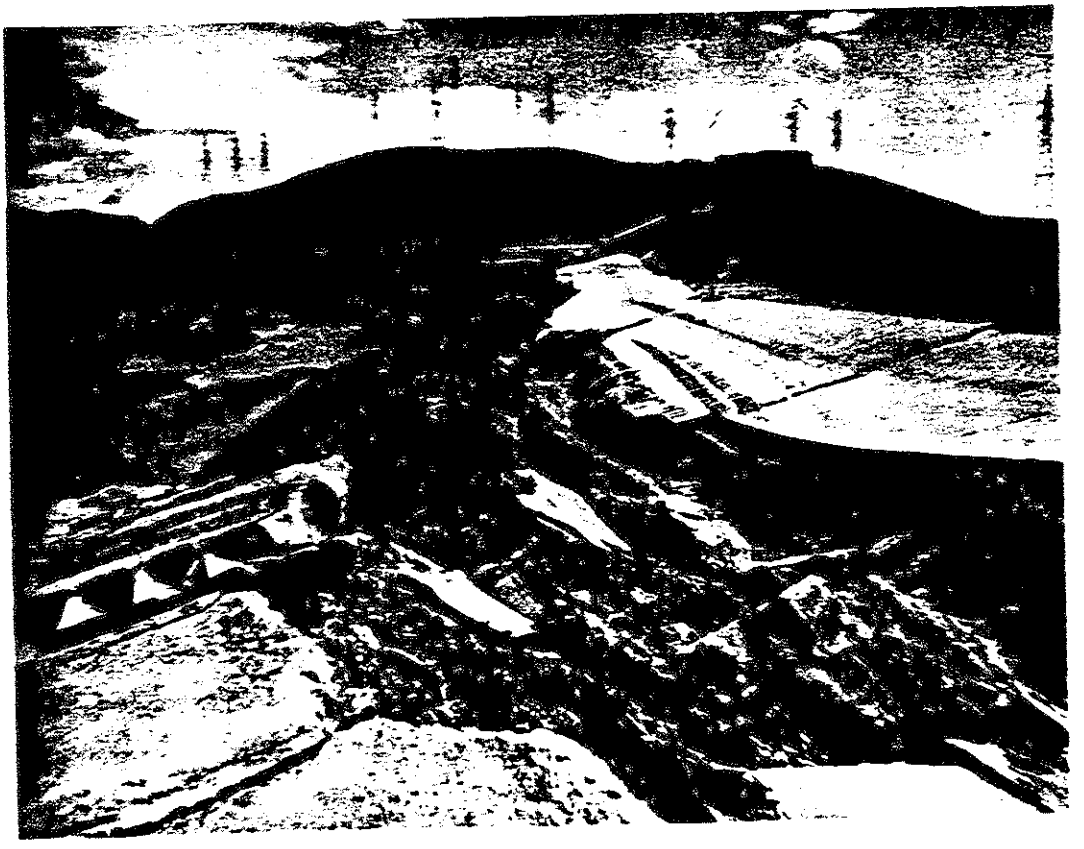

FIG. III – 22 SLIDE DEBRIS – LOWER SAN FERNANDO DAM

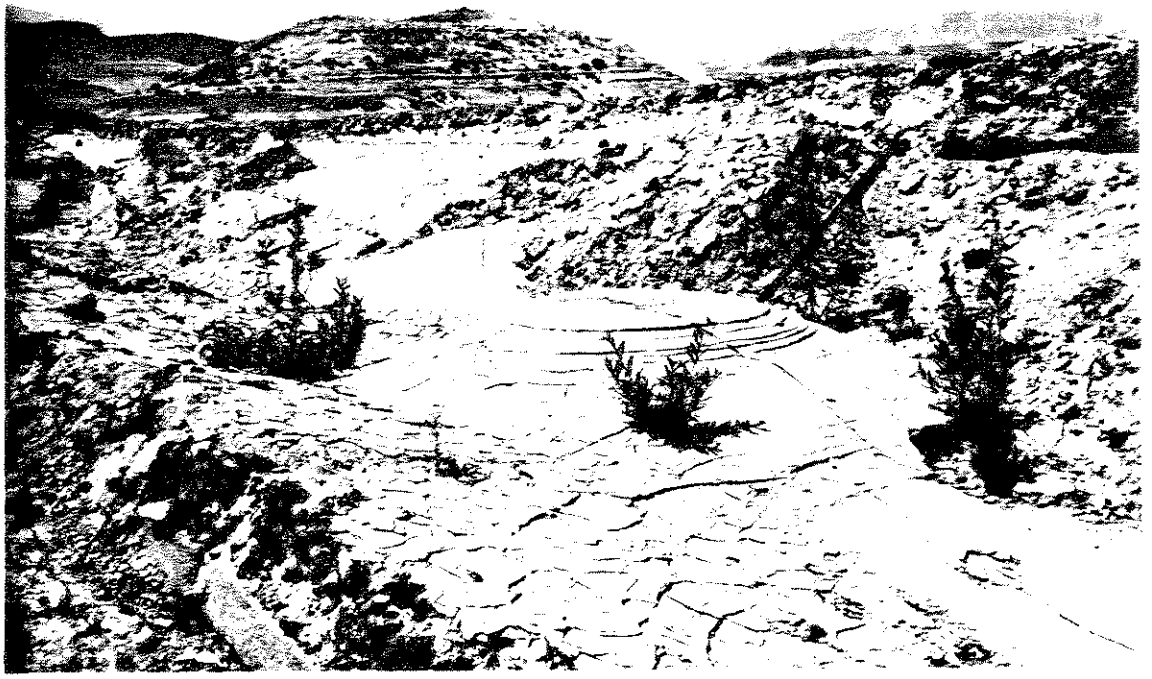

FIG. III–23 SAND BOILS IN THE DEPRESSION SCARPS NEAR THE TOE OF THE SLIDE DEBRIS, LOWER SAN FERNANDO DAM.

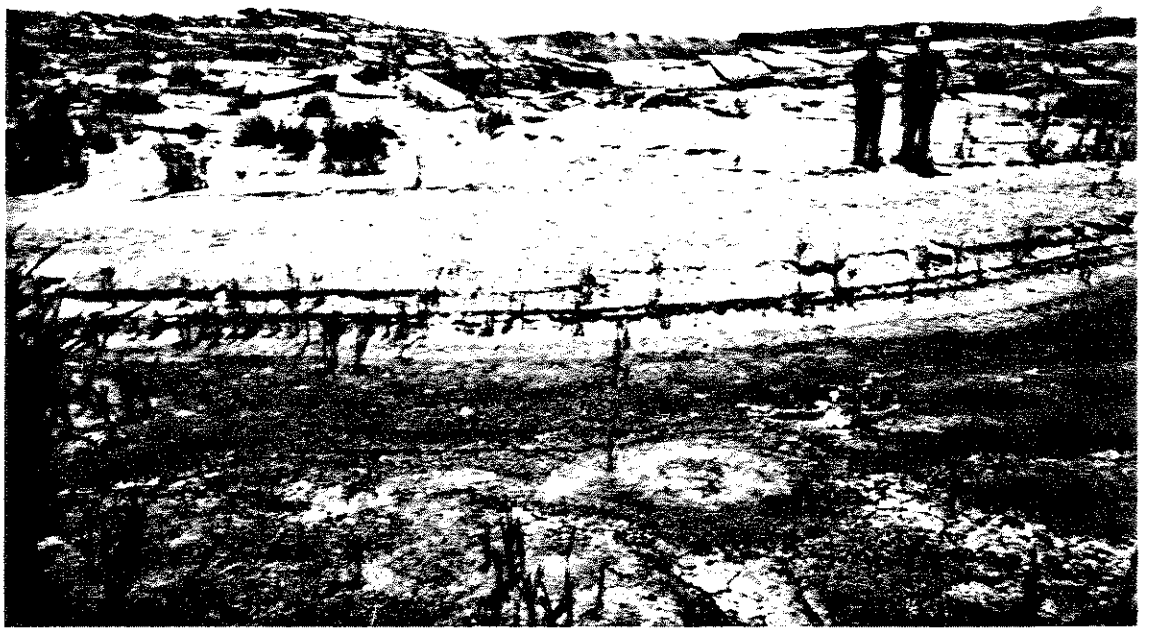

FIG. III–24 TOE OF THE SLIDE DEBRIS, LOWER SAN FERNANDO DAM.

(3) Large increases in water pressure in the observation wells within the embankment which later decreased with time.

(4) The presence of sand boils which developed in the graben area near the toe of the slide where the overburden was shallow.

(5) The nature of the toe of the slide which indicated that the material had simply flowed out over the existing reservoir sediments suggested that much of the material within the dam had been reduced to a fluid consistency.

It was surmised from these observations that probably a major zone of soil within the dam liquefied under the effect of the seismic loading during the later stages of the earthquake. This zone of liquefied soil was contained by an outer zone of stronger material which did not liquefy. With the strength of the internal material reduced to that of a viscous fluid mass the upper rolled fill and the outer shell began to move outwards and downwards. As the movements developed the stronger zones broke into smaller blocks, and near the toe where the overburden was sufficiently low, dykes of the liquefied sand found their way to the surface through cracks in the stronger material where they deposited themselves in the form of sand volcanos. The higher water pressures within the liquefied zone later began to subside as the soil reconsolidated under the new conditions.

Part IV - Field and Laboratory Investigations - Upper San Fernando Dam

Introduction

A program of field and laboratory investigations of the characteristics of the soils comprising the embankments of the Upper and Lower San Fernando Dams was initiated almost immediately after the earthquake. The scope and the timing of these investigations were governed to some extent by the physical conditions at the dams. For example, at the Upper Dam it was impractical to lower substantially the water in the reservoir or to operate a drilling rig from a barge floating within the reservoir; accordingly, the investigation was limited to the portion of the dam downstream from the shoreline on the upstream slope. At the Lower Dam the field investigation was delayed until the water level in the reservoir had subsided and the slide debris on the upstream slope had dried out sufficiently to permit access by the drilling equipment.

Field Investigations

The field investigations at the Upper Dam consisted of a series of trenches, borings, and seismic surveys. Four trenches were excavated across the top of the downstream berm and three of these trenches extended down the downstream slope to the toe of the dam. A total of 17 drill holes were made along three sections of the dam extending from the upstream shoreline to the downstream toe. Each of these drill holes extended through the hydraulic fill and alluvium into the bedrock foundation. Seismic surveys were conducted between selected adjacent drill holes and at selected locations below the dam to determine the seismic wave velocities within the fill, the alluvium and the bedrock materials.

Trenches

A plan view of the Upper Dam is presented in Fig. IV-1 which shows the locations of three of the four trenches and the drill holes. These trenches and drill holes are located along three transverse sections, A, B, and C shown on Figs. IV-2, IV-3 and IV-4 respectively.

A fourth trench somewhat shorter than the other three was excavated several months later between sections B and C for the purpose of obtaining some special samples and checking the characteristics of the fill. A photograph showing the eastern wall of this fourth trench is shown in Fig. IV-5. This view was taken from the shoulder of the berm looking in an upstream direction toward the man standing approximately at the toe of the slope leading up to the crest of the dam.

The walls of this trench were typical of the walls of the other three trenches previously excavated. The hydraulic fill exposed in the walls of the trench consisted of alternating layers of fairly clean sands and silty to clayey sands with occasional layers of clay. The layering was most pronounced near the outer parts of the embankment where the soil appeared to be generally coarser than that near the central portion of the dam, where the layering became almost indistinct and the soil was a fairly homogeneous fine sandy silt with occasional areas of more clayey material.

A number of field density tests were taken in the bottom of these trenches and additional soil from around the field density holes was taken into the laboratory for further testing. The results of these and other tests will be described in a later section of this report. However the grain size distributions from this series of samples taken at various locations along the base of one of the trenches provide a good indication of the progressive change in soil characteristics. These data are shown

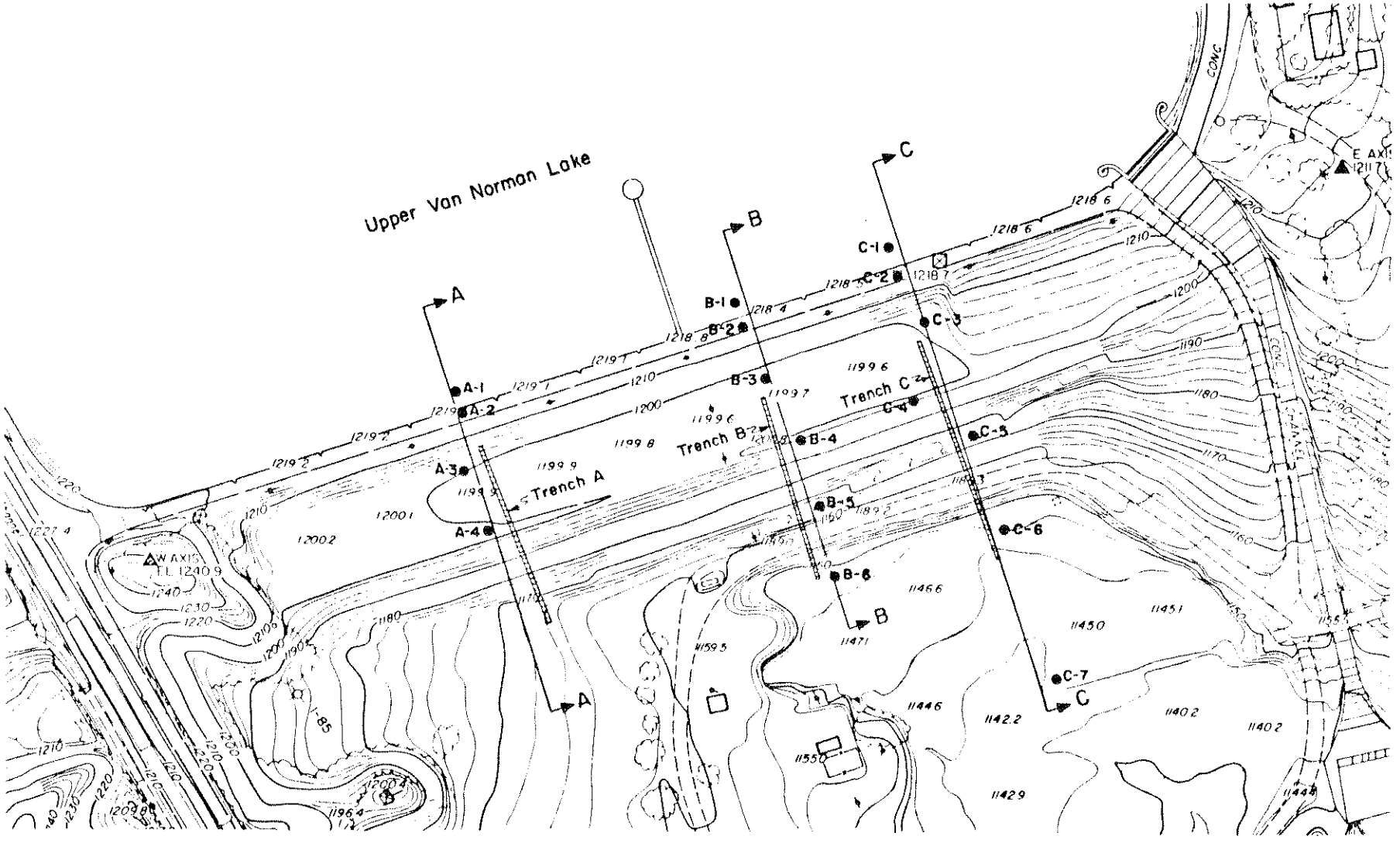

Fig. IV–1 PLAN OF UPPER SAN FERNANDO DAM.

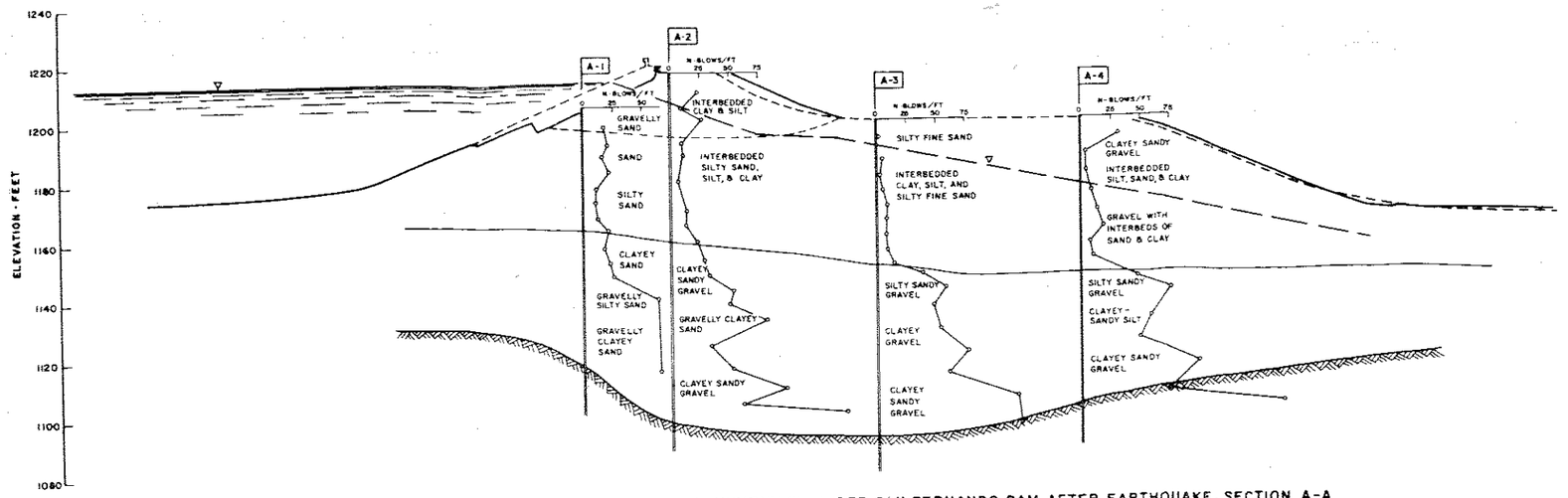

Fig IV-2 CROSS-SECTION THROUGH EMBANKMENT OF UPPER SAN FERNANDO DAM AFTER EARTHQUAKE, SECTION A-A

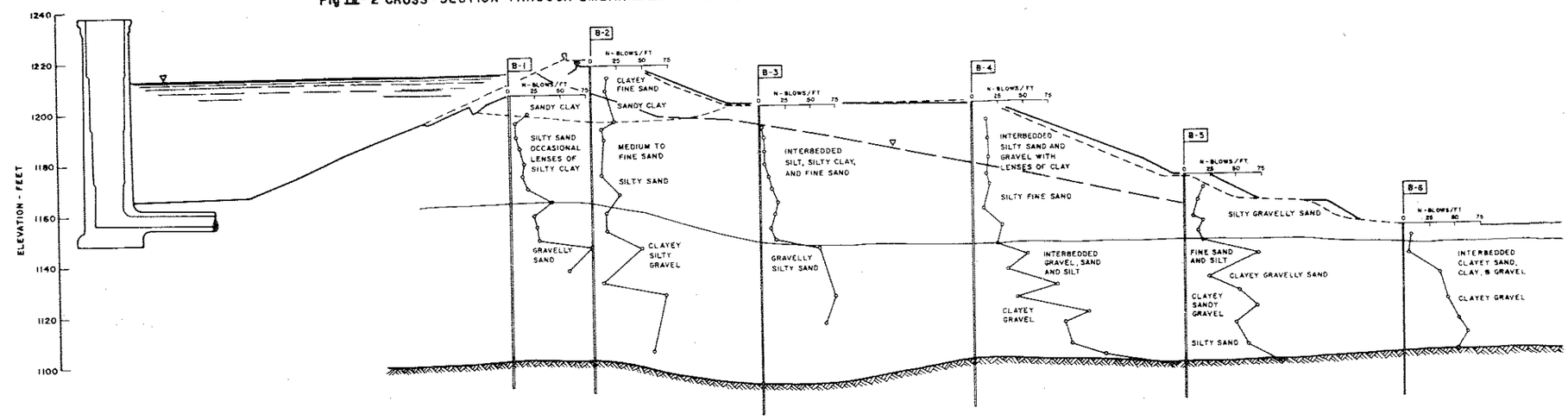

Fig IV-3 CROSS-SECTION THROUGH EMBANKMENT OF UPPER SAN FERNANDO DAM AFTER EARTHQUAKE, SECTION B-B

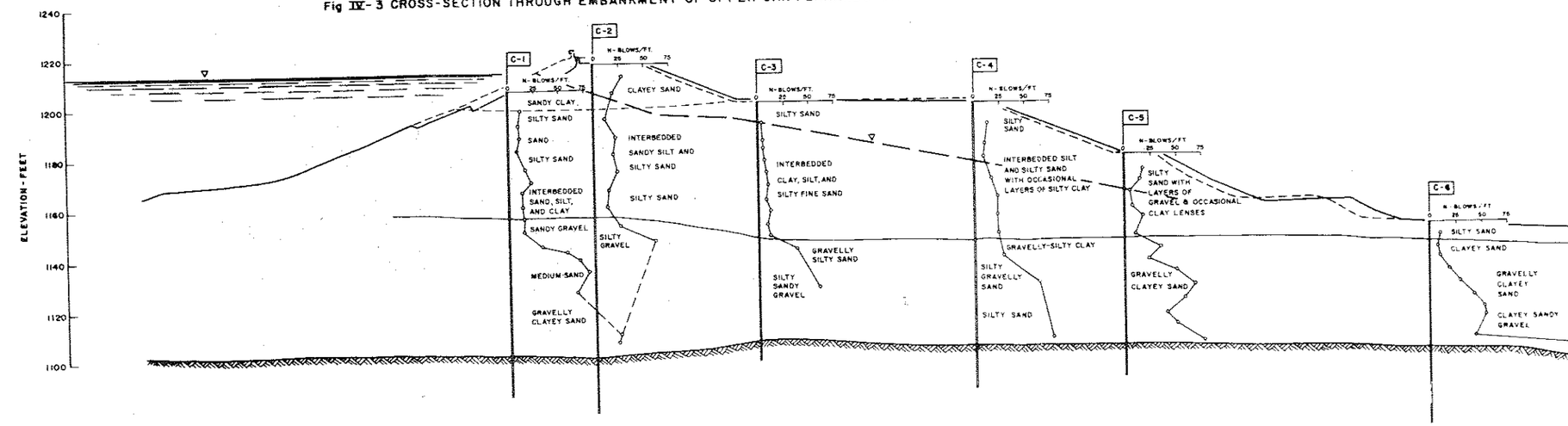

Fig IV-4 CROSS-SECTION THROUGH EMBANKMENT OF UPPER SAN FERNANDO DAM AFTER EARTHQUAKE, SECTION C-C

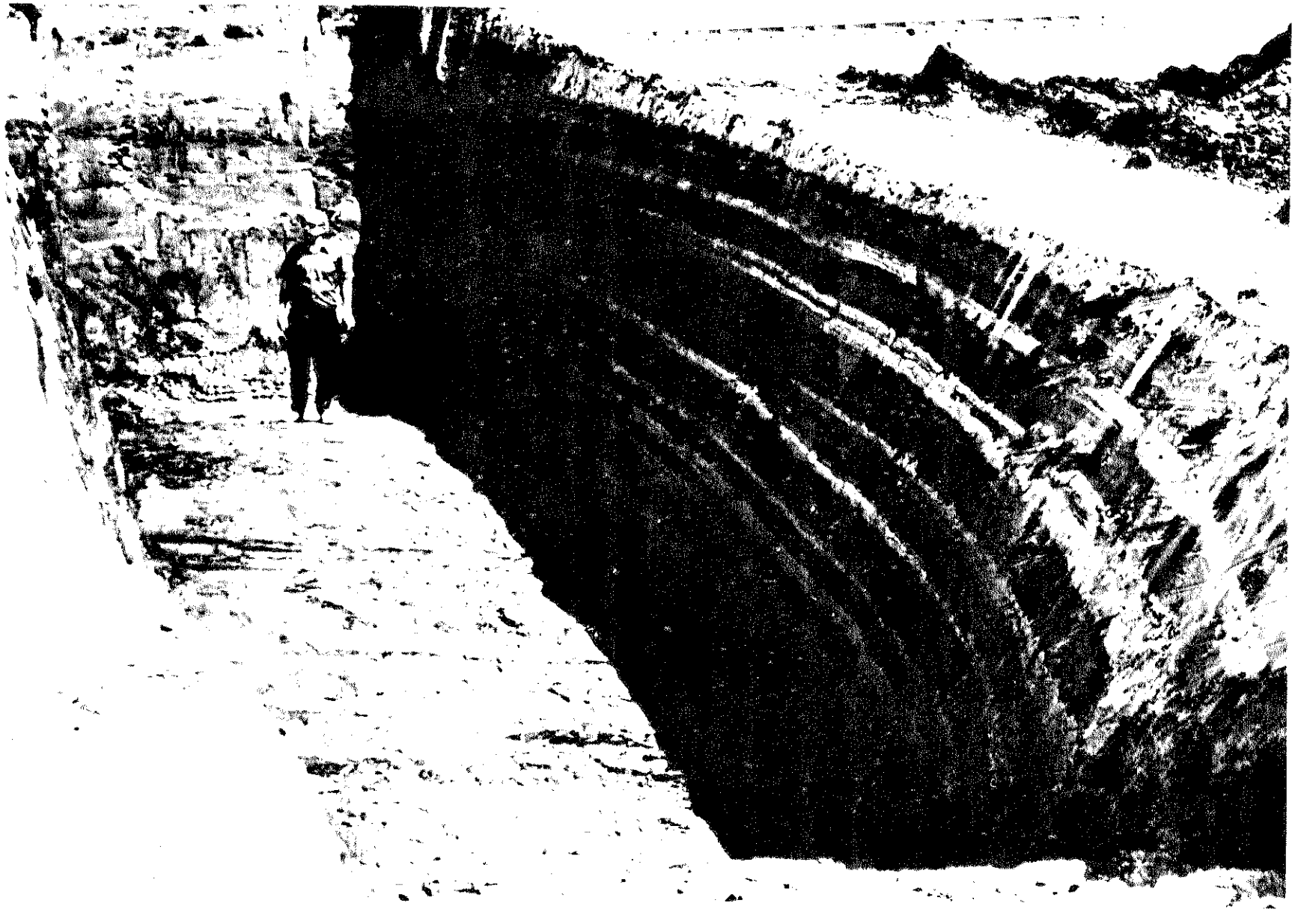

FIG. IV–5 SOIL STRATIFICATION ALONG WALL OF INSPECTION TRENCH – UPPER SAN FERNANDO DAM.

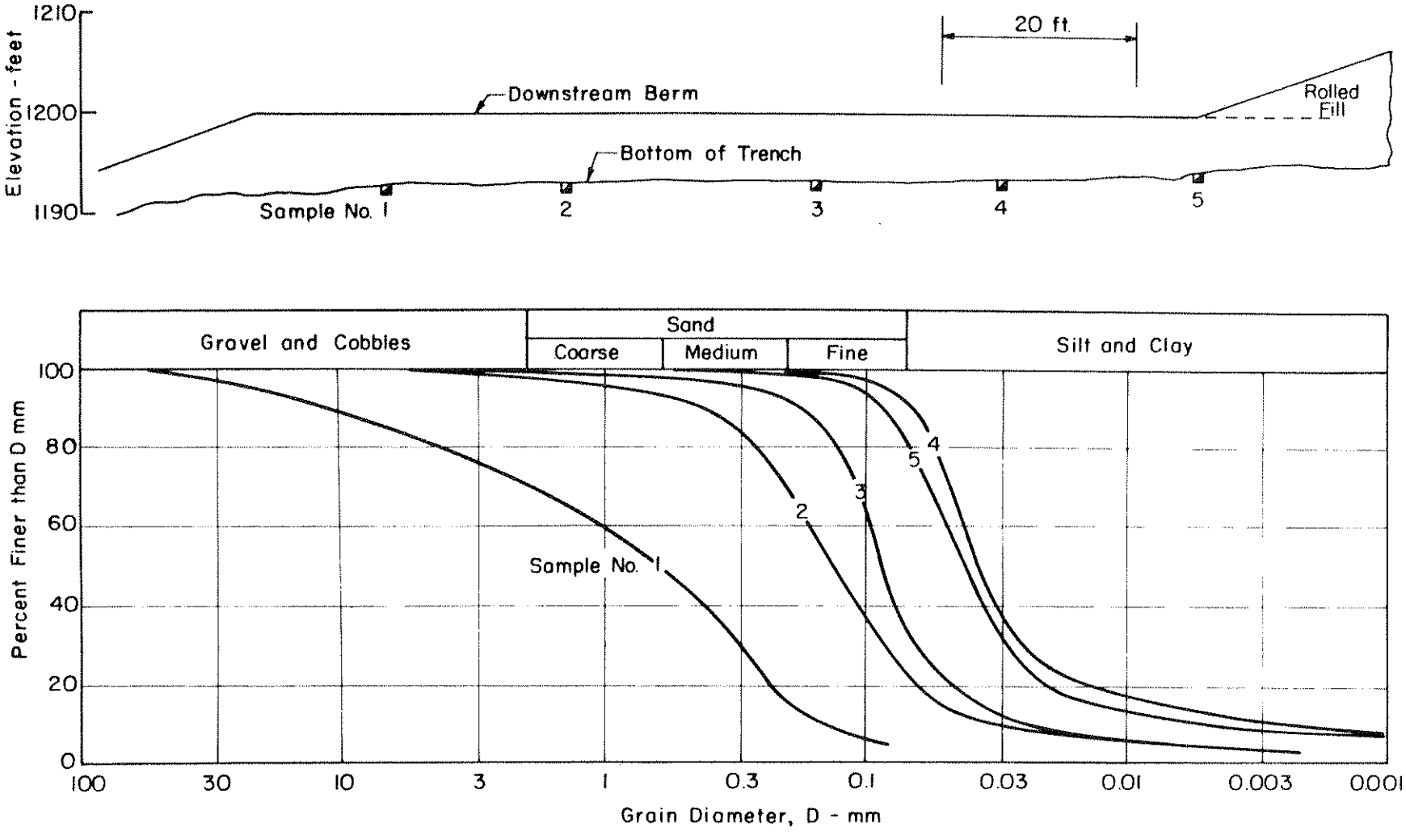

Fig. IV–6 DISTRIBUTION OF GRAIN SIZES IN HYDRAULIC FILL FROM OUTER SHELL TOWARDS CENTER OF EMBANKMENT – UPPER SAN FERNANDO DAM.

on Fig. IV-6 for the trench at section A. The locations of the field density samples are shown in the upper portion of the figure and the grain size distribution curves for the samples are shown in the lower portion of the figure. It may be seen that sample No. 1 near the downstream shoulder of the berm is a coarse gravelly sand. Proceeding in an upstream direction towards the center of the dam the samples become progressively finer until samples Nos. 4 and 5 near the central part of the embankment are predominantly silt and clay.

Drill Holes

Cross sections through the Upper Dam at Sections A, B, and C are shown on Fig. IV-2, IV-3, and IV-4 respectively. The locations of each of the 16 drill holes are shown on these three sections, along with an abbreviated drill log.

Each of the drill holes was 6 inches in diameter and made with drilling mud without the use of any casing. Sampling was almost continuous and consisted of a standard penetration test on a split spoon sampler followed by a 3 inch diameter thin wall Shelby tube sample every 5 ft. An experienced geologist was with each drill rig at all times. He opened every split spoon standard penetration sample in the field and examined the ends of every Shelby tube sample as it was extracted from the ground. The abbreviated drill logs shown on the cross sections were obtained primarly from these field soil classifications.

In addition to the abbreviated soil classifications, the results of standard penetration tests are also shown on the cross sections. It may be seen that the penetration resistance (N-values) were very low in the silt and clay core of the central portion of the hydraulic fill, whereas the blow counts in the outer sands and gravels of the shell were somewhat

higher. In most of the holes there was a significant increase in penetrative resistance in the alluvium as compared to the hydraulic fill. Subsequent examination of the Shelby tube samples taken within the alluvium indicated a very heterogeneous soil ranging from layers or pockets of clay to layers or pockets of sands and gravels. This heterogeneity in the alluvium is reflected by the rather erratic variations in blow counts in most of the drill holes through the alluvium as compared to the more consistent values within the hydraulic fill.

On the basis of the information obtained from the drilling and sampling, the boundaries between the four major zones on each section (bedrock, alluvium, hydraulic fill, and the small cap of rolled fill at the crest of the dam) were established as shown in the sections.

Seismic Surveys

In order to determine the dynamic shear moduli of the soils in the Upper San Fernando Dam, field seismic surveys were made to determine the velocities of compression and shear wave propagation in the embankment and foundation soils. These investigations were made by cross-hole measurements at various elevations. Measured values of shear wave velocity, v_s, for the hydraulic fill and base rock formation are presented in the following table:

Formation	Depth - ft	v_s - fps
Hydraulic Fill	40	≈600
Rock	100	≈3300

Shear moduli can readily be determined from the shear wave velocities using the relationship

$$v_s = \sqrt{\frac{G \cdot g}{\gamma}}$$

where G = shear modulus

g = acceleration of gravity

γ = unit weight of formation

For analysis purposes, the shear modulus of granular soils may be expressed by the relationship

$$G = 1000 \cdot K_2 \cdot (\sigma_m')^{1/2} \text{ psf}$$

where K_2 is a soil constant which depends on the strain amplitude of the shear deformations and σ_m' is the mean effective pressure acting on the soil (Seed and Idriss, 1970).

For the measured values of shear wave velocity shown above, the corresponding value of K_2 for the hydraulic fill at the small strain levels of the wave propagation tests is about 30. In the alluvium the velocities of wave propagation were considerably more variable. In the deeper alluvium values of shear wave velocity ranged from about 1480 to 1850 fps but in one traverse, the compression wave velocity was only about 1200 fps, indicating a shear wave velocity of only about 400 fps. Since the borings indicated a marked stiffening of the alluvium with depth it was considered that the higher velocities would be applicable to the lower zone of alluvium but that substantially lower values would be more appropriate for the upper alluvium. On this basis values of K_2 for the alluvium were estimated to be as follows:

Upper foundation alluvium $K_2 \simeq 40$

Lower foundation alluvium $K_2 \simeq 110$

Laboratory Investigations

The laboratory testing of the samples obtained during the field investigations was divided among three cooperating laboratories: The Department of Water Resources Laboratory at Sacramento (DWR), The City of Los Angeles Department of Water and Power Laboratory (DWP), and The Soil Mechanics Laboratory, at the University of California, Los Angeles (UCLA). Most of the static strength testing and some of the compaction tests were done at the DWR lab in Sacramento. The field density samples and corresponding compaction and grain size tests were processed at the DWP lab in Los Angeles. Most of the cyclic load tests were performed at UCLA.

On inspection of the soil exposed in the test trenches and after examining several of the Shelby tube samples, it appeared that the hydraulic fill soil could be divided into three major categories: coarse sand, fine sand or silty sand, and clay. Since previous studies have shown that clay soils are not susceptible to liquefaction under cyclic loading, samples of clay were not extensively tested and the test programs were conducted primarily on the fine and coarse sands. Since it was felt that the fine sand, and the coarse sand materials might have significantly different strength properties, samples of these two materials were tested separately. Also because the field investigation had indicated that the alluvium was considerably denser and therefore stronger than the hydraulic fill, the test programs for the alluvium were less extensive than those for the hydraulic fill materials.

Grain Size Distribution

The range of grain size curves for the coarse sand and for the fine sand of the hydraulic fill in the Upper Dam are shown on Fig. IV-7.

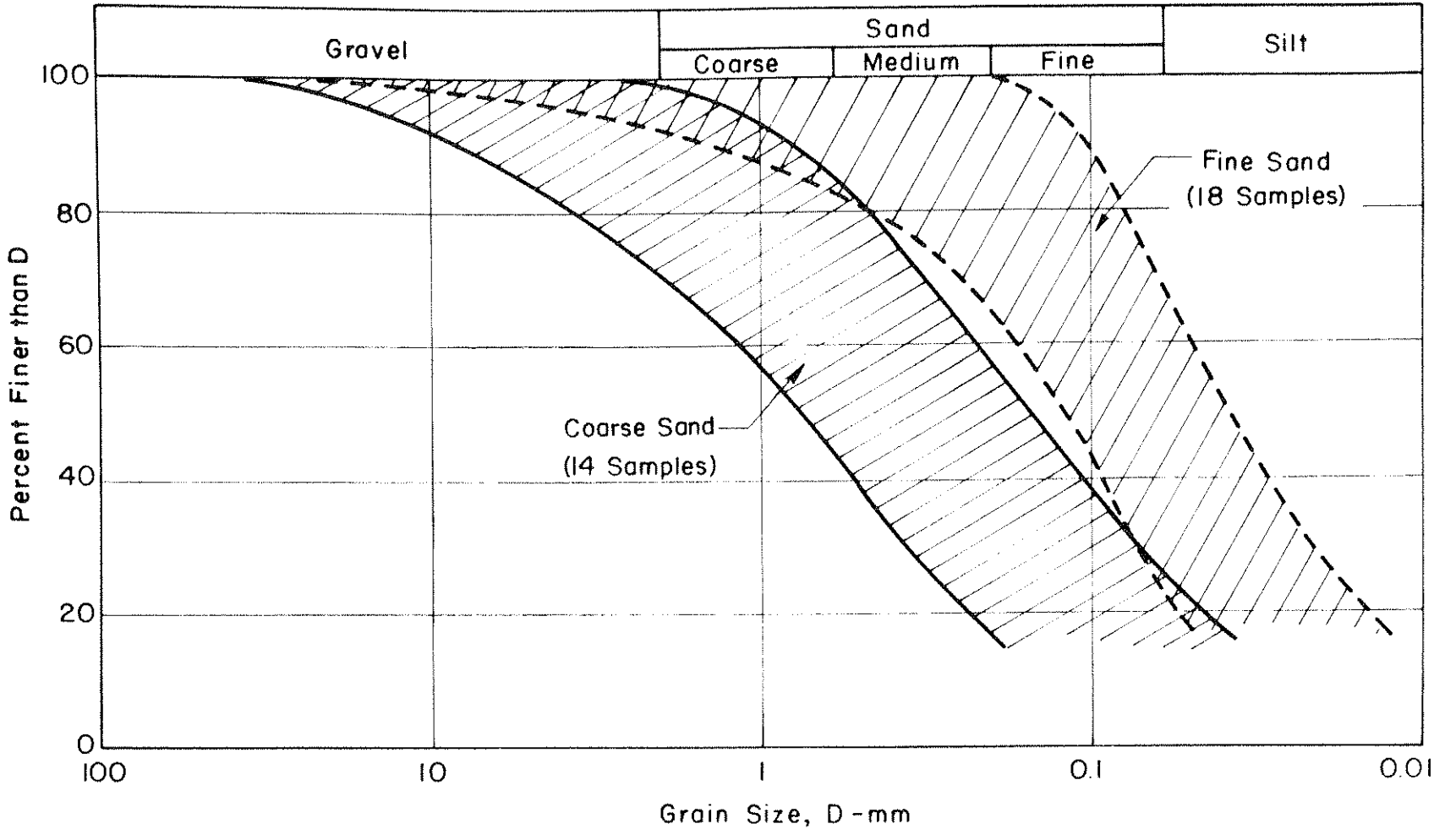

Fig. IV–7 RANGES OF GRAIN SIZE DISTRIBUTION CURVES FOR HYDRAULIC FILL – UPPER SAN FERNANDO DAM.

Ranges of the grain size curves for the coarse and fine alluvium are shown on Fig. IV-8. Comparison of these data indicate that the alluvium is somewhat coarser than the hydraulic fill in both the coarse sand and the fine sand classifications. Also, the alluvium tends to be a little better graded than the hydraulic fill.

Field Density and Relative Density Data

Field density and relative density data were obtained from three sources: densities of the undisturbed Shelby tube samples, field density tests made in the bottom of the inspection trenches along the downstream berm, and correlations with standard penetration test results obtained during the drilling operations.

The undisturbed samples were obtained by cutting the Shelby tubes into 7 inch lengths and extruding an undisturbed sample of soil. Each of these samples was weighed and measured to determine the dry density. In addition grain size determinations were made on a large number of these individual test specimens.

A summary of all the field density data from the hydraulic fill and alluvium at the Upper Dam is presented on Fig. IV-9 in the form of frequency distribution diagrams. Data are presented for alluvium, coarse hydraulic fill and fine hydraulic fill. These data also indicate that the alluvium was somewhat denser than the hydraulic fill.

As previously noted there was a fairly wide range of grain sizes present ranging from very fine silty sands up to coarse sands and gravel. Because soils of different grain size characteristics would have different absolute and relative densities, the compilation summary in Fig. IV-9 presents a somewhat oversimplified view of the density distribution within the dam and the foundation soil. This is illustrated by the field density

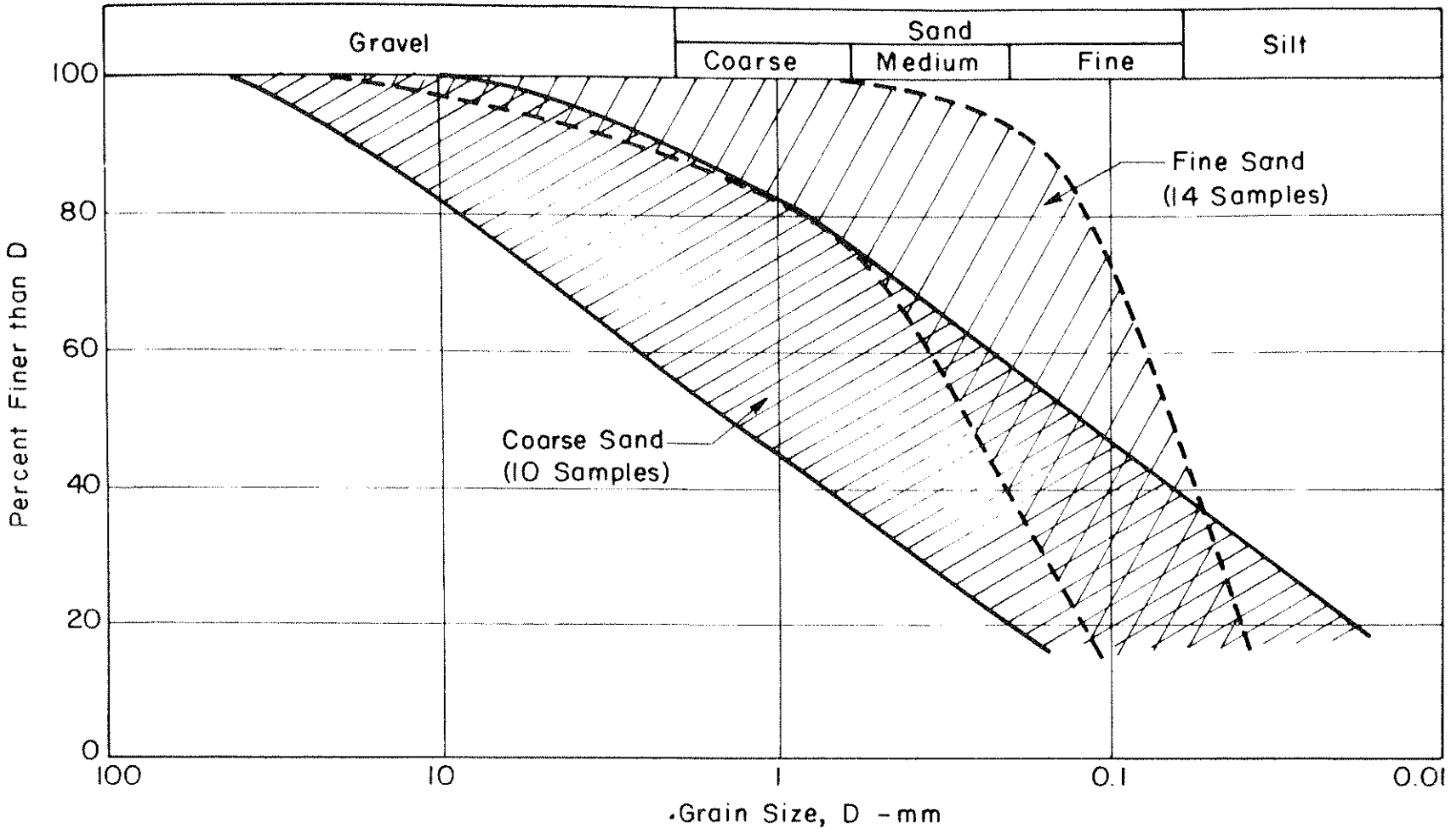

Fig. IV-8 RANGES OF GRAIN SIZE DISTRIBUTION CURVES FOR ALLUVIUM - UPPER SAN FERNANDO DAM.

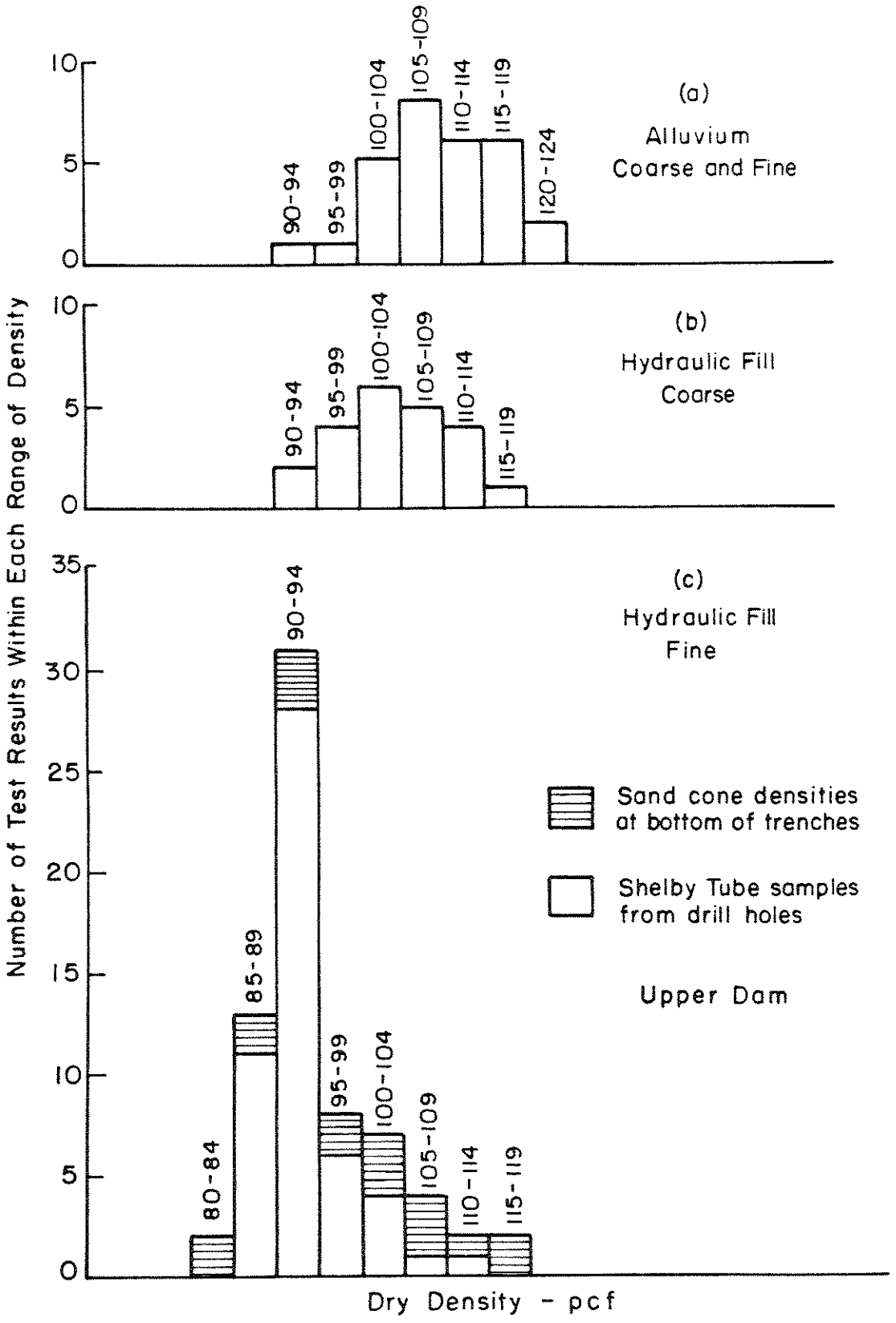

Fig. IV-9 SUMMARY OF FIELD DENSITY TESTS - UPPER SAN FERNANDO DAM.

data taken from the bottom of the inspection trenches and presented on Fig. IV-10. The measured field densities shown by solid dots are plotted against the mean grain size of the soil in the test specimen. With some scatter there is a fairly well defined trend of decreasing field density with decreasing grain size.

In addition to the field density tests, sufficient soil was brought to the laboratory to perform compaction and minimum density tests on each of the samples. The compaction test was performed using the modified AASHO (1961) procedure.* The minimum density test was performed by an ASTM procedure which consisted of pouring the oven dry soil through a funnel into a mold. The minimum and maximum density values obtained by these procedures are also shown on Fig. IV-10, where they may readily be compared with the field density of the same sample.

As with the field densities there is some scatter in the limiting density data but there is a general trend of decreasing density with decreasing grain size. Visual comparison of the field density with the two limiting densities of any particular sample indicates a substantial range in relative density data. While this may be a true situation it should also be noted that a small error in any one of the three densities determined for any sample could lead to a rather large apparent error in the corresponding relative density. Accordingly, it was felt to be more appropriate to approach the question of relative density of the soil within the dam and its foundation on the basis of average general trends rather than on an individual test by test basis. This approach is discussed more fully in the following paragraphs.

---

*1/30 cu ft mold, 10 lb hammer, 18 inch drop, 5 layers, 25 blows per layer.

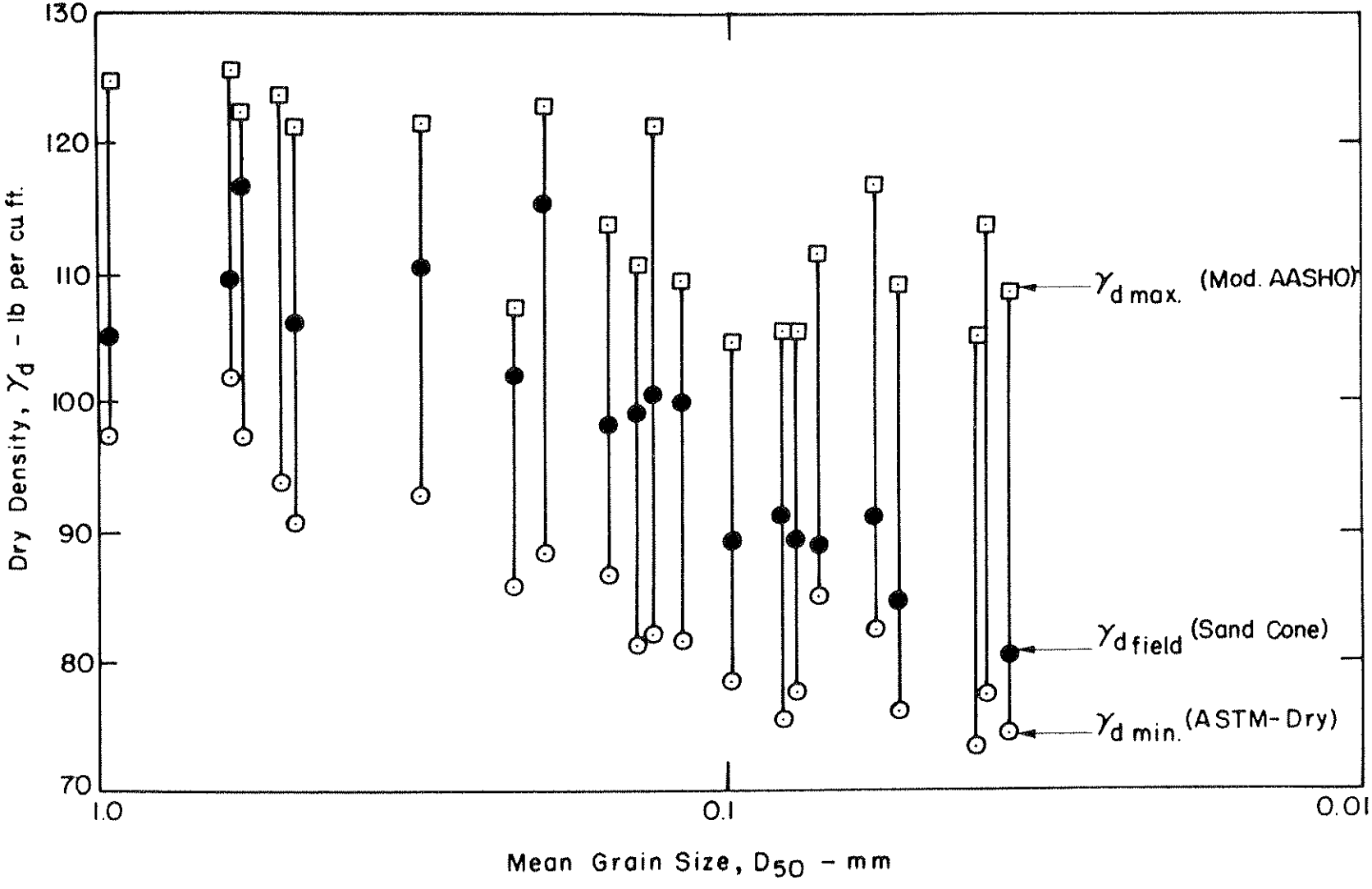

Fig. IV-10 MAXIMUM, MINIMUM AND FIELD DENSITIES FOR SAMPLES OF HYDRAULIC FILL FROM TRENCH SECTIONS – UPPER SAN FERNANDO DAM.

All of the field density data for the hydraulic fill are plotted on Fig. IV-11. The data obtained from undisturbed Shelby tube samples are shown by solid points whereas data obtained from the field density sand cone tests in the bottom of the trenches are shown by open points. There appears to be no major difference in the data obtained by either of these two methods. In spite of some scatter there appears to be a fairly well defined trend of decreasing field density with decreasing grain size. The best fit line drawn through this data on Fig. IV-11 was used in subsequent calculations of the average relative density of the soil in the hydraulic fill zone of the dam.

Definition of relative density requires not only a determination of the field density but determination of both the maximum and minimum limiting densities as well. Ideally these limiting densities are readily determined by standard test methods. However, from a practical point of view there are often many problems and many inconsistencies in such determinations.

Most of the soils encountered in the dam, and in the foundation were fine to coarse silty sands and it was not immediately clear which of the many possible test methods would be most appropriate for determining the maximum and minimum densities. As a result several different test methods were used.

Maximum Density Tests

Maximum density values were performed using three procedures: impact compaction by the modified AASHO (1961) test procedure, vibratory compaction of very wet soil, and vibratory compaction of oven dry soil. Except for the field density samples taken from the trenches, there was not sufficient soil from any single Shelby tube test specimen to perform a complete

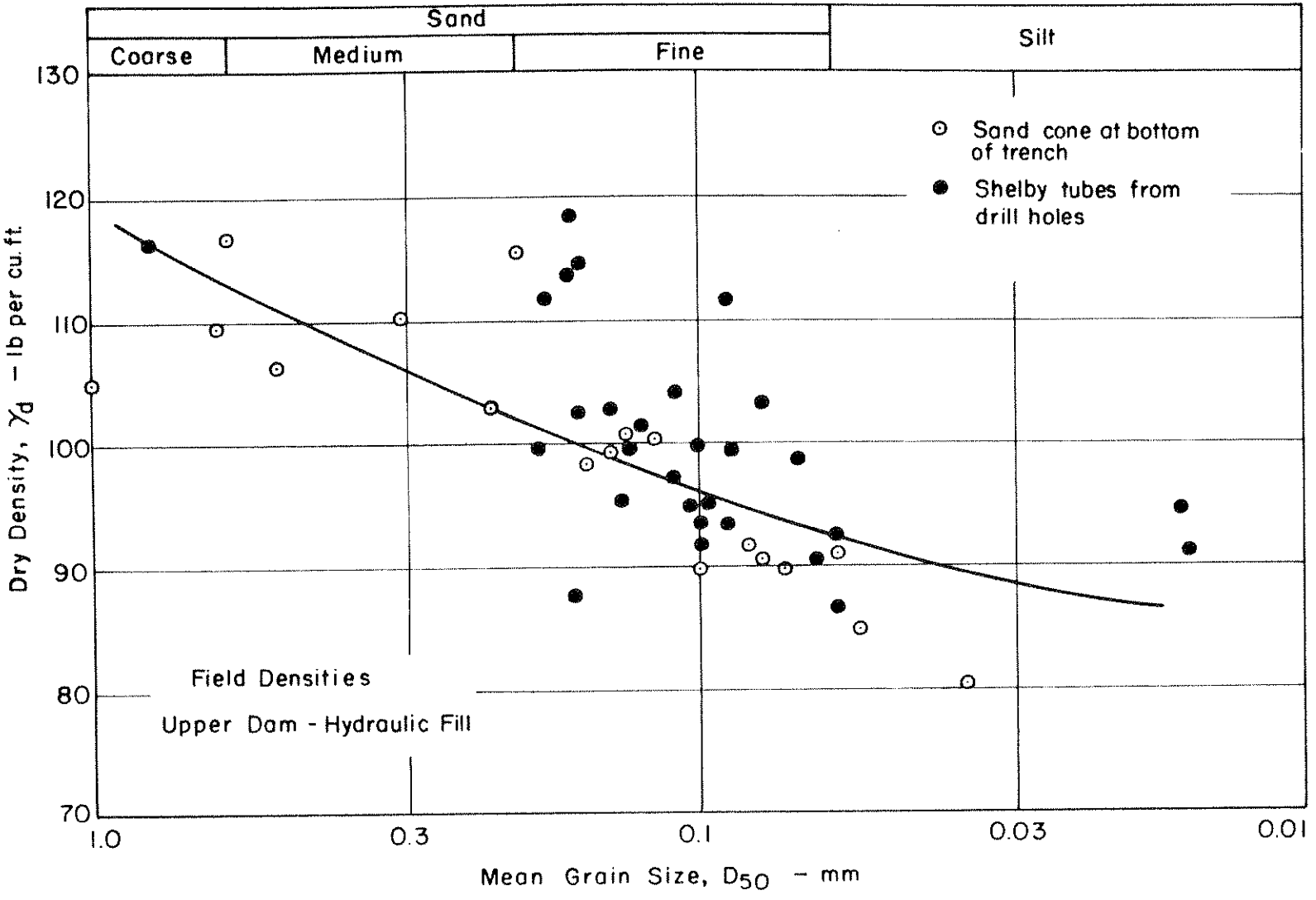

Fig. IV–11 FIELD DENSITIES FOR SAMPLES OF HYDRAULIC FILL – UPPER SAN FERNANDO DAM.

maximum density test by any one of the three procedures. Therefore as a compromise, composite samples were formed from several of the test specimens to make enough soil to perform a maximum density test. The results of these three types of maximum density tests on seven different composite samples of hydraulic fill are presented on Fig. IV-12.

Since similar studies were made for soil from the Lower San Fernando Dam and because the soils from both dams were very similar and showed the same general trends, the data are plotted together in Fig. IV-12. In addition, because compaction tests were performed at three different laboratories, it was decided to perform some check tests by having each laboratory compact the same sample of soil to see if comparable results would be obtained. These correlation data are also presented on Fig. IV-12.

Examination of the maximum density data for the seven composite samples, leads to the following conclusions.

1. For the modified AASHO (1961) test there was fair to good agreement between the data obtained from the three different participating laboratories.
2. There was a fairly large difference in maximum density of any sample obtained by vibration of a wet sample as compared to vibration of a dry sample. For the fine samples the highest densities were obtained by vibrating the dry soil whereas for the coarse samples the highest density was obtained by vibrating the soil in a wet condition.
3. The maximum vibrated density appeared to be about 5 to 6 lb/ft^3 greater than the maximum density obtained by the modified AASHO (1961) test procedure.

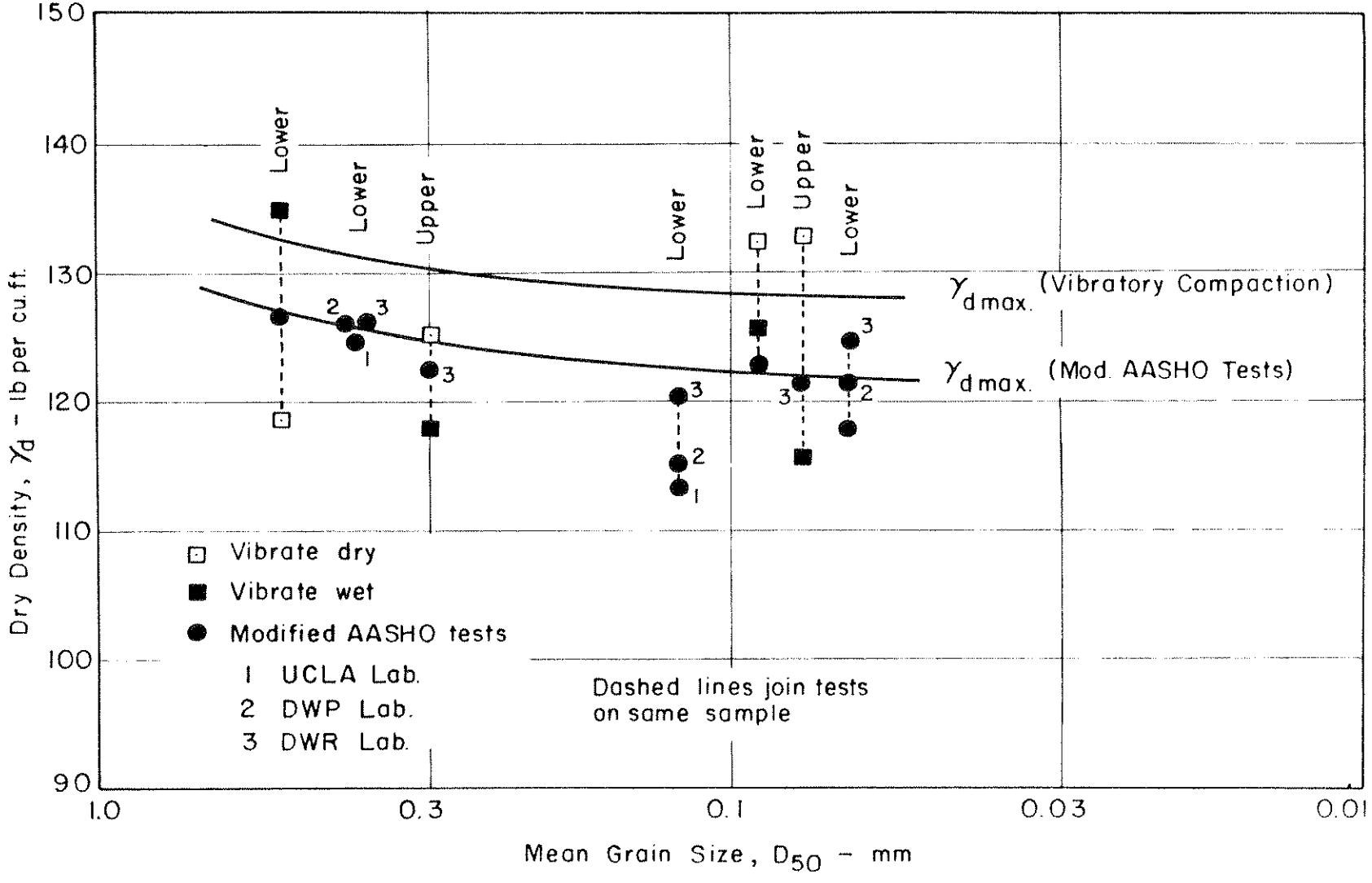

Fig. IV-12 RESULTS OF MAXIMUM DENSITY TESTS ON COMPOSITE SAMPLES OF HYDRAULIC FILL - UPPER AND LOWER SAN FERNANDO DAMS.

A similar series of compaction tests were performed on two samples of alluvium. These data will be presented later, but they showed the same general trends as discussed above for the hydraulic fill samples. It may also be noted that similar results have been reported by Felt (1959).

It is important to note that the compaction test data presented on Fig. IV-12 were all obtained from composite samples: that is, samples made up of a mixture of soil from several different specimens. Because of this it seems probable that the values of maximum density shown on Fig. IV-12 may be somewhat greater than values of maximum density obtained from individual samples compacted by the same procedures. This trend may be demonstrated by comparing the compaction test maximum density at any value of mean grain size for the composite samples on Fig. IV-12 with the corresponding maximum densities obtained on individual samples shown on Fig. IV-10. For this reason the maximum density line shown in Fig. IV-12 was not used as a measure of the maximum density of the soil in the field. Instead the maximum density of the soil in the field was taken as about 5 to 6 lb/ft^3 greater than the values of maximum density obtained by modified AASHO (1961) compaction tests on individual field samples. These data are shown on Fig. IV-13 for samples of hydraulic fill. Each of the data points represents the maximum density obtained in a modified AASHO (1961) compaction test on an individual sample taken from the field. A best fit line was drawn through these somewhat scattered data and then a dashed line drawn at 5 to 6 lb/ft^3 higher to indicate the estimated maximum densities of the different soils.

Because a number of agencies still use the standard AASHO* compaction procedure for regulating the compaction of soil in the field, it was

---

*1/30 cu ft mold, 5.5 pound hammer, 12 inch drop, three layers, 25 blows per layer.

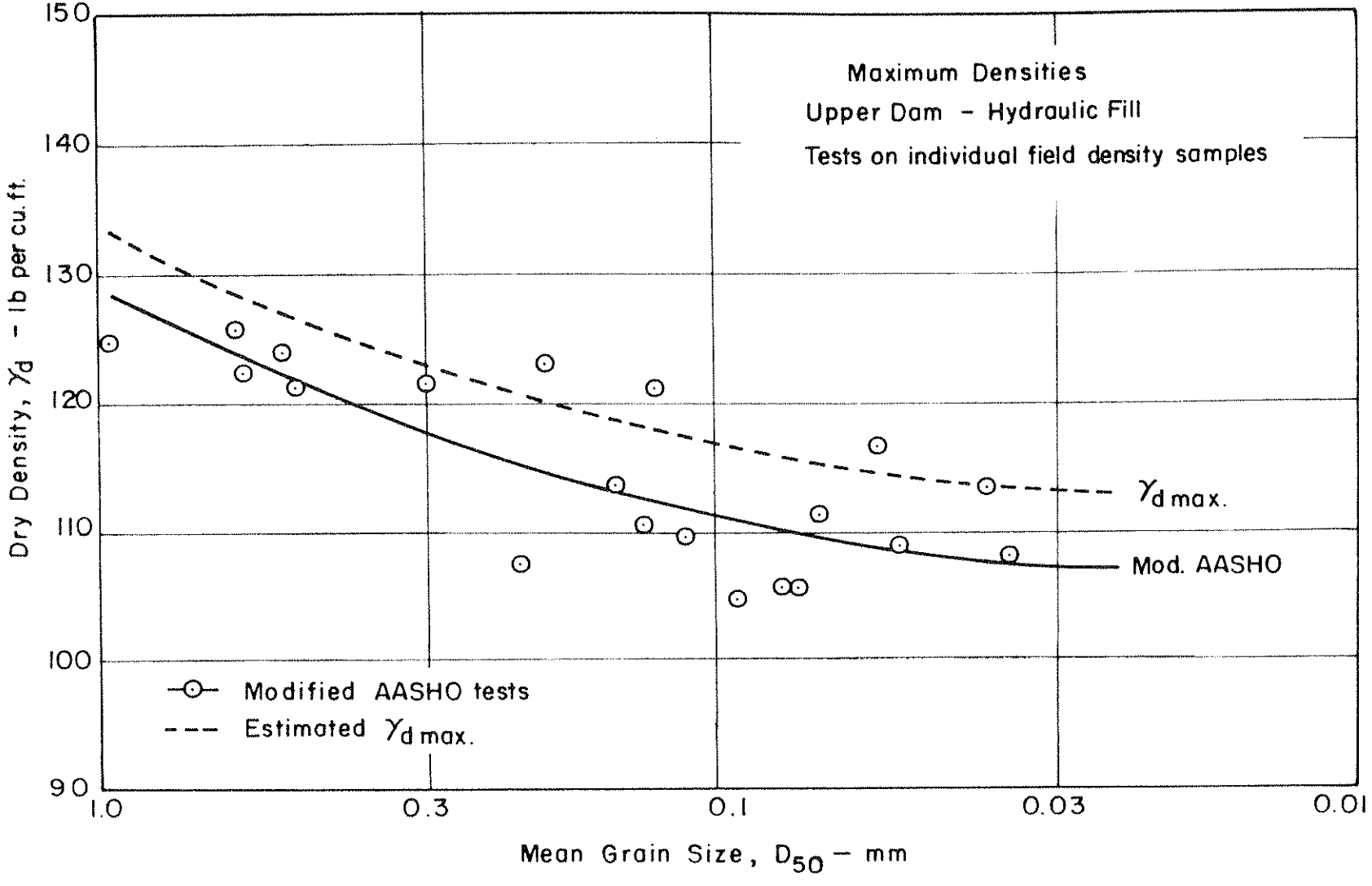

Fig. IV-13 RESULTS OF MAXIMUM DENSITY TESTS ON SAMPLES OF HYDRAULIC FILL - UPPER SAN FERNANDO DAM.

decided to perform standard AASHO tests on many of the field samples to provide data for comparison purposes. The results of these tests are summarized on Fig. IV-14 for samples of hydraulic fill. The open data points refer to tests performed on individual samples taken from the dam, whereas the two solid points refer to tests on composite samples. As suggested previously the maximum densities for the composite samples are somewhat higher than those for individual field samples. A best fit line through the individual field sample data is shown on the figure.

Minimum Density

Four different types of minimum density tests were performed on two different composite samples of the hydraulic fill from the Upper Dam. The results of these four tests are shown by the solid points on Fig. IV-15. Test method No. 1 was the ASTM standard method for obtaining the minimum density of oven dry soil (ASTM designation D2049-69). The method consists of pouring oven dry soil through a standard funnel into a steel mold. Test method No. 2 was similar to the ASTM method but used a funnel with a smaller opening. As indicated by the data on Fig. IV-15 this method led to a lower minimum density in both cases. Test method No. 3 was similar to that developed by Kolbuzewski (1948). Approximately 300 c.c. of oven dried soil were placed in a 1,000 c.c. graduate flask. The flask was then very slowly turned end for end and rotated to thoroughly stir the soil without vibration into a loose state. The data obtained by this method were similar to those obtained by method No. 2.

These three methods all used oven-dried soil, whereas the soil placed in the field was in a saturated state. Method No. 4 was developed in an attempt to simulate this saturated condition. Four to five 100-gram samples of soil were thoroughly mixed separately with water. A 1,000 c.c.

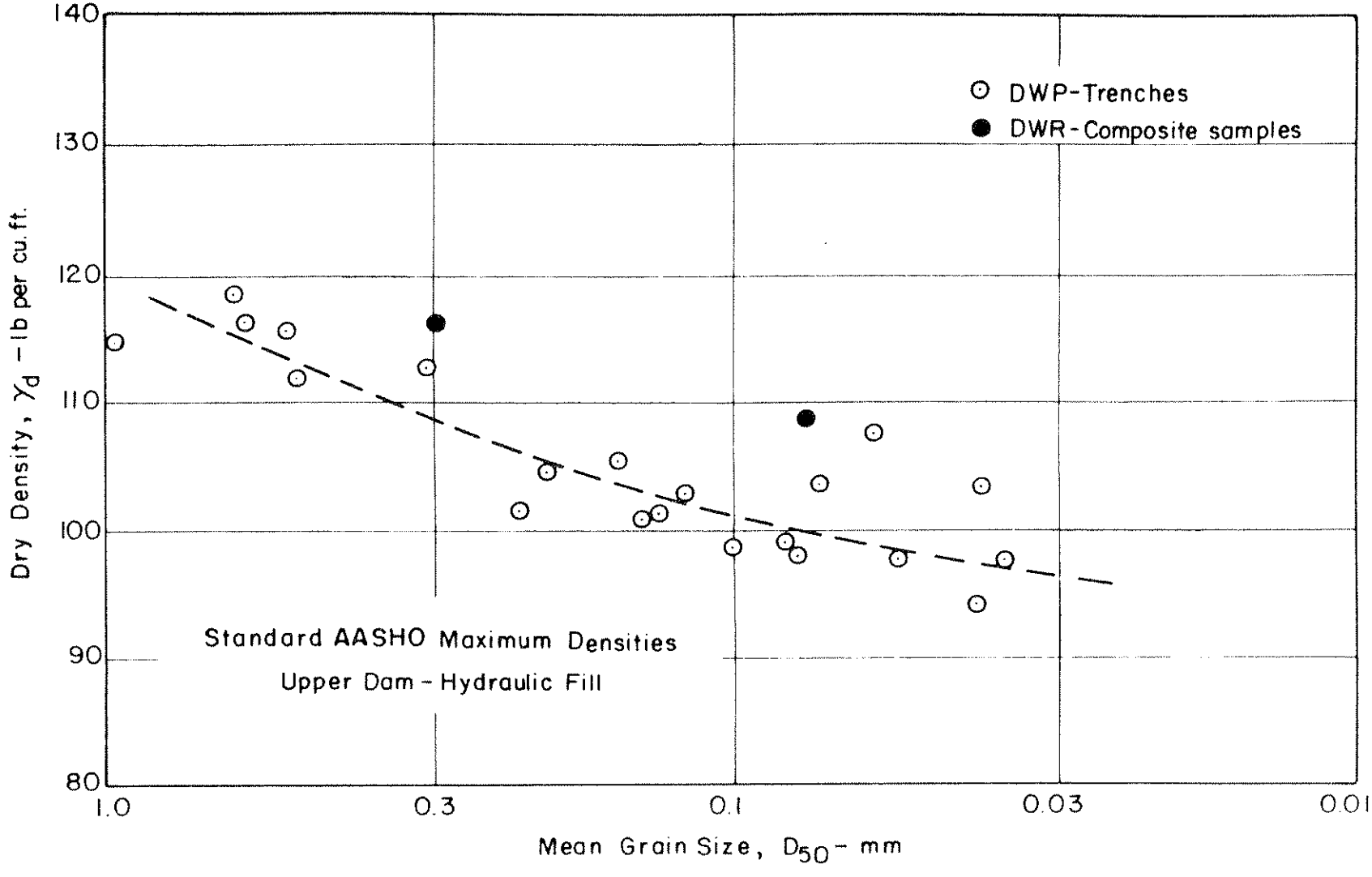

Fig. IV–14 STANDARD AASHO MAXIMUM DENSITIES FOR SAMPLES OF HYDRAULIC FILL – UPPER SAN FERNANDO DAM.

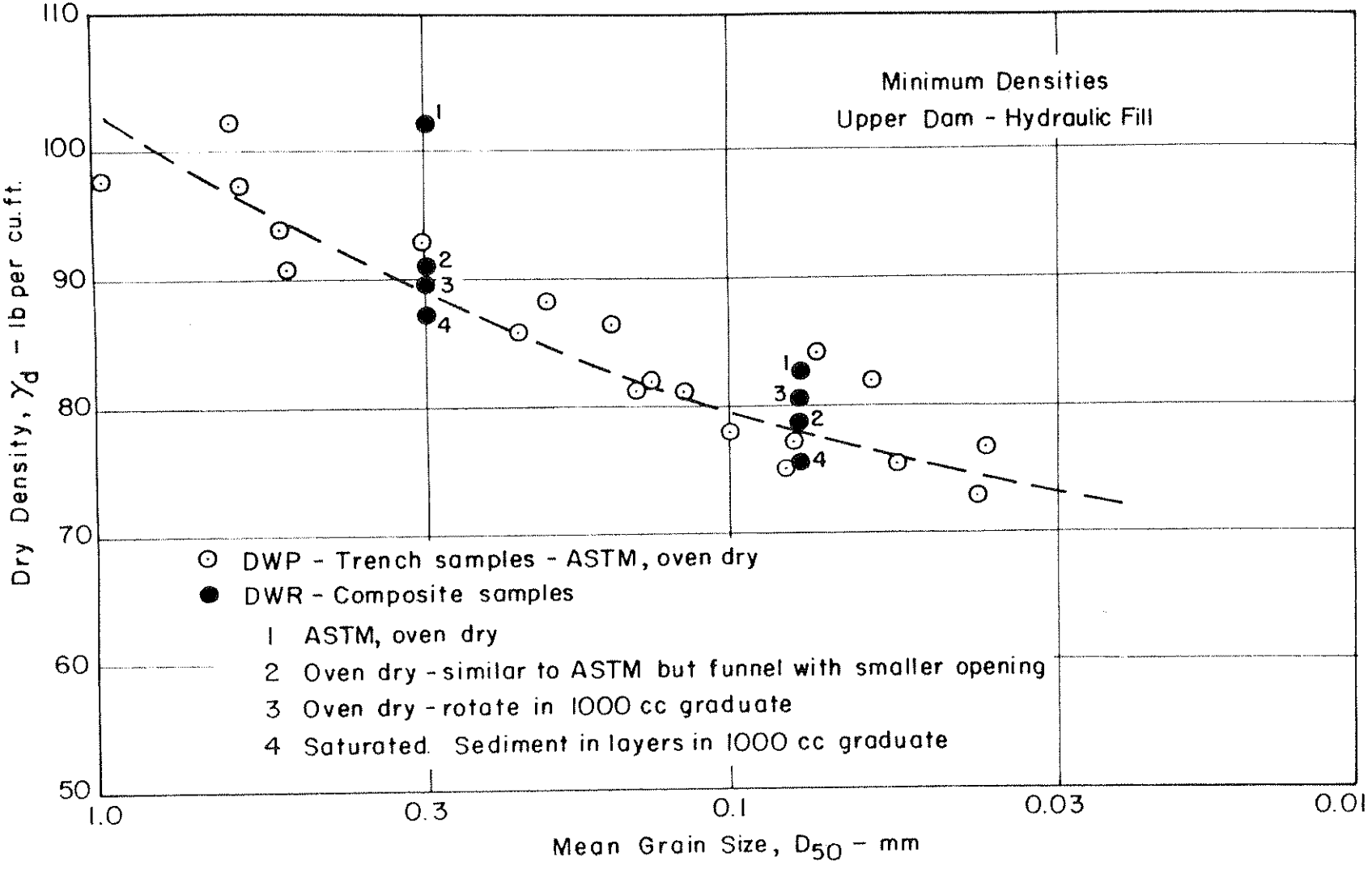

Fig. IV–15 MINIMUM DENSITIES FOR SAMPLES OF HYDRAULIC FILL – UPPER SAN FERNANDO DAM.

graduate flask was filled with clear water, and one of the 100-gram batches of soil was slowly poured into the graduate. The first batch of soil was allowed to settle for one day and then the second batch of soil was poured in. The process was repeated until all of the individual batches of saturated soil were poured into the large graduate. The final volume of soil which settled to the bottom of the graduate was read and the minimum density calculated. Minimum densities by this method were slightly lower than any of the minimum densities obtained using dry soil.

This sedimentation procedure is likely to introduce some error since it causes particle size segregation, with the coarse soil in each batch settling out faster than the finer portion. In fact the finest portion never did completely consolidate to a solid condition at the bottom of the graduate. Thus the measured final volume was probably too large and the resulting minimum densities were probably somewhat too low to be realistic.

Minimum density data by the ASTM Method for oven-dried soil is also shown on Fig. IV-15 for the individual field samples. The data is somewhat less scattered than the corresponding data for the maximum density tests on these same samples and shows a clear relation of decreasing minimum density with decreasing grain size. The best fit line was drawn slightly on the low side to allow for the fact that the ASTM Method used to obtain the data appeared to give slightly high results as compared to other methods.

Relative Density and Relative Compaction

The best fit curves for the maximum, minimum, compaction and field density test data described above are presented together on Fig. IV-16 for comparison purposes. It may be seen that they present a consistent

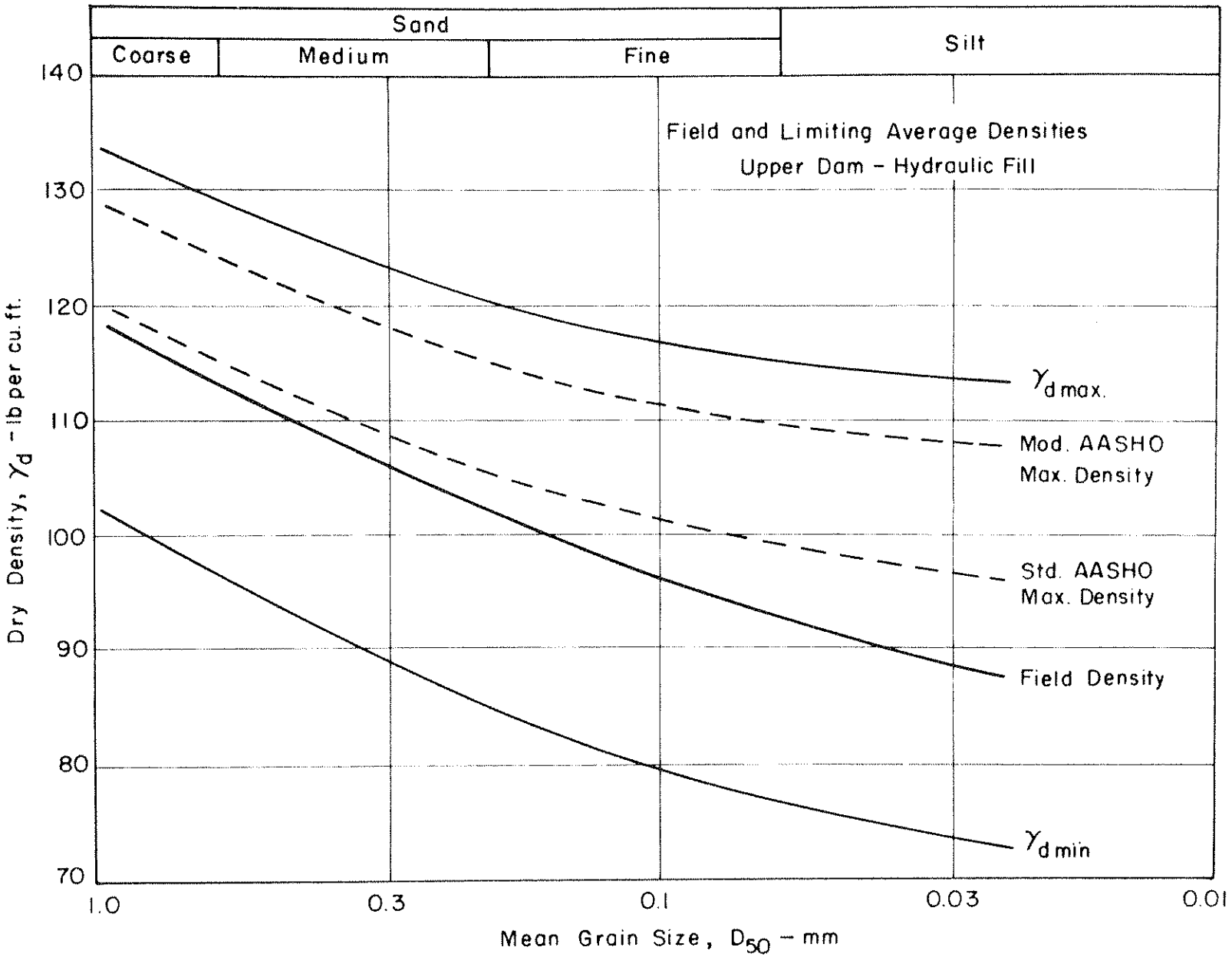

Fig. IV-16 SUMMARY OF FIELD AND LIMITING DENSITY DATA FOR HYDRAULIC FILL - UPPER SAN FERNANDO DAM.

pattern of decreasing density with decreasing grain size along more or less parallel curves.

From these data it is a straight forward matter to compute the relative density of the field curve at each grain size. This was done using the relationship:

$$D_r = \frac{\gamma_{d_{max}}}{\gamma_d} \left(\frac{\gamma_d - \gamma_{d_{min}}}{\gamma_{d_{max}} - \gamma_{d_{min}}} \right) \times 100\% \qquad (2)$$

The calculated relative densities based on the field and limiting densities shown in Fig. IV-16 are plotted in Fig. IV-17. It may be seen that the relative density of the hydraulic fill in the Upper Dam, determined by this procedure, is approximately 54 percent for all grain sizes. This relative density is similar to that reported by others (Whitman, 1970; Turnbull, 1972) for other hydraulic fills (45 to 60%).

The relative compaction of a soil is defined as the ratio of the field density to the maximum density obtained by some standard laboratory procedure. Values based on the standard AASHO range from 92 to 99 percent and values based on the modified AASHO (1961) test are considerably lower ranging between 83 and 92 percent.

For purposes of comparison, relative compaction values corresponding to minimum density conditions and based on a laboratory test producing maximum density results are shown by a dashed curve on Fig. IV-18. These values range from about 65 to 75 percent and indicate that a relative compaction of at least 65 to 75 percent will automatically be obtained no matter how poorly the fill is placed in the field. Thus as previously discussed by Lee and Singh (1971) the useful range of relative compaction values is very narrow, and it can be expected that many physical properties of the soil are quite sensitive to small changes in relative compaction.

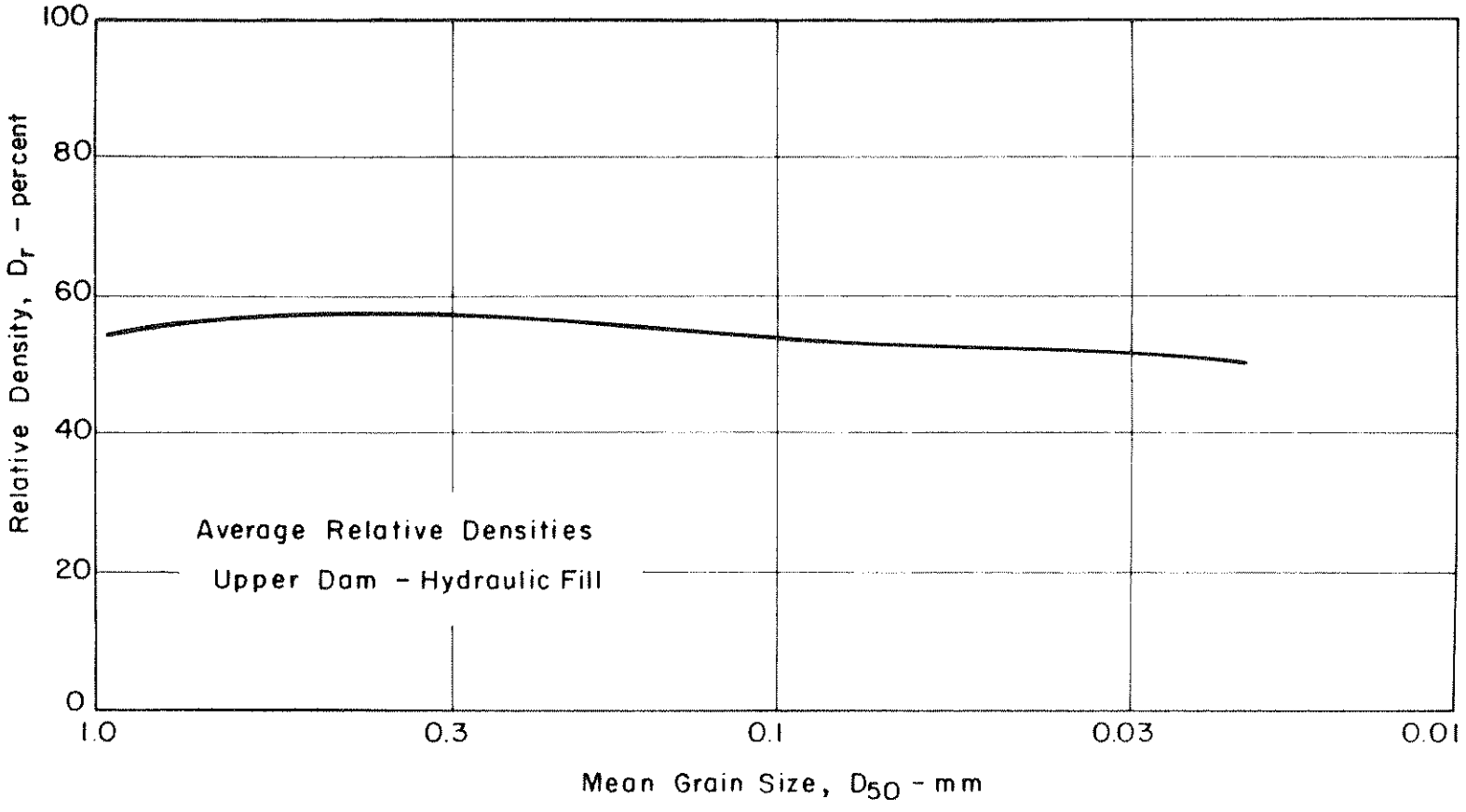

Fig. IV-17 AVERAGE RELATIVE DENSITIES FOR HYDRAULIC FILL - UPPER SAN FERNANDO DAM.

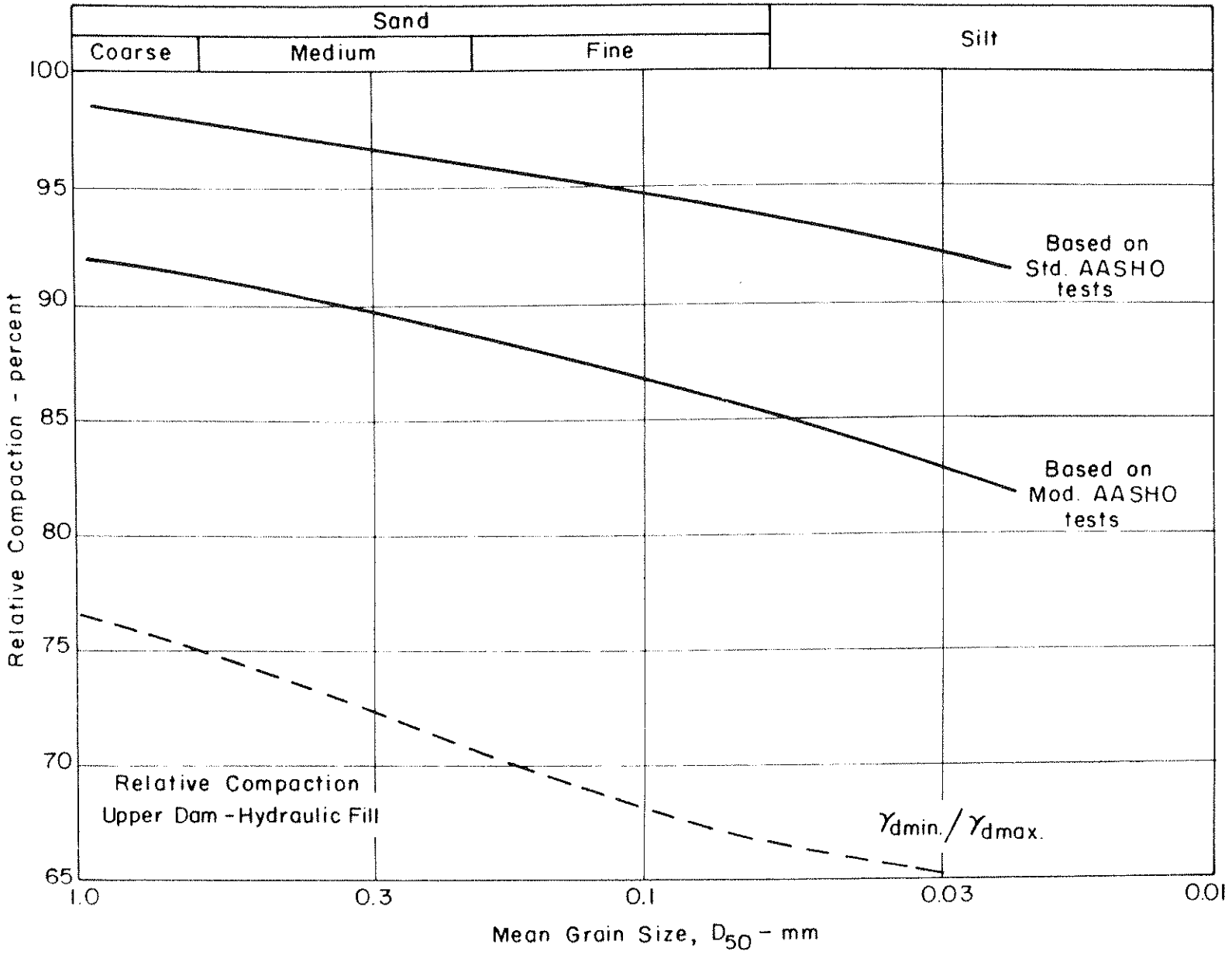

Fig. IV-18 AVERAGE VALUES OF RELATIVE COMPACTION FOR HYDRAULIC FILL - UPPER SAN FERNANDO DAM.

Density of the Alluvium

Using a similar procedure to that described above for the hydraulic fill, studies were also made to determine the absolute and relative densities of samples of soil from the underlying alluvium. In making this study it was recognized that the alluvium at both the Upper and Lower Dam sites was of essentially the same geological formation and the samples from each site appeared to be very similar material. Moreover because there was only a relatively small amount of alluvium at the Lower Dam, and because triaxial tests indicated it to be stronger than the hydraulic fill, testing on samples of alluvium from the Lower Dam was not as extensive as that for the alluvium at the Upper Dam. For these reasons the density tests from the alluvium at both dams are presented together.

A summary of the field and limiting density data for the alluvium at both the Upper and Lower Dams is presented on Fig. IV-19. It may be seen that the field density data for both dams are similar, and as for the hydraulic fill, indicate a trend of decreasing density with decreasing grain size.

Maximum density tests on composite samples performed by the three methods described previously are also shown on Fig. IV-19. The vibration methods led to higher maximum densities than the modified AASHO (1961) compaction method.

Because the alluvium at the damsites was inaccessible to field trenching no field density tests were performed and therefore no single samples could be obtained large enough to perform compaction tests on individual samples. Accordingly it was necessary to estimate the probable maximum density corresponding to the field samples based on the maximum densities obtained from the composite samples. This estimated relationship

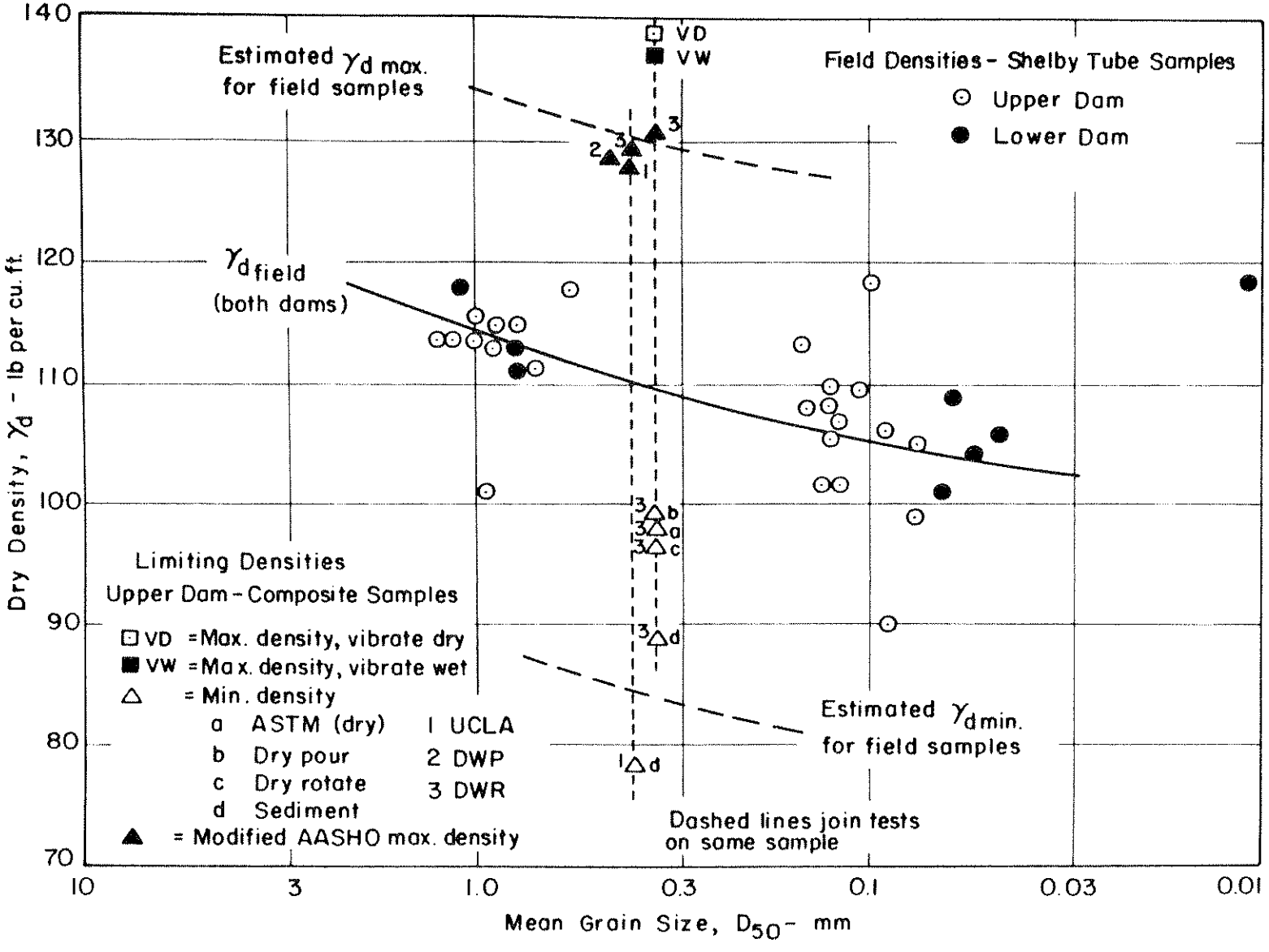

Fig. IV-19 FIELD AND LIMITING DENSITIES FOR SAMPLES OF ALLUVIUM - UPPER AND LOWER SAN FERNANDO DAMS

for various grain sizes is shown on Fig. IV-19. Similarly it was necessary to estimate the probable minimum field density for individual field samples based on the results of minimum density tests performed on composite samples. The estimated minimum density values are also shown on Fig. IV-19.

On the basis of these results and field densities obtained from Shelby tube samples, the average relative density of the alluvium appears to be about 67 percent, or some 10 percent higher than the average relative density of the hydraulic fill. This value of the relative density is considered to represent a lower range of density in the alluvium corresponding to some of the weaker zones or pockets in this extremely heterogeneous soil. When the samples were opened for testing many were discarded because they contained gravels or very coarse sand in a dense silty clay matrix. The testing program for the alluvium was designed to determine the characteristics of the weaker samples and therefore these obviously denser and stronger samples were not tested.

Relative Density by Standard Penetration Tests

As previously described, a standard penetration test was performed every five feet in each of the drill holes, and the variations of penetration resistance with depth for each of the holes are shown on the cross-sections, Figs. IV-2 to IV-4. These sections also show the major soil boundaries.

From these data and the field density data, values of effective overburden pressure at the location of each standard penetration test can readily be computed and used with the penetration test data to determine the relative density of the soil from the correlation between standard penetration resistance, effective overburden pressure, and relative

density of granular soils presented by Gibbs and Holtz (1957). Values of relative density obtained in this way are summarized on Fig. IV-20.

For convenience the relative density values from several holes are combined on each of the figures. For example the data from three holes drilled in the upstream slope of the dam, starting at about the same elevation, are all presented on Fig. IV-20a. All the holes drilled from the crest of the dam are presented on Fig. IV-20b, etc. The approximate average soil boundaries for each of these sets of holes are also shown. The data for the hydraulic fill material are shown as open points whereas the data from the rolled fill and underlying alluvium are shown as solid points.

As is generally observed with standard penetration test data there is considerable scatter. No doubt some of the abnormally high relative densities were caused by the sampling spoon encountering a rock in the soil while some of the abnormally low values could have been caused by the sampling spoon penetrating one of the many seams of clay.

The possibility that lower penetration resistance values may be due to clay seams beccmes more apparent from a review of the penetration resistance profile along any one of the cross sections. The N-values in Holes A3, B3 and C3 are considerably lower than those for the hydraulic fill in any other holes. It is noted that Holes A3, B3 and C3 are in the center of the dam where one would expect to find the greatest concentration of clay. This is also borne out by the soil conditions described in the drill logs. For this reason the standard penetration data from these three holes through the clay core, were not included with the data in Fig. IV-20.

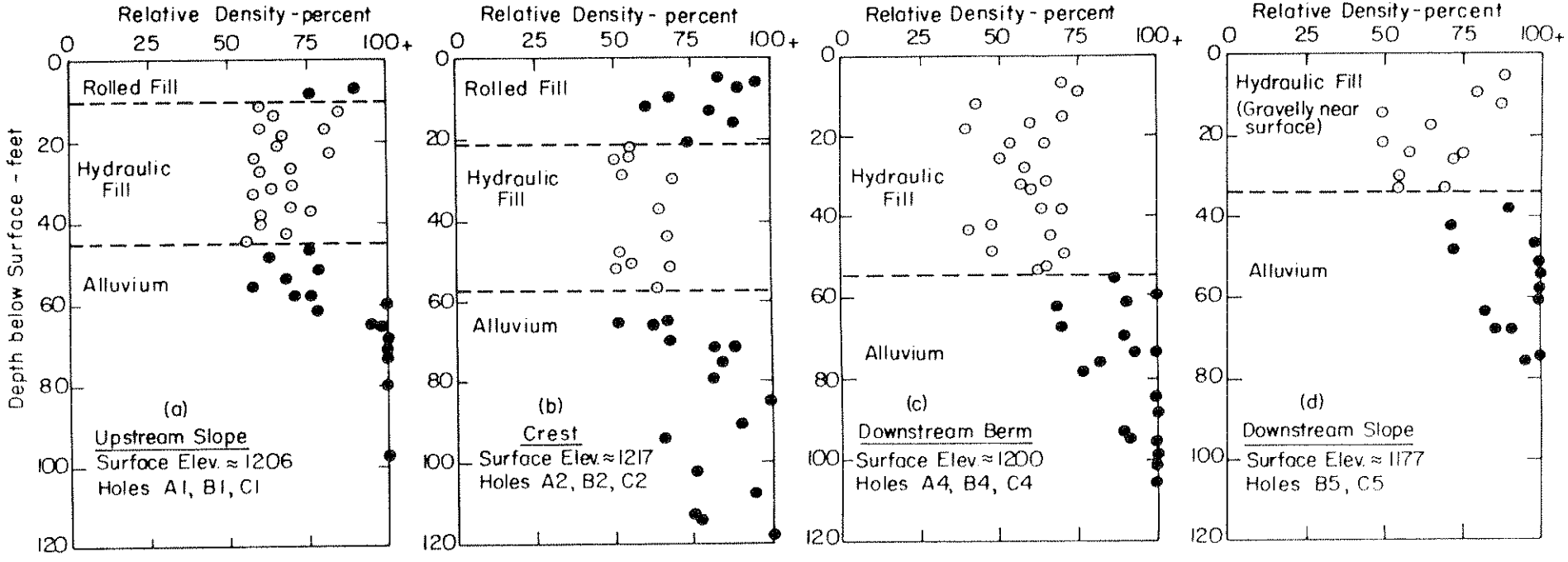

Fig. IV–20 RELATIVE DENSITIES DETERMINED FROM STANDARD PENETRATION TEST DATA – UPPER SAN FERNANDO DAM

Discounting or de-emphasizing the few abnormally high and abnormally low relative densities, the large bulk of the data in Fig. IV-20 indicates that the relative density in the hydraulic fill at the Upper Dam was approximately 45 to 70% which correlates well with the average relative density of about 54 percent obtained from the field and the laboratory compaction data. The data on Fig. IV-20 also shows that the relative density in the upper rolled filled portion of the dam is significantly higher than the relative density in the hydraulic fill.

The relative densities calculated for the alluvium are quite erratic as might be expected from the known heterogenic nature of the material. Near the surface of the alluvium the relative density appears to be only slightly greater than the relative density of the hydraulic fill, but with depth the relative density of the alluvium increases to very high values.

Static Strength Tests on Granular Soils

A total of about 50 static loading triaxial tests were performed on undisturbed samples from the hydraulic fill and alluvium of the Upper Dam. One purpose for performing these tests was to obtain the strength data required to evaluate the stress condition in the dam prior to the earthquake and for use in pseudo-static analyses of seismic stability. Another purpose for performing the tests was to obtain the static loading stress-strain parameters required for the static finite element analysis to determine the equilibrium stress conditions in the dam prior to the earthquake.

Test specimens for these and all other tests on undisturbed samples were obtained in the same way. The Shelby tubes of soil obtained from the field were sawn into 7 inch lengths and the undisturbed sample was

extruded from this 7 inch length of tube. The top, bottom and the sides of this sample were carefully examined in the laboratory to determine the nature and consistency of the soil. In general, the samples could be classified as either fine sand, coarse sand, or clay. Occasionally, the samples contained an interface between two types of soils. In this case the sample was either discarded or it was divided at the interface and the two parts spliced into a similar soil from another sample. The occasional samples which contained large pieces of gravel were discarded.

The samples were tested as they were extruded from the tubes without further trimming on the sides. A little soil was trimmed from each end to make the sample approximately six inches high. The diameter of the samples was slightly less than three inches.

The static tests were carried out in standard triaxial cells using top and bottom drainage with back pressure to bring the samples to saturation. The samples were consolidated isotropically under effective stresses ranging from 1.0 to 4.0 kg per sq cm. Two types of tests were performed: consolidated-drained tests with volume change measurements, and consolidated-undrained tests with pore pressure measurements.

The stress strain curves for typical drained and undrained triaxial tests on the hydraulic fill of the Upper Dam are shown on Fig. IV-21. Each of these samples was consolidated to an isotropic effective stress of 2.0 kg per sq cm and then axially loaded to failure. For the drained tests, volume change measurements were made and for the undrained tests pore water pressure measurements were made throughout.

The behavior of these samples under static loading is similar to that obtained from static loading tests on other granular soils. The drained test shows some decrease in volume followed by a slight tendency for

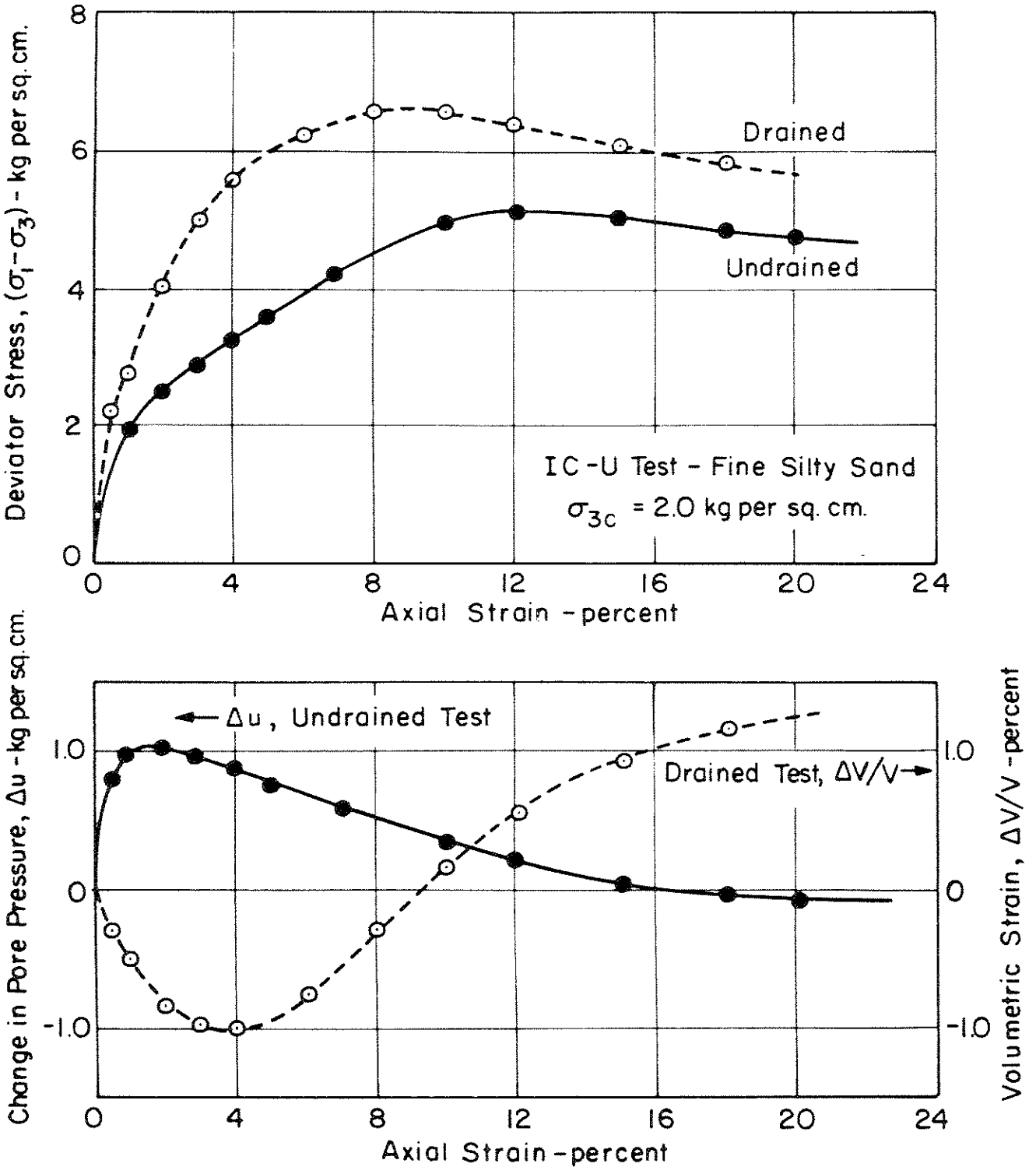

Fig. IV-21 TYPICAL STRESS-STRAIN CURVES IN STATIC LOADING TRIAXIAL TESTS ON SAMPLES OF HYDRAULIC FILL - UPPER SAN FERNANDO DAM.

dilation near and beyond failure. The undrained test shows an initial increase in pore water pressure, changing to a slight decrease at high strains. While there is a definable peak in the stress strain curve there is no significant decrease in strength beyond the peak which would suggest a tendency for serious loss in strength after large strains.

Similar stress-strain-pore pressure change curves were obtained from triaxial tests on all of the samples tested under consolidation pressures of 1.0, 2.0 and 4.0 kg per sq cm. As the confining pressures increased the tendency for dilation was found to decrease, but in no case was there any indication of a significant rapid loss in strength beyond the peak stress condition.

Strength data for all of the tests performed on the hydraulic fill material are presented on Fig. IV-22 on a modified Mohr diagram. Strength data, on a total stress basis, for the consolidated-undrained tests are presented in the upper diagram, Fig. IV-22a. Strength data, on an effective stress basis, from both the drained tests and the consolidated-undrained tests are presented on the lower diagram, Fig. IV-22b. Data from these two different types of tests are distinguished by different symbols on the diagram, as are data from consolidated-undrained tests on coarse sand and fine sand. It may be seen from the data that there is virtually no difference in the strength parameters of the coarse sand and the fine sand of the hydraulic fill, and there is virtually no difference between the strength parameters, on an effective stress basis, determined from drained test data or from undrained tests with pore pressure measurements. Conversion of the test data in Fig. IV-22 to show the relationship between the shear stress on the failure plane at the time of failure τ_{ff}, and the normal stress on the failure plane after consolidation σ_{fc} is shown on Fig. IV-23.

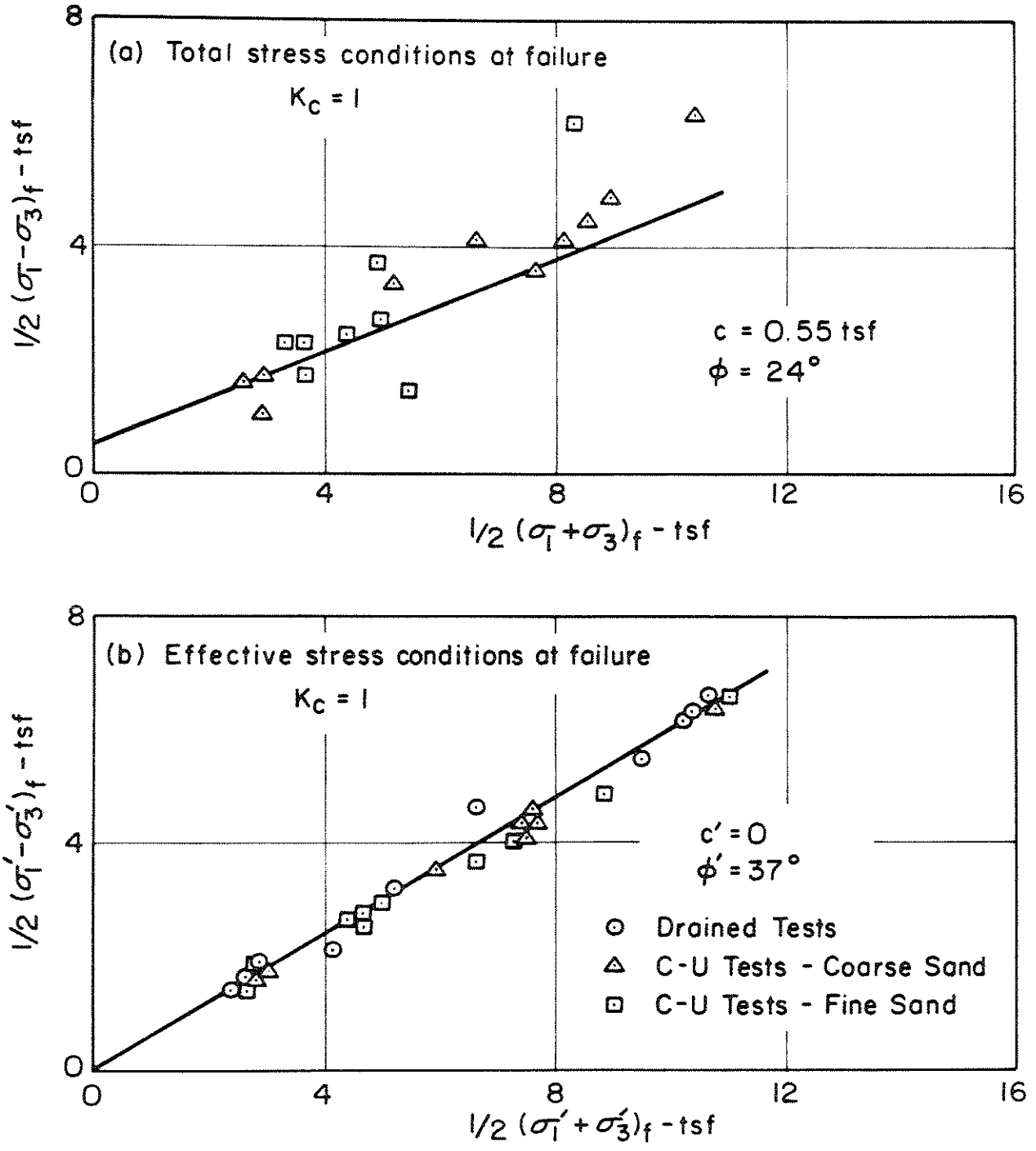

Fig. IV-22 RESULTS OF TRIAXIAL TESTS ON SAMPLES OF HYDRAULIC SAND FILL FROM UPPER SAN FERNANDO DAM (Data from State of California Department of Water Resources 1971).

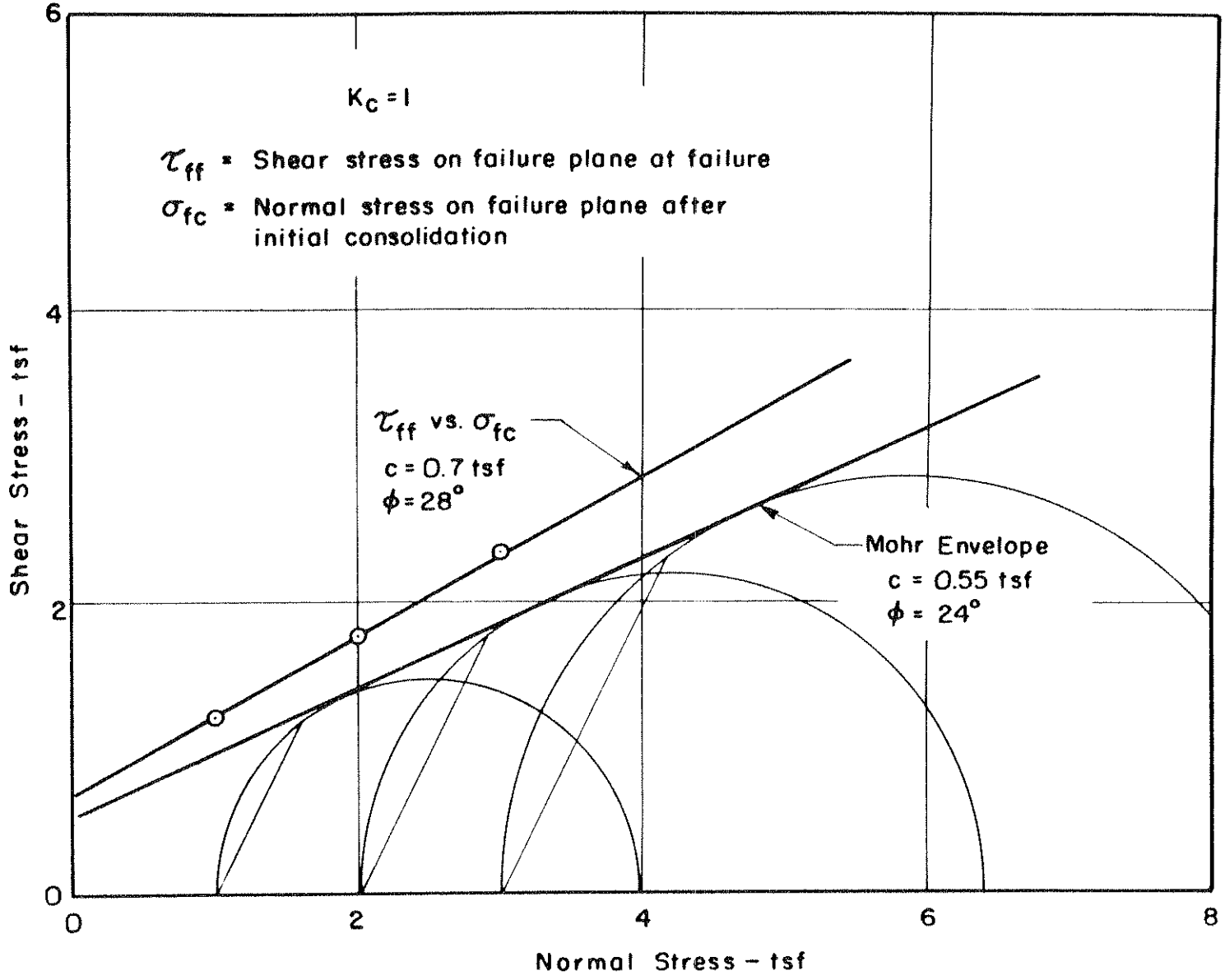

Fig. IV-23 MOHR ENVELOPE AND τ_{ff} vs σ_{fc} RELATIONSHIPS DETERMINED BY CONSOLIDATED-UNDRAINED TRIAXIAL TESTS ON SAMPLES OF HYDRAULIC SAND FILL -UPPER SAN FERNANDO DAM (Data from State of California Department of Water Resources, 1971).

Similar data obtained from triaxial tests on undisturbed samples of the alluvium are presented on Fig. IV-24. Again there appears to be no significant difference between the data from the coarse sand and the data from the fine sand samples.

Comparison of the strength data from these figures indicates that the strength of the alluvium is somewhat greater than that of the hydraulic fill. The strength parameters shown on these figures were used in the pseudo-static stability analyses which were performed to determine the factor of safety of of the dam against earthquake effects.

A dynamic stability analysis of an earth dam requires a detailed knowledge of the stress distribution in the dam and its foundation prior to the earthquake. These stresses are obtained by performing a finite element analysis which simulates construction of the dam in stages and which uses stress-strain properties for the soil which vary non-linearly with increasing stress. The static stress analysis used in this study has been described by Kulhawy, Duncan, and Seed (1969). The computer program uses stress-strain and volume change properties defined by two hyperbolic relationships. The soil properties used to define these relationships are determined from the stress-strain relationships obtained from drained triaxial tests. A summary of these parameters for the rolled fill, the hydraulic fill, and the alluvium materials is presented in Table IV-1. The data for the hydraulic fill and the alluvium were obtained from the testing program on undisturbed samples. They are generally similar to values given in a compilation of data presented by Kulhawy, Duncan and Seed (1969) for similar soils.

Undrained Strength of Clay

As described previously there were numerous thin layers of clay within the hydraulic fill; in addition, the central core of the embankment was predominantly clay material. This clay was insensitive, in that it did not lose strength on remolding. Since previous studies have shown that clays are considerably stronger than saturated sands at a corresponding

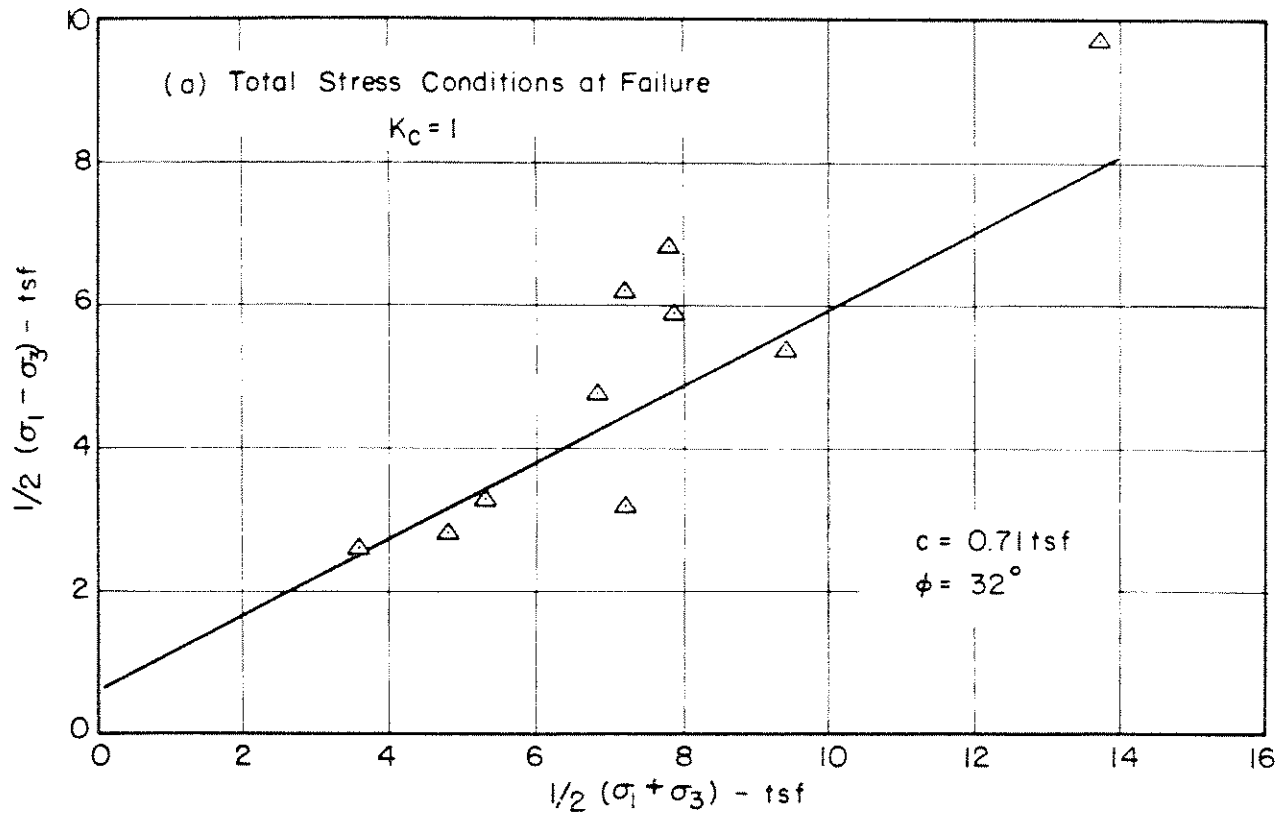

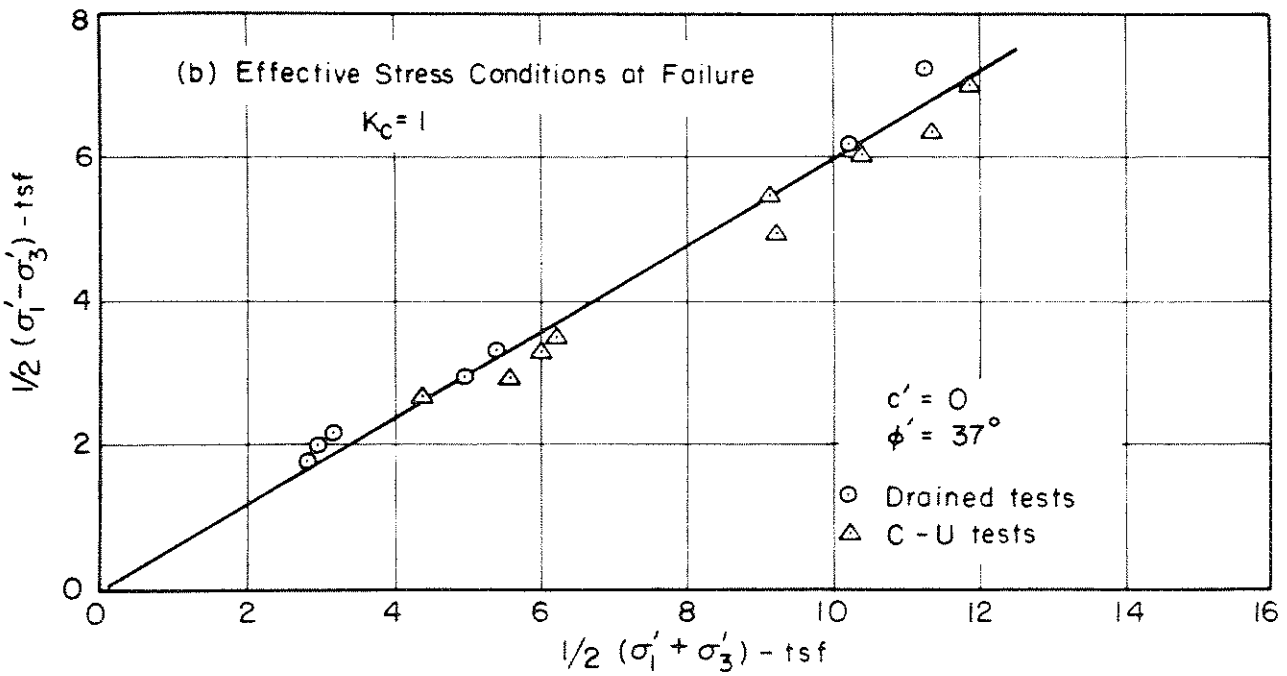

Fig. IV–24 RESULTS OF TRIAXIAL TESTS ON SAMPLES OF ALLUVIUM FROM UPPER SAN FERNANDO DAM. (Data from State of California Department of Water Resources, 1971).

Table IV-1

Summary of Stress-Strain-Strength Parameters used in Static Finite Element Stress Analysis, Upper Dam

	Parameter	Zone		
		Rolled Fill	Hydraulic Fill	Alluvium
Unit Weights	γ_t (above Wt.) lb/ft^3	134	120	--
	γ_b (below Wt.) lb/ft^3	78	60	67
Strength Parameters	c ton/ft	1.3	0	0
	ϕ degrees	25	37	37
	R_f	0.90	0.78	0.66
Young's Modulus Parameters	K	300	420	280
	n	0.76	0.52	0.80
Poisson's Ratio Parameters	G	0.30	0.33	0.32
	F	0.10	0.12	0.10
	D	3.80	10.00	9.00

γ_t = total unit weight
γ_b = buoyant unit weight
c = cohesion intercept
ϕ = angle of internal friction
R_f, K, n, G, F, D = nonlinear stress-strain parameters, assumed the same above or below the water table

density under cyclic loading conditions (Lee and Fitton, 1969; Seed and Chan, 1966), it was considered that the clay did not play a significant part in causing the seismic instability of the dam. Accordingly, a comprehensive testing program was not carried out on the clay soil.

Nevertheless, a fairly large number of small torvane shear tests were performed on the larger clay seams that were found in the Shelby tubes when the samples were extruded. Other torvane tests were performed on some of the clay seams exposed in the shallow inspection trenches excavated along the downstream berm. The results of these tests are plotted on Fig. IV-25 which shows shear strength plotted against the effective overburden or consolidation pressure. Although the data is somewhat scattered there is a fairly well defined trend of shear strength increasing linearly with depth below the water table, as would be expected for a normally consolidated clay soil. The ratio of shear strength to consolidation stress is approximately 0.24.

Atterberg limit tests were performed on various samples of the clay. The liquid limit ranged from about 37 to 60 and the PI values ranged from about 20 to 40. Compilations of data from other normally consolidated clays indicates an approximate empirical relationship between undrained strength Su, consolidation pressure, p, and plasticity index PI as follows (Terzaghi and Peck, 1967):

$$\frac{Su}{p} = 0.11 + 0.0037\ PI \qquad (1)$$

On the basis of this equation and the Atterberg limit data, the ratio Su/p for the clay in this dam would be expected to range between about 0.18 and 0.25, which correlates reasonably well with the measured strengths. Torvane tests made on samples taken from above the water table were relatively stronger, due to the effects of desiccation in these upper zones.

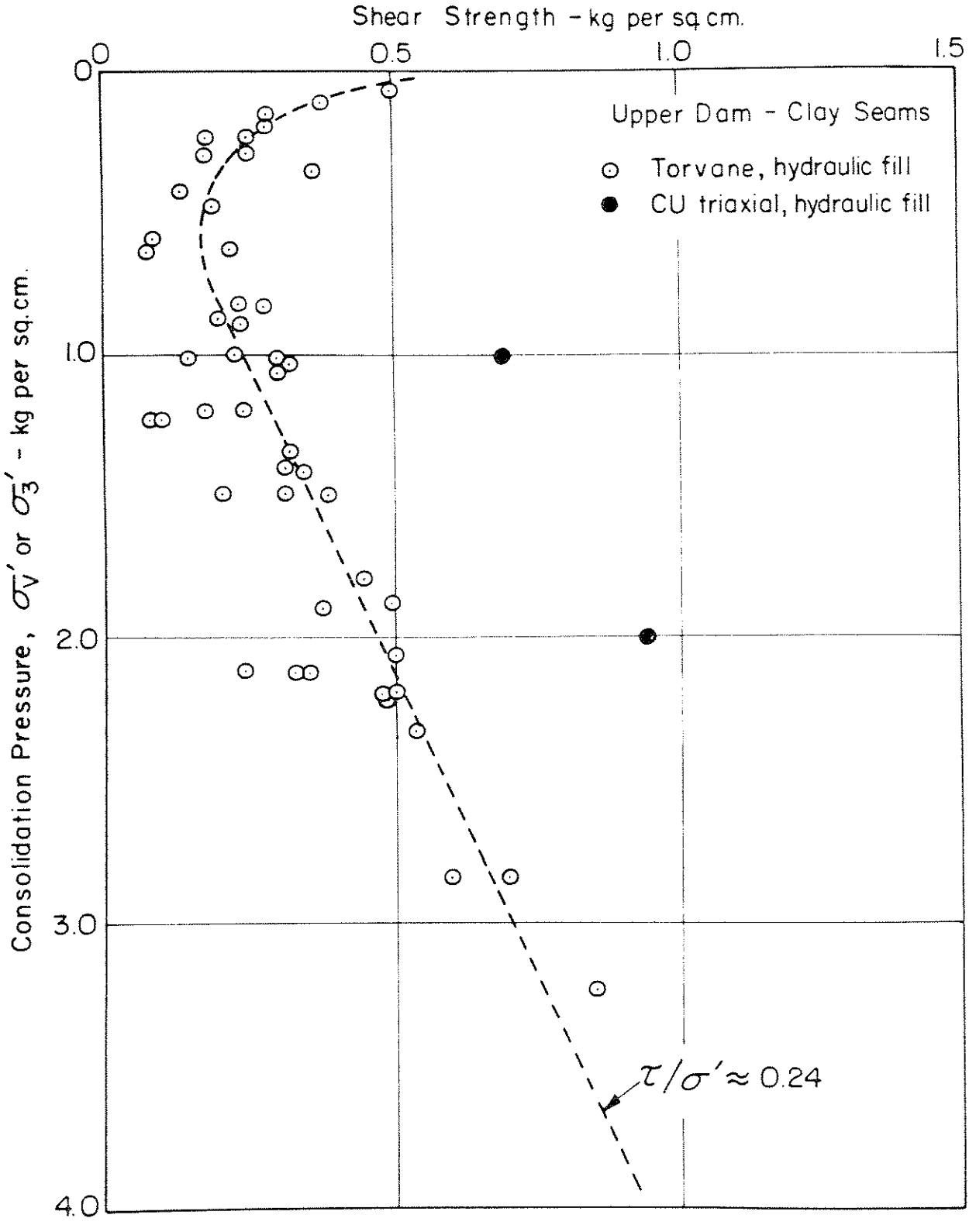

Fig. IV-25 UNDRAINED SHEAR STRENGTH OF CLAY - UPPER SAN FERNANDO DAM.

Two consolidated undrained tests were performed on undisturbed samples of clay taken from the dam. These data are also plotted on Fig. IV-25, and indicate shear strengths substantially higher than those obtained from the small torvane tests. No satisfactory explanation was found for this apparent discrepancy.

Cyclic Load Tests on Hydraulic Fill and Alluvium

A total of 46 cyclic loading triaxial tests were performed on samples of hydraulic fill from the Upper Dam. Samples were prepared for testing in exactly the same way as for the static load triaxial tests. The 3 inch diameter Shelby tube samples were cut in seven inch lengths and an undisturbed sample of soil extruded and examined to determine its suitability for testing. Samples containing large amounts of gravel or clay seams were discarded. Satisfactory samples were trimmed to a length of about six inches prior to testing. They were then weighed and measured, placed in a standard triaxial cell with top and bottom drainage, saturated using a back pressure, and consolidated under the desired effective stress conditions.

Samples were consolidated under both isotropic and anisotropic stress conditions using lateral consolidation pressures of 1.05 and 2.10 kg per sq cm. The principal stress ratio during consolidation, $K_c = \frac{\sigma_{1c}}{\sigma_{3c}}$, ranged from 1.0 to 2.0.

The behavior of saturated cohesionless materials subjected to cyclic loading triaxial tests has been described in a number of previous publications (Seed and Lee, 1966; Lee and Seed, 1967; Finn et al 1970; Seed and Peacock, 1971). However to illustrate the methods used to reduce the data, a brief summary of typical test results is presented in the following paragraphs.

In a typical test on an isotropically-consolidated sample of hydraulic fill subjected to a series of uniform cyclic or pulsating loads, σ_{dp}, records were made of the increase in pore water pressure and the axial strains developed with increasing number of cyclic stress applications. Usually after a relatively small number of cycles the peak pore pressure developed in any one pulse reached a value equal to the applied confining pressure. In this instant of time the effective stress in the sample was reduced to zero, and the soil had no resistance to deformation. This condition occured when the cyclic stress was zero; that is, when the sample was under an isotropic stress condition.

As the applied pulsating stress moved away from its zero position in either direction for the next cycle, the sample, having virtually no strength at that instant, deformed considerably, causing dilation and a corresponding reduction in the pore water pressure. Then the sample began to gain strength, ultimately arresting the movement induced by the pulsating load. This process continued with increasing deformation on each successive cycle until the magnitude of the deformations reached the limitations of the testing equipment.

As a first step in reducing the data it has been found convenient to plot the maximum peak to peak strain (Fig. IV-26a) and the maximum pore pressure developed (Fig. IV-26b) in different numbers of stress cycles. The pore pressure values are presented as the ratio of the change in pore pressure Δu to the initial consolidation stress, σ_{3c}. A maximum pore pressure ratio, $\frac{\Delta u}{\sigma_{3c}}$, of 1 represents a transient condition of zero effective stress and is referred to as initial liquefaction. Continuing the test beyond this point usually results in a rapid increase in strain with each succeeding stress cycle. The number of cycles required to reach

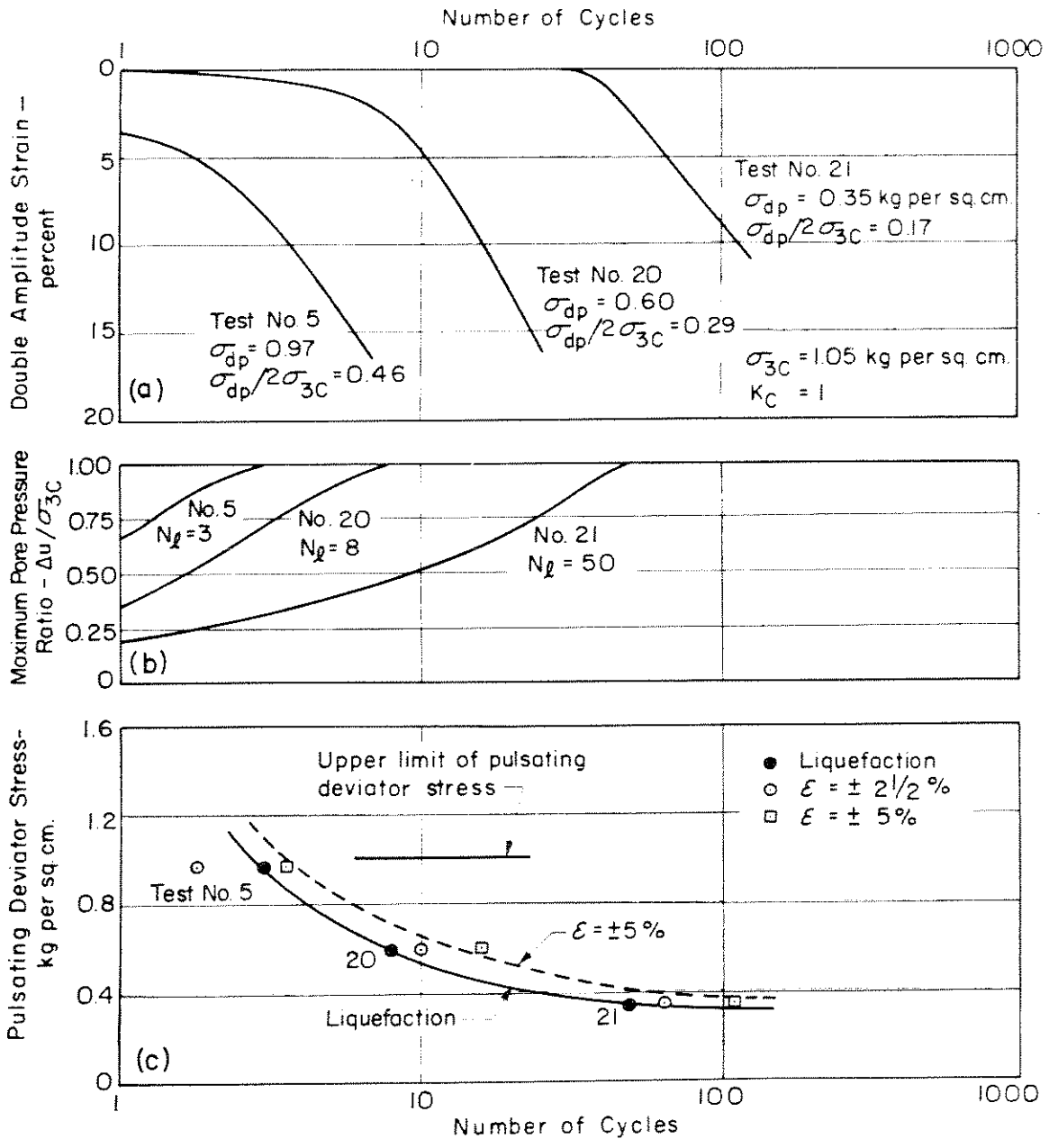

Fig. IV–26 RESULTS OF CYCLIC LOAD TESTS ON ISOTROPICALLY CONSOLIDATED SAMPLES OF HYDRAULIC SAND FILL – UPPER SAN FERNANDO DAM.

this initial liquefaction, N_ℓ, is indicated for each test on Fig. IV-26b.

For the three tests shown in Fig. IV-26, the number of stress cycles required to cause liquefaction, N_ℓ, for different values of the cyclic deviator stress, σ_{dp} is shown in the lower part of the figure.

For analysis purposes it is often desirable to define the cyclic loading strength in terms of a limiting axial strain rather than in terms of initial liquefaction. This information is readily obtained from the curves shown on Fig. IV-26a, and the numbers of cycles required to cause ±2-1/2 and ±5 percent strain for different values of the cyclic stress are also shown on Fig. IV-26c. It may be seen that the strength data for an axial strain of ±2-1/2 percent is quite close to that for initial liquefaction. This latter observation was consistently observed in all of the tests on isotropically consolidated samples for both the Upper and Lower Dams and had previously been observed by Lee and Fitton (1969). Thus in general, test data were reduced for failure defined as ±5 percent strain and initial liquefaction, and ±10 percent axial strain.

The data in Fig. IV-26 represents the results for three of a large number of tests performed on isotropically-consolidated samples. Data from 10 other tests on undisturbed samples of the hydraulic sand fill, all isotropically consolidated to 1.0 or 1.05 kg per sq cm are summarized on Fig. IV-27. The results are shown in terms of the cyclic stress ratio $\sigma_{dp}/2\sigma_{3c}$ to eliminate the effect of small changes in confining pressure. These data include tests on samples of coarse sand and fine sand performed at the UCLA and DWR laboratories. All of the data define a smooth curve typical of cyclic loading test results obtained in other investigations. On the basis of these data, it was concluded that the strength of the

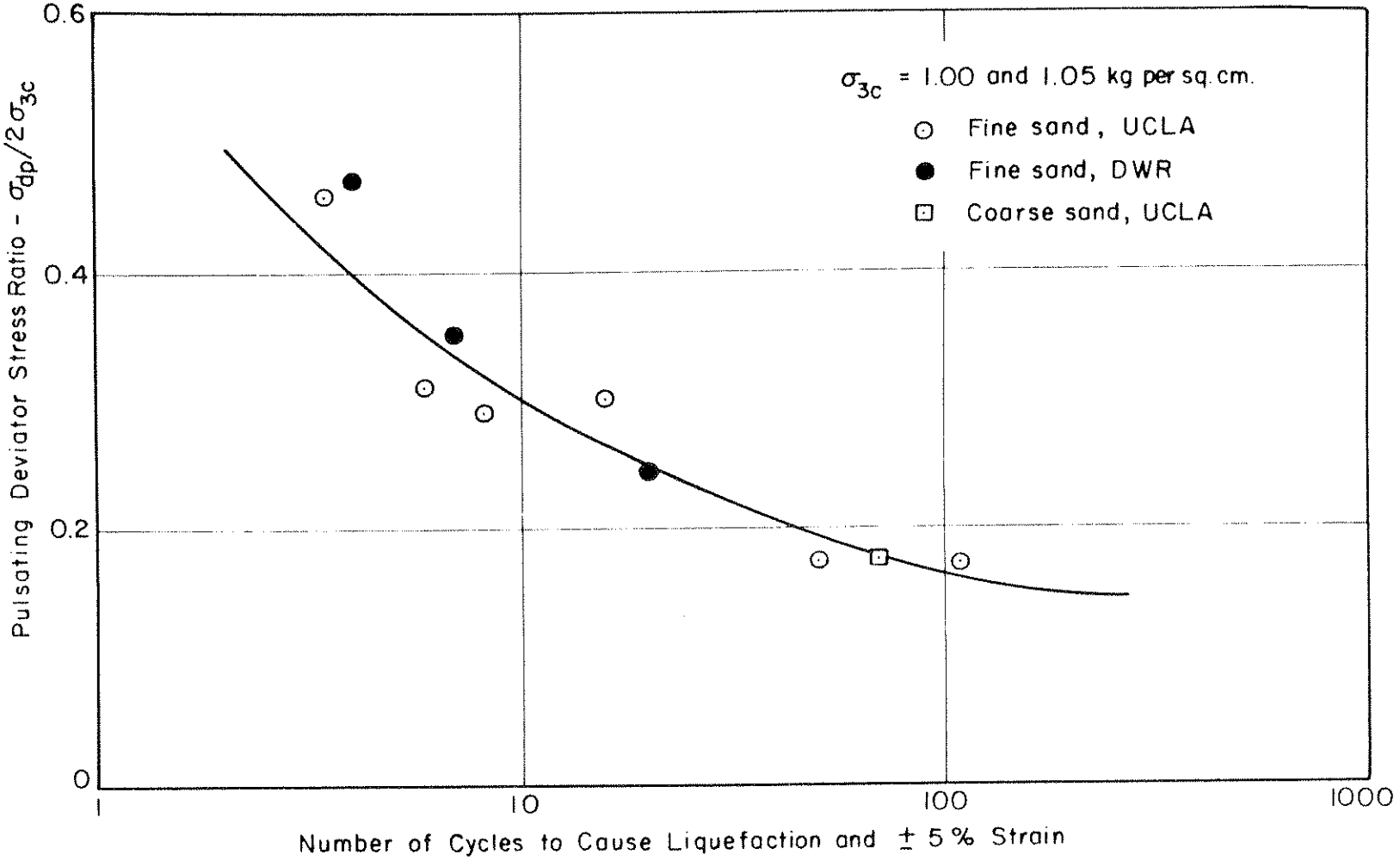

Fig. IV-27 RESULTS OF CYCLIC LOAD TESTS ON ISOTROPICALLY CONSOLIDATED SAMPLES OF HYDRAULIC SAND FILL -UPPER SAN FERNANDO DAM.

hydraulic fill under cyclic loading was not significantly dependent on the grain size distribution of the soil. Accordingly, in subsequent tests at different consolidated pressures, no distinction was made between tests on fine and coarse sands.

The results of a similar series of tests performed on undisturbed samples of the alluvium from the Upper San Fernando Dam at the same consolidation pressure are summarized on Fig. IV-28. Again there is little difference in the results obtained from tests on fine and coarse sand samples, adding further justification to the conclusion that the cyclic loading strength was essentially independent of the grain size within the ranges found within the dam and the alluvium foundation. Also, as observed for the hydraulic fill, there was no significant difference between the results obtained from different laboratories.

A comparison of the strengths of the hydraulic sand fill and the alluvium under cyclic loading conditions is presented in Fig. IV-29. The curves shown in this figure are the same as those determined by the data in Figs. IV-27 and IV-28, together with an additional curve for tests on the hydraulic sand fill under a confining pressure of 2.15 kg per sq cm. It may be seen that at the same confining pressure the alluvium was about 25 to 30% stronger than the hydraulic fill under cyclic loading conditions. This is consistent with the previous observation that the alluvium was denser than the hydraulic fill. As a result of this finding, no further cyclic loading tests were performed on the alluvium from the Upper Dam.

Test data on isotropically-consolidated samples are intended to simulate a field condition in which there is no initial static shear stress acting on a horizontal plane prior to the earthquake. As discussed

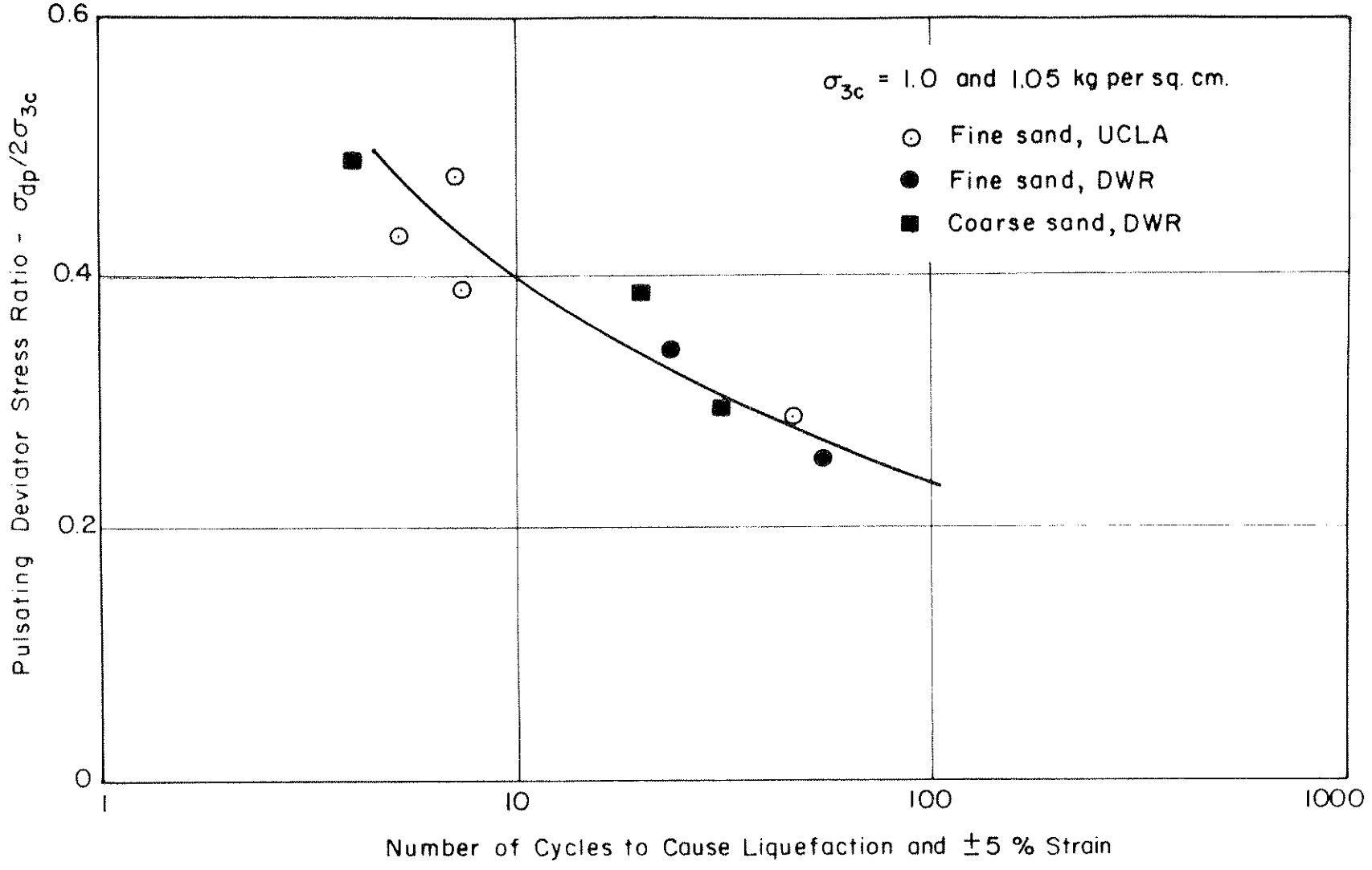

Fig. IV-28 RESULTS OF CYCLIC LOAD TESTS ON ISOTROPICALLY CONSOLIDATED SAMPLES OF ALLUVIUM - UPPER SAN FERNANDO DAM.

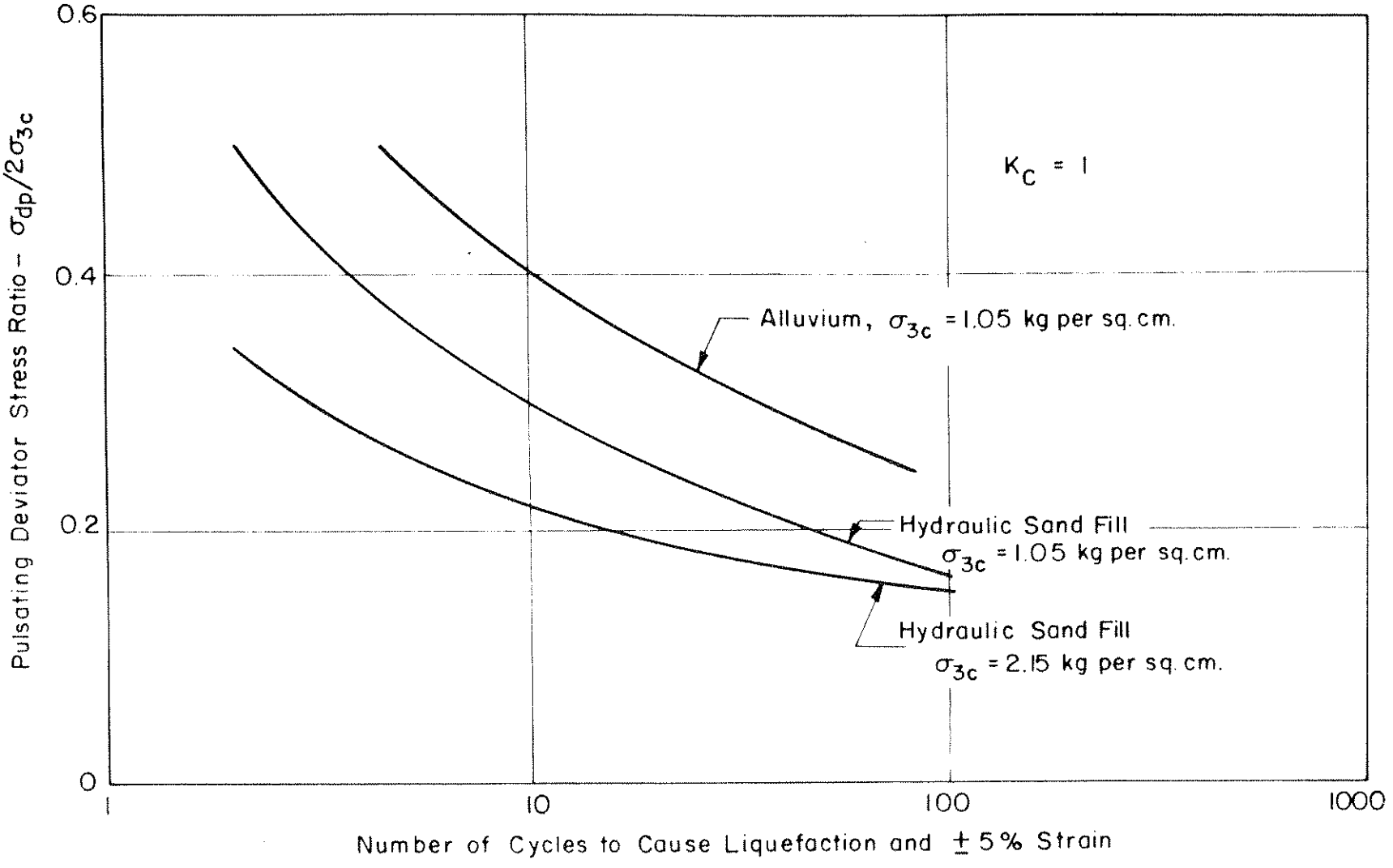

Fig. IV-29 COMPARISON OF CYCLIC LOAD TEST DATA FOR HYDRAULIC SAND FILL AND ALLUVIUM -UPPER SAN FERNANDO DAM.

in connection with the analysis of the Sheffield Dam failure (Seed et al, 1969), this condition is appropriate for soil within the central portion of a dam. However, in the outer portion of an embankment the initial shear stresses on horizontal planes are significant and this condition is best simulated in the laboratory by anisotropic consolidation of triaxial test specimens using an effective stress ratio, ($K_c = \sigma_{1c}/\sigma_{3c}$), greater than 1.0 prior to application of the cyclic stresses. As described elsewhere, (Lee and Seed, 1967; Seed and Lee, 1969), under these conditions the sample may respond in two different ways depending on the initial anisotropic stress ratio and the amount of applied pulsating deviator stress.

In cases where $\frac{\sigma_{dp}}{2\sigma_{3c}} < \frac{K_c - 1}{2}$ there will be no reversal in the direction of application of shear stresses during any part of the cyclic loading test; that is, during the extension as well as on the compression part of the loading cycle, the net axial stress will always be the major principle stress. On the other hand, if the stress ratio $\frac{\sigma_{dp}}{2\sigma_{3c}} > \frac{K_c - 1}{2}$ there will be a stress reversal on each cycle. Previous studies have shown that conditions of stress reversal or very near stress reversal, are required in order for the pore water pressure in a sample to build up to the value of the applied confining pressure and therefore to attain a condition of initial liquefaction. If there is no stress reversal then samples tend to deform progressively during each successive load cycle but the pore pressure does not usually increase sufficiently to produce a transient state of liquefaction leading to a rapid increase in strain.

Regardless of the stress conditions, the data may be plotted in the same way as shown on Fig. IV-26, but using the maximum compressive

strain after any cycle as a measure of the effect of the cyclic stress applications on the soil. In the same way as before, failure may be defined as the number of cycles required to reach initial liquefaction or to reach a limiting axial strain.

A summary of the cyclic stresses causing five percent strain in different numbers of stress cycles for samples consolidated under an initial lateral pressure of 1.05 kg per sq cm but with different principal stress ratios is shown on Fig. IV-30. It may be seen that the peak deviator stress required to cause 5% strain in a given number of cycles increases with increasing values of the principal stress ratio during consolidation.

For tests with K_c = 2.0 and 1.5, the boundaries between reversing and non-reversing stress conditions, which also represent the approximate boundaries between development of a transient state of liquefaction and no liquefaction, are indicated in Fig. IV-30. It may be seen that for failure in less than about 40 cycles (or more for lower K_c ratios) there will always be stress reversal resulting in some degree of liquefaction. Since the San Fernando Earthquake produced much less than 40 significant cycles, the development of large strains in soil elements consolidated under pressures of about 1 kg per sq cm during this earthquake loading would be expected to produce a transient liquefaction condition, as indicated by the development of peak pore pressures equal to the overburden pressure, even in the outer parts of the embankment of the Upper Dam.

A summary of the results of cyclic load tests on undisturbed hydraulic fill samples consolidated under lateral pressures of 2.15 kg per sq cm and at different principal stress ratios is shown on Fig. IV-31. These data have the same general form as the data from tests at the lower

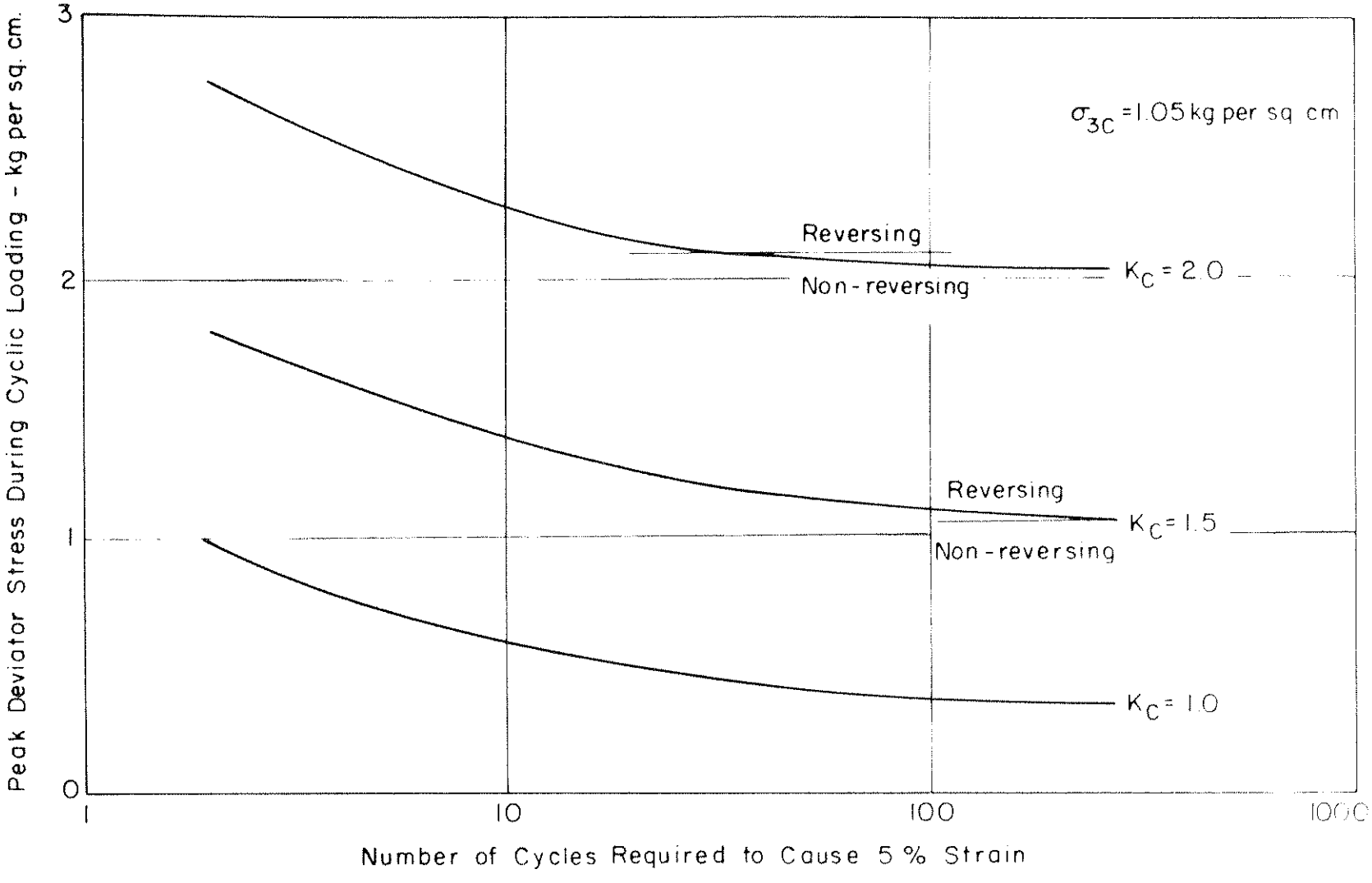

Fig. IV–30 RESULTS OF CYCLIC LOAD TESTS ON ANISOTROPICALLY CONSOLIDATED SAMPLES OF HYDRAULIC SAND FILL – UPPER SAN FERNANDO DAM.

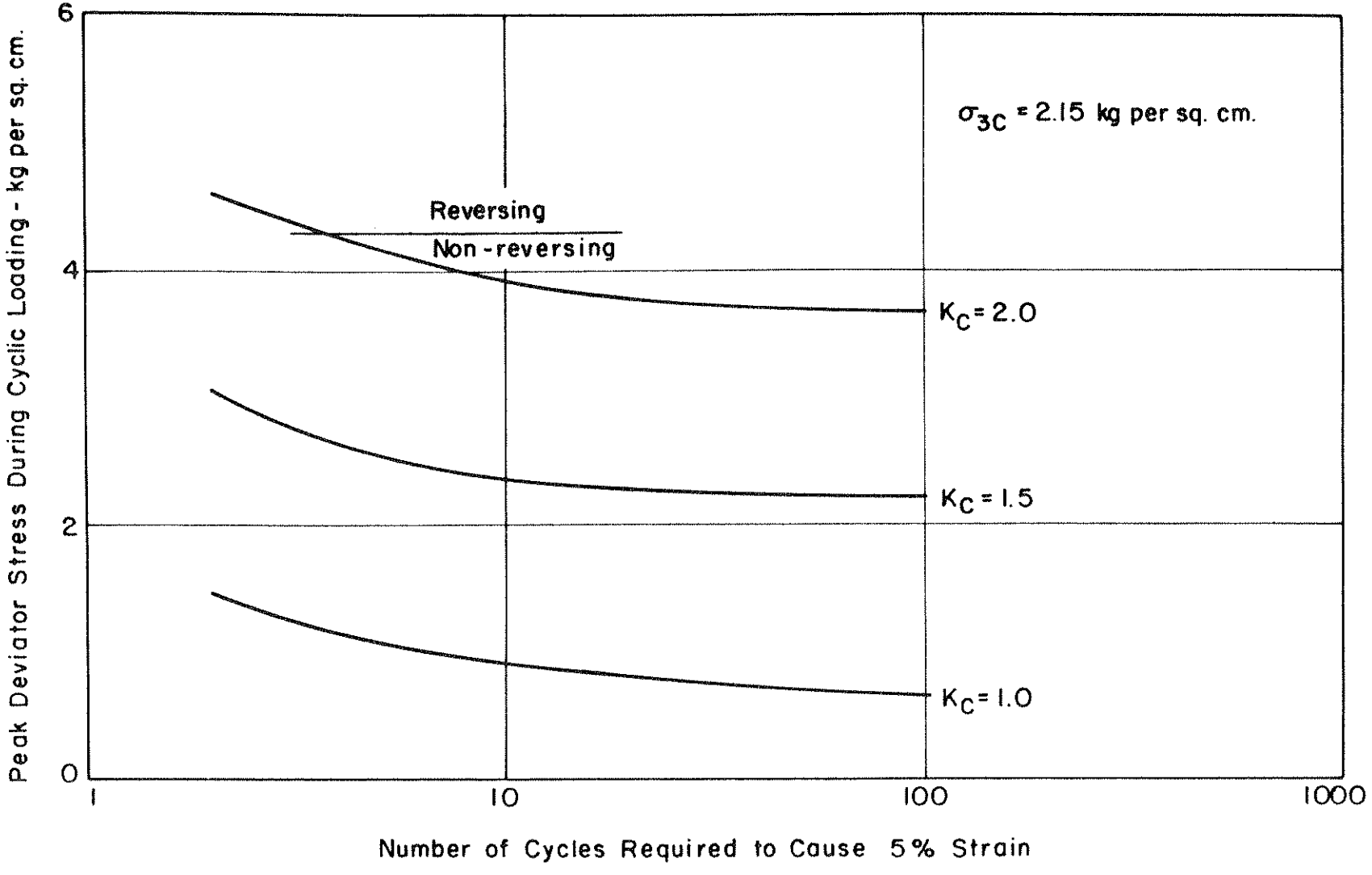

Fig. IV–31 RESULTS OF CYCLIC LOAD TESTS ON ANISOTROPICALLY CONSOLIDATED SAMPLES OF HYDRAULIC SAND FILL – UPPER SAN FERNANDO DAM.

consolidation pressure. However the limit between reversing and non-reversing stress conditions occurs at a lower number of cycles for this higher consolidation pressure condition. For samples consolidated under a principal stress ratio of 2, for example, the development of large strains in more than about 4 to 6 cycles would not be accompanied by even transient liquefaction. Thus under somewhat higher pressures in the embankment, development of large strains would not necessarily be associated with a large pore pressure increase for numbers of stress cycles which might develop during earthquakes.

The cyclic loading test data summarized on Figs. IV-30 and IV-31, together with similar data obtained for other failure strain criteria provide the basic data used in the dynamic analysis of embankment stability discussed in later sections of this report. For this purpose it is convenient to determine combinations of static and cyclic stress conditions causing limiting strains in a given number of stress cycles. The data from Figs. IV-30 and IV-31 is replotted in Fig. IV-32, for example, to show the maximum deviator stress developed during cyclic loading required to cause 5% strain and initial liquefaction in 2 cycles for samples consolidated to different values of minor principal stress and for different K_c values. Similar data obtained in tests on the hydraulic sand fill from the Lower Dam are included in this figure since they help to establish the positions of the curves at higher consolidation pressures.

Similar results for the cyclic stress conditions causing 5% strain and initial liquefaction in 5 cycles are shown in Fig. IV-33.

In utilizing the results of cyclic load tests in a dynamic analysis it is convenient to determine the deformations produced by known values

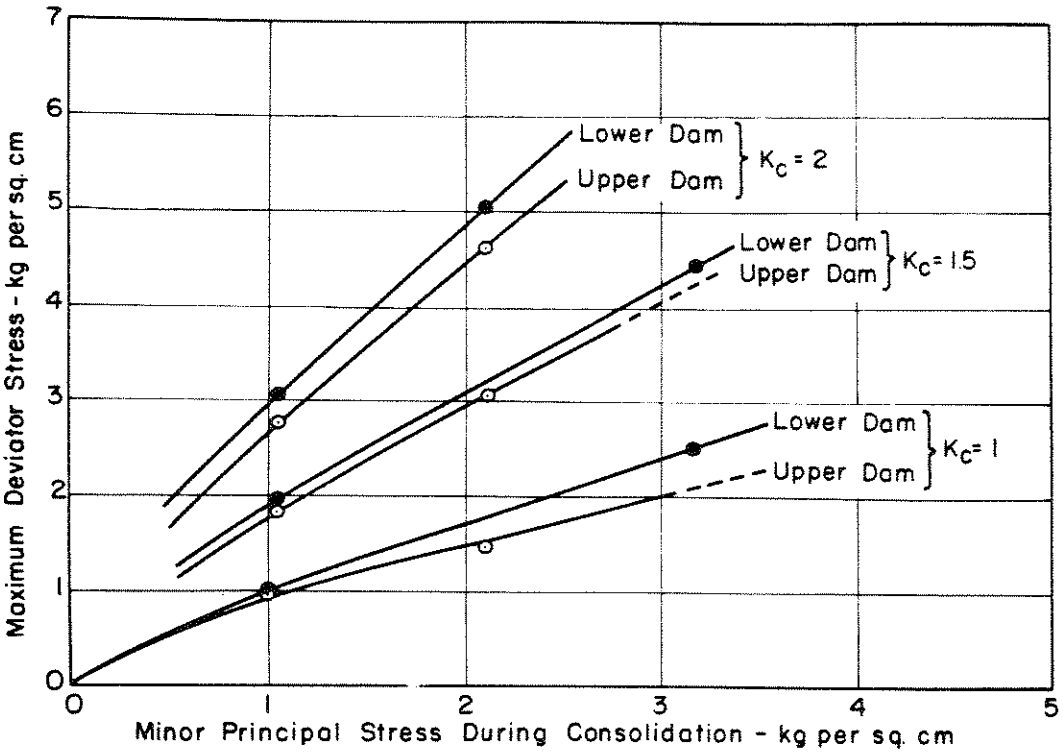

Fig. IV–32 CYCLIC STRESSES CAUSING LIQUEFACTION AND 5% STRAIN IN 2 CYCLES FOR HYDRAULIC SAND FILL.

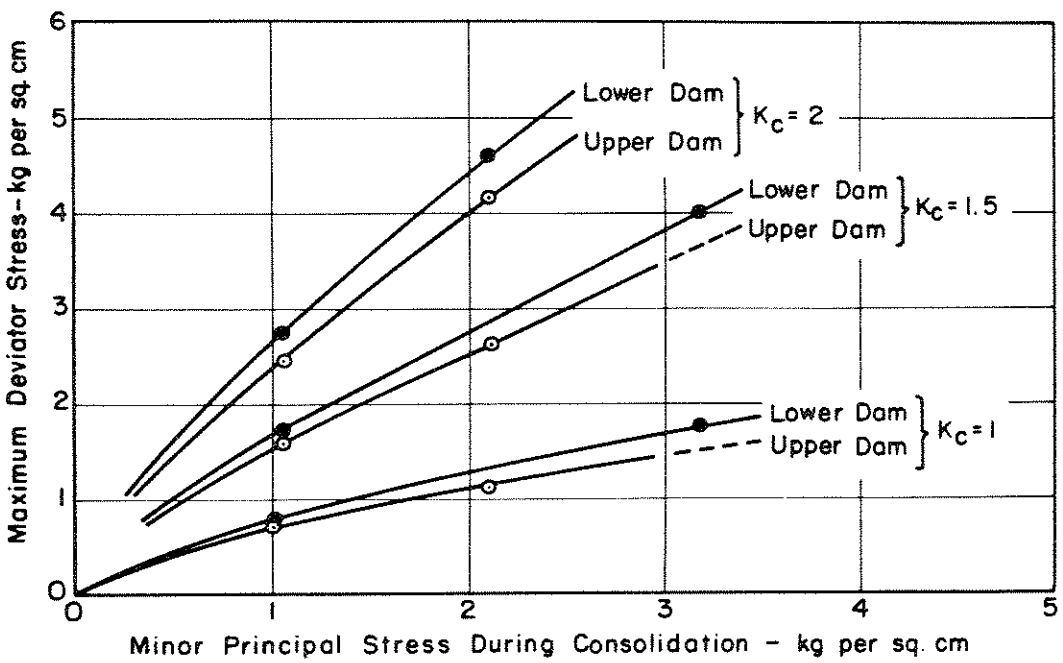

Fig. IV–33 CYCLIC STRESSES CAUSING LIQUEFACTION AND 5% STRAIN IN 5 CYCLES FOR HYDRAULIC SAND FILL.

of cyclic shear stress superimposed on the initial (pre-earthquake) static stress conditions. For this purpose the cyclic load test data presented in Figs. IV-32 and IV-33 must be interpreted in terms of the cyclic shear stress developed in the primary direction of potential failure.

For samples initially consolidated under an isotropic stress condition, representing soil elements in the field with zero shear stress on horizontal planes, the superimposed cyclic shear stress applied to such a plane may be taken as about 60% of the maximum shear stress in the laboratory test specimen (Seed and Peacock, 1971; Finn, 1972). For anisotropically-consolidated samples, it seems reasonable to assume that the primary direction of failure and movement will be along planes inclined at $45 + \phi'/2$ to the horizontal and thus the cyclic shear stress applied to such planes, for different values of the initial static stresses on these planes, may be determined by the construction procedure shown in Fig. IV-34.

Following these procedures the cyclic load test data in Figs. IV-32 and 33 leads to the results plotted in Figs. IV-35 and IV-36 respectively. In these figures, the initial static stress conditions on a soil element are expressed by the value of σ_{fc}, the normal stress on the potential failure surface when the element is in equilibrium before the earthquake, τ_{fc} the shear stress on the same surface at the same time and $\alpha = \tau_{fc}/\sigma_{fc}$. Values of the cyclic shear stress to be applied in the direction of potential failure to cause 5% axial strain in 2 and 5 cycles, for different initial stress conditions, are shown in the figures. The laboratory test data provides results for values of α equal to 0, 0.185 and 0.330. Stress conditions causing 5% strain for other values of α have been interpolated and plotted as shown.

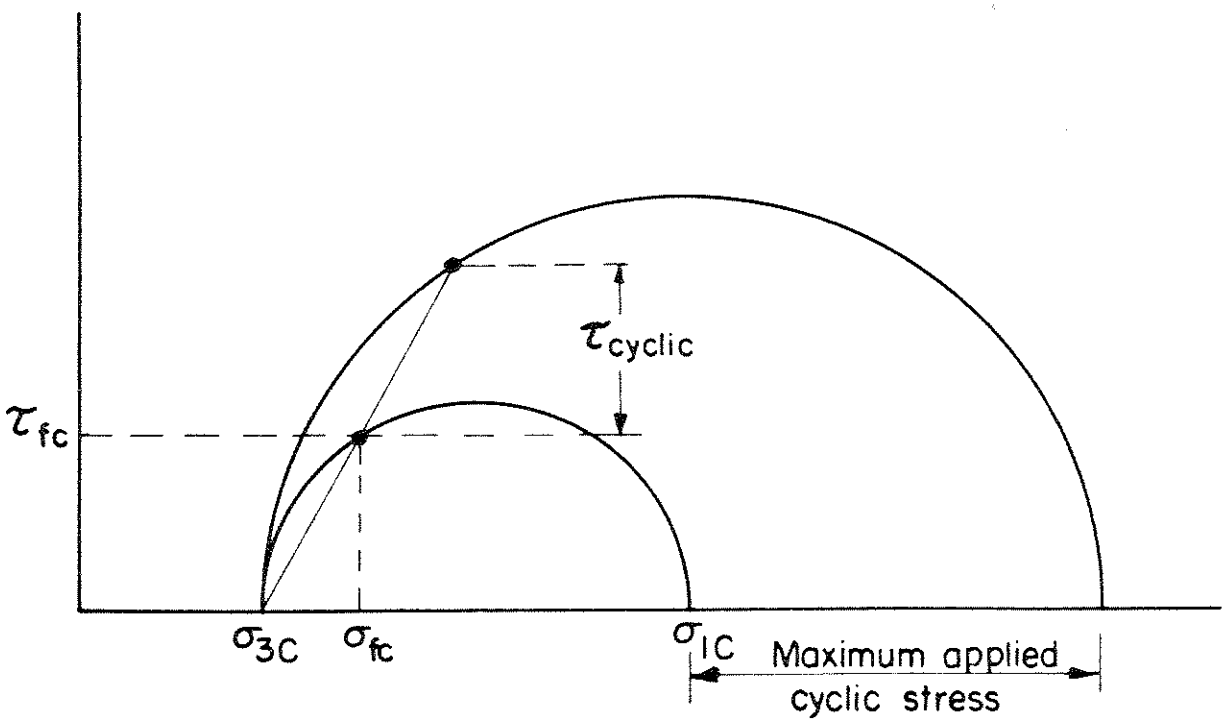

τ_{fc} = Initial shear stress on potential failure surface

σ_{fc} = Initial normal stress on potential failure surface

$\alpha = \tau_{fc}/\sigma_{fc}$

τ_{cyclic} = Cyclic shear stress developed on potential failure surface

Fig. IV-34 PROCEDURE FOR INTERPRETING CYCLIC LOAD TRIAXIAL TEST DATA TO DETERMINE CYCLIC SHEAR STRESS ON POTENTIAL FAILURE SURFACE.

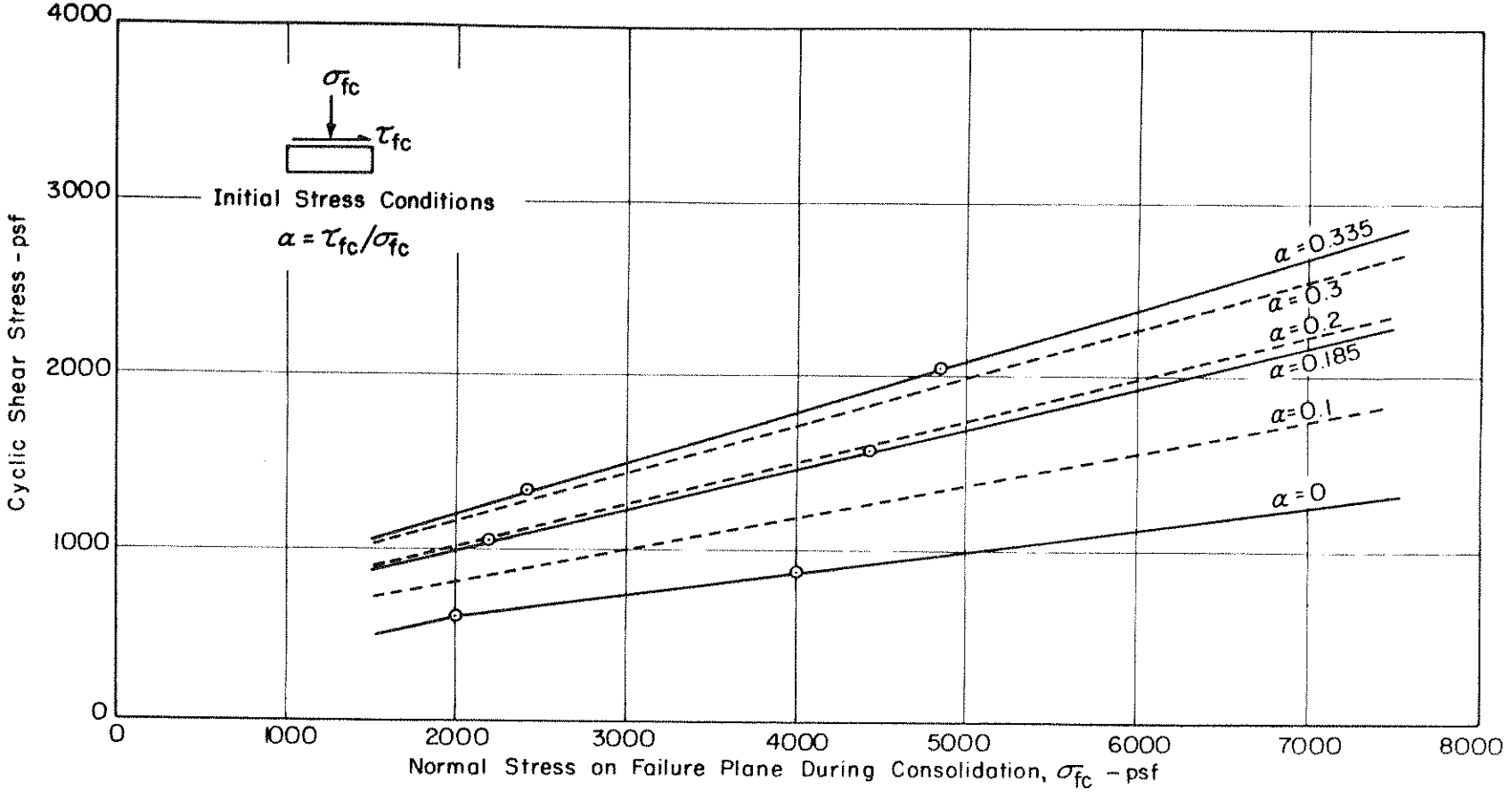

Fig. IV–35 CYCLIC STRESS CONDITIONS CAUSING 5% STRAIN AND LIQUEFACTION IN 2 CYCLES FOR HYDRAULIC SAND FILL – UPPER SAN FERNANDO DAM.

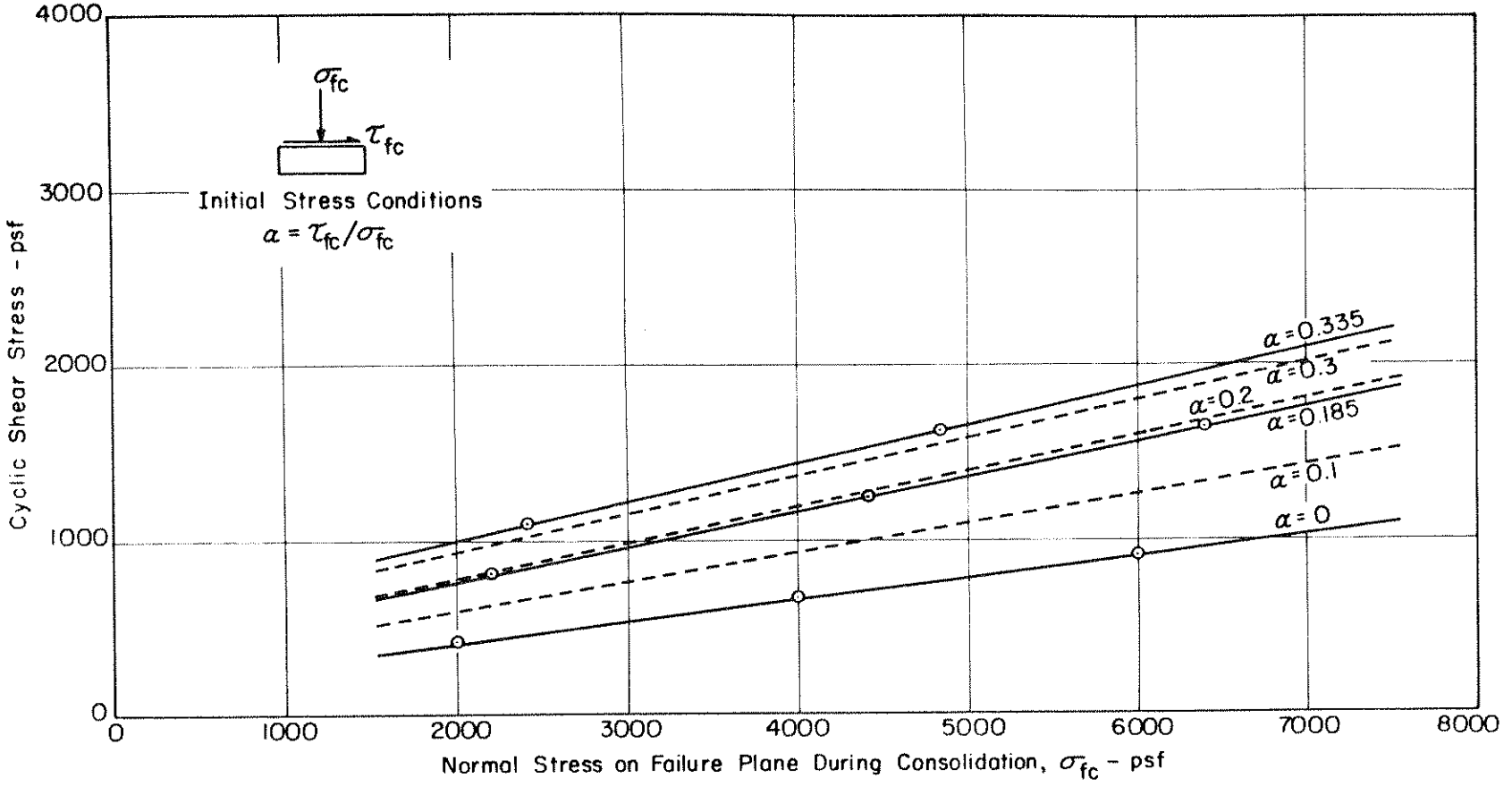

Fig. IV–36 CYCLIC STRESS CONDITIONS CAUSING 5% STRAIN AND LIQUEFACTION IN 5 CYCLES FOR HYDRAULIC SAND FILL – UPPER SAN FERNANDO DAM.

It may be noted that the shear strain in a test specimen of saturated hydraulic sand fill under plane strain conditions will be about twice the major principal strain in a triaxial compression test. Thus the stress conditions shown in Figs. IV-35 and 36 might be considered representative of those causing 5 percent axial strain or about 10 percent shear strain of soil elements on which they are developed.

Part V - Field and Laboratory Investigations--Lower San Fernando Dam

Introduction

In general the field and laboratory investigations for the Lower Dam were similar to those described for the Upper Dam, involving trenching, boring and sampling, and seismic surveys followed by both static and dynamic laboratory testing of the soil samples recovered. Because the Lower Dam was considerably larger and because the conditions were somewhat more complicated, the investigation at the Lower Dam was in many respects more detailed. However, because of certain similarities in materials it was possible to translate some of the experience gained from studies of the Upper Dam to the Lower Dam and thereby to curtail in some respects the extent of the soil testing programs.

Field Investigations

Large Trench Excavation

Although the downstream slope of the Lower Dam remained intact it was not practical to trench through this slope into the hydraulic fill. As shown in Fig. II-3, a large berm of dense rolled fill had been placed over the downstream hydraulic fill in 1940. The upper part of the remaining crest of the dam was also a rolled fill. Thus the sections of hydraulic fill which remained undisturbed following the earthquake were buried too deeply below the rolled fills to make it practical to expose them by trenching from the surface. It was therefore necessary to investigate this undisturbed portion of the hydraulic fill by means of drill holes.

However, it was considered essential to cut a trench through the slide debris on the upstream face of the dam in order to expose the

hydraulic fill in that zone and locate failure zones or surfaces that developed during the sliding. Accordingly a large trench was excavated into the slide debris on the upstream face at about the position of the central tower which had failed during the earthquake. A photograph of the western face of this trench is shown in Fig. V-1. The maximum depth of the trench was about sixty feet and the base was still about twenty feet above the top of the alluvium.

The trench exposes most of the significant zones of fill as they appeared in their displaced positions following the slide. The upper part of the excavation exposes the rolled fill, under which is the relatively thin zone of hydraulically placed ground-up shale. These two zones are almost indistinguishable from each other, and even on close examination it was not possible to clearly define the boundary between them.

Immediately below the rolled and ground-shale fill is a zone of medium to coarse sand. In the field it had a bright yellow color and in the photograph it appears as a light colored zone. It was about four feet thick where it intersected the upstream face and tapered to almost zero thickness towards the left side of the photograph. In the extreme lower right hand corner of the photograph more of this same zone of soil is seen. Apparently during the slide a large block of soil slid down the present slope, twisted somewhat in the process and came to rest with horizontal layers in almost a vertical position.

Below this marker bed of yellow sand are a large number of alternating light and dark layers of relatively undisturbed hydraulic fill. The fill in this zone closely resembled the undisturbed hydraulic fill exposed in the trenches at the Upper Dam. The darker layers are silty to clayey material and the lighter layers are fine to coarse sands. These layers were more or less horizontal except toward the left hand side of the

FIG. V-1 PHOTOGRAPH OF TEST TRENCH THROUGH A PORTION OF THE SLIDE DEBRIS - LOWER SAN FERNANDO DAM

photograph where they begin to curve noticeably downward; presumably they were pushed into this position by the slide movements.

Below and to the left of this stratified hydraulic fill was a large dark zone of homogeneous clay. This appears to have been the displaced clay core of the dam which had been pushed out into the sand layers of the hydraulic fill during the slide. The lower portions of the hydraulic fill exposed in the trench to the right of this mass of clay showed considerable disturbance.

A similar photograph of the trench section is presented in Fig. V-2. Superimposed on this photograph are a number of letters designating points of interest. Close-up photographs of the soil at these points are presented in Figs. V-3 to V-9.

Fig. V-3 shows a close-up view at the location of point A, where a block of the upper rolled fill material had moved down and sheared into the layered hydraulic fill without creating significant disturbance in either zone. The contact shear zone between these two types of soil is readily apparent in the photograph. Fig. V-4 shows a close-up view of the light colored sand layer described previously; originally a horizontal layer above the hydraulic fill and below the rolled fill, the portion shown in this photograph had apparently slid down from its original position and tilted to an almost vertical orientation. The broken outlet tower is shown in the background of the photograph some fifty feet away.

Fig. V-5 shows a close-up view of location C at the contact between the clay core and the hydraulic fill. The contact is close to the position of the geological hammer. To the right of the contact the layers of sand in the hydraulic fill are seen to be considerably disturbed. To the left of the geological hammer there are several cracks in the clay core.

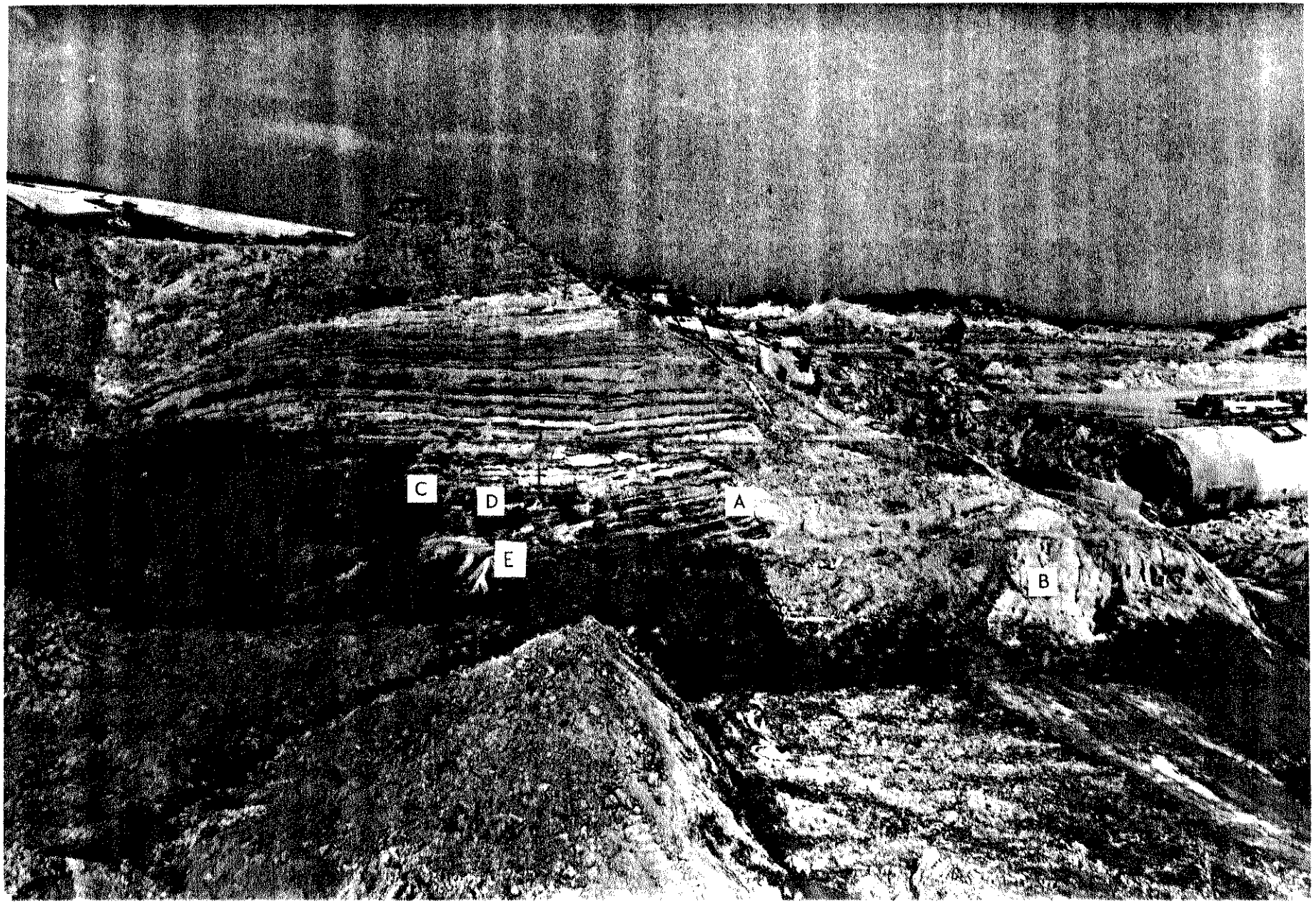

FIG. V–2 VIEW OF TEST TRENCH THROUGH SLIDE DEBRIS OF LOWER DAM SHOWING LOCATIONS OF ENLARGED PHOTOGRAPHS.

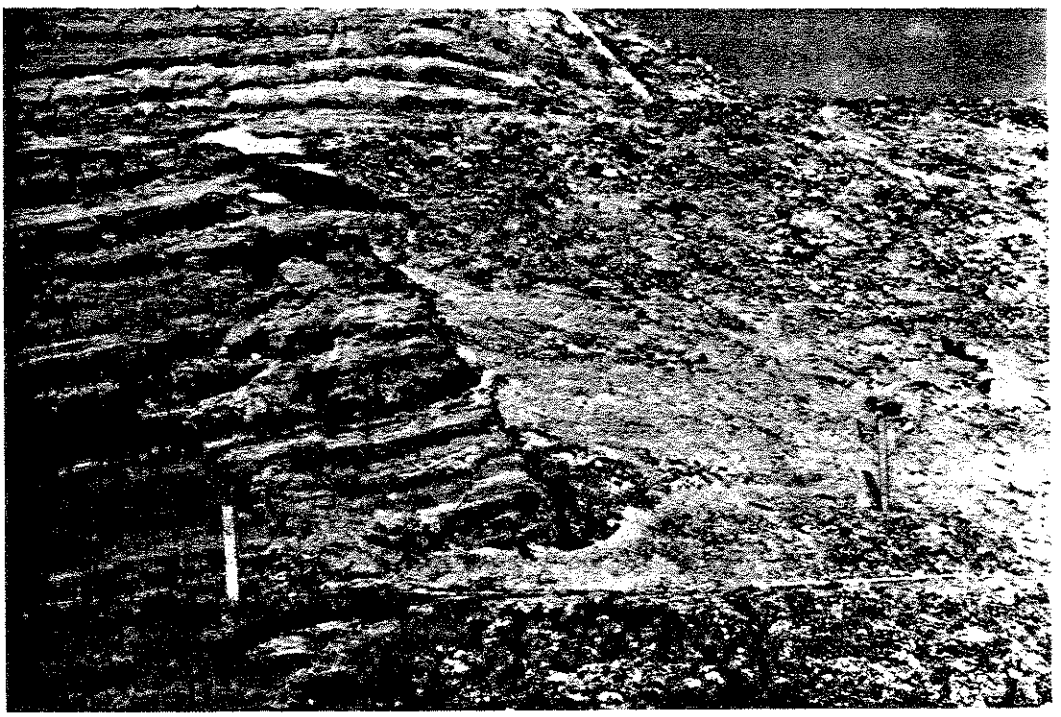

FIG. V-3 ENLARGED VIEW OF LOCATION A ON FIG. V-2
ROLLED FILL SHEARED DOWN OVER THE HYDRAULIC FILL.

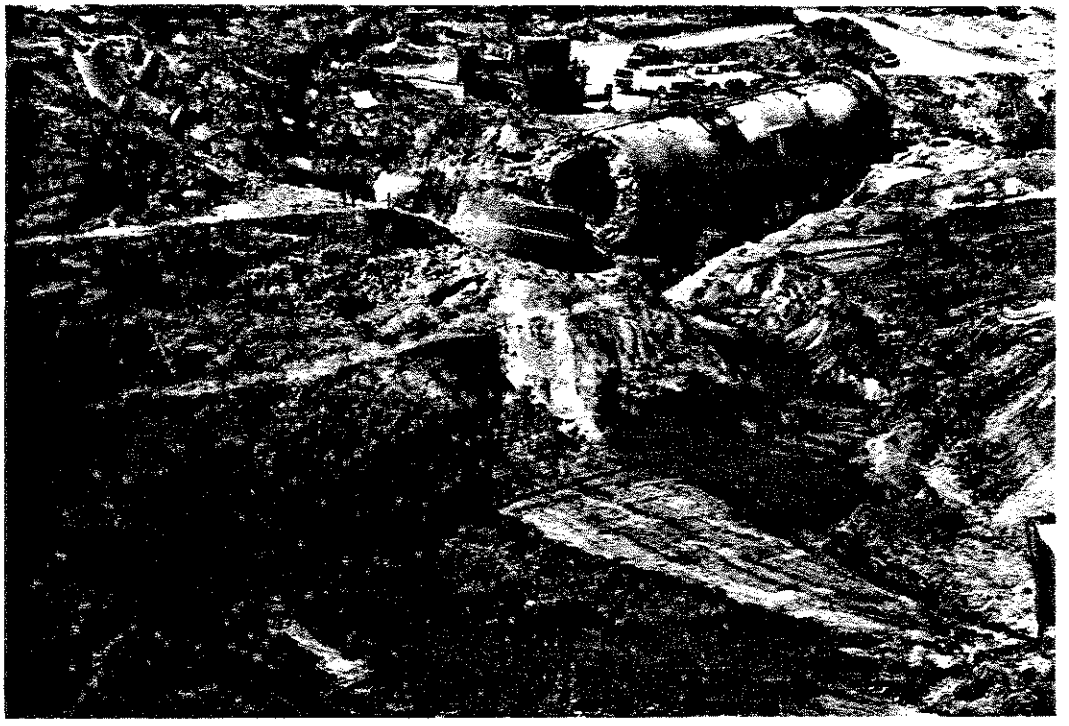

FIG. V-4 ENLARGED VIEW OF LOCATION B ON FIG. V-2. LIGHT COLORED MARKER BED OF SAND FROM TOP OF HYDRAULIC FILL SLID DOWN TO LOWER POSITION.

A close-up of one of these cracks is shown in Fig. V-6. The crack is filled with sand. It has a vertical orientation and presumably developed during the slide becoming filled with sand as a result of liquefaction in this zone of the embankment.

Two close-up views near location D are shown in Figs. V-7 and V-8. The dark material on top was a layer of sandy clay overlying the lighter layer of fairly clean sand. No doubt these layers were originally fairly smooth as shown in the undisturbed part of the hydraulic fill in Fig. V-1. However the movements during the slide have created shear zones through these layers of sand and clay which are clearly visible in the photograph. Although some of the cleaner sand has penetrated into cracks in the clay, the clearly defined shear zones in the light colored sands indicate that these materials did not liquefy during the earthquake. The relative movements in this zone appear to have occurred along shear surfaces rather than resulting from flow of a viscous material such as liquefied sand. However the sand-filled crack in Fig. V-3 would seem to indicate some degree of liquefaction of the sand.

Near the bottom of the trench, location E, there was strong evidence of liquefaction of the sandy materials. A close-up view of this area is shown in Fig. V-9. A vertical tongue or dyke of light colored sand had extruded up through the darker soils, producing a configuration which could only have occurred if the sand dyke were moving as a fluid. Had there been a very shallow overburden of soil at this site, it is quite possible that the light colored sand dyke would have reached the surface and formed a sand boil. It will be recalled that sand boils were found near the upstream toe of the debris where the overburden was very thin (Fig. III-23).

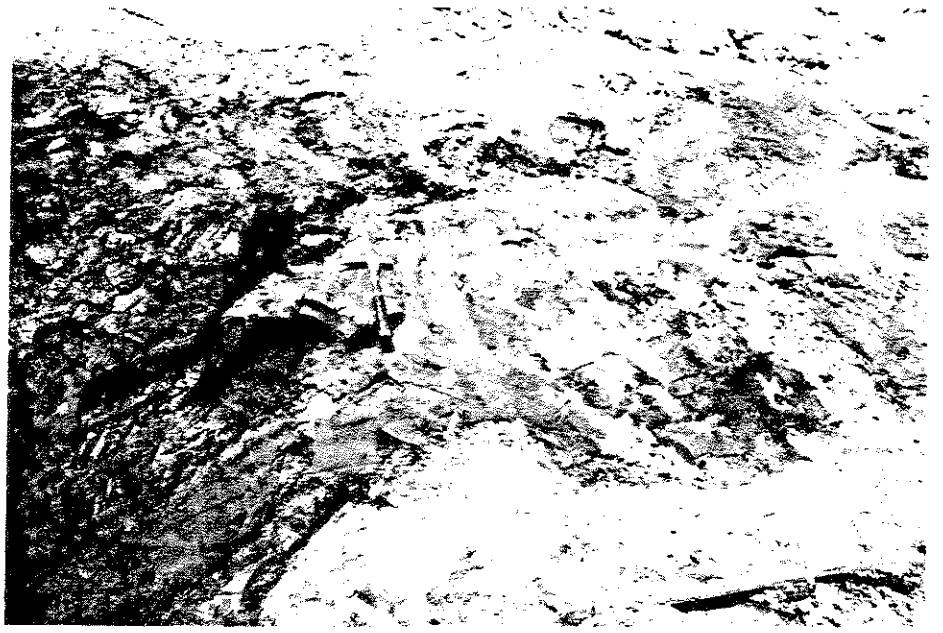

FIG. V–5 ENLARGED VIEW OF LOCATION C ON FIG. V–2. CLAY CORE AT LEFT HAS PUSHED INTO AND OVER LAYERS OF HYDRAULIC SAND FILL.

FIG. V–6 ENLARGED VIEW OF CRACK IN CLAY CORE TO LEFT OF HAMMER SHOWN ON FIG. V–5 – NOTE FRESH CRACK IN CLAY FILLED WITH SAND WHICH ENTERED DURING THE SLIDING.

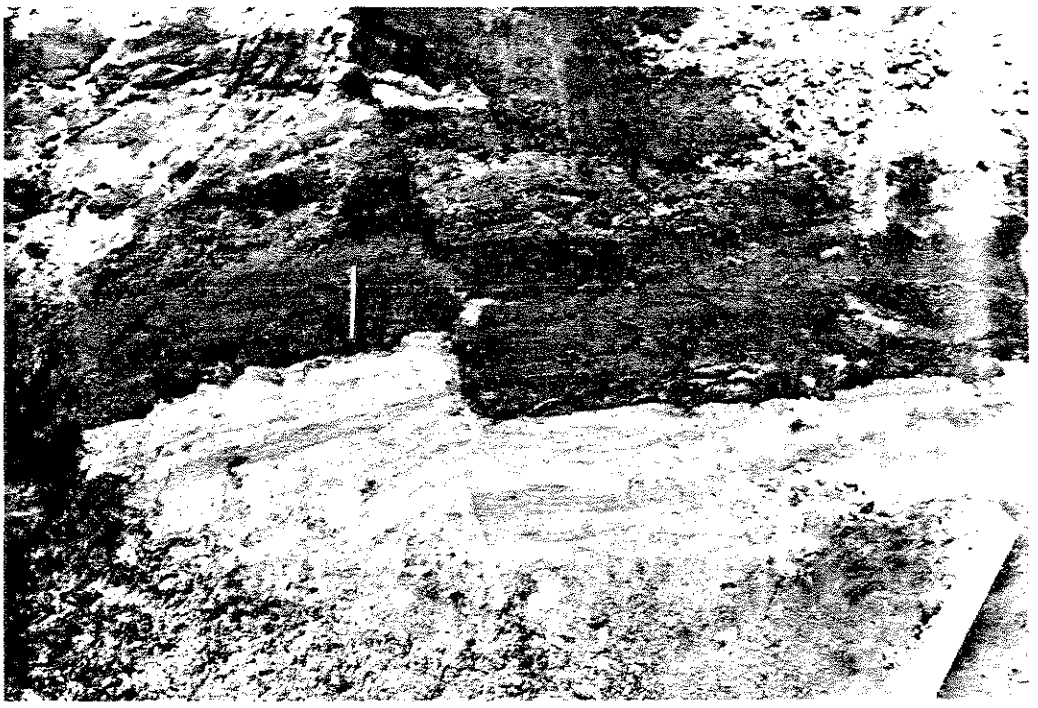

FIG. V–7 ENLARGED VIEW OF LOCATION D ON FIG. V–2. SAND HAS BEEN SHEARED AND DISTORTED IN SLIDE MOVEMENT

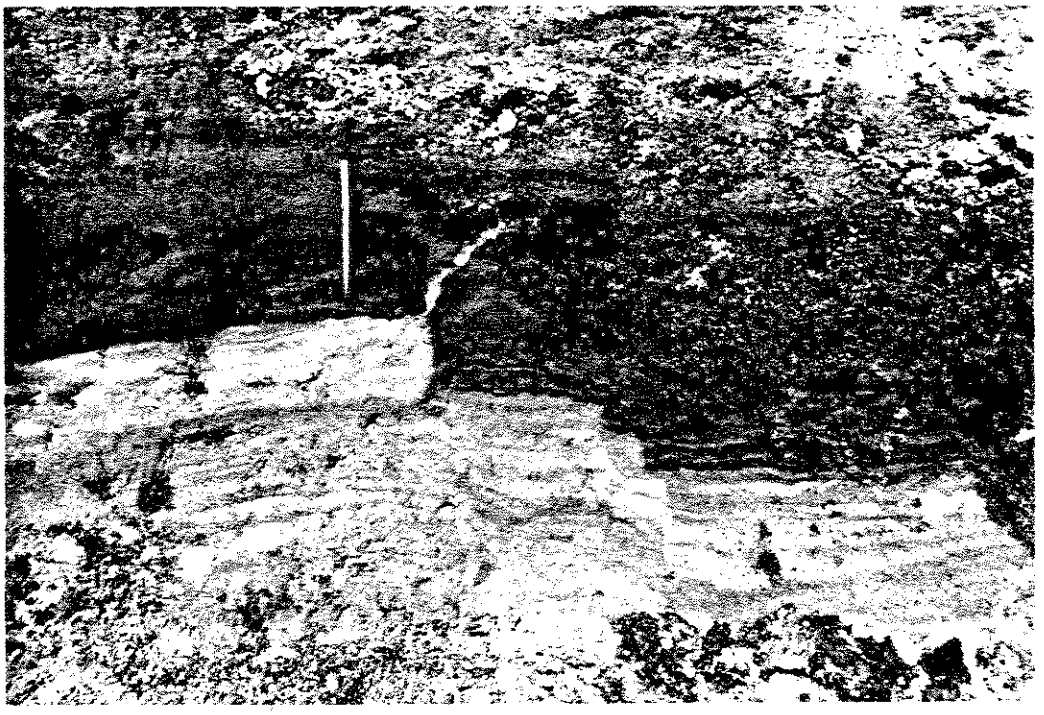

FIG. V–8 ENLARGED VIEW, NEAR LOCATION D ON FIG. V–2. SAND LAYER IN HYDRAULIC FILL HAS BEEN DISTORTED AND SHEARED DURING SLIDE.

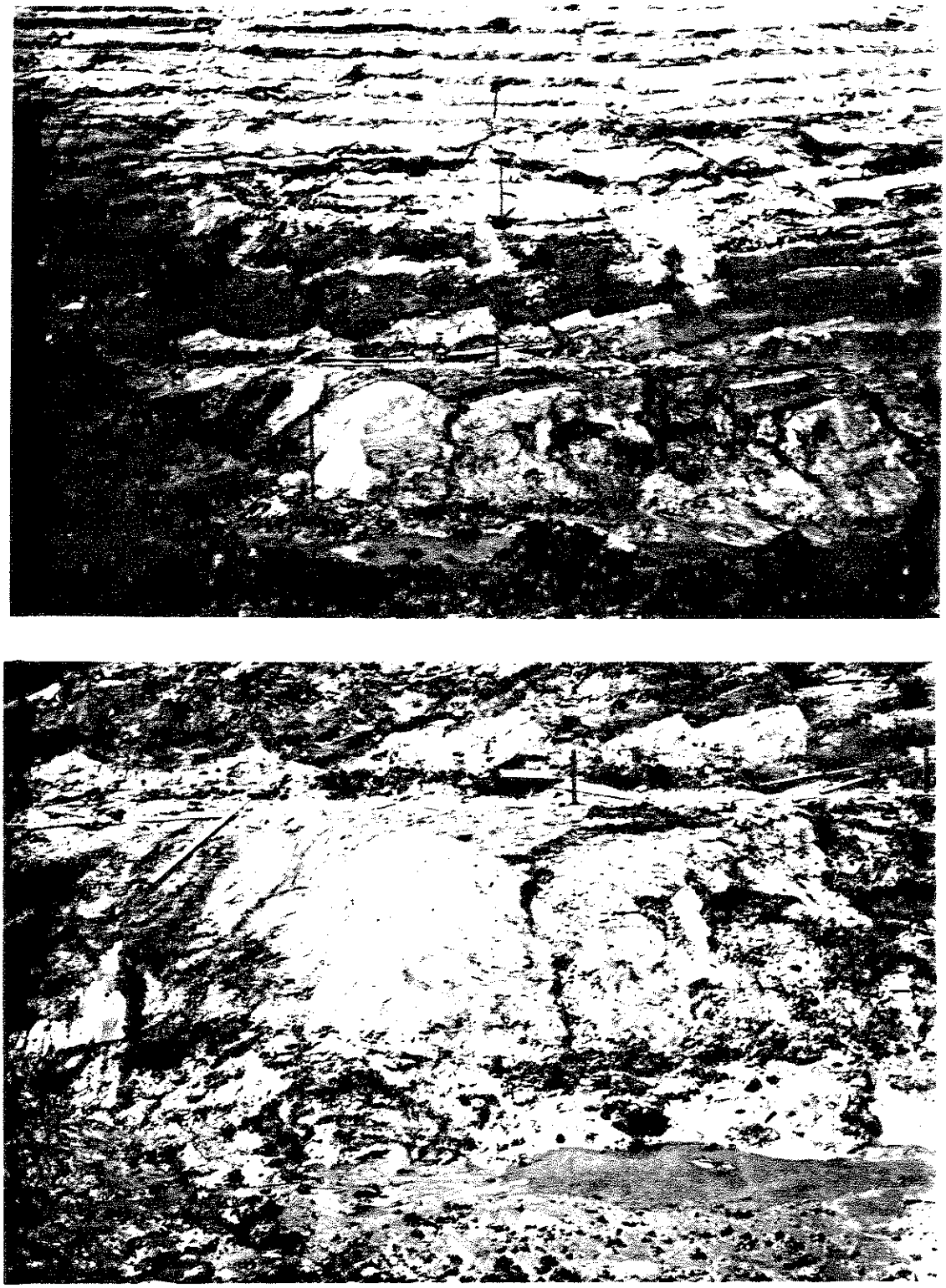

FIG. V-9 ENLARGED VIEWS OF LOCATION E, IN FIG. V-2. THE LIGHT COLORED VERTICAL ZONE AT THE BOTTOM OF THE PHOTOGRAPH IS A SAND DIKE OF LIQUEFIED SAND WHICH HAS BEEN EXTRUDED UPWARD FROM BELOW.

When the trench section had been cut to a depth of about 60 ft there were indications that the slope was becoming unstable, and it was considered unsafe to carry the excavation any deeper. Work was therefore discontinued for a few weeks to give the soil a chance to drain and further excavation was then continued by means of a slit trench, as shown in Figs. V-10 and V-11. This trench extended about sixteen feet below the base of the large trench before it had to be discontinued because of incipient failures in the side walls.

Most of this trench was cut through heavy clay material displaced from the core of the dam. The clay exposed in the walls of this deeper trench also contained a number of near-vertical cracks which were filled with sand (see Fig. V-12). Very soon after excavation ceased the eastern wall of the trench collapsed. (The beginning of the failure can be seen at the bottom of the trench of Fig. V-11.) The failure occurred along several of the sand-filled cracks within the clay. These sand-filled cracks could only have developed during the slide when the sand liquefied and flowed as a fluid into the fissures which developed in the distorting clay core.

Fortunately the trench remained open long enough to permit a careful inspection of the walls. A close-up view of the trench wall near the base is shown in Fig. V-13. The material at the upper part of the photograph is a homogeneous stiff clay. From about the middle of the photograph to the bottom, pockets of sand about the size of baseballs, can be seen mixed within this homogeneous clay. It seems likely that these sand pockets were formed by the clay sliding over a bed of sand which had very little strength such that it could be picked up and mixed in the clay. This photograph was taken some 70 feet or more below the original surface

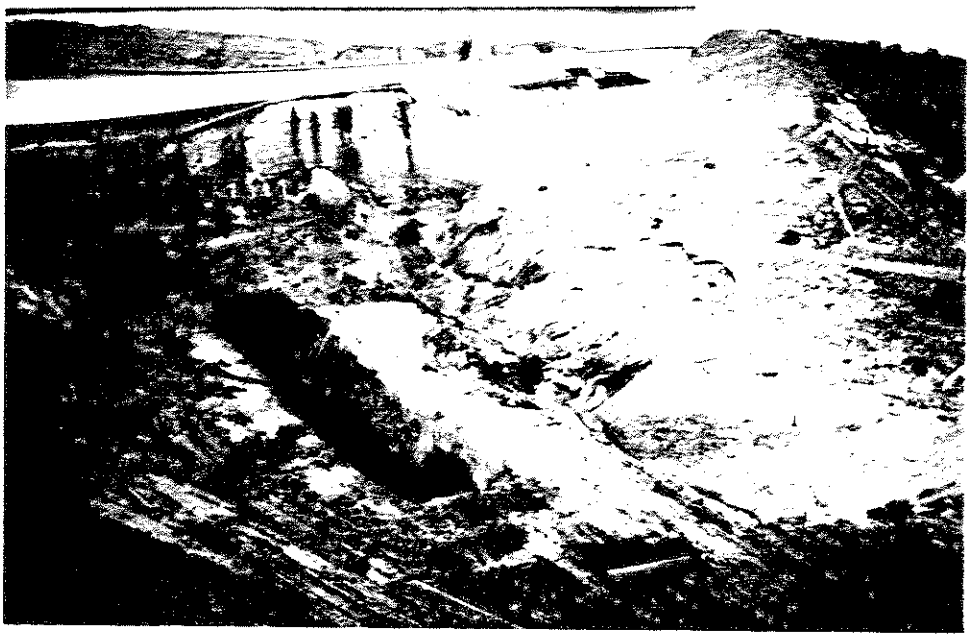

FIG. V-10 SLIT TRENCH EXCAVATED SOME 16 FT INTO BASE OF LARGE INSPECTION TRENCH.

FIG. V-11 CLOSE UP VIEW OF SLIT TRENCH SHOWN IN FIG. V-10. NOTE FAILURE JUST BEGINNING AT THE LEFT LOWER SIDE.

FIG. V-12 CLOSE UP OF ONE VERTICAL SAND-FILLED CRACK IN THE CLAY CORE. CRACK IS ABOUT 3/4 INCH WIDE.

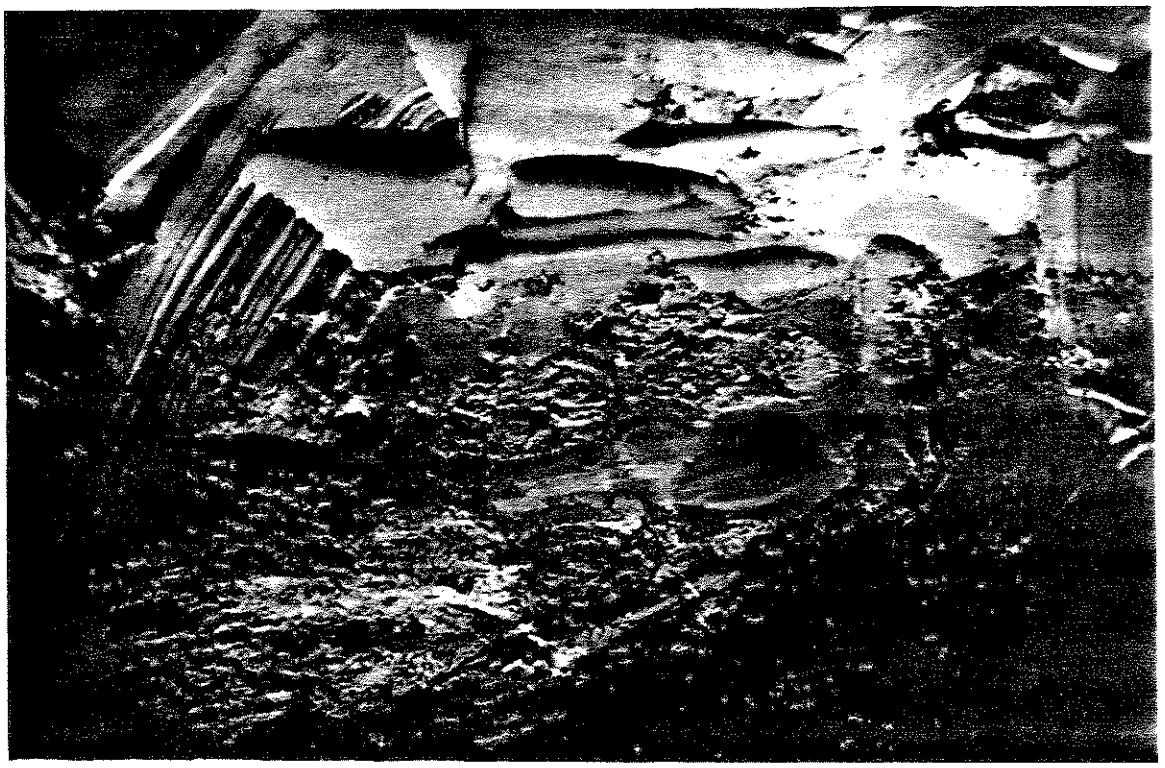

FIG. V-13 SAND POCKETS EMBEDDED IN CLAY IN THE LOWER PART OF THE SLIT TRENCH.

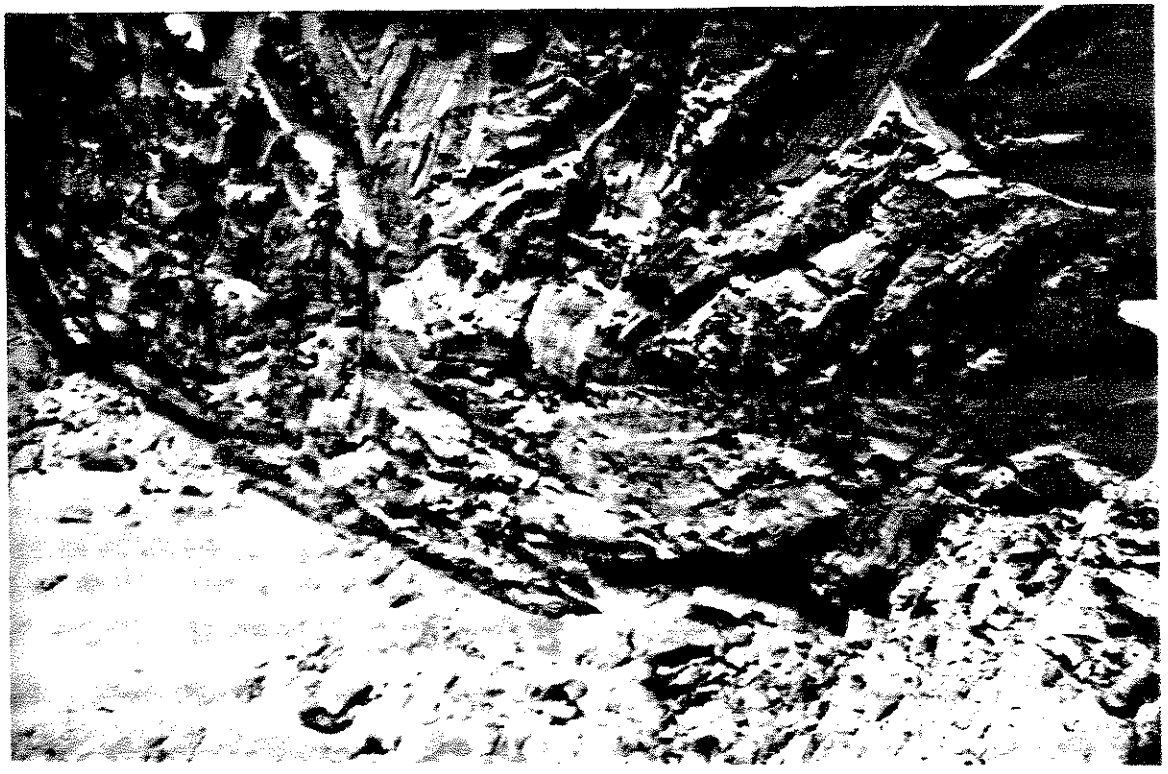

FIG. V-14 WATER BEARING SAND BELOW THE CLAY AT THE BASE OF THE SLIT TRENCH.

of the dam where, without liquefaction, the sand would have had considerable strength as a result of the heavy overburden pressure. Any static failure which would occur at this depth without liquefaction would presumably have been within the weaker clay materials. The fact that the sand had been picked up and molded into the clay material strongly suggests that the sand must have been weakened considerably if not completely liquefied as a result of the earthquake.

A close-up view of the bottom of the trench is shown on Fig. V-14. This photograph was taken at a location about two feet below Fig. V-13 and shows the presence of water bearing sand below the upper clay core material. The homogeneous clay extends about 15 feet vertically above the underlying sands. The bottom of the trench is still about four feet above the alluvium and is therefore still within the hydraulic fill. The relative position of a thick layer of clay overlying sand is not at all typical of hydraulic fill in a normal condition. The clay must have been moved into its position over the sand sometime during the slide.

The information gained from examination of the soils exposed by the trenches through the slide debris on the upstream face of the dam indicates that liquefaction did not occur within the hydraulic fill in the upper regions towards the outside face of the dam. On the other hand the evidence suggests that liquefaction did occur within the hydraulic sand fill in the lower central regions, and as a result, clay material from the central core was able to move out in an upstream direction over this liquefied zone. As it did so some of the liquefied sand became mixed with the lower portion of the clay, and in some cases where cracks developed some of the liquefied sand was extruded upwards filling cracks and forming sand dykes. On the upper surface of this tongue of clay which

was pushed out into the sand, the clay merely pushed aside and through the layers of hydraulic fill, bending and shearing the previously horizontal stratifications.

Boring and Sampling

Two types of boring and sampling were carried out at the Lower Dam. By far the greatest amount of boring was done in exactly the same way as for the Upper Dam using 6 inch diameter uncased auger holes and drilling mud. A total of 19 of this type of drill holes were made along four sections across the dam from the surface of the slide debris as well as from the surface of the downstream slope.

A plan view of the Lower Dam, showing the location of these 19 holes is presented on Fig. V-15. Cross-sections DD, EE, FF and GG through the dam are shown in Figs. V-16 to V-19 respectively. These four sections show in dashed outline the original profile of the dam, and in bold outline the surface profile of the dam as it was surveyed after the slide and after the water in the reservoir had been removed. An abbreviated log for each of the drill holes is also shown on these sections.

Following the same procedure as used for the Upper Dam a standard penetration test and an undisturbed three inch diameter Shelby tube sample were taken every five feet in each of the borings. Standard penetration resistance values for the soils are also shown with the abbreviated drill logs on the sections. The blow counts within the sandy layers appeared to be a little higher than those measured at the Upper Dam. However, the depth of these layers was also somewhat greater than for the Upper Dam, which would account for some increase in penetration resistance.

The large trench excavation discussed in the previous section was made along Section E-E. An outline of this trench is shown on the drawing

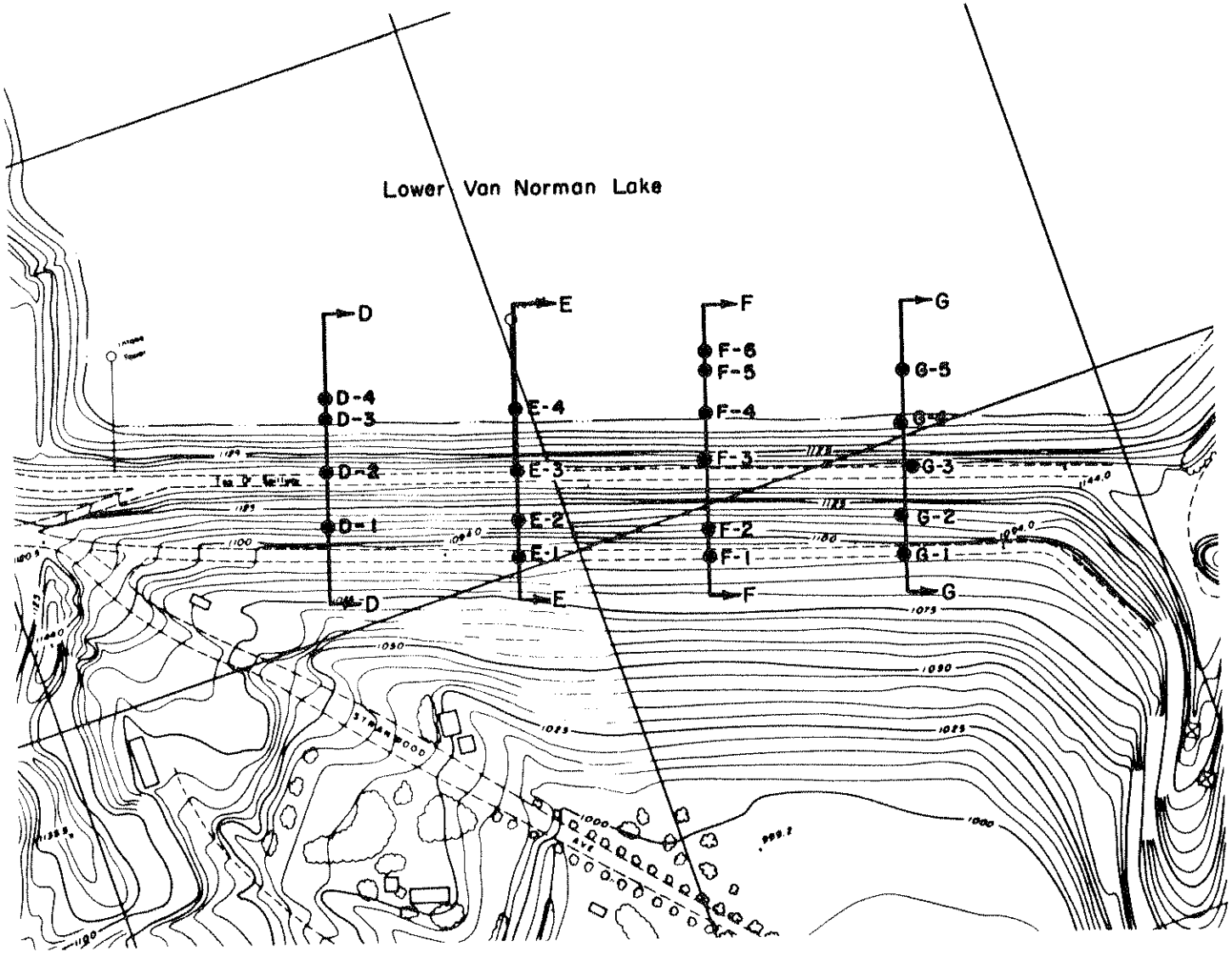

Fig. V–15 PLAN OF LOWER SAN FERNANDO DAM.

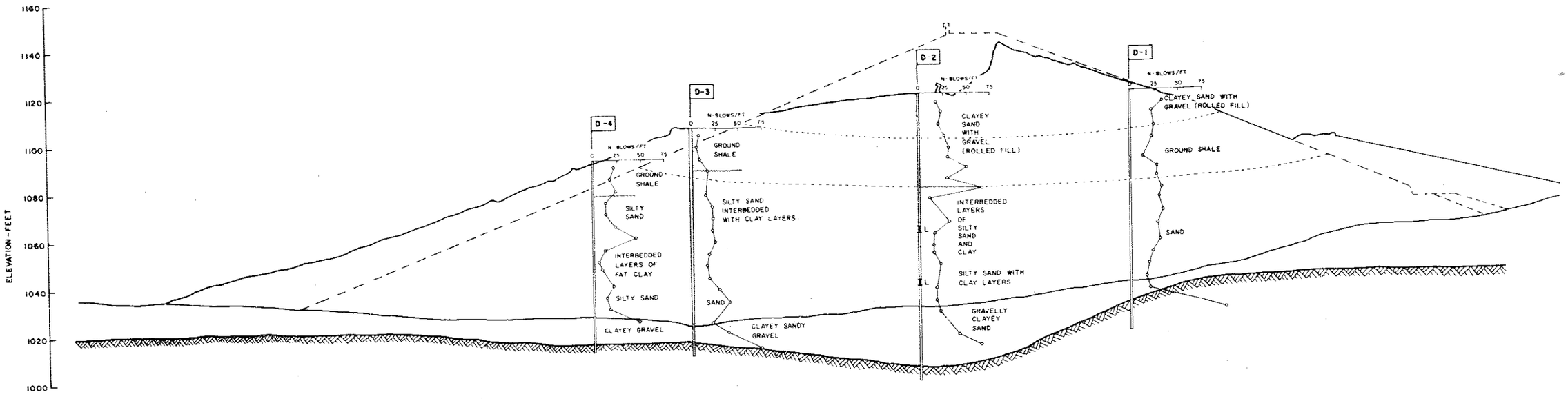

IL LIQUEFIED ZONE

Fig. V-16 CROSS-SECTION THROUGH EMBANKMENT OF LOWER SAN FERNANDO DAM AFTER EARTHQUAKE, SECTION D-D

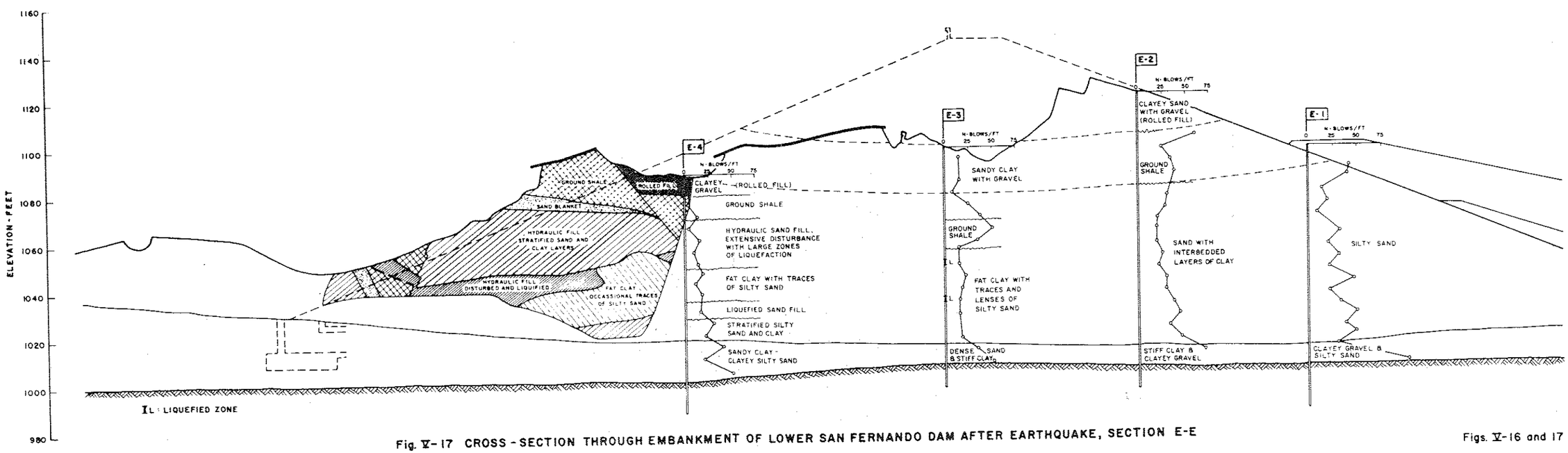

IL : LIQUEFIED ZONE

Fig. V-17 CROSS-SECTION THROUGH EMBANKMENT OF LOWER SAN FERNANDO DAM AFTER EARTHQUAKE, SECTION E-E

Figs. V-16 and 17

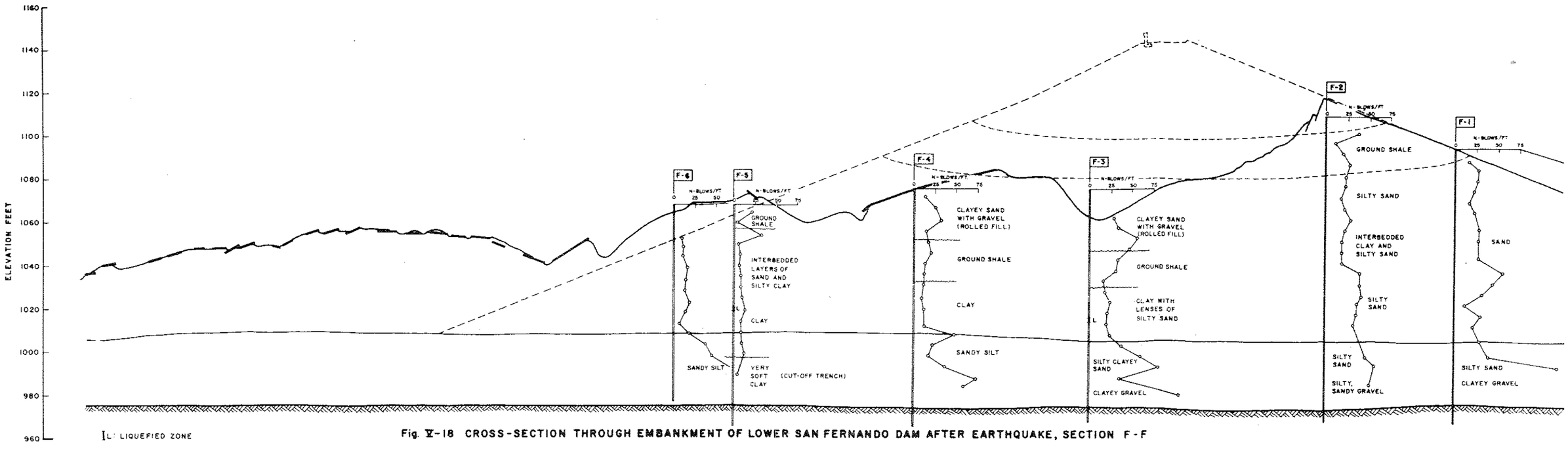

Fig. V-18 CROSS-SECTION THROUGH EMBANKMENT OF LOWER SAN FERNANDO DAM AFTER EARTHQUAKE, SECTION F-F

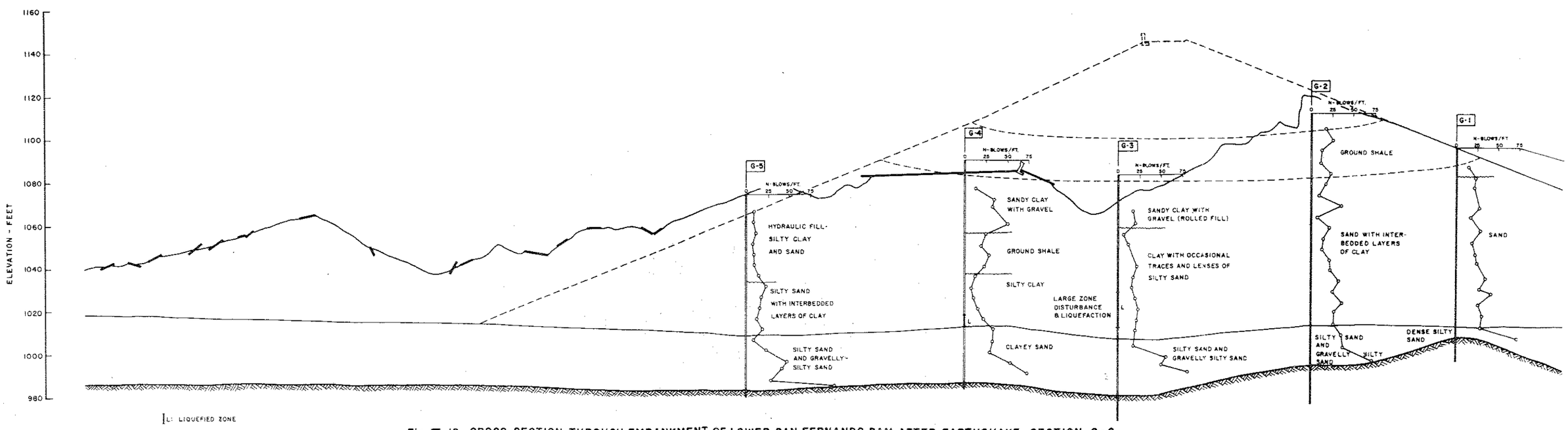

Fig. V-19 CROSS-SECTION THROUGH EMBANKMENT OF LOWER SAN FERNANDO DAM AFTER EARTHQUAKE, SECTION G-G

Figs. V-18 and 19

of Section E-E, Fig. V-17. The major zones of soil found on the walls of this trench excavation are also shown on Fig. V-17.

The information obtained from the trench excavation and from the drilling and sampling program as shown on these four sections, provided the basic data for determining the nature of the soil within the dam, and for analyzing the movements that occurred as a result of the earthquake. Reference to the sectional views, shows that the holes drilled from the downstream berm of the dam passed through soil which did not participate in the slide and was therefore probably not seriously disturbed as a result of the earthquake. For this reason, the undisturbed Shelby tube samples from the downstream holes were used exclusively for the laboratory strength tests. On the other hand, the holes drilled through the central and upstream portions of the dam passed through materials which participated in the slide and were probably significantly disturbed because of the slide movements. Shelby tube samples from these areas were therefore used only to identify the nature and extent of the slide movements which occurred.

Each of the Shelby tube samples from the central and upstream holes was split open in a longitudinal direction and carefully examined for evidence of disturbance during the slide. Photographs of the soil in two of these tubes are shown in Fig. V-20. The soil in Fig. V-20a consisted of stratified hydraulic fill overlying alluvium. The contact between these two zones is clearly evident in the photograph. The hydraulic fill consisted of numerous very thin layers of silty sand sandwiched between thicker layers of clay. All of the layers were plane and well defined indicating that there had been virtually no disturbance of the soil in this zone.

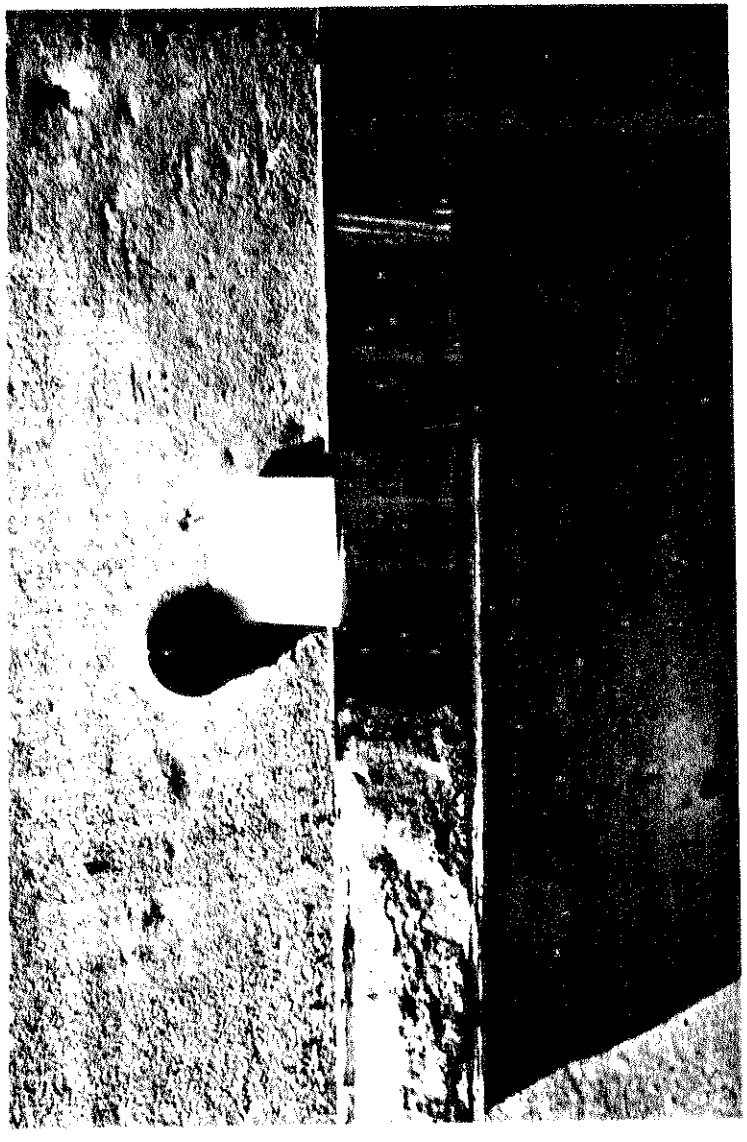

(a) HYDRAULIC FILL ABOVE ALLUVIUM – NO LIQUEFACTION.

(b) SAND MIXED WITH CLAY IN STREAKS INDICATES LIQUEFACTION.

FIG. V–20 EXAMPLES OF SHELBY TUBE SAMPLES OF SOIL FROM THE LOWER DAM

In contrast, the soil in the Shelby tube shown on Fig. V-20b, consisted of very distorted streaks of sand and clay. There had obviously been a considerable amount of disturbance which could only have been produced by the sand losing strength and mixing with the clay.

Close-up views of two other Shelby tube samples are shown in Fig. V-21. These photographs show dark streaks of clay and silty sand distorted and mixed in a zone of lighter colored sand, again indicating a large amount of disturbance. The pattern of coarse streaks within the sand shown in Fig. V-21 could only have formed if the sand had been in a very weak or liquefied condition.

These four photographs are typical of the soil that was found within the Shelby tubes taken from drill holes in the slide area through the upstream portion of the dam. Many of the samples showed no disturbance whatsoever while other samples showed a considerable amount of disturbance. The nature of each of these samples was recorded and noted on the drill hole logs. The major zones of liquefaction disturbance as indicated above were noted on the drill logs and shown on the four sections through the dam, Figs. V-16 to V-19. As described in a subsequent section, these zones of disturbance played a key role in helping to reconstruct the movement which occurred as a result of the earthquake.

The Shelby tube samples from holes made in the downstream portion of the dam were shipped to the laboratories for strength testing purposes. The same procedure for sample preparation and testing employed with samples from the Upper Dam was followed for samples from the Lower Dam. The Shelby tubes, still full of soil, were sawn in seven inch lengths and then the soil within each short length of tube was extruded, examined, and tested.

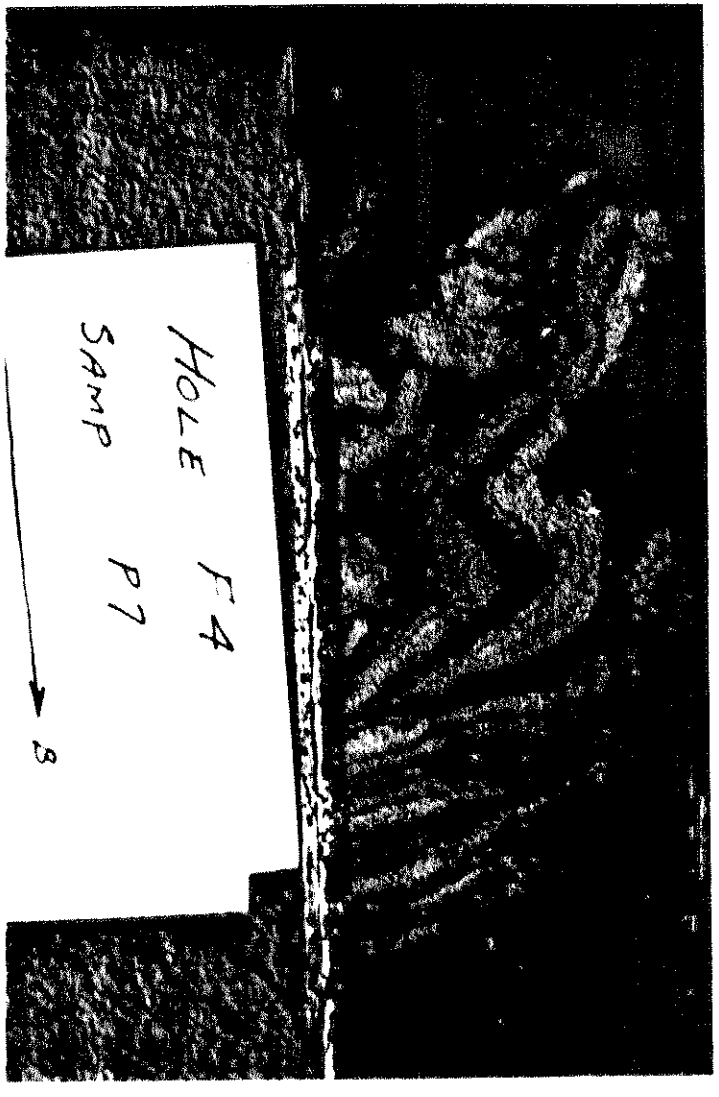

(a) DARK SILTY SAND STREAKS MIXED WITH LIGHTER COLOR COARSE SAND.

(b) CLAY STREAKS MIXED WITH SAND.

FIG. V-21 CLOSE UP VIEWS OF TWO SHELBY TUBE SAMPLES OF SOIL FROM THE UPSTREAM PORTION OF THE LOWER DAM SHOWING DISTURBED AREAS.

As anticipated, there was very little evidence of soil disturbance in the samples taken from the downstream portion of the dam. However, in a few rare cases, some indication of minor disturbance was noted and in these cases the samples were discarded and not used for testing. An example of this is shown in the photograph in Fig. V-22. Here a three inch long seam of clay was sandwiched between an upper and lower layer of medium to coarse sand. The clay contained a vertical crack about one half inch wide which was completely filled with sand. Occasional vertical cracks such as this would seem to indicate that there may have been some zones of liquefaction within the sand even in the downstream portion of the dam. However, because of the large, massive berm the downstream slope remained stable and no slide movements developed.

Bucket Auger Holes

Although some field density tests by the sand cone method were made on the inclined walls of the large trench, it was felt that these data were insufficient to establish the density of the sand within the undisturbed portion of the hydraulic fill. Accordingly, two 36-inch diameter bucket auger holes were made from the downstream berm of the Lower Dam penetrating well into the old hydraulic fill material. As these holes were being drilled, field density tests by the sand cone method were performed at the bottom of the holes at several locations within the hydraulic fill.

After the holes were completed the walls were carefully inspected. The soil conditions exposed on the walls of these holes were very similar to the soil conditions in the undisturbed portions of the wall of the large trench previously described: alternating strata of clean sand and silty sand or clay in 6 to 12-inch layers. There was no evidence of any disturbance from sliding or from liquefaction in these downstream holes.

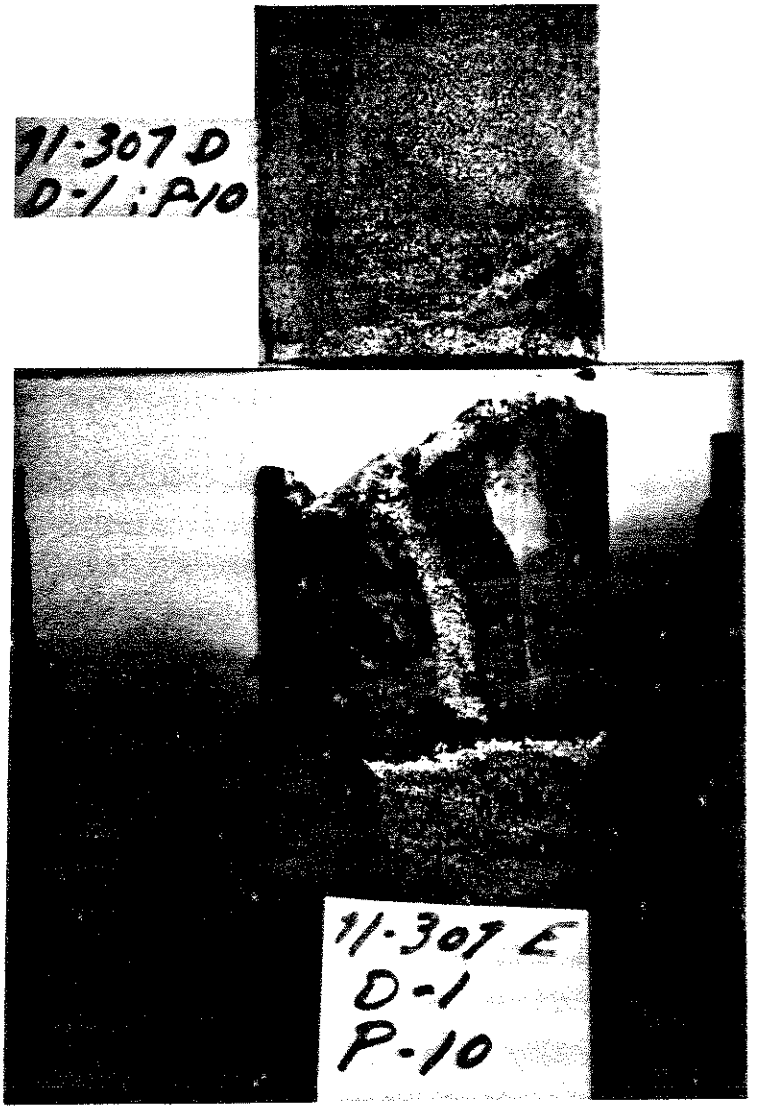

FIG. V-22 SAND DIKE THROUGH A CLAY SEAM IN A SHELBY TUBE SAMPLE FROM THE DOWNSTREAM PORTION OF THE LOWER DAM. ONLY A FEW SUCH SAMPLES WERE FOUND IN THE DOWNSTREAM BORINGS.

The bucket auger holes extended to depths of 28 and 38 feet below the surface level of the downstream berm. They were stopped because of difficulties encountered at the bottom of the holes due to the walls caving and water seepage. Although these two holes were drilled in January of 1972, almost a full year after the earthquake and after the water in the reservoir had been drained, the soil in this area still retained a sufficiently high water content that at a depth of thirty feet below the downstream berm the water would flow freely out of the soil into the hole.

Seismic Surveys

As for the Upper Dam, field seismic surveys were made to determine the velocities of shear wave propagation in the embankment and foundation soils of the Lower San Fernando Dam. These investigations were made by cross-hole measurements at various elevations. Measured values of shear wave velocity, v_s, are presented in the following table:

Formation	Depth-ft	v_s - fps
Hydraulic Fill	50	≃750
Rock	110	≃3600

A limited number of measurements in the lower alluvium gave shear wave velocities similar to those determined for the Upper Dam (v_s ≃ 1500-1800 fps).

Shear moduli can readily be determined from these results (see page 35) and expressed by the relationship

$$G = 1000 \cdot K_2 \cdot (\sigma_m')^{1/2} \text{ psf}$$

where K_2 is a soil constant which depends on the strain amplitude of the shear deformations and σ_m' is the mean effective pressure acting on the

soil. For the measured value of shear wave velocity shown above, the corresponding value of K_2 for the hydraulic fill at the small strain levels of the wave propagation tests is in the range 40 to 45. Values of K_2 at small strains for the foundation alluvium are similar to those shown in Part IV for the Upper Dam.

Grain Sizes

Grain size determinations were made on each of the individual field density samples taken from the walls of the large trench and from the bucket auger holes. In addition, grain size determinations were made on many individual triaxial test specimens. A summary of the grain size distribution curves from the hydraulic fill materials is presented in Fig. V-23. It may be seen that some of the field density samples were a little coarser than the range of grain sizes found within the Shelby tube samples used for triaxial testing purposes. In all, the grain sizes ranged from coarse through fine sand and silty sand materials. Reference to Fig. IV-7, which shows a similar range of grain sizes for the Upper Dam, indicates that the grain size distributions for the hydraulic fill in each dam were quite similar.

Grain size distribution curves were determined for only 9 samples from the alluvium at the Lower Dam. These included 6 samples of fine alluvium and 3 samples of coarse alluvium. The ranges of grain size distributions for these samples are shown in Fig. V-24. These soils would be classified as silty clays and sandy gravels.

Field Densities

Field density data at the Lower Dam were obtained from 3 sets of measurements: the triaxial test specimens extruded from the undisturbed three inch diameter Shelby tubes; sand cone tests made at selected locations

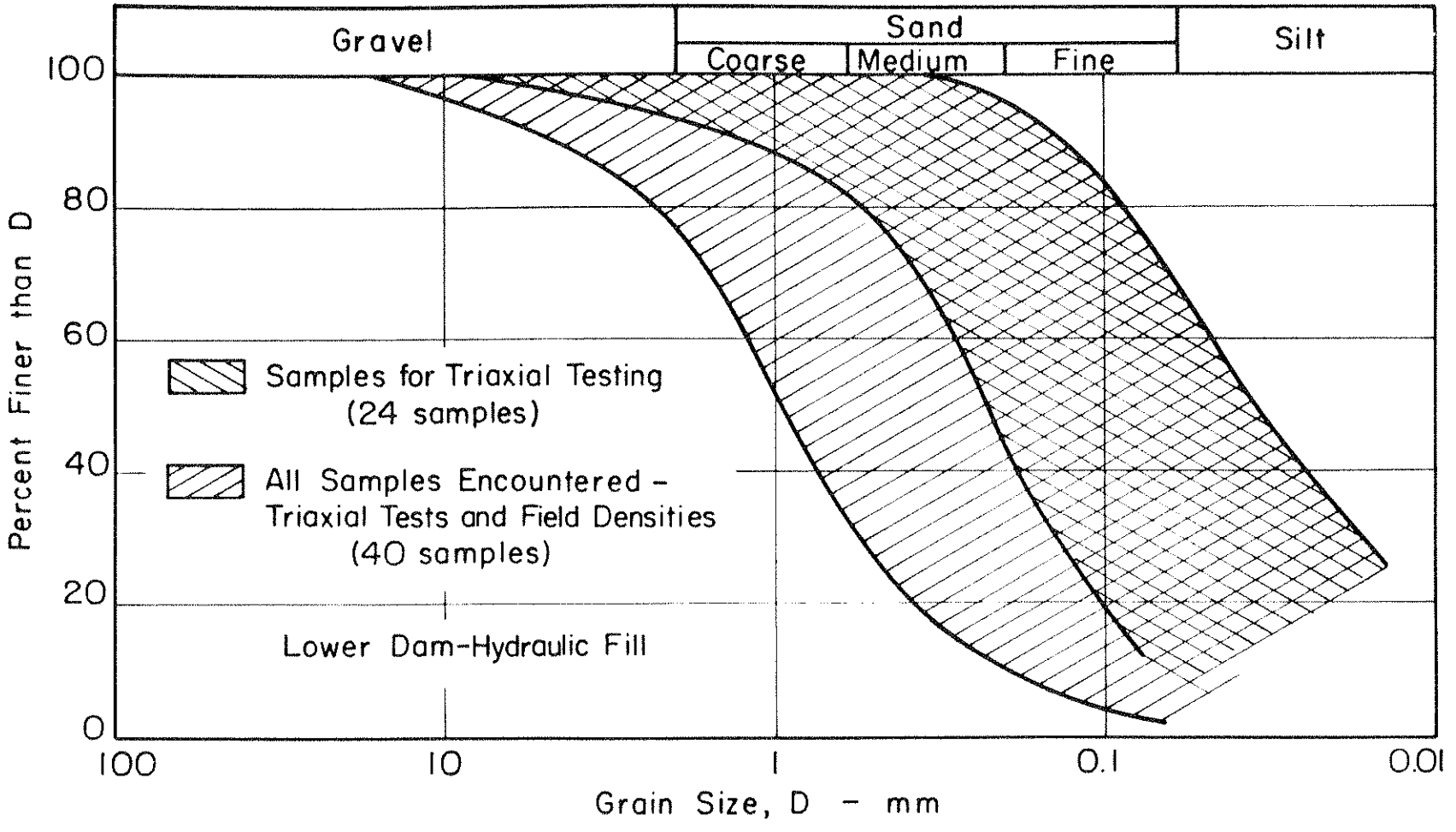

Fig. V-23 RANGES OF GRAIN SIZE DISTRIBUTION CURVES FOR HYDRAULIC FILL - LOWER SAN FERNANDO DAM.

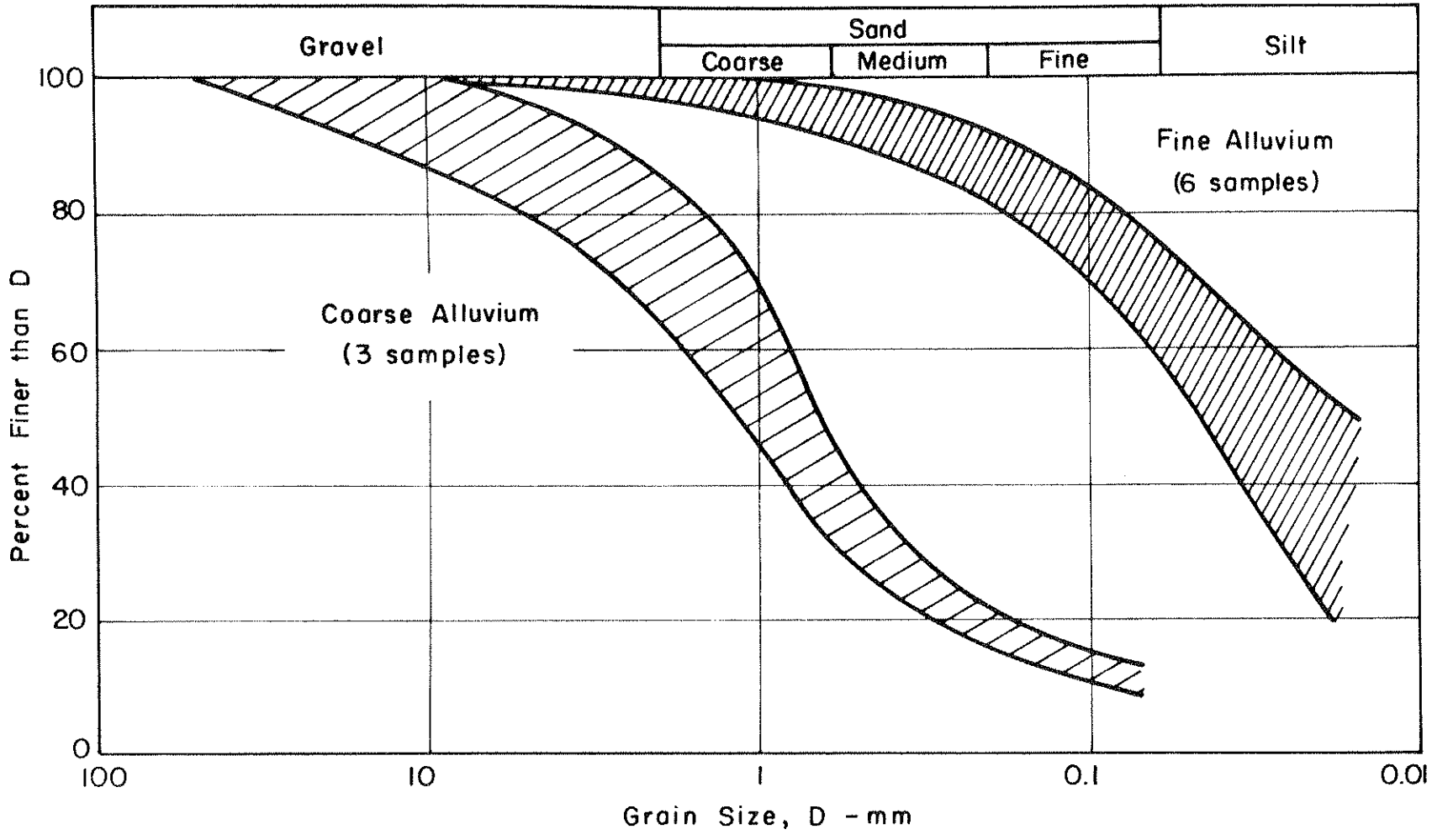

Fig. V–24 RANGES OF GRAIN SIZE DISTRIBUTION CURVES FOR SAMPLES OF ALLUVIUM – LOWER SAN FERNANDO DAM

on the sides of the large trench; and sand cone tests made at various locations in the bottom of the bucket auger holes as these holes were being drilled. A summary of all the field density data from these three sources is presented in Fig. V-25 in the form of frequency distribution charts. The data indicate that the alluvium was somewhat more dense than the hydraulic fill and that the coarse hydraulic fill was somewhat more dense than the fine fill material.

Field density data measured directly by the sand cone method at locations on the walls of the large trench and in the bottom of the bucket auger holes are shown in Fig. V-26. When these field density tests were made, additional soil from the same areas was also taken to the laboratory and used for determinations of the minimum and maximum densities. In these cases the maximum density was obtained by the modified AASHO (1961) test procedure and the minimum density was defined by the ASTM standard test on oven-dried soils.

These limiting density data are also shown in Fig. V-26 where they may be readily compared with the field density at the same site. Although there is considerable scatter, there is nevertheless a distinguishable trend of decreasing field density with decreasing grain size. The compilation of all field density determinations both from the Shelby tubes and from the sand cone tests is presented in Fig. V-27. These data cover a wider range of grain sizes and lead to a more clearly defined trend of density versus grain size than was seen from the previous figure.

As observed at the Upper Dam there appears to be no significant difference between the field densities measured from the undisturbed Shelby tube samples and the field densities determined directly by the sand cone method. All of the field densities shown in Fig. V-27 for

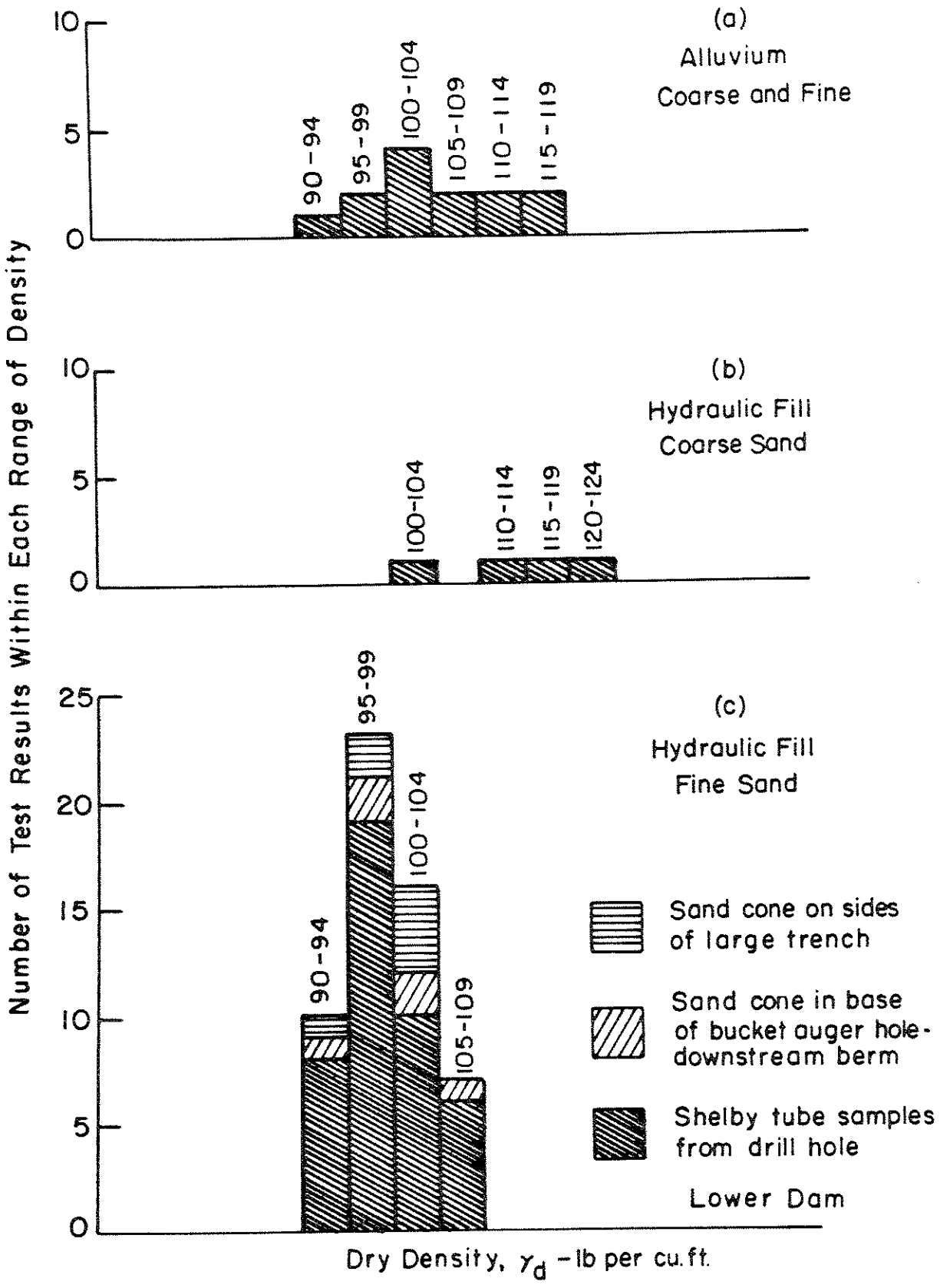

Fig. V-25 SUMMARY OF FIELD DENSITY TESTS - LOWER SAN FERNANDO DAM.

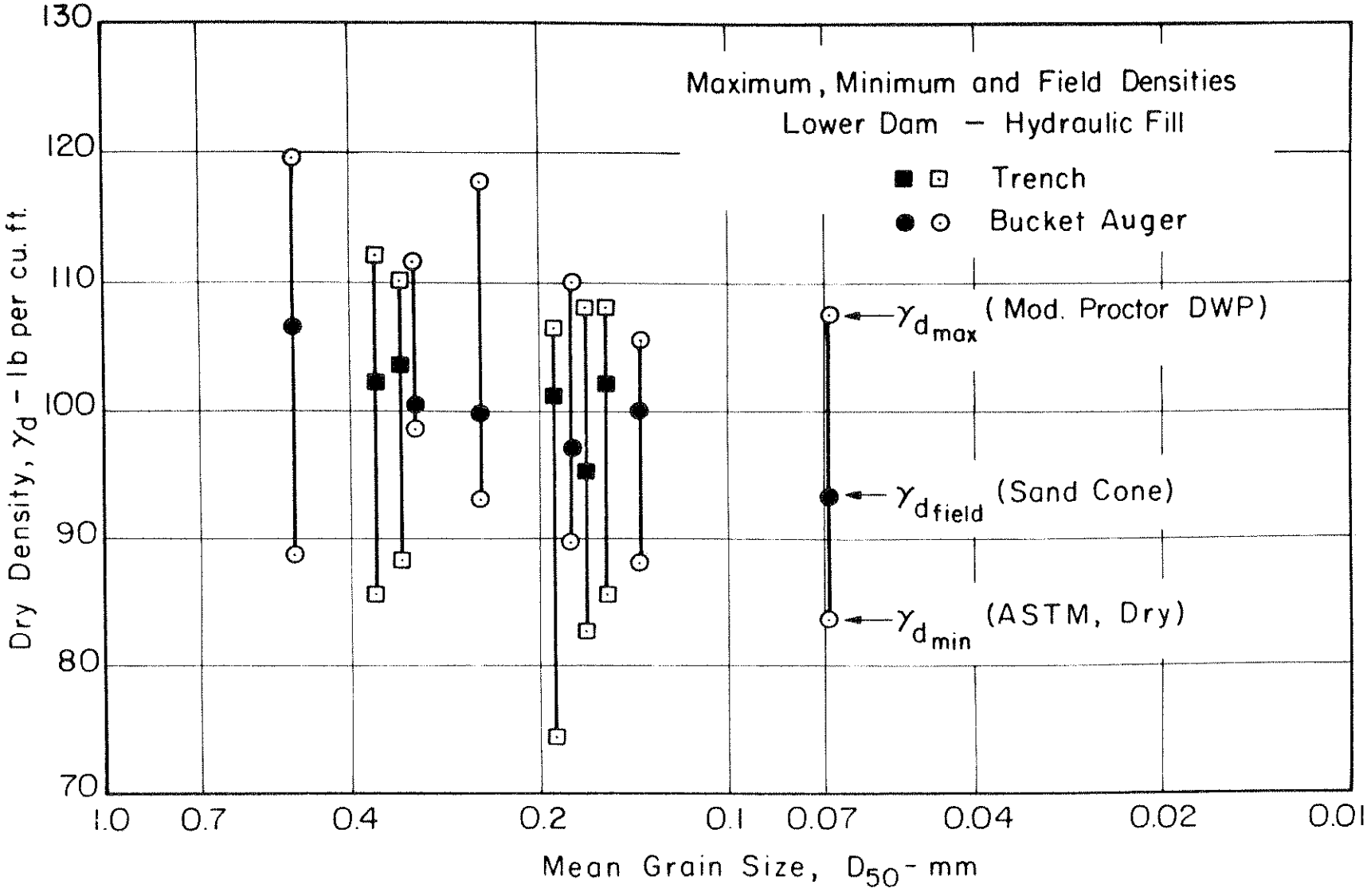

Fig. V–26 MAXIMUM, MINIMUM AND FIELD DENSITIES FOR SAMPLES OF HYDRAULIC FILL – LOWER SAN FERNANDO DAM.

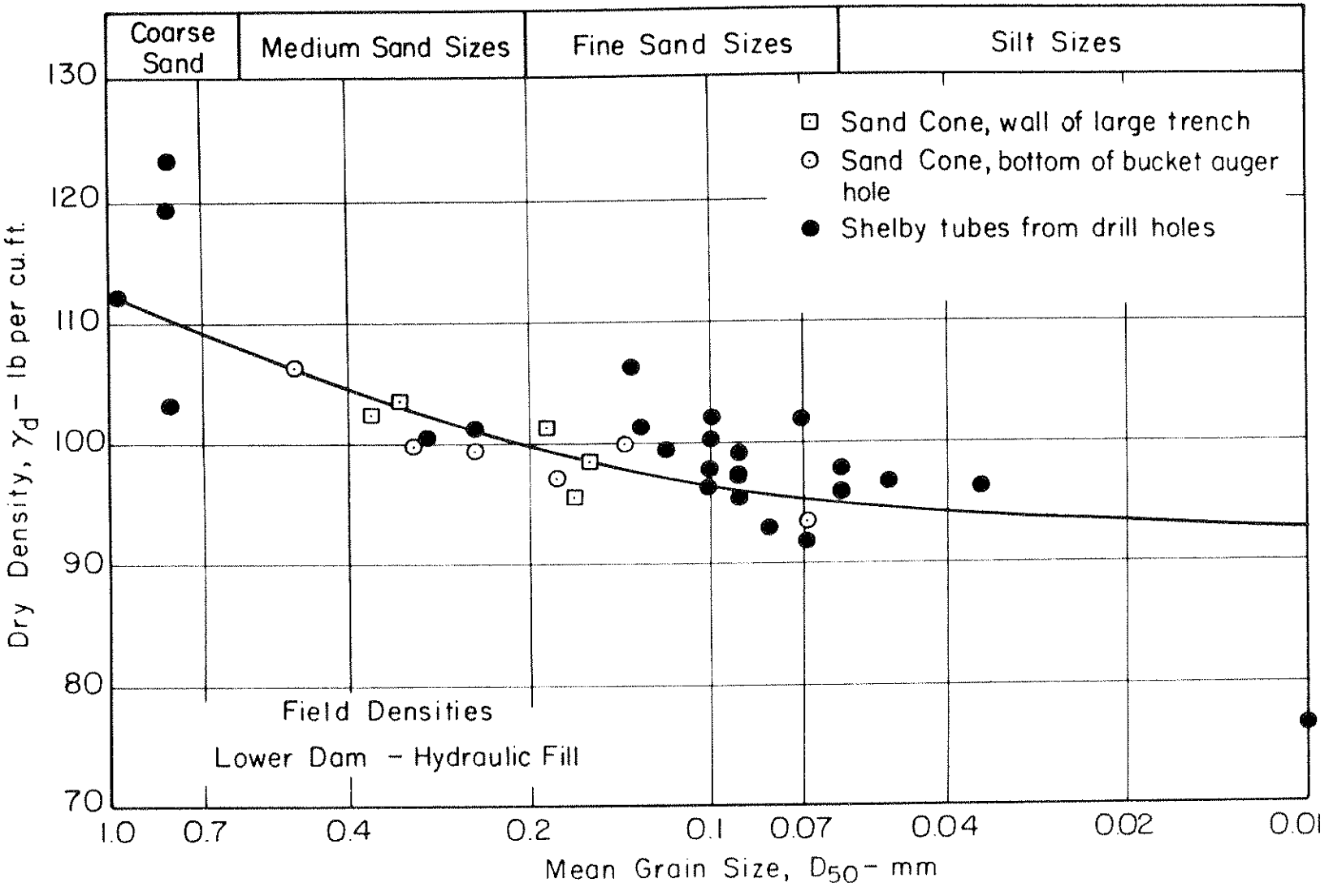

Fig. V-27 FIELD DENSITIES FOR SAMPLES OF HYDRAULIC FILL - LOWER SAN FERNANDO DAM.

samples taken from the large trench were from areas which appeared to have suffered no disturbance during the slide and they agree well with the field densities from the other zones of undisturbed hydraulic fill material. The solid line through the data shown in Fig. V-27 was taken as representing the average field density of the hydraulic fill throughout the range of grain sizes shown.

Maximum Density Tests

The problems involved in determining the maximum densities of the materials from these dams were discussed in some detail in the previous section dealing with the Upper Dam. Three types of maximum density tests were performed on composite samples from both the Upper and the Lower Dams and it was determined that the maximum density was about 5 to 6 lb per cu ft greater than the modified AASHO (1961) maximum density. The study which led to this conclusion was based on data from both the Upper and Lower Dams as shown in Fig. IV-12. Therefore, this same criteria was used to define the maximum density for the Lower Dam material.

The maximum densities obtained from modified AASHO (1961) compaction tests on the field density samples are shown in Fig. V-28. The solid line indicates the average densities determined by the data points. The dashed line drawn about this solid line represents the probable maximum densities for the different grain sizes of the material in the field.

It will be recalled from the discussion of the Upper Dam that maximum densities for composite mixtures of samples could be expected to be somewhat greater than the maximum density of the individual samples. This is shown by the solid data points in Fig. V-28, each of which represent the maximum modified AASHO (1961) density for composite samples of the hydraulic fill. These data points are significantly higher than the modified AASHO (1961) densities

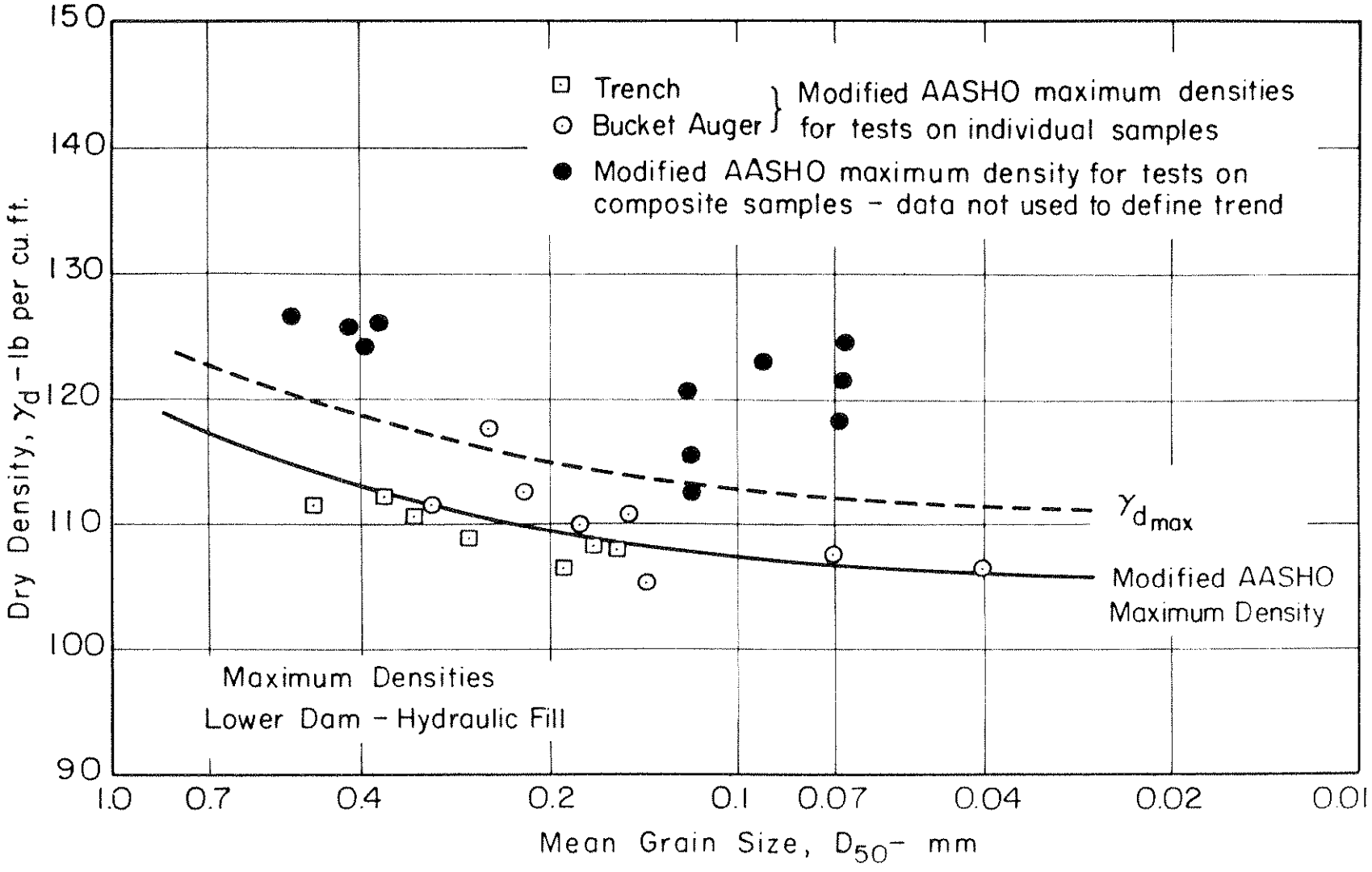

Fig. V-28 MODIFIED AASHO MAXIMUM DENSITIES FOR SAMPLES OF HYDRAULIC FILL - LOWER SAN FERNANDO DAM.

of the individual samples shown by open data points. Accordingly test data from the composite samples were not considered to be representative of the maximum densities of the soil within the embankment.

Maximum density data from standard AASHO tests are summarized in Fig. V-29. It will be noted again that the maximum standard AASHO densities from composite samples were found to be significantly greater than those from individual field samples.

Minimum Densities

Minimum density tests were performed by the four different procedures described previously in the discussion of the Upper Dam. Data from all of the minimum density tests are summarized in Fig. V-30. These data also show a trend of decreasing minimum density with decreasing grain size. The best fit line drawn through the data points obtained by the ASTM standard method of test on individual samples of oven-dried soil is shown on this figure and was taken as the minimum density relation for the hydraulic sand fill at the Lower Dam.

Relative Density and Relative Compaction

A comparative summary of each of the density vs grain-size relationships for the Lower Dam is presented on Fig. V-31. These data show that the field density is approximately midway between the minimum and maximum densities for all soils and approximately equivalent to the standard AASHO maximum density. Values of average relative density computed from these relationships are shown in Fig. V-32; values ranged between about 50 and 54 percent. This is almost identical to the values determined for the hydraulic fill at the Upper Dam, and similar to relative densities reported for other hydraulic fills (Whitman, 1970; Turnbull, 1972).

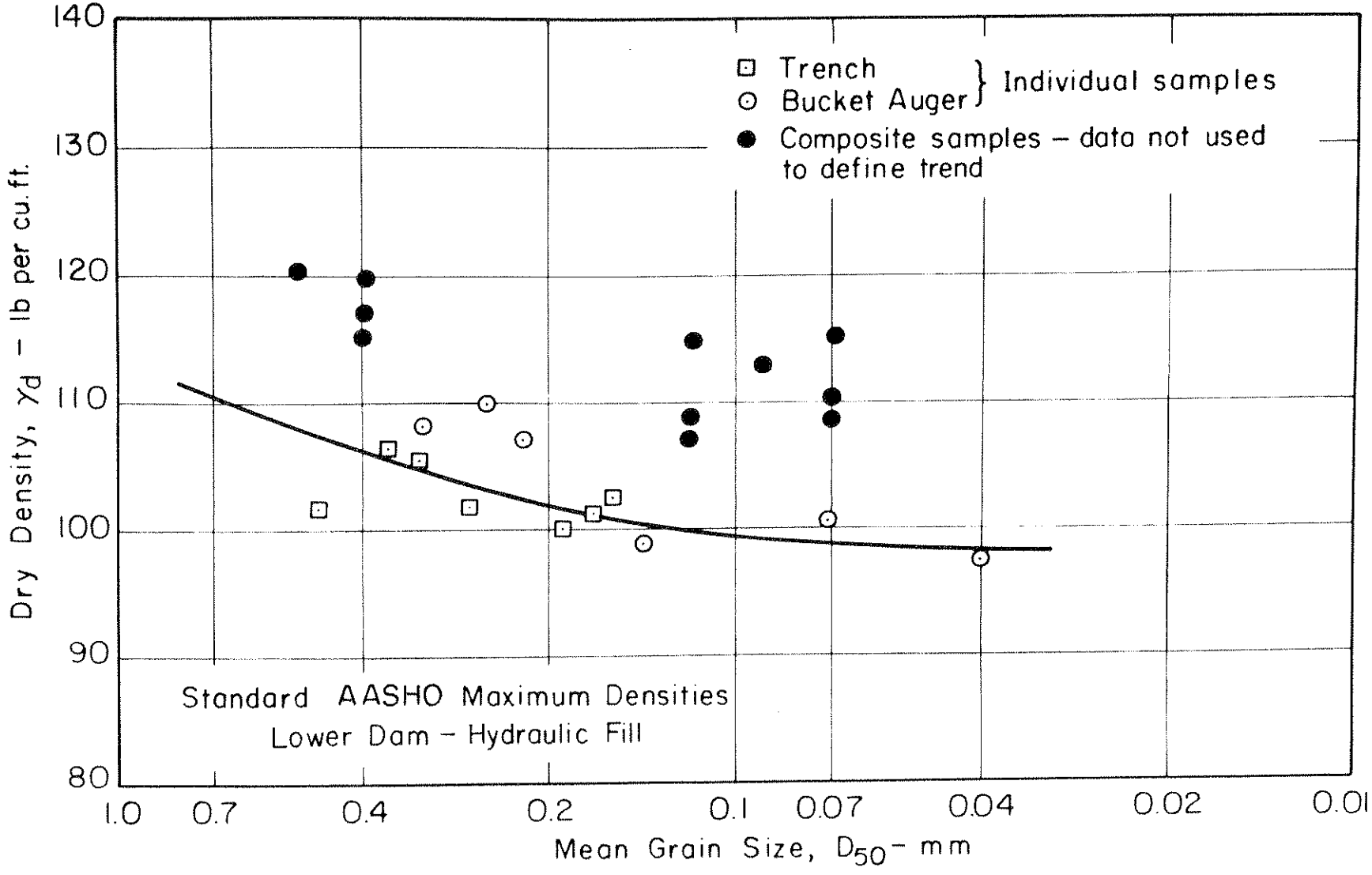

Fig. V–29 STANDARD AASHO MAXIMUM DENSITIES FOR SAMPLES OF HYDRAULIC FILL – LOWER SAN FERNANDO DAM.

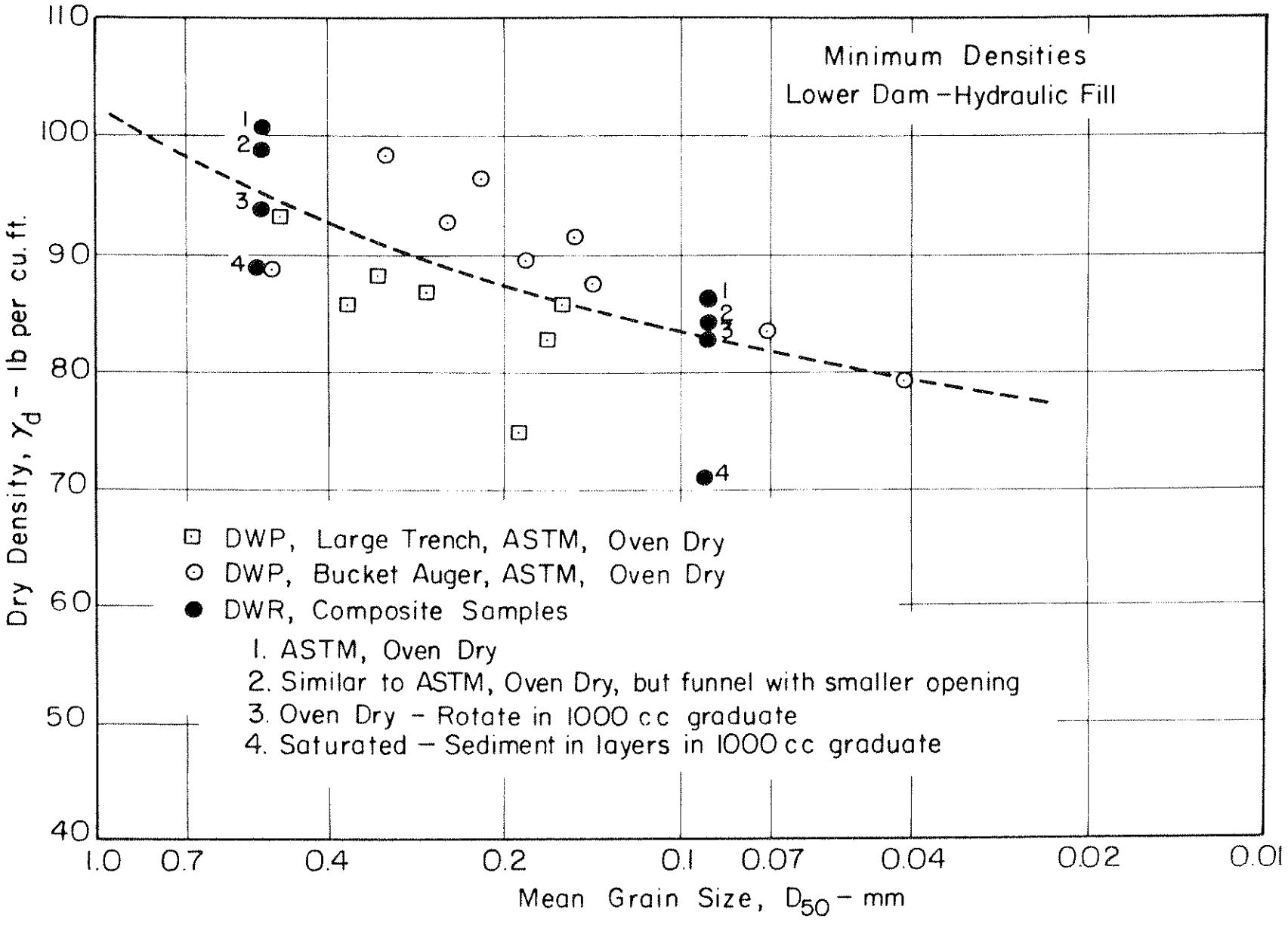

Fig. V–30 MINIMUM DENSITIES FOR SAMPLES OF HYDRAULIC FILL – LOWER SAN FERNANDO DAM

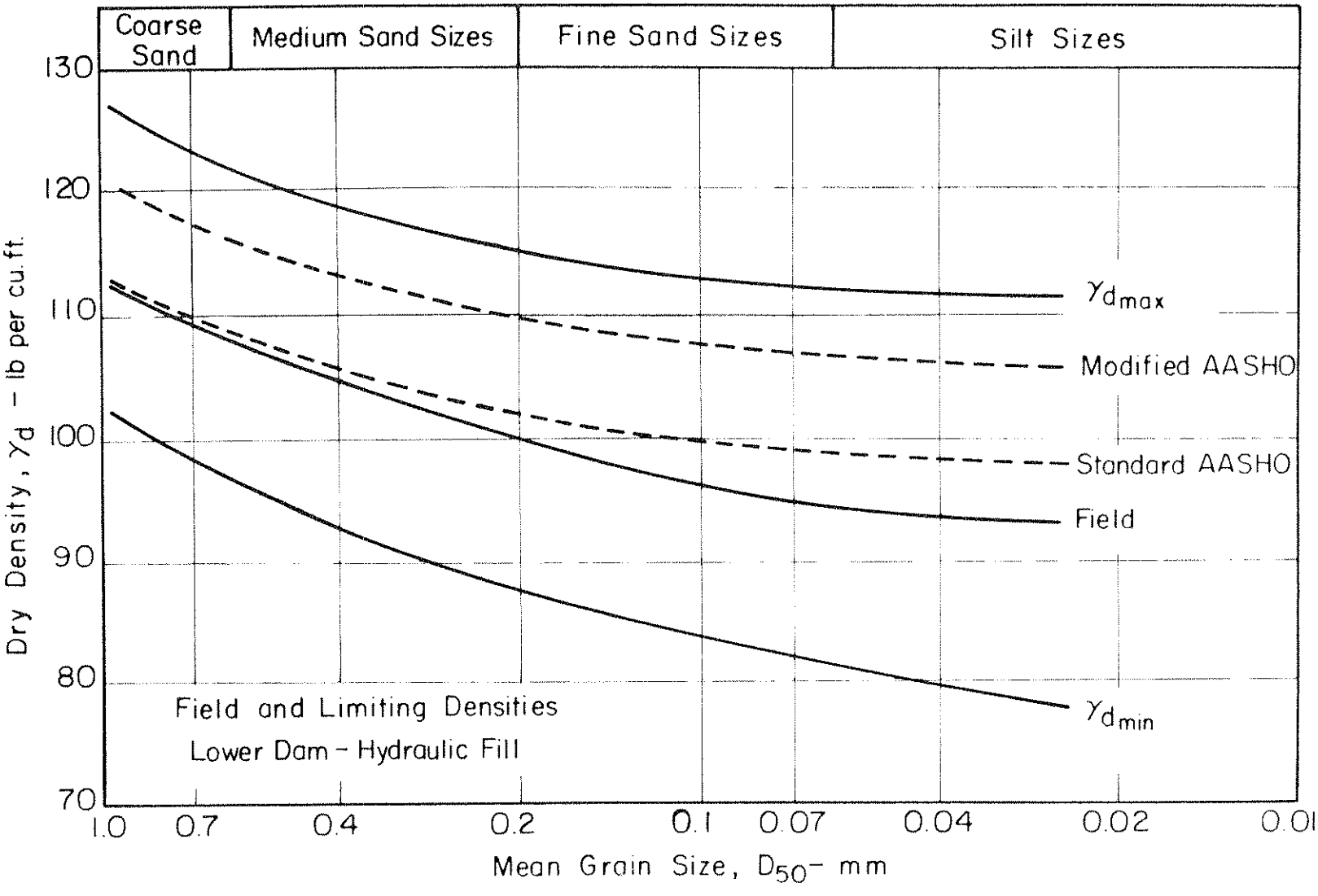

Fig. V-31 SUMMARY OF FIELD AND LIMITING DENSITY DATA FOR HYDRAULIC FILL - LOWER SAN FERNANDO DAM.

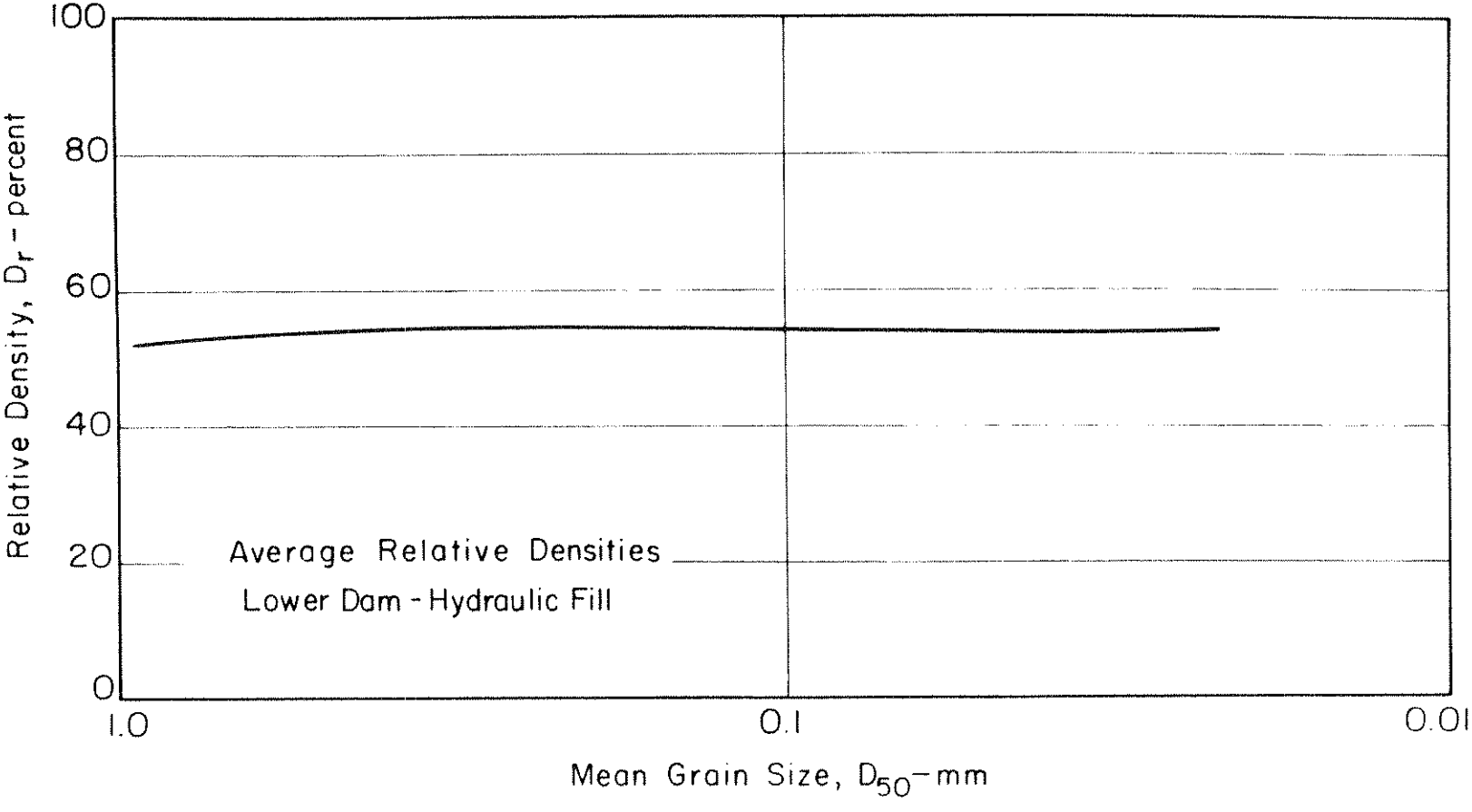

Fig. V-32 AVERAGE RELATIVE DENSITIES FOR HYDRAULIC FILL - LOWER SAN FERNANDO DAM.

The relative compaction of a soil is defined as the ratio of field density divided by some specified laboratory maximum density. Values of relative compaction based on the standard and the modified AASHO (1961) compaction tests are summarized in Fig. V-33. The average relative compaction of the sand fill based on the standard AASHO test ranged from about 95 to 100 percent depending on the grain size of the material. The relative densities based on the modified AASHO (1961) compaction test ranged from about 88 to 93 percent, increasing with increasing grain size.

Also shown in Fig. V-33 for comparative purposes is a relative compaction calculated by the ratio of minimum to maximum density. This relative compaction ranged from about 70 to about 80 percent, indicating that without any compaction whatsoever the relative compaction of a loosely placed fill would always be at least 70 to 80 percent of the maximum possible density.

Relative Densities by the Standard Penetration Test

Standard penetration tests were performed at five-foot intervals in every drill hole in the Lower Dam. The penetration resistance values determined from these tests are summarized on the sections through the dam on Figs. V-16 to V-19. The drill holes through the central and upstream portions of the dam penetrated through predominantly disturbed material in the slide debris and the standard penetration blow counts in these holes were not used in defining the relative density of the material prior to the earthquake. However, the drill holes downstream of the slide debris penetrated through apparently undisturbed material and the standard penetration resistance values from these holes were considered to be representative of the fill material unaffected by the earthquake.

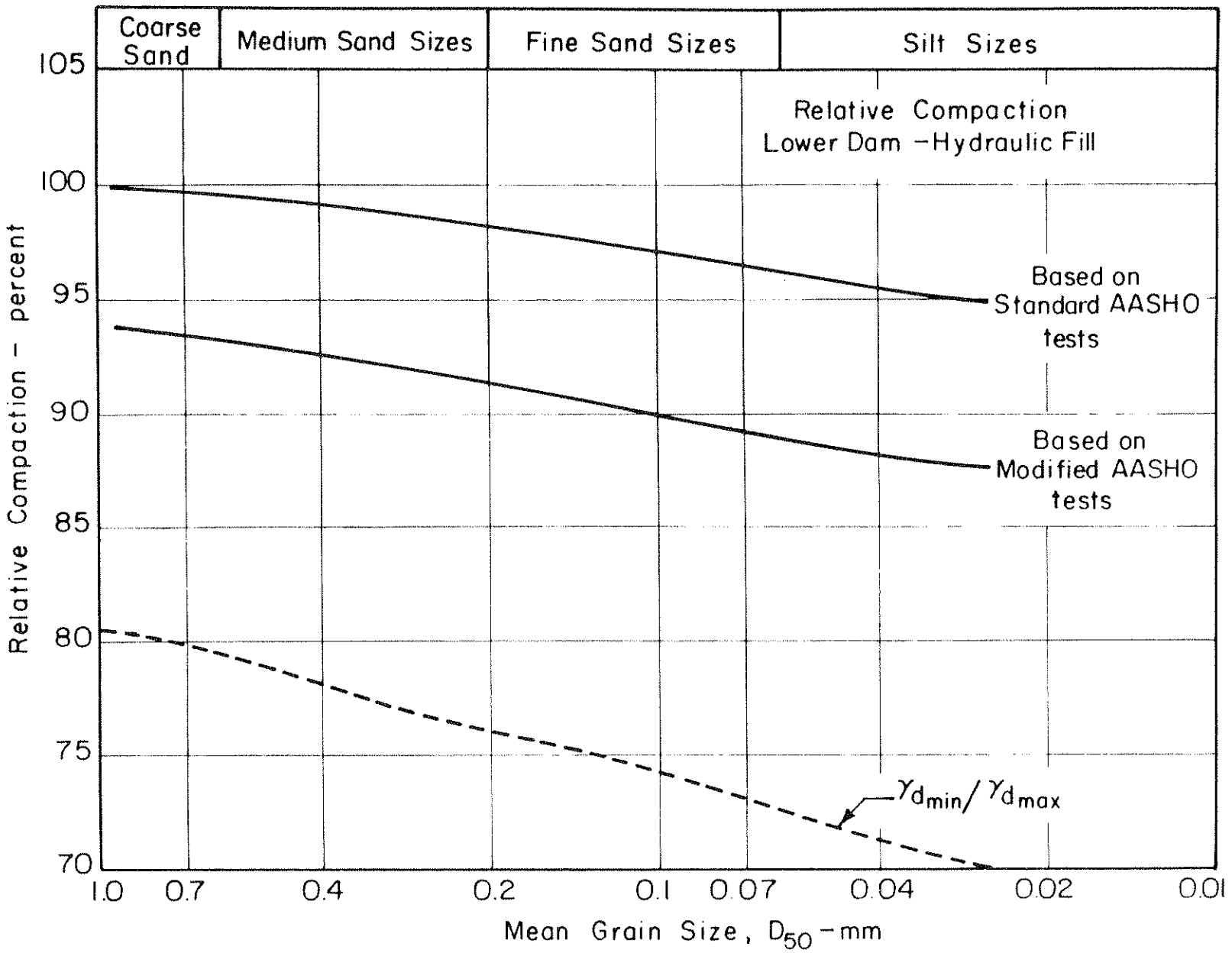

Fig. V-33 AVERAGE VALUES OF RELATIVE COMPACTION FOR HYDRAULIC FILL LOWER SAN FERNANDO DAM

The standard penetration test data were used to determine values of relative density for the embankment and foundation soils using the correlation chart proposed by Gibbs and Holtz (1957). The values of relative density determined in this way for all the drill holes at comparable locations on the downstream berm are combined and presented together in Figs. V-34a and b.

As observed for the Upper Dam there are occasional erratic data points probably due to the penetration spoon encountering either a clay seam which would give a low value, or coarse gravel which would give a high value. However, the majority of data presents a fairly well defined relationship of relative density vs. depth. These data indicate that within the hydraulic fill material the relative density ranged from about 45 to 65 percent, which is comparable to the relative densities obtained by direct measurement. The relative densities obtained by this method in the rolled fill, ground shale, and the alluvium appear to be significantly higher.

Relative densities were also determined from penetration test data obtained from a boring made from the downstream berm before the earthquake, as shown in Fig. V-34c. While the data are limited in number, the results are generally similar to the data obtained from the holes made from similar locations during the 1971 investigation following the earthquake, and thus substantiate the suggestion that the hydraulic fill material in the downstream portion of the dam was not significantly disturbed as a result of the earthquake.

Static Loading Triaxial Tests

A number of static loading triaxial tests were performed on undisturbed samples from both the hydraulic fill and the alluvium from the

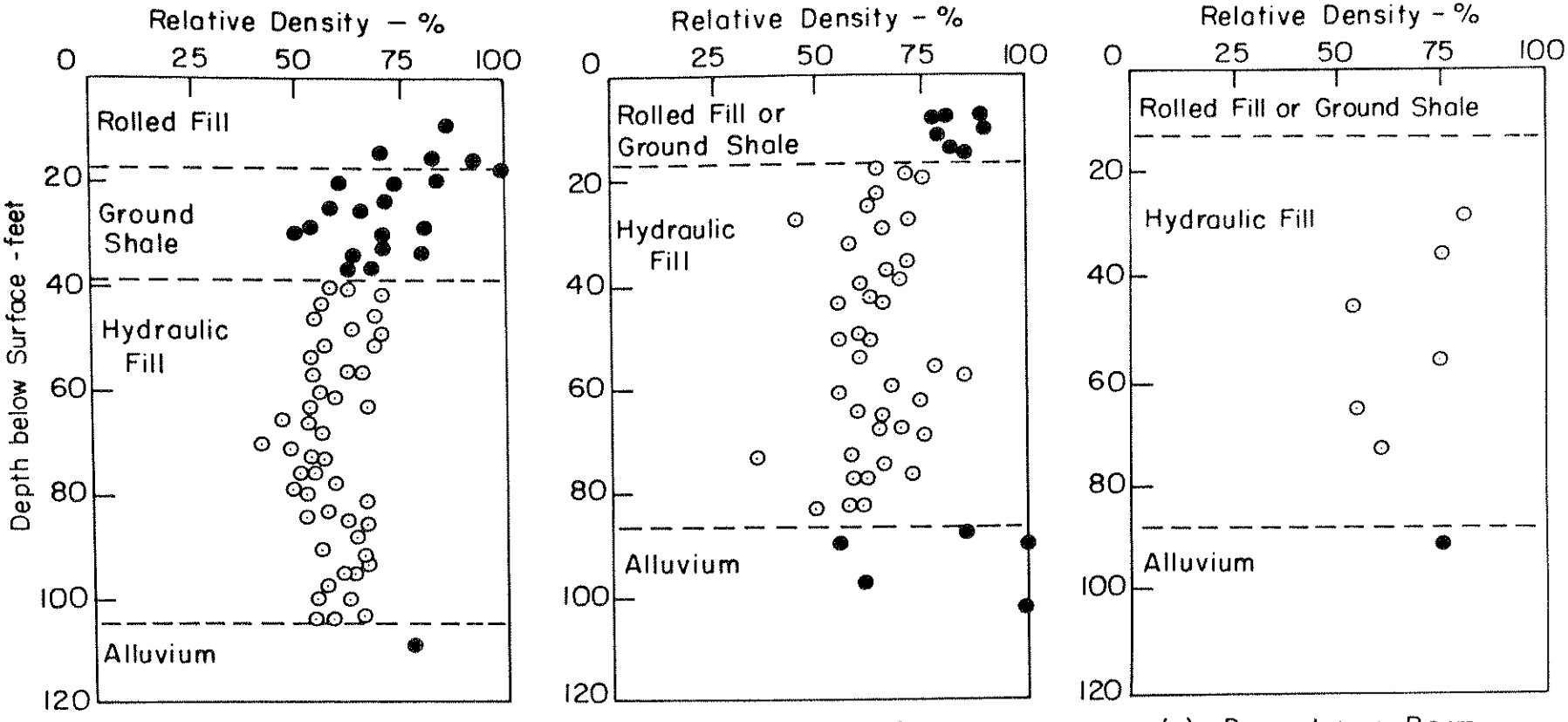

(a) Downstream Slope
Surface Elevation ≈ 1112
Holes D1, E2, F2, G2
(After Earthquake)

(b) Downstream Berm
Surface Elevation ≈ 1095
Holes E1, F1, G1
(After Earthquake)

(c) Downstream Berm
Surface Elevation ≈ 1095
Hole CH-67-A
(Before Earthquake)

Fig. V–34 RELATIVE DENSITIES DETERMINED FROM STANDARD PENETRATION TEST DATA. – LOWER SAN FERNANDO DAM

Lower Dam. All of the test specimens were obtained by extruding the soil directly from the seven inch lengths of Shelby tubes which, after squaring off the ends, resulted in a sample approximately six inches long and three inches in diameter. Each sample was saturated in a triaxial chamber under a back pressure and isotropically consolidated under an effective confining pressure of 1.0, 2.0 or 4.0 kg per sq cm.

Two types of tests were performed; consolidated-drained tests and consolidated-undrained with pore pressure measurements. In both types of tests, failure was defined as the peak axial stress developed during the test.

Typical stress-strain curves for static loading triaxial tests on drained and undrained samples of hydraulic fill from the Lower Dam are shown in Fig. V-35. Each of these samples was isotropically consolidated under an effective stress of 2.0 kg per sq cm, and then statically loaded under controlled strain conditions until the peak stress had been obtained. Similar data were obtained from all static loading triaxial tests on hydraulic fill and on alluvial materials. In no case was there any significant loss in strength at strains beyond the peak axial stress, which would suggest the possibility of large movements after the earthquake-induced stress changes had ceased.

Modified Mohr diagrams showing the peak stress conditions at failure for both types of tests are presented in Fig. V-36 together with an interpreted straight line Mohr envelope through the data points. The total stress data from the CU tests are somewhat more scattered than the effective stress data. However, it will be noted that there appears to be no significant difference between the data from tests on coarse sand and fine sand materials. On an effective stress basis the test data from

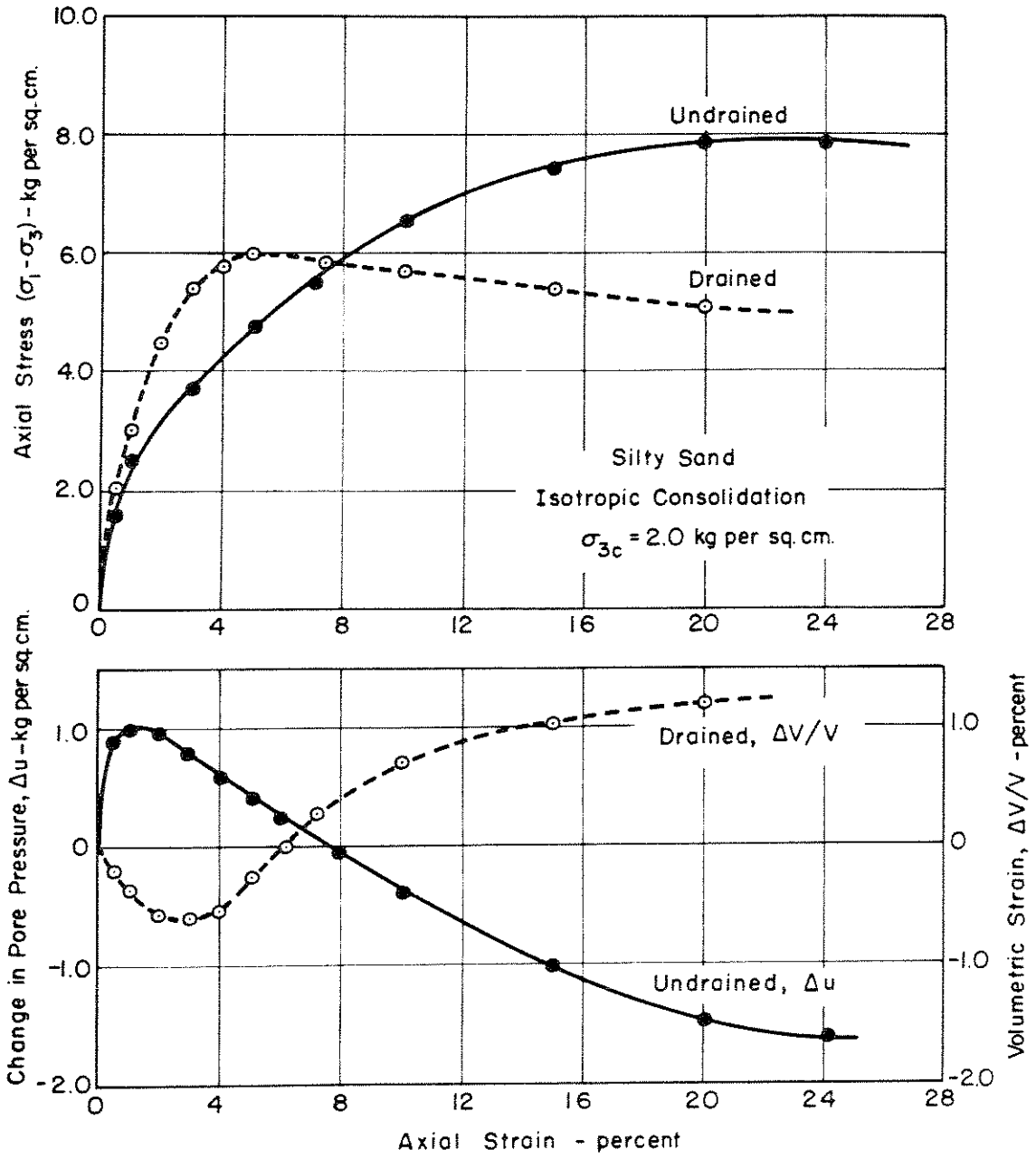

Fig. V-35 TYPICAL STRESS-STRAIN CURVES IN STATIC LOADING TRIAXIAL TESTS ON SAMPLES OF HYDRAULIC FILL - LOWER SAN FERNANDO DAM.

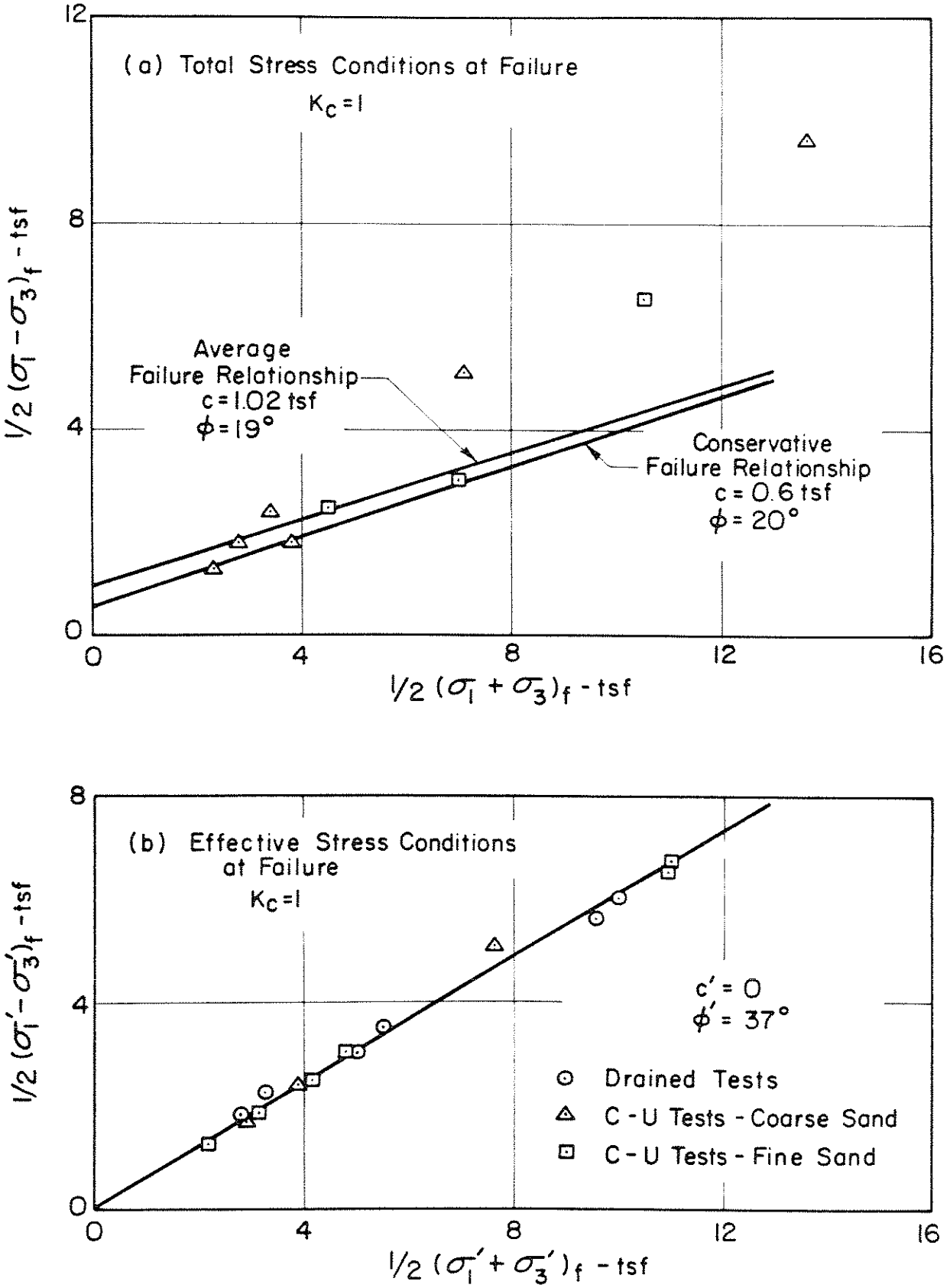

Fig. V–36 RESULTS OF TRIAXIAL TESTS ON SAMPLES OF HYDRAULIC SAND FILL FROM LOWER SAN FERNANDO DAM. (Data from State of California Department of Water Resources, 1972).

drained tests and from CU tests with pore pressure measurements led to the same failure envelope.

The results of the static loading triaxial tests on samples of alluvium in the Lower Dam are presented in Fig. V-37. Relationships between the shear stress on the failure plane (τ_{ff}) and the effective normal stress on the failure plane (σ_{fc}) corresponding to the Mohr envelopes for the soils are shown in Fig. V-38.

The shear strength parameters, cohesion and angle of internal friction, obtained from these data were used in the static stability analyses performed on the Lower Dam. In addition the dynamic analysis required a detailed knowledge of the equilibrium static stress condition within the embankment before the earthquake. These static stresses were calculated by means of a finite element analysis (Kulhawy et al, 1969) which used incremental loading to simulate construction and nonlinear stress-strain parameters for the soil. The stress-deformation parameters used in this analysis were obtained from the stress-strain curves of the static triaxial tests.

A summary of these nonlinear stress-strain parameters for the significant zones of the Lower Dam is presented on Table V-1. The data shown in this table for the rolled fill section of the dam was interpreted from a large collection of data on a wide variety of materials presented by Kulhawy, Duncan and Seed (1969).

Undrained Shear Strength of Clay in the Hydraulic Fill

A limited number of Torvane shear tests and Atterberg limit tests were performed on samples of clay from the core of the dam. Values of liquid limit ranged from 41 to 70 and corresponding values of plasticity index from 19 to 46. Shear strengths near the upper part of the core had

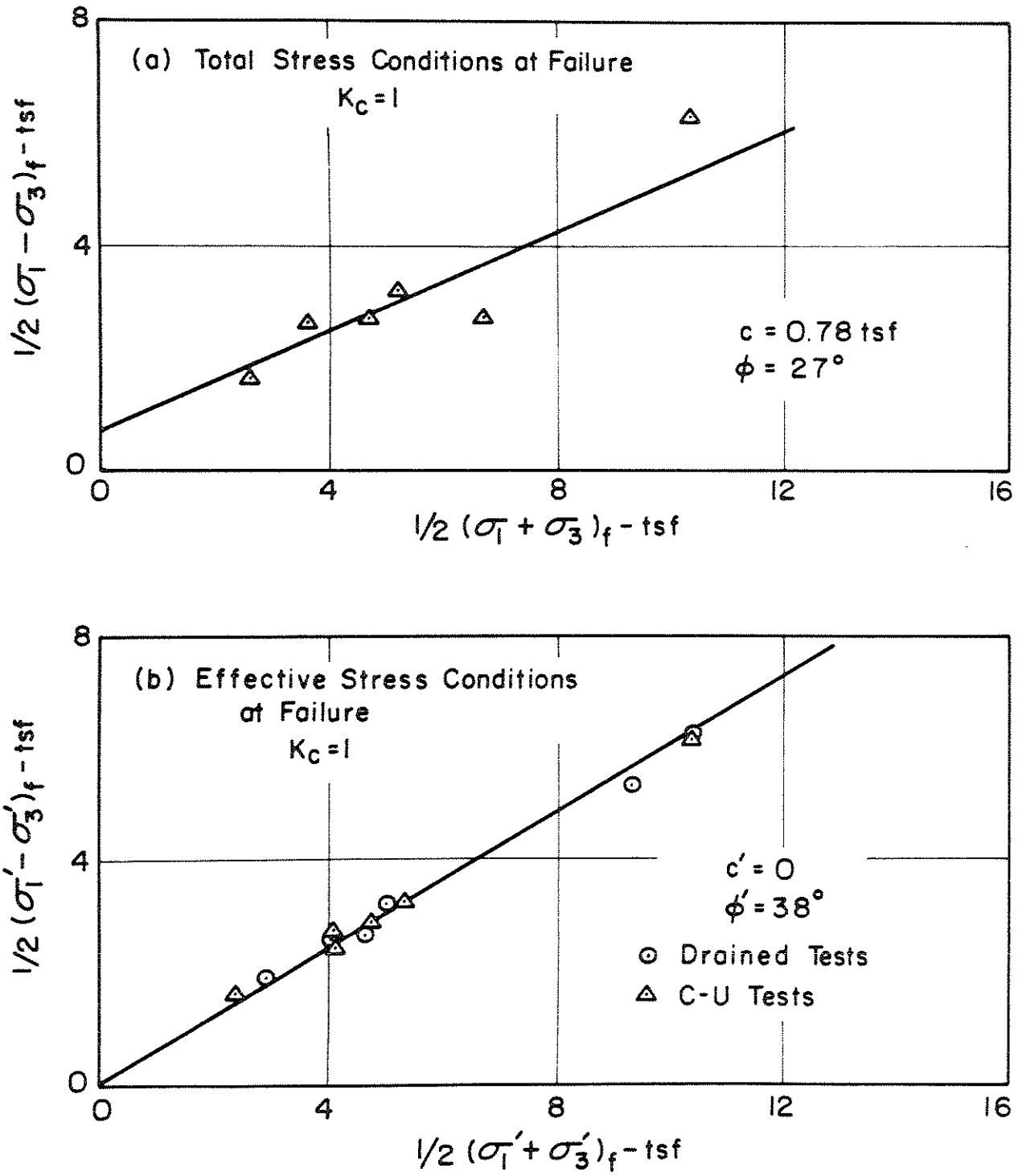

Fig. V-37 RESULTS OF TRIAXIAL TESTS ON SAMPLES OF ALLUVIUM FROM LOWER SAN FERNANDO DAM. (Data from State of California Department of Water Resources, 1972).

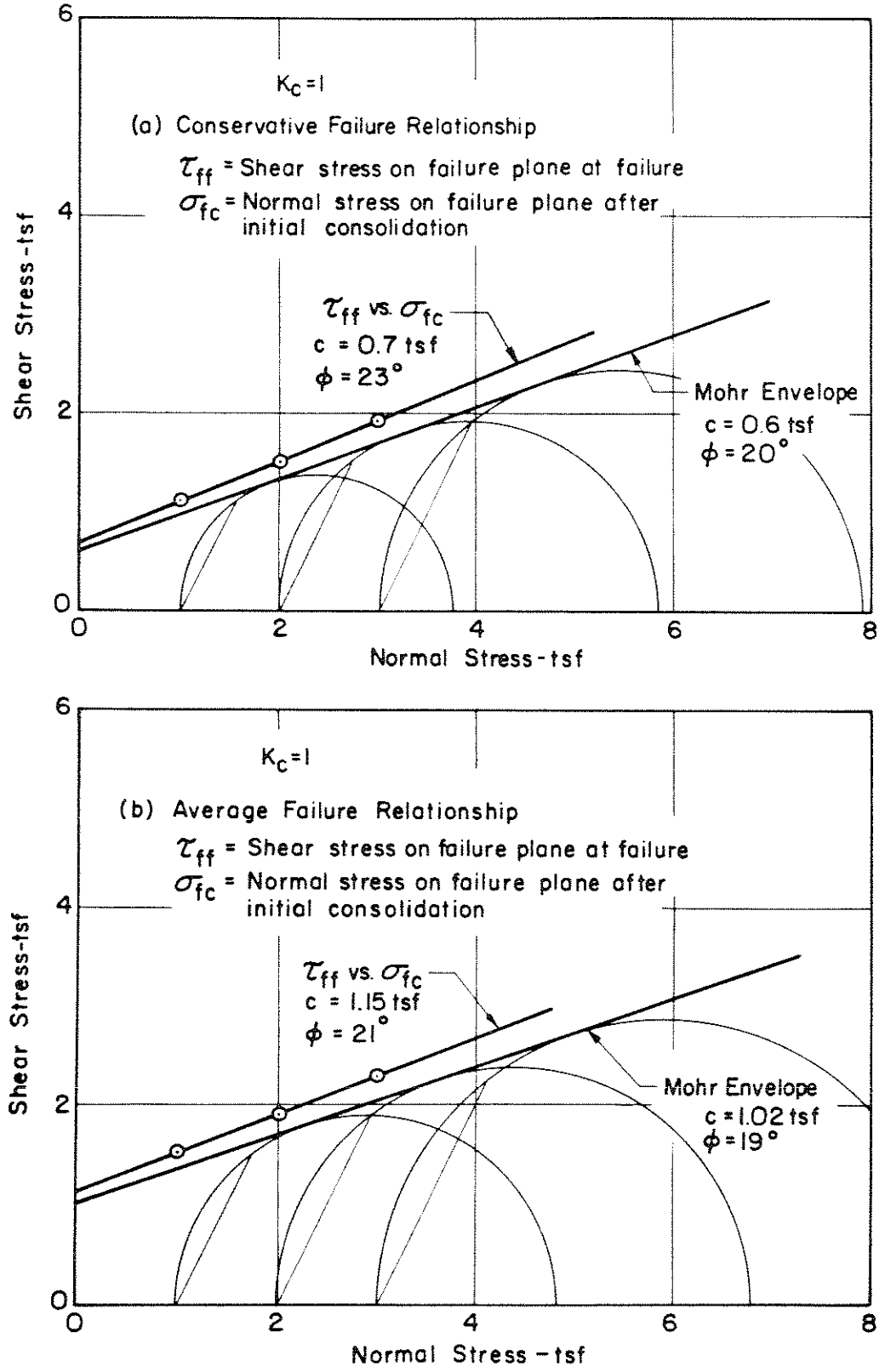

Fig. V–38 MOHR ENVELOPE AND τ_{ff} VS σ_{fc} RELATIONSHIPS DETERMINED BY CONSOLIDATED–UNDRAINED TRIAXIAL TESTS ON SAMPLES OF HYDRAULIC SAND FILL – LOWER SAN FERNANDO DAM. (Data from State of California Department of Water Resources, 1972)

Table V-1

Summary of Stress-Strain-Strength Parameters used in Static Finite Element Stress Analysis, Lower Dam

	Parameter	Zone		
		Rolled Fill	Hydraulic Fill	Alluvium
Strength Parameters	γ_t (above Wt.) lb/ft^3	134	128	--
	γ_b (below Wt.) lb/ft^3	78	64	68
	c ton/ft^2	1.3	0	0
	ϕ degrees	25	37	38
	R_f	0.90	0.72	0.76
Young's Modulus Parameters	K	300	510	330
	n	0.76	0.54	0.41
Poisson's Ratio Parameters	G	0.30	0.41	0.40
	F	0.10	0.23	0.16
	D	3.80	9.40	5.80

γ_t = total unit weight

γ_b = buoyant unit weight

c = cohesion

ϕ = angle of internal friction

R_f, K, n, G, F, D = nonlinear stress-strain parameters, assumed the same above or below the water table

values ranging from 1200 to 1700 psf, corresponding to a shear strength/effective overburden pressure ratio of about 0.3.

Laboratory Cyclic Load Tests

A total of 49 cyclic load triaxial tests were performed on undisturbed samples of hydraulic fill and alluvium from the Lower Dam. The procedures for preparing the samples, performing the tests and interpreting the data were identical to those used for samples from the Upper Dam and generally similar results were observed. The stress conditions causing liquefaction and 5 percent strain for samples of hydraulic sand fill and alluvium, isotropically consolidated under a confining pressure of 1.05 kg per sq cm are shown in Fig. V-39. It may be seen that the stresses required to cause liquefaction of the alluvium are about 70 percent greater than those causing liquefaction in the hydraulic fill. It should be noted that a similar observation was made concerning the tests on samples from the Upper Dam. The relatively higher strength observed for the alluvium as compared to the hydraulic fill is compatible with the observed higher relative densities in the alluvium. Because of its greater stability, no further tests were performed on the alluvium from the Lower Dam Site.

The stress conditions causing 5 percent strain and liquefaction in 2, 3, 4, 5, 10 and 20 cycles in tests on undisturbed samples of the hydraulic sand fill are presented in Figs. V-40 to V-45. It should be noted that for most of the tests, the pore pressure built up to a value equal to the applied confining pressure, even for the samples consolidated under anisotropic stress conditions.

Using the same data analysis procedure as that described in conjunction with the cyclic load tests on samples from the Upper Dam, the data in Figs. V-40 to V-45 have been replotted in Figs. V-46 to V-51 to show values

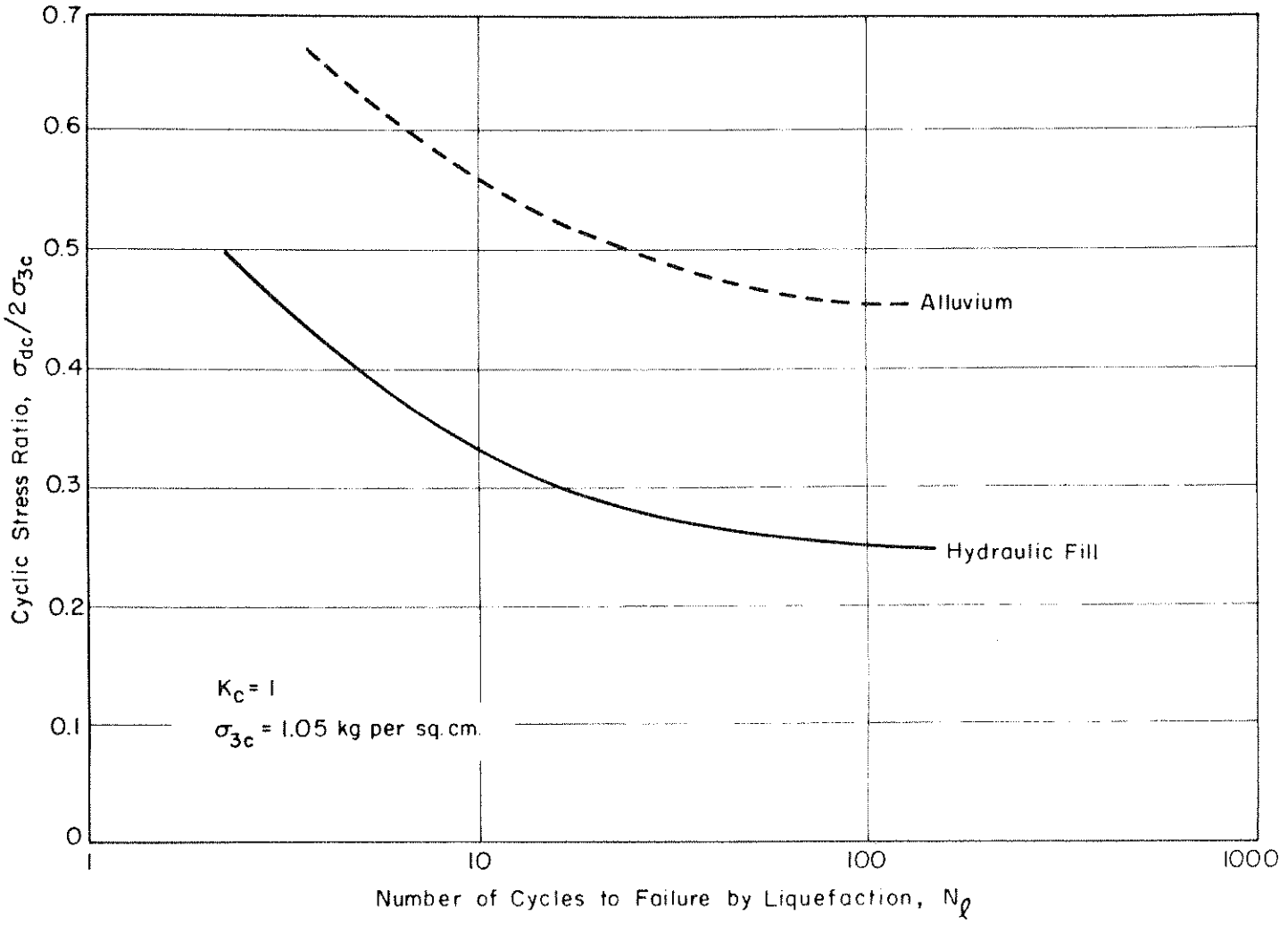

Fig. V–39 COMPARISON OF CYCLIC LOAD TEST DATA FOR HYDRAULIC SAND FILL AND ALLUVIUM – LOWER SAN FERNANDO DAM.

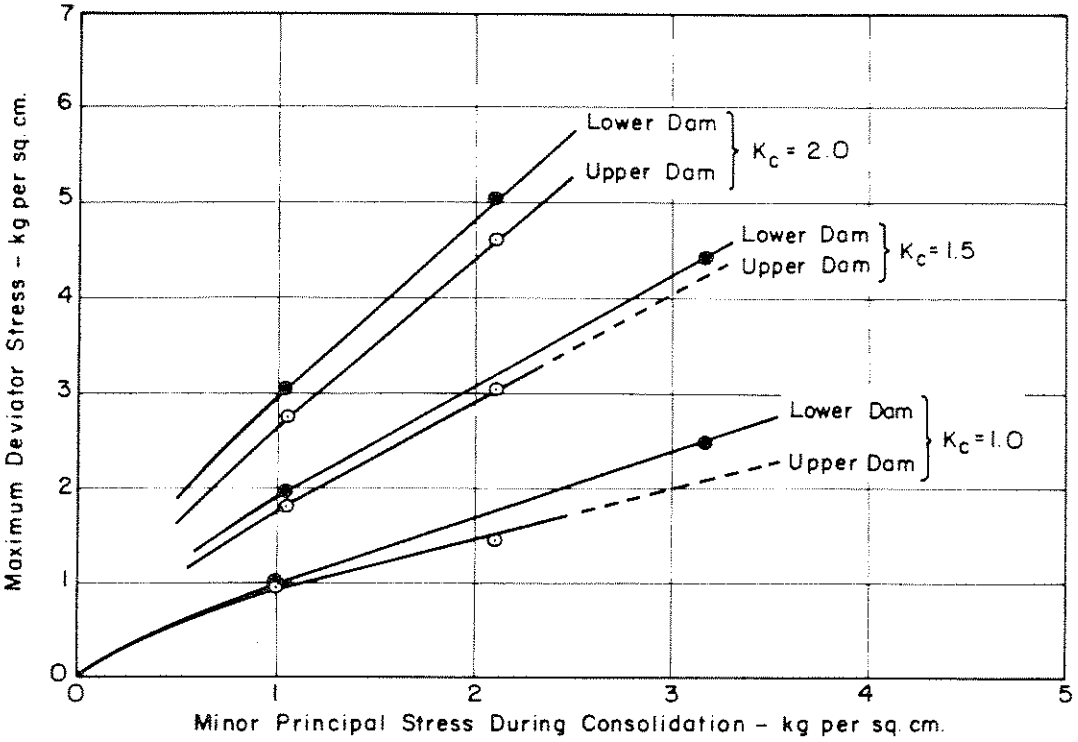

Fig. V-40 CYCLIC STRESSES CAUSING LIQUEFACTION AND 5% STRAIN IN 2 CYCLES FOR HYDRAULIC SAND FILL.

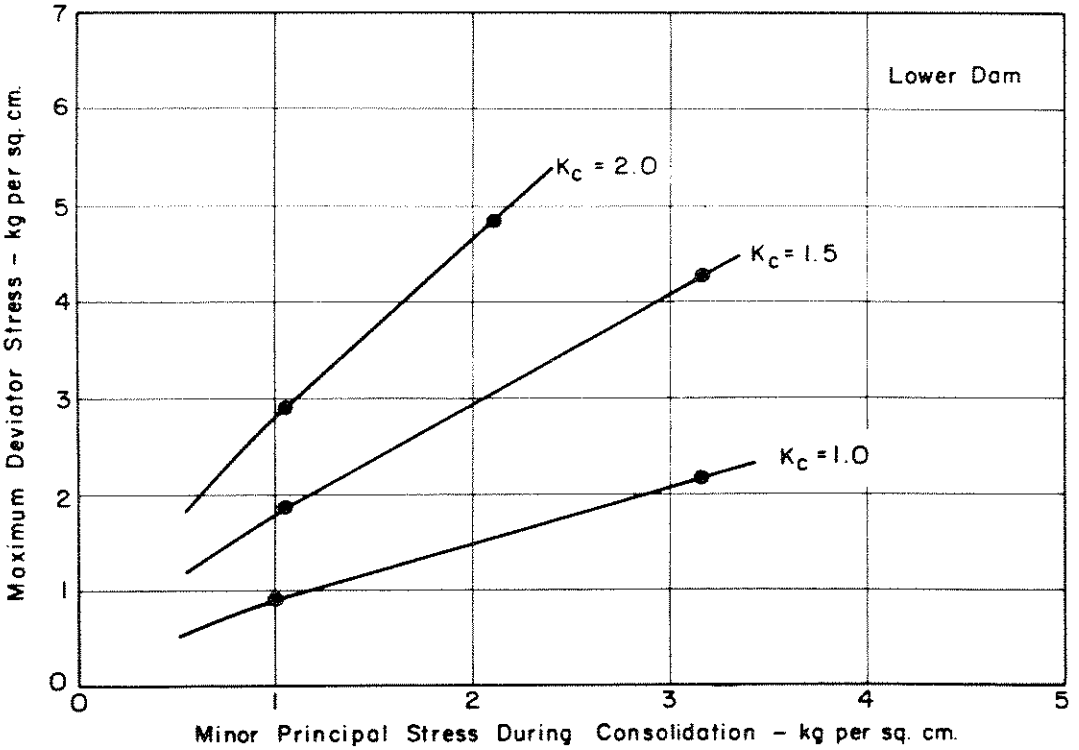

Fig. V-41 CYCLIC STRESSES CAUSING LIQUEFACTION AND 5% STRAIN IN 3 CYCLES FOR HYDRAULIC SAND FILL.

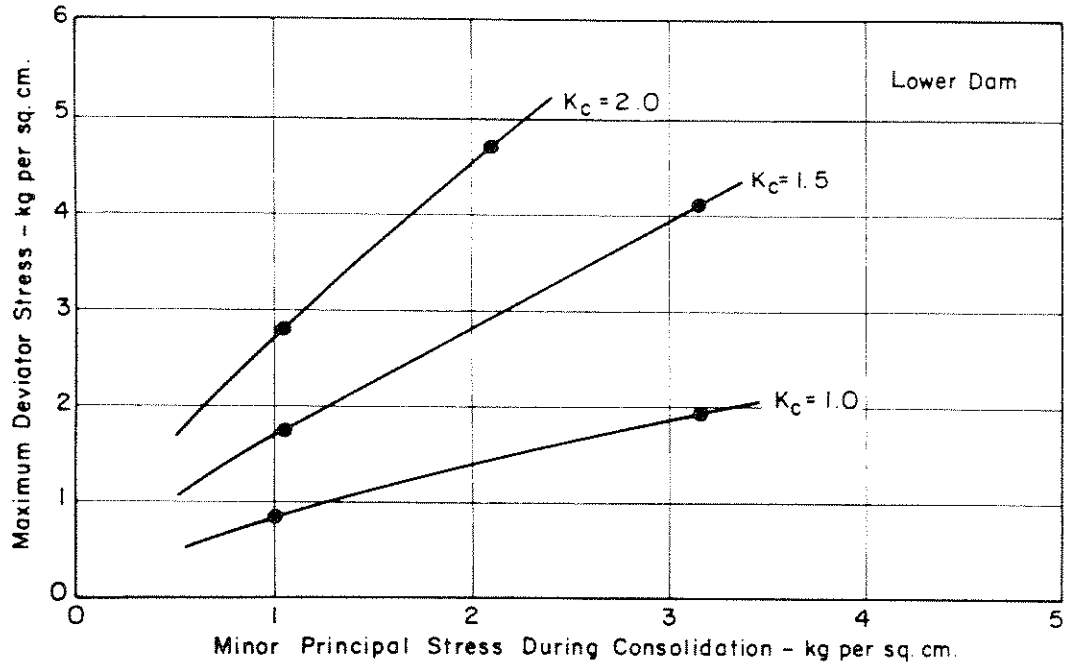

Fig. V-42 CYCLIC STRESSES CAUSING LIQUEFACTION AND 5% STRAIN IN 4 CYCLES FOR HYDRAULIC SAND FILL.

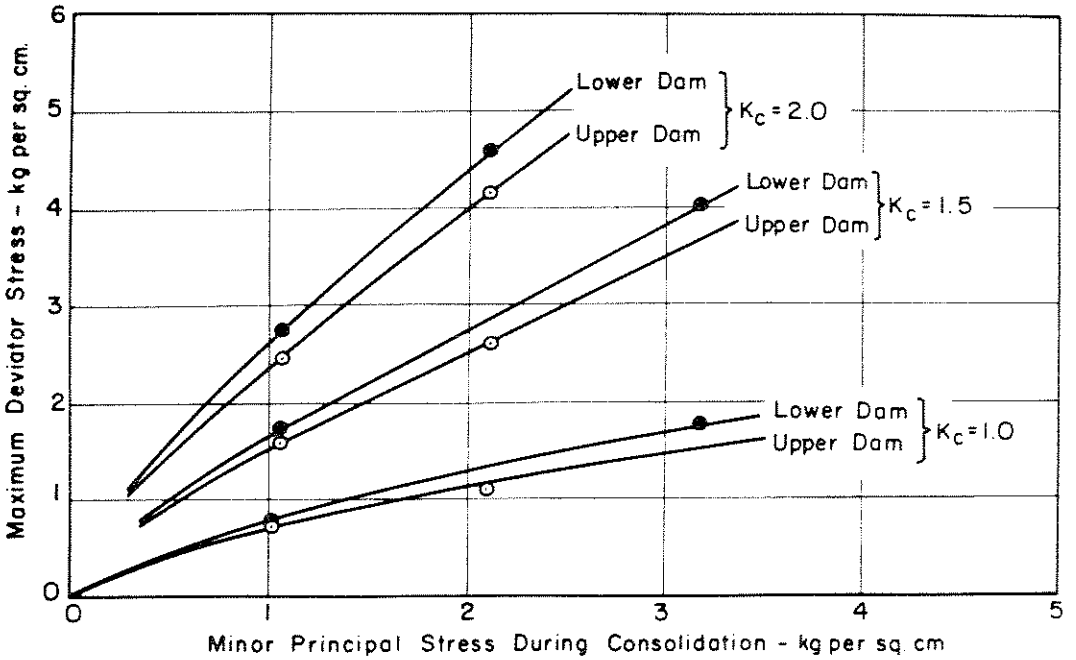

Fig. V-43 CYCLIC STRESSES CAUSING LIQUEFACTION AND 5% STRAIN IN 5 CYCLES FOR HYDRAULIC SAND FILL.

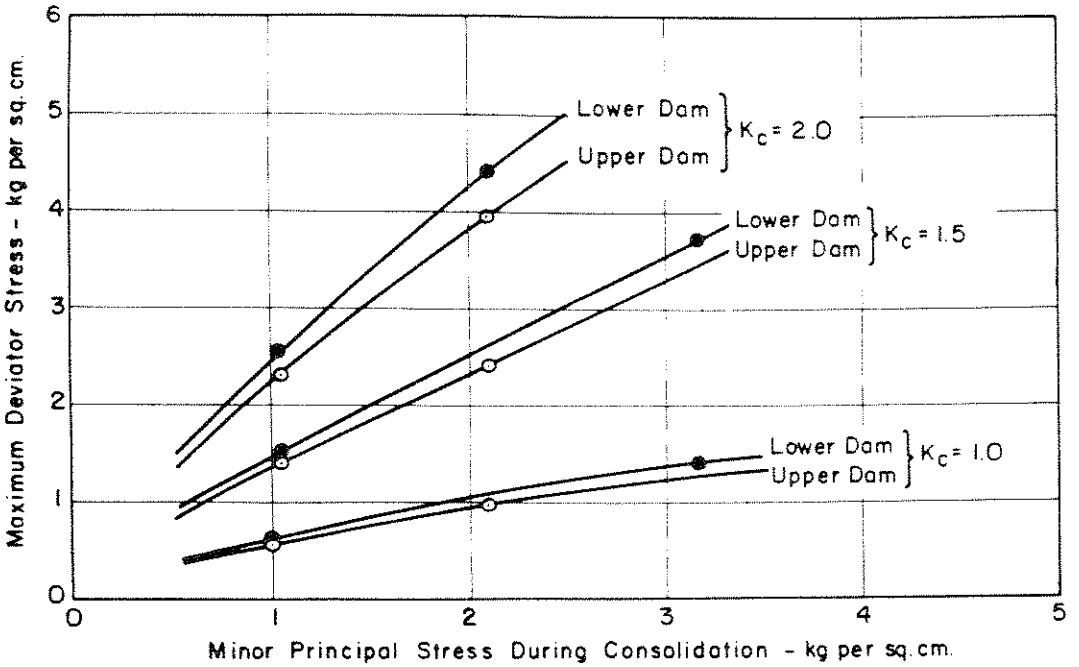

Fig. V-44 CYCLIC STRESSES CAUSING LIQUEFACTION AND 5% STRAIN IN 10 CYCLES FOR HYDRAULIC SAND FILL.

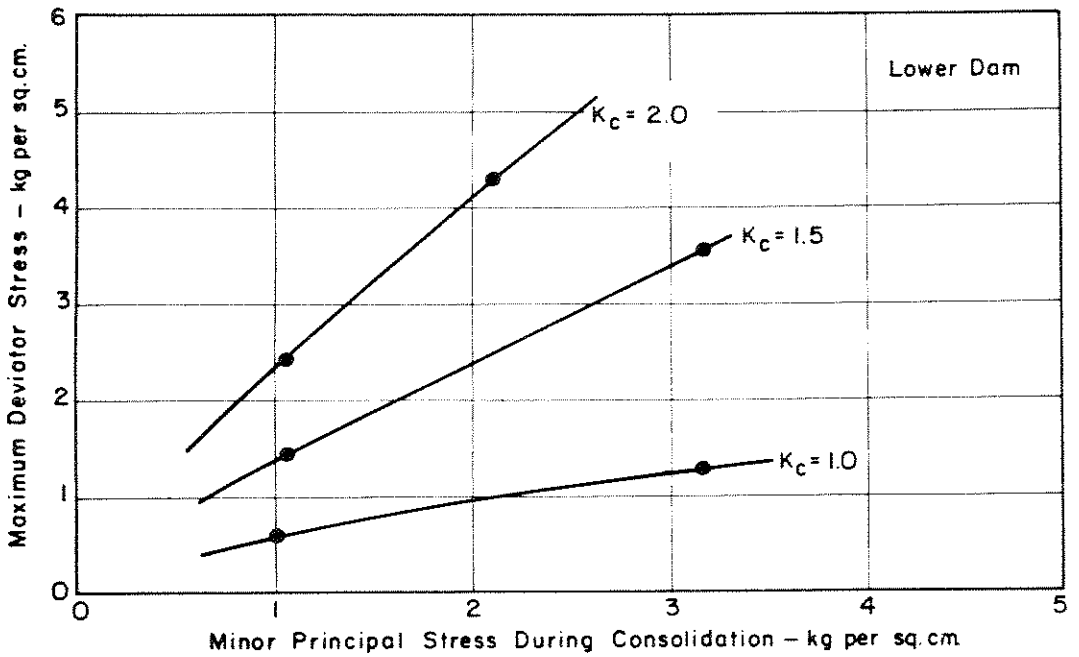

Fig. V-45 CYCLIC STRESSES CAUSING LIQUEFACTION AND 5% STRAIN IN 20 CYCLES FOR HYDRAULIC SAND FILL.

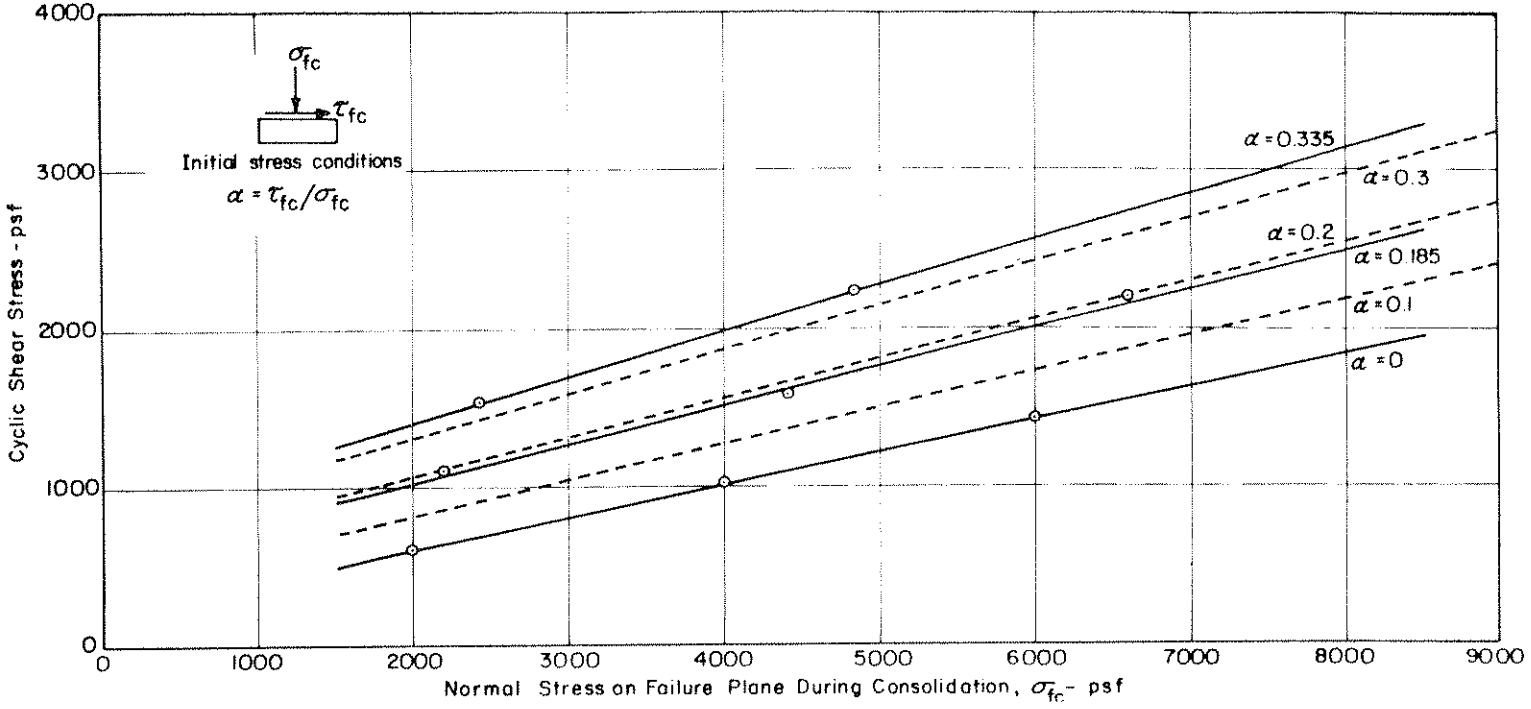

Fig. V-46 CYCLIC STRESS CONDITIONS CAUSING 5% STRAIN AND LIQUEFACTION IN 2 CYCLES FOR HYDRAULIC SAND FILL - LOWER SAN FERNANDO DAM.

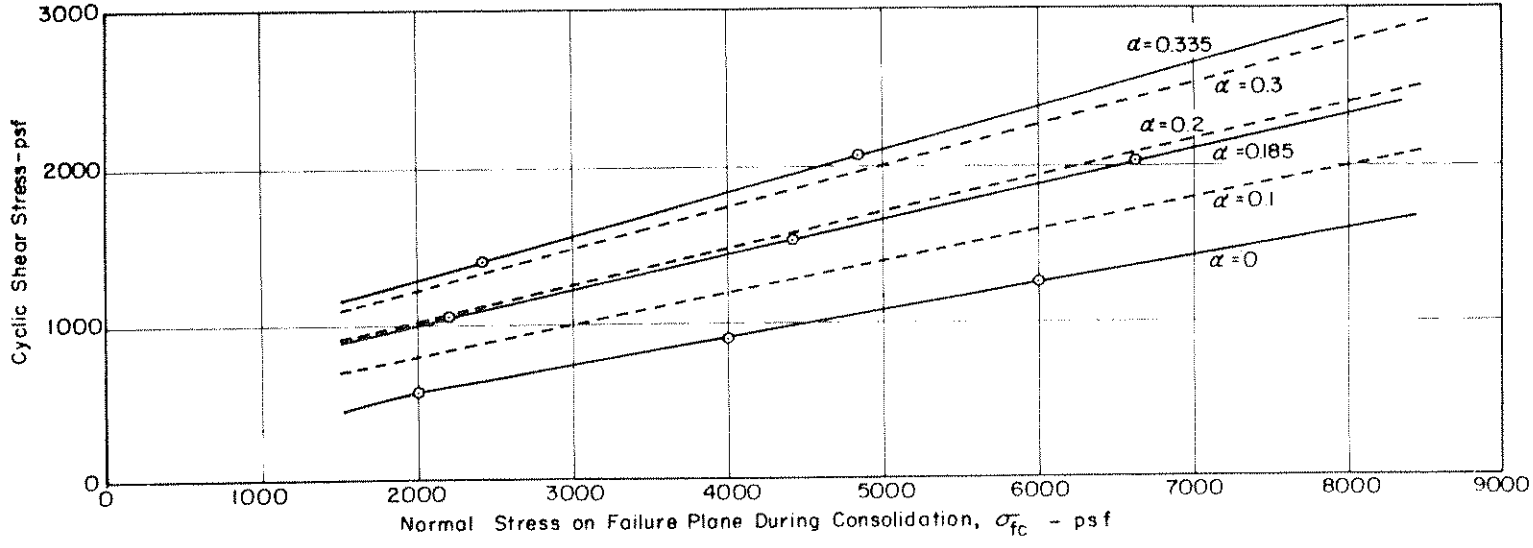

Fig. V-47 CYCLIC STRESS CONDITIONS CAUSING 5% STRAIN AND LIQUEFACTION

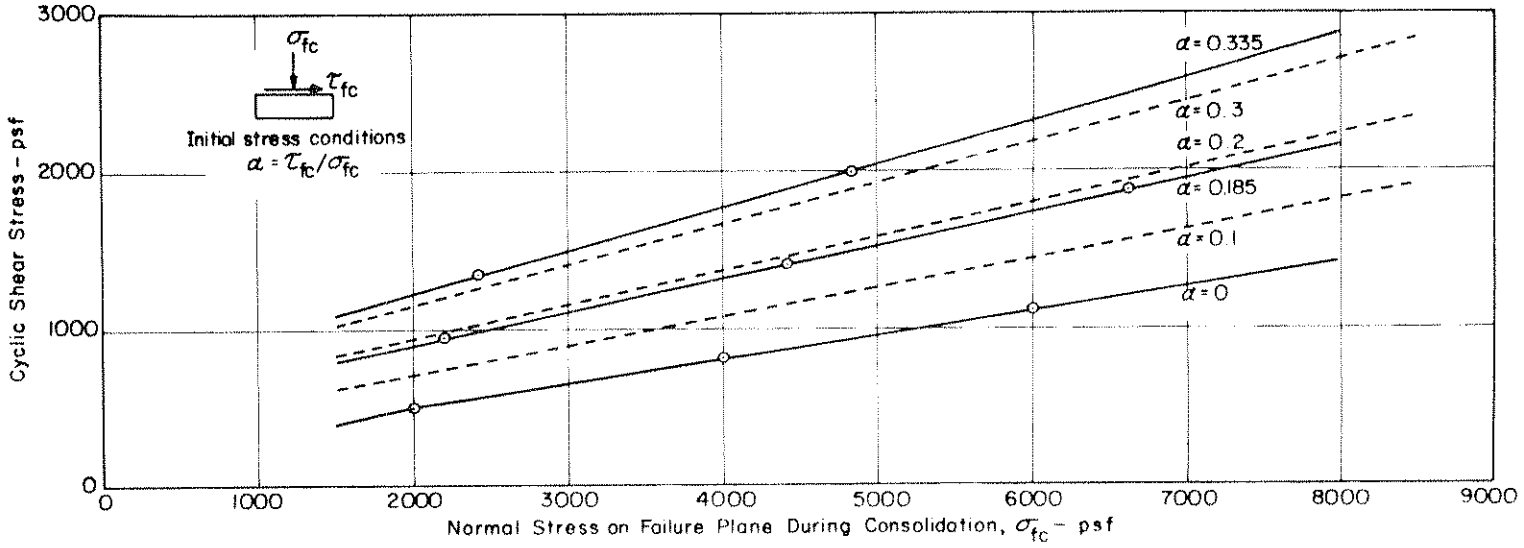

Fig. V-48 CYCLIC STRESS CONDITIONS CAUSING 5% STRAIN AND LIQUEFACTION IN 4 CYCLES FOR HYDRAULIC SAND FILL - LOWER SAN FERNANDO DAM.

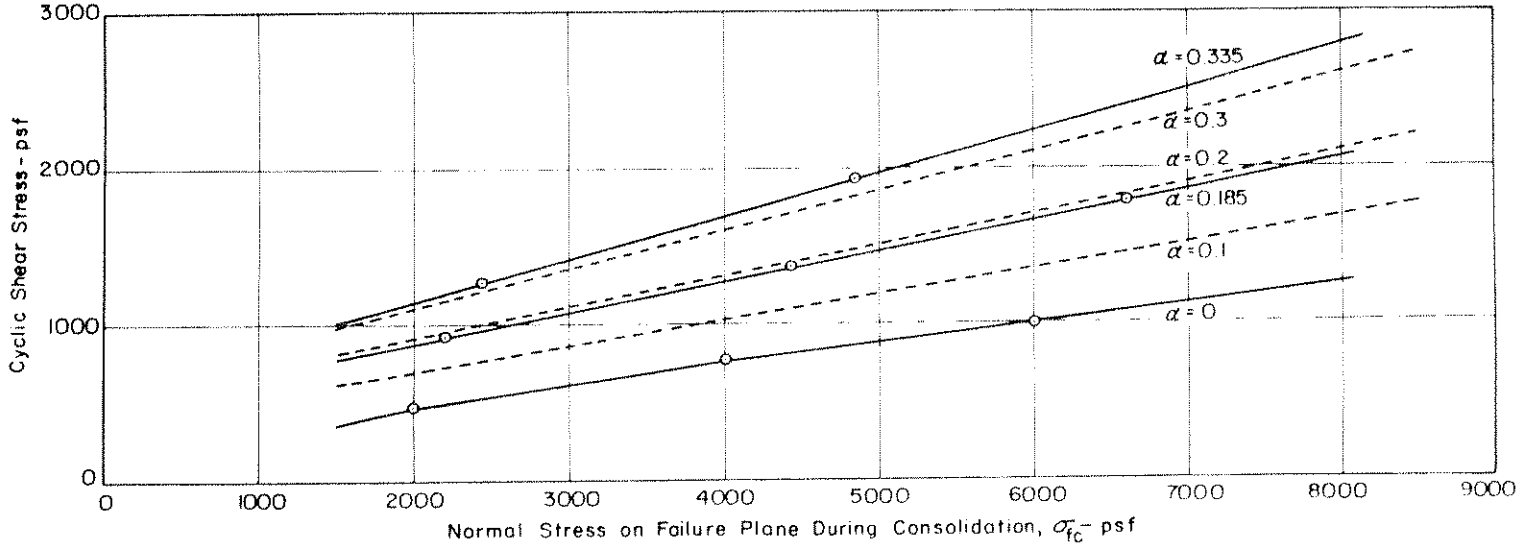

Fig. V-49 CYCLIC STRESS CONDITIONS CAUSING 5% STRAIN AND LIQUEFACTION IN 5 CYCLES FOR HYDRAULIC SAND FILL - LOWER SAN FERNANDO DAM.

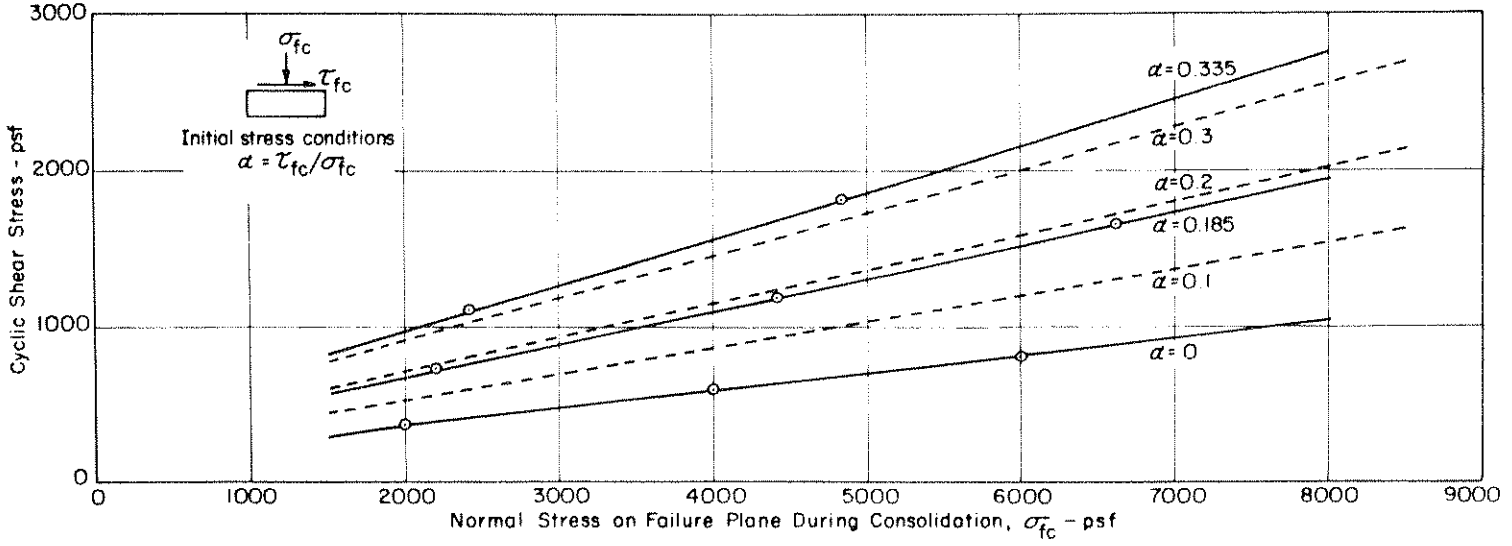

Fig. V-50 CYCLIC STRESS CONDITIONS CAUSING 5% STRAIN AND LIQUEFACTION IN 10 CYCLES FOR HYDRAULIC SAND FILL - LOWER SAN FERNANDO DAM.

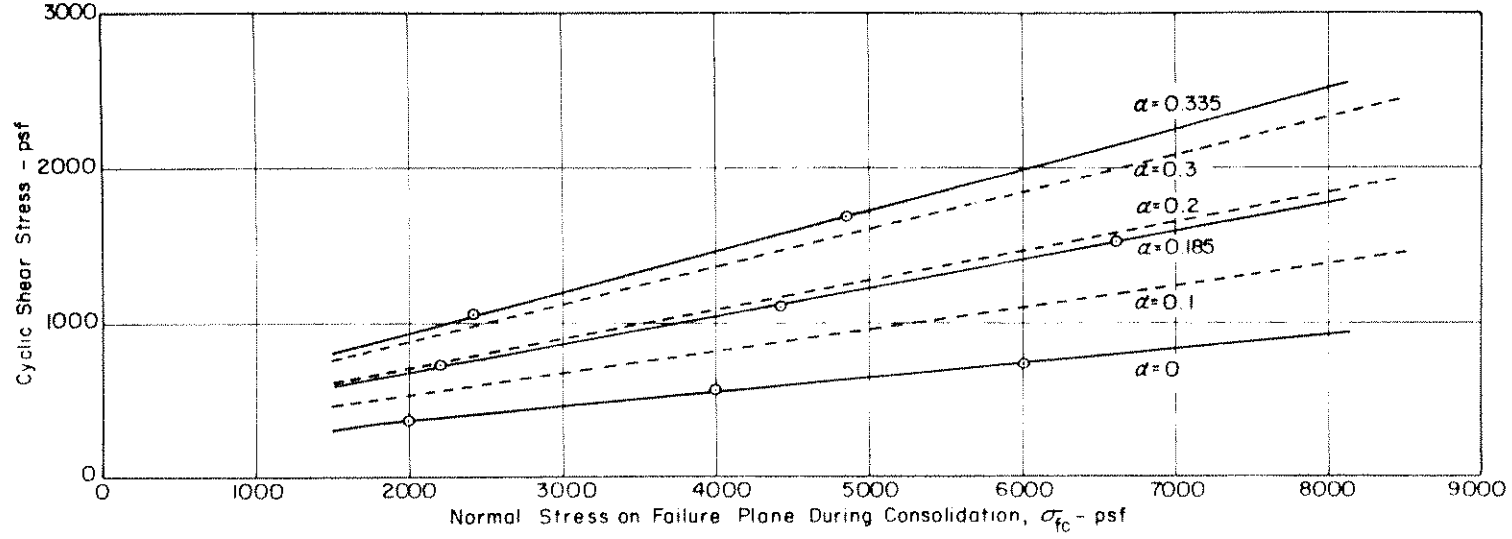

Fig. V-51 CYCLIC STRESS CONDITIONS CAUSING 5% STRAIN AND LIQUEFACTION IN 20 CYCLES FOR HYDRAULIC SAND FILL - LOWER SAN FERNANDO DAM.

of the cyclic shear stress which must be applied in the direction of potential failure to cause 5 percent axial strain and liquefaction, for samples initially consolidated under different initial stress conditions. The results in this form are required for use in the dynamic analysis of the stability of the Lower Dam during the San Fernando earthquake, presented in Part VIII.

Finally it should be noted that the data presented in Figs. V-40 to V-51 show the cyclic stresses causing liquefaction and 5 percent strain. Because the samples did not liquefy completely after initial liquefaction had developed, somewhat higher stresses were required to cause higher strains. In general it was found that the cyclic shear stresses required to cause compression strains of 10 and 20 percent were greater than those required to cause 5 percent strain by the following factors:

$$\frac{\text{Cyclic stress required to cause 20\% strain}}{\text{Cyclic stress required to cause 5\% strain}} = 1.15$$

$$\frac{\text{Cyclic stress required to cause 10\% strain}}{\text{Cyclic stress required to cause 5\% strain}} = 1.06$$

With the aid of these relationships and the data presented in Figs. V-40 to V-51, the stresses causing any level of strain in any number of stress cycles can readily be determined.

Part VI - Reconstruction of Mechanics of Sliding for Lower San Fernando Dam

From the field and laboratory studies described in the preceding section the following conclusions can be drawn concerning the slide in the Lower San Fernando Dam:

1. There was no evidence of failure in the foundation soils.
2. The slide occurred as a result of failure in a zone of soil about 20 ft thick in the hydraulic fill near the base of the embankment.
3. Failure was accompanied by some liquefaction of the hydraulic sand fill.

Recognition of these facts, together with the possibility of identifying large blocks of undisturbed soil in the slide mass, made it possible to reconstruct the probable mechanics of sliding.

Consider for example the section EE shown in Plate 1. The trench section showed that a large block of soil, block number 7 in Plate 1b, had moved intact during the slide. The original position of this block in the embankment could be located in three ways:

1. By measuring the length of the pieces of concrete slab behind this soil block in the failure zone and measuring this distance down from the original position of the parapet wall.
2. By knowing the original position of the hydraulic shale fill forming the top of this block.
3. By measuring the volume of soil in the slide zone behind this block and, on the assumption that very little slide debris had passed below the block, finding a position retaining an equal volume of soil in the original cross-section.

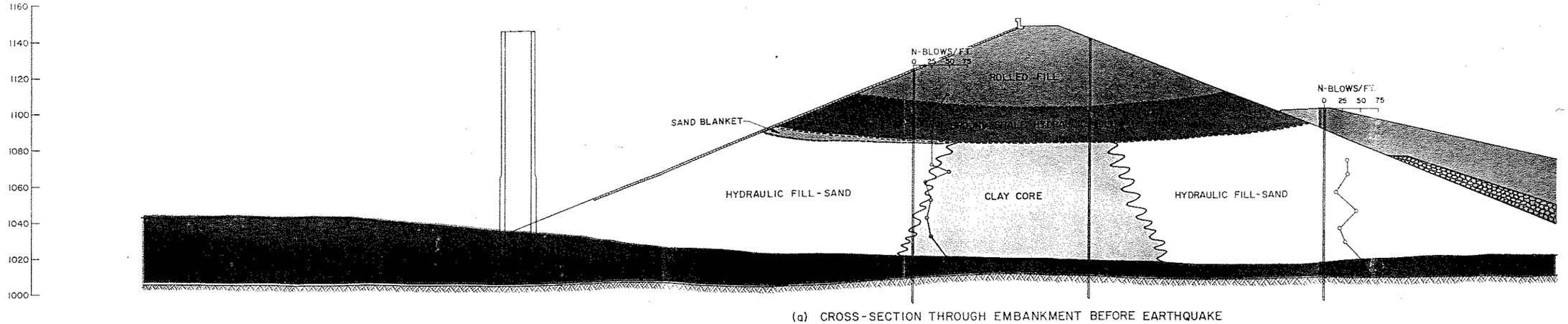

(a) CROSS-SECTION THROUGH EMBANKMENT BEFORE EARTHQUAKE

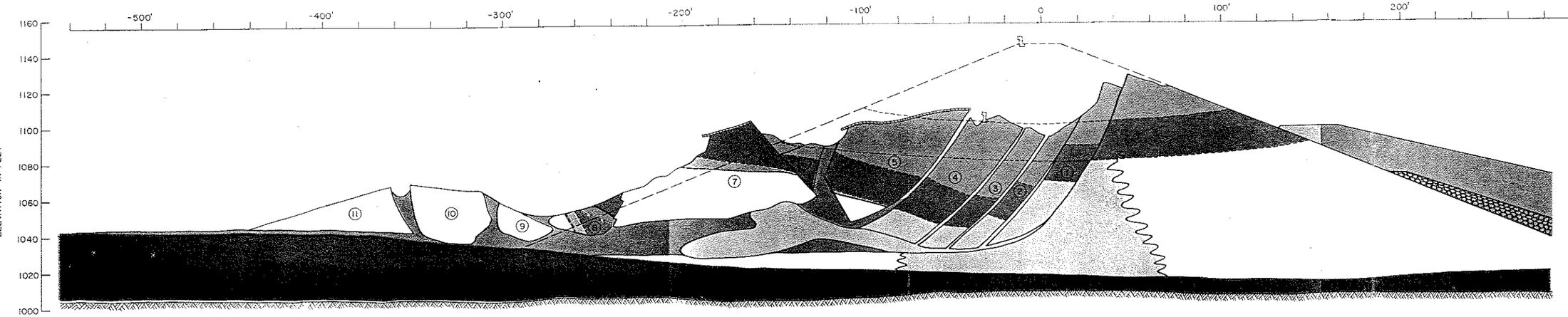

(b) CROSS-SECTION THROUGH EMBANKMENT AFTER EARTHQUAKE

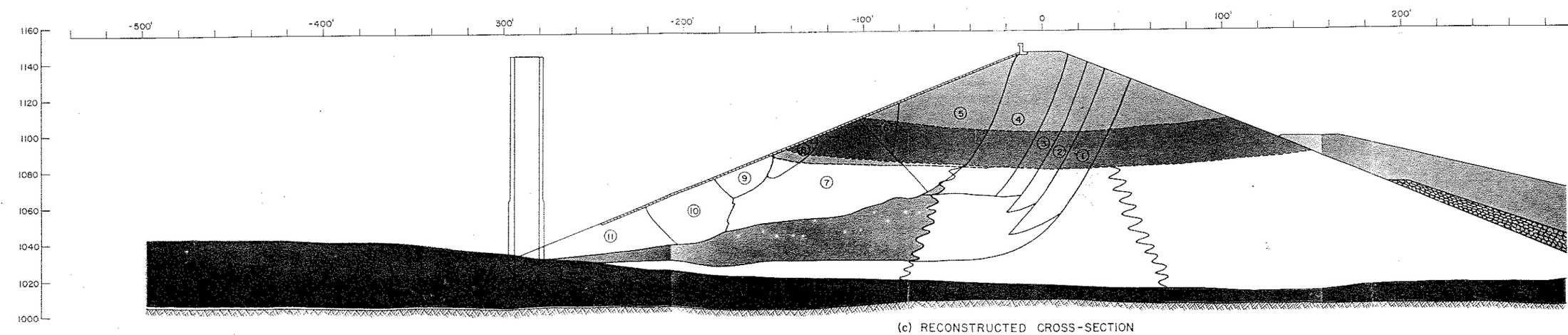

(c) RECONSTRUCTED CROSS-SECTION

LEGEND

- ROLLED FILL
- GROUND SHALE - HYDRAULIC
- HYDRAULIC FILL - SAND
- CLAY CORE
- ALLUVIUM
- ROCK DRAIN
- SAND BLANKET
- LIQUEFIED ZONE

LOWER SAN FERNANDO DAM

CROSS-SECTIONS THROUGH EMBANKMENT

SECTION E-E

PLATE 1

All three of these procedures gave similar initial locations for the block and it was determined to have moved from the location shown in Plate 1c.

With the aid of the surface boundaries indicated by the original roadway across the top of the dam, the parapet wall, and the concrete slab facing for the upstream slope and the internal boundaries between different zones of soil within the embankment which could be identified from the trench section and the boring logs, it was possible to recognize the large relatively undisturbed blocks of soil numbered 1 to 11 in Plate 1b. Using techniques similar to those described above, the original positions of these blocks were then determined as shown in Plate 1c. It was found that the blocks fitted together extremely well and formed the upper part of the original embankment. However no blocks of soil could be identified as having moved from the zone colored blue along the base of the embankment in this figure. It appeared that this soil had spread throughout the slide zone, infiltrating between the large blocks of undisturbed material, extruding below the toe of the original embankment and sometimes rising to the surface within the slide zone.

Thus by reconstructing the original positions of the slide debris in this way, it was concluded that the slide must have been triggered by liquefaction of the hydraulic fill near the base of the embankment. The soil above this fill had then broken into blocks which moved laterally through distances varying from 30 to 150 feet as the sliding progressed, thereby removing support from the upstream side of the clay core. At this stage the core could no longer support the overlying mass of soil causing a secondary slide movement involving the crest of the dam and the upper part of the downstream slope. During these movements the clay core was extruded by the overlying mass of soil to form the tongue-like section shown in Plate 1.

Similar reconstructions of the original and final locations of the soils in the slide zone along sections FF and GG are shown in Plates 2 and 3. In these cases also, the mechanics of sliding appears to be very similar to that described above with the primary zone of failure being in the hydraulic sand fill near the base of the embankment. Again the diffusion of this material throughout the slide zone provides convincing evidence that it was liquefied by the earthquake shaking. Taken in conjunction with the other evidence of liquefaction observed in the field (sand-filled cracks, sand boils, large lateral movements, extrusion of liquefied sand from the toe of the embankment) there seems to be little doubt that liquefaction of the hydraulic sand fill was the primary cause of the slide movements in this embankment.

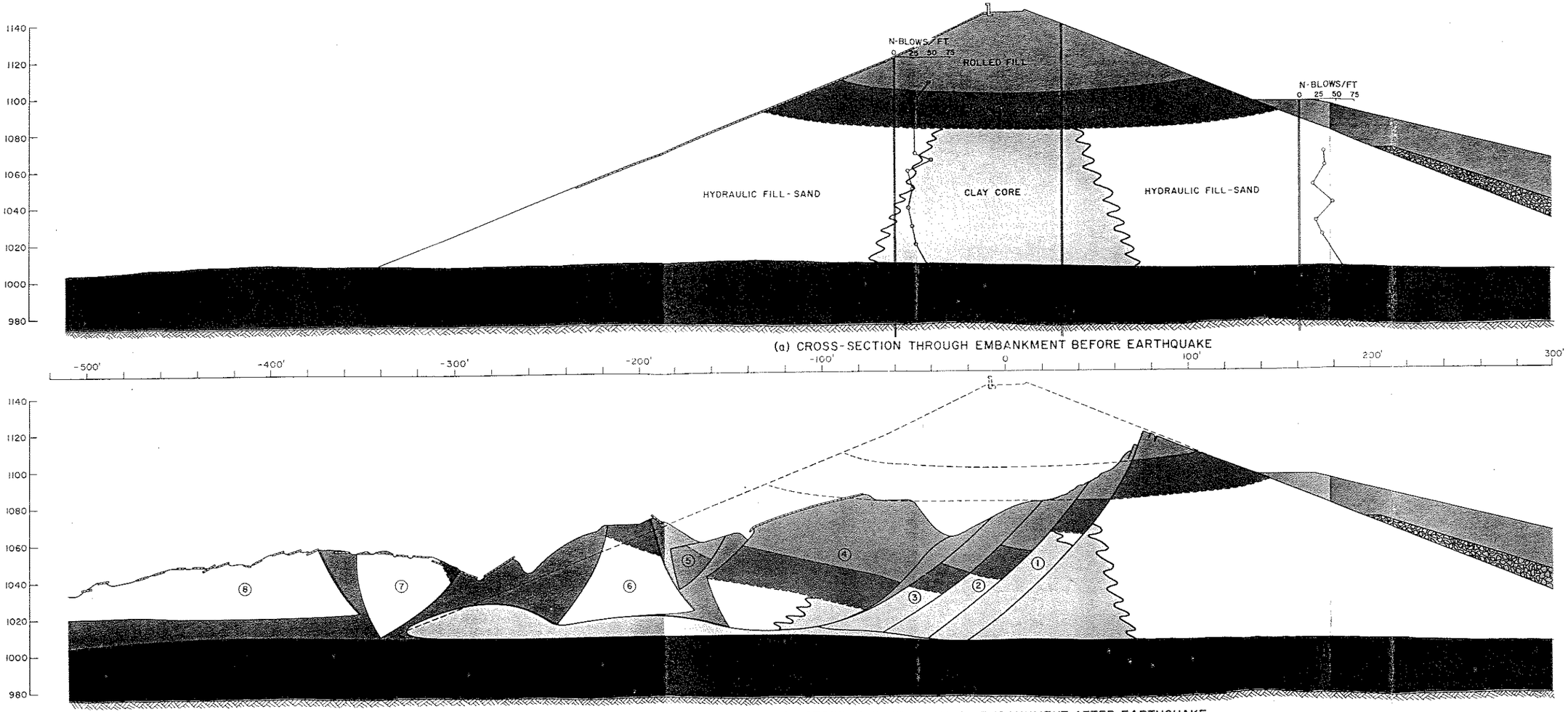

(a) CROSS-SECTION THROUGH EMBANKMENT BEFORE EARTHQUAKE

(b) CROSS-SECTION THROUGH EMBANKMENT AFTER EARTHQUAKE

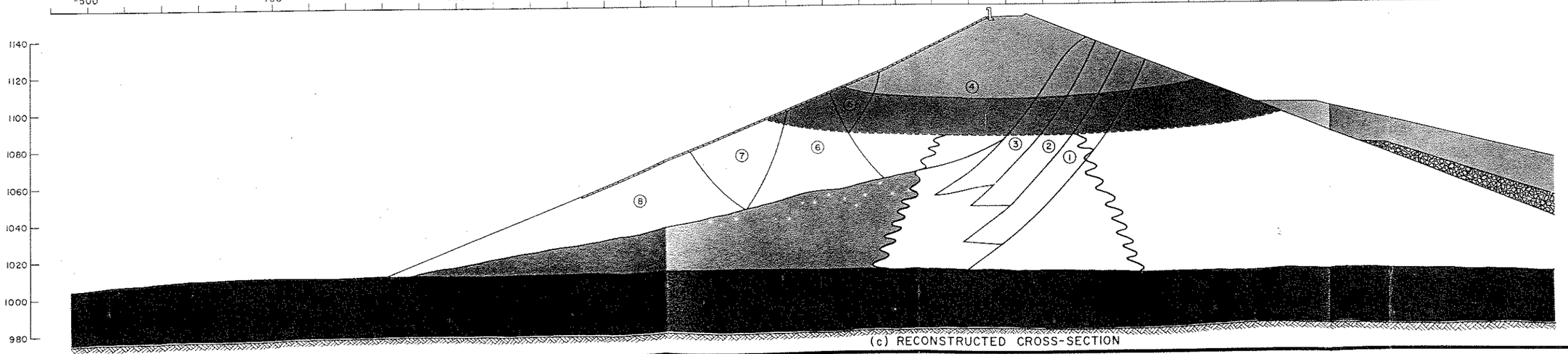

(c) RECONSTRUCTED CROSS-SECTION

LEGEND

- ROLLED FILL
- GROUND SHALE-HYDRAULIC F
- HYDRAULIC FILL-SAND
- CLAY CORE
- ALLUVIUM
- ROCK DRAIN
- LIQUEFIED ZONE

LOWER SAN FERNANDO DAM

CROSS-SECTIONS THROUGH EMBANKMENT

SECTION F-F

PLATE 2

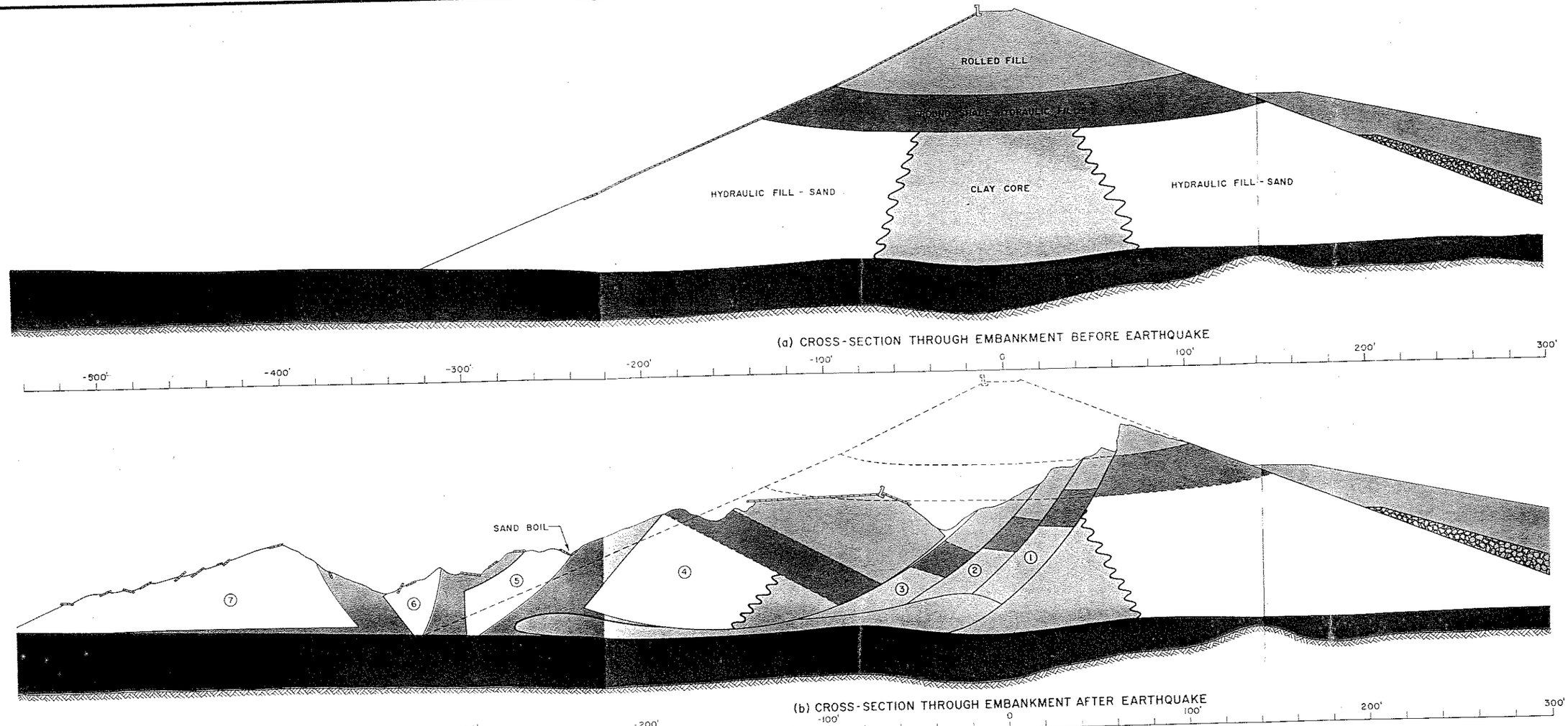

(a) CROSS-SECTION THROUGH EMBANKMENT BEFORE EARTHQUAKE

(b) CROSS-SECTION THROUGH EMBANKMENT AFTER EARTHQUAKE

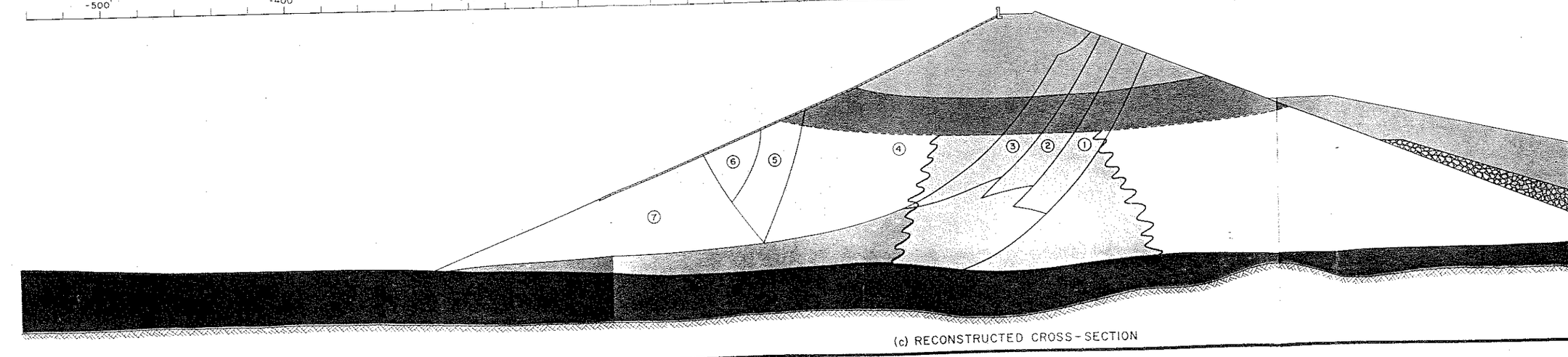

(c) RECONSTRUCTED CROSS-SECTION

LEGEND

- ROLLED FILL
- GROUND SHALE-HYDRAULIC FIL
- HYDRAULIC FILL-SAND
- CLAY CORE
- ALLUVIUM
- ROCK DRAIN
- LIQUEFIED ZONE

LOWER SAN FERNANDO DA

CROSS-SECTIONS
THROUGH EMBANKMENT
SECTION G-G
PLATE 3

Part VII - Pseudo Static Analyses of Stability of Embankments

With few exceptions, analyses of the stability of embankment dams during earthquakes are conventionally made using pseudo-static methods. In this approach the stability of a potential sliding mass is determined as for static loading conditions and the effects of an earthquake are taken into account by including an equivalent horizontal force, acting on the potential sliding mass, in the computations. The horizontal force representing earthquake effects is expressed as the product of the weight of the sliding mass under consideration and a seismic coefficient, k.

In United States practice, the value of the seismic coefficient is normally selected on the basis of the seismicity of the region in which the dam is to be constructed, values in California ranging from a lower limit of 0.05 to an upper limit of about 0.15. For the San Fernando dams in the 1971 earthquake, a value of 0.15 would therefore represent most normal design practices; this value was in fact used to evaluate the seismic stability of the Lower Dam in 1966.

In order to evaluate the applicability of this method of approach for determining the stability of the San Fernando dams in the 1971 earthquake, analyses have been made using the conventional method of slices to compute the factors of safety for the dams using a seismic coefficient of 0.15 and, since both dams presumably reached the point of incipient failure during the earthquake (the 5 ft downstream movement of the Upper Dam is about the limit of tolerable movements), the values of seismic coefficient which would lead to a computed factor of safety of unity.

Lower San Fernando Dam

Computation of the factor of safety against sliding of the upstream slope of the Lower Dam using a pseudo-static approach is complicated by the availability of different strength parameters for the embankment soils. For the short duration of the earthquake of Feb. 9, 1971 it is apparent that strength parameters should correspond to undrained loading conditions. Thus the test data for consolidated-undrained triaxial compression tests shown in Fig. V-36 provide an appropriate basis for analysis.

Reference to Fig. V-36 shows that there is considerable scatter of the test results obtained on undisturbed samples of the hydraulic fill, reflecting the variability of the soil in the embankment. Thus it is possible to interpret the data to determine a lower bound or conservative strength relationship for the shell material or to draw an average line through the data points (Fig. V-36). Strength parameters defining the envelope of failure for total stresses in consolidated-undrained tests on the shell material are therefore as follows:

Conservative: $c = 1200$ psf; $\phi = 20°$

Average: $c = 2040$ psf; $\phi = 19°$.

These strength parameters are somewhat higher than those used by the Los Angeles Department of Water and Power in the 1966 stability studies ($c = 720$ psf and $\phi = 25°$) because of the even more conservative evaluation of the test data made at that time.

The undrained shear strength of the core material was determined from the shear strength/effective pressure ratio of 0.3 indicated by the test data previously discussed. Shear strength values varied from about 1700 psf near the top of the core to about 2600 near the base. Test

data for the foundation soils gave considerably higher strength parameters (c = 1560 psf and $\phi = 27°$) than for the hydraulic fill, as shown in Fig. V-37.

In using the test data for stability computations it is possible to use the strength parameters directly to determine the soil strength in the embankment or to convert the Mohr envelope into a relationship between the shear stress on the failure plane at failure, τ_{ff}, and the normal stress on the failure plane at the end of the consolidation phase of the tests, σ_{fc}. Both procedures are apparently used in practice and accordingly, analyses were made using both procedures in the present study.

The critical surfaces of sliding determined by the analyses are shown in Fig. VII-1 and the computed factors of safety for different seismic coefficients, as determined by the conventional method of slices, are presented in Table VII-1. It may be seen that the computed locations of the most critical sliding surface are in reasonably good agreement with the position of the slide zone in the embankment, and that the analyses correctly indicate that failure would not extend into the foundation Soils. However, for a seismic coefficient of 0.15, the computations indicate factors of safety ranging from about 1.22 for a conservative interpretation of the test data combined with a Mohr envelope method of data use, to about 1.61 for an average interpretation of the test data combined with the use of the τ_{ff} vs σ_{fc} strength relationship.

Since it has been common practice to interpret a computed factor of safety exceeding about 1.1 to be indicative of adequate seismic stability for an embankment, it is clear that the use of conventional pseudo-static analyses would not have predicted the failure which actually occurred.

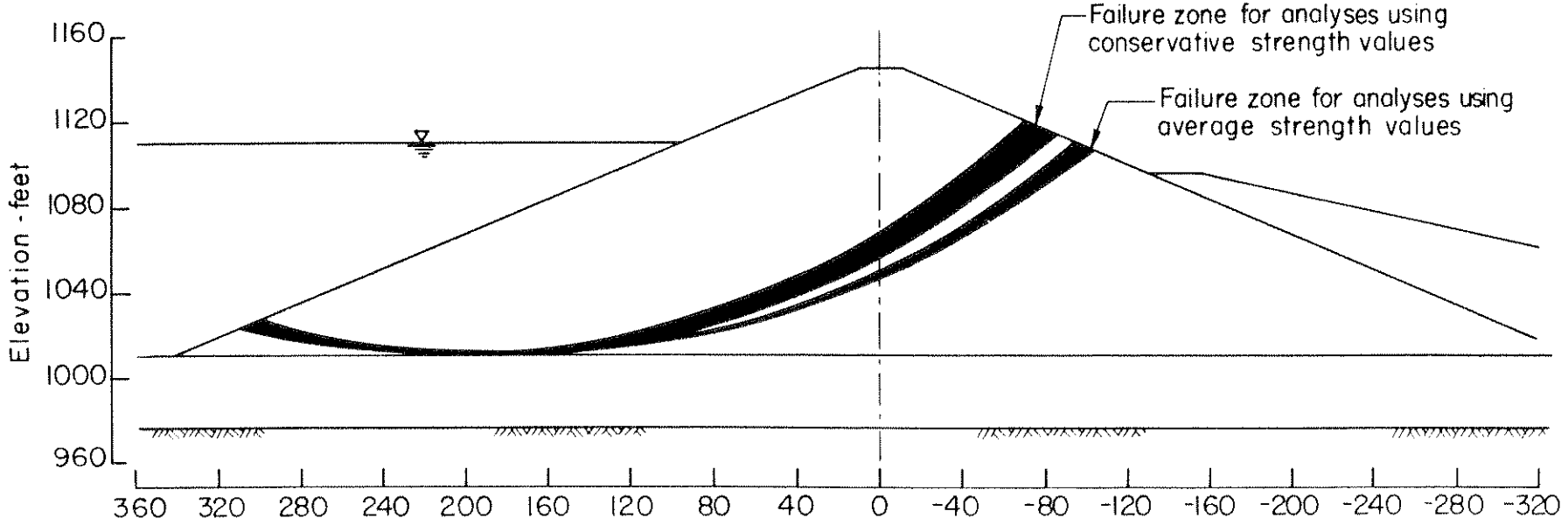

Fig. VII-1 FAILURE ZONES INDICATED BY PSEUDO-STATIC STABILITY ANALYSES - LOWER SAN FERNANDO DAM.

Table VII-1

Results of Pseudo Static Analyses of Stability of Lower San Fernando Dam

Embankment Strength Characteristics		Data form used in analysis	Factor of Safety for Seismic Coefficient k = 0.15	Seismic Coefficient, k, for Factor of Safety = 1
c-psf	ϕ - degrees			
1200	20	Mohr envelope	1.22	k = 0.22
1200	20	τ_{ff} vs σ_{fc}	1.37	k = 0.25
2040	19	Mohr envelope	1.47	k = 0.29
2040	19	τ_{ff} vs σ_{fc}	1.61	k = 0.34

However, as shown in Table VII-1, the use of seismic coefficient values ranging from about 0.22 to 0.34, depending on the method of data interpretation, would have led to a computed factor of safety of unity. Presumably values of this order of magnitude would be required in pseudo-static analyses, even when other computational details are selected to minimize the computed factor of safety, to give factors of safety indicative of failure for earthquake motions comparable to those developed in the San Fernando area during the 1971 earthquake.

Upper San Fernando Dam

Similar computations to those described above were made for the Upper San Fernando Dam. The strength parameters for consolidated-undrained triaxial compression tests for the embankment and foundation soils of this dam were as follows (Figs. IV-22 and IV-23):

Embankment: $c = 1100$ psf; $\phi = 24°$

Foundation: $c = 1420$ psf; $\phi = 32°$.

The results of the pseudo-static analyses are shown in Figs. VII-2 to VII-4 and Table VII-2. The computed position of the critical sliding surface (Fig. VII-2) is again in reasonable agreement with the observed behavior of the embankment during the earthquake, in that downstream movement occurred with the formation of scarps on the upstream face in approximately the same position as that indicated by the analysis. However for a seismic coefficient of 0.15, the computed factor of safety was about 2.0 for soil strengths determined from a standard Mohr envelope or 2.5 for strengths determined from the τ_{ff} vs σ_{fc} form of data representation. In either case the analysis indicates an ample margin of safety against slide movements developing--a result in marked contrast to the actual behavior of the embankment.

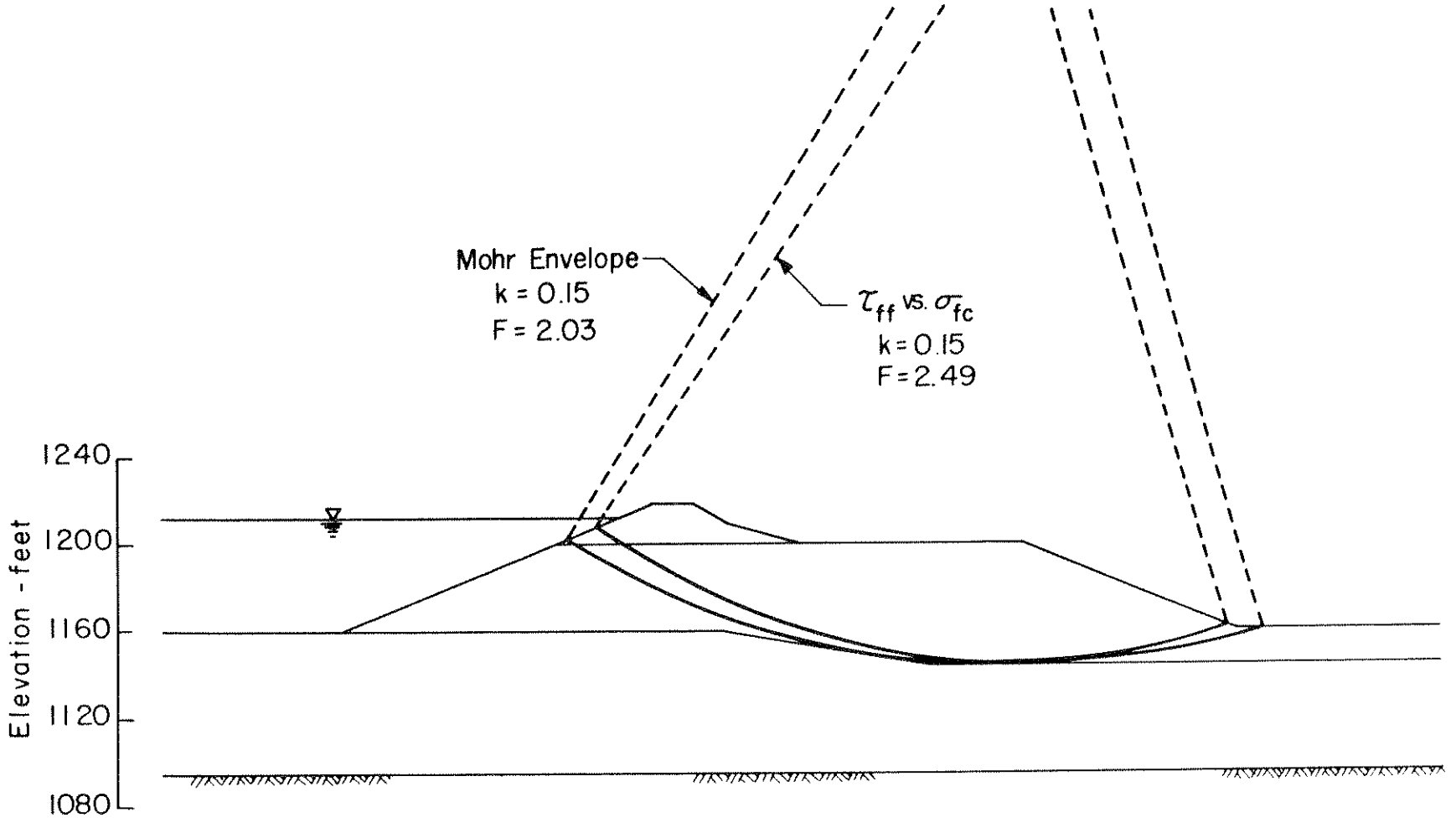

Fig. VII-2 RESULTS OF PSEUDO-STATIC ANALYSES OF EMBANKMENT STABILITY - UPPER SAN FERNANDO DAM.

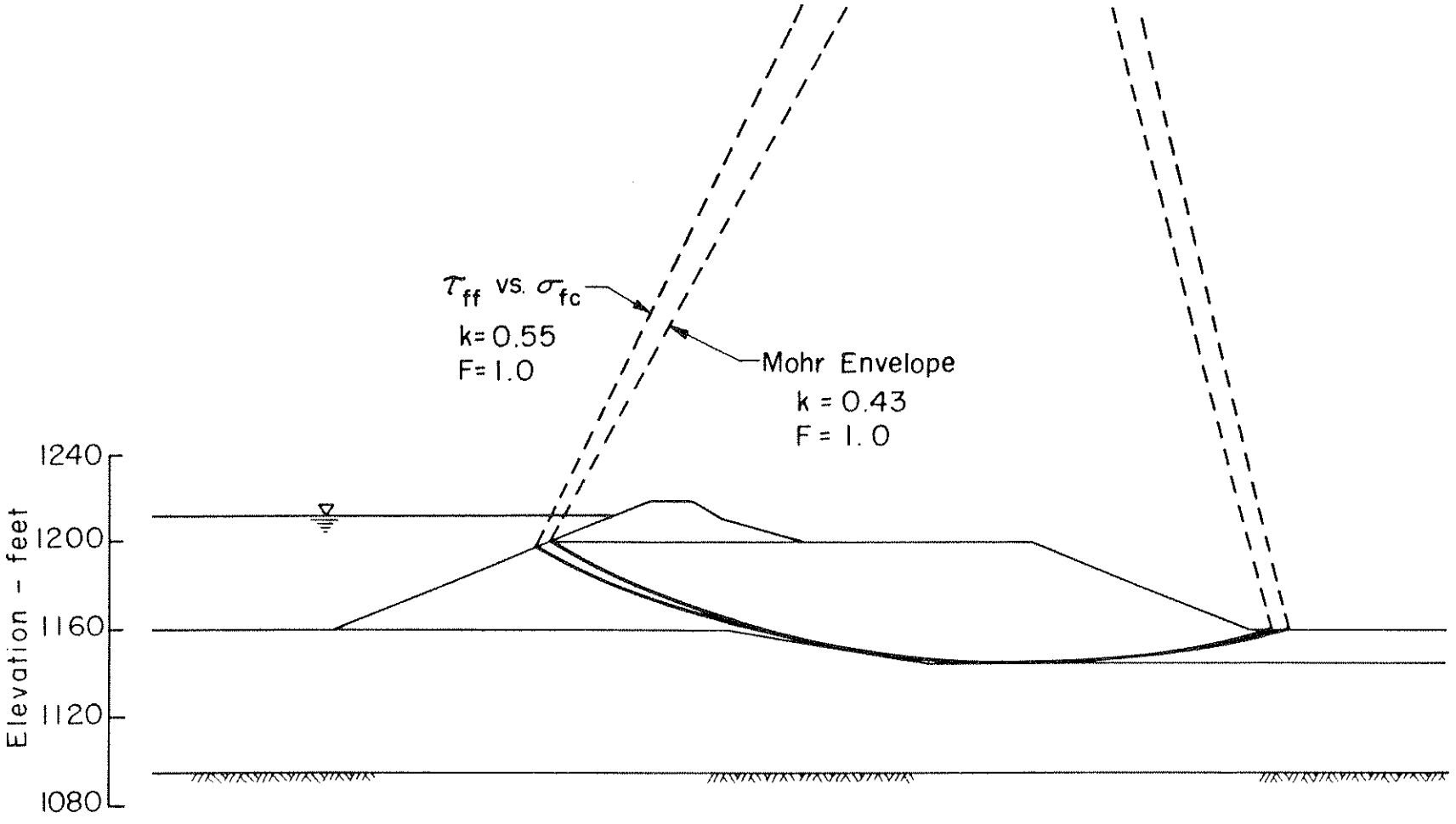

Fig. VII-3 RESULTS OF PSEUDO-STATIC ANALYSES OF STABILITY OF DOWNSTREAM SLOPE -UPPER SAN FERNANDO DAM.

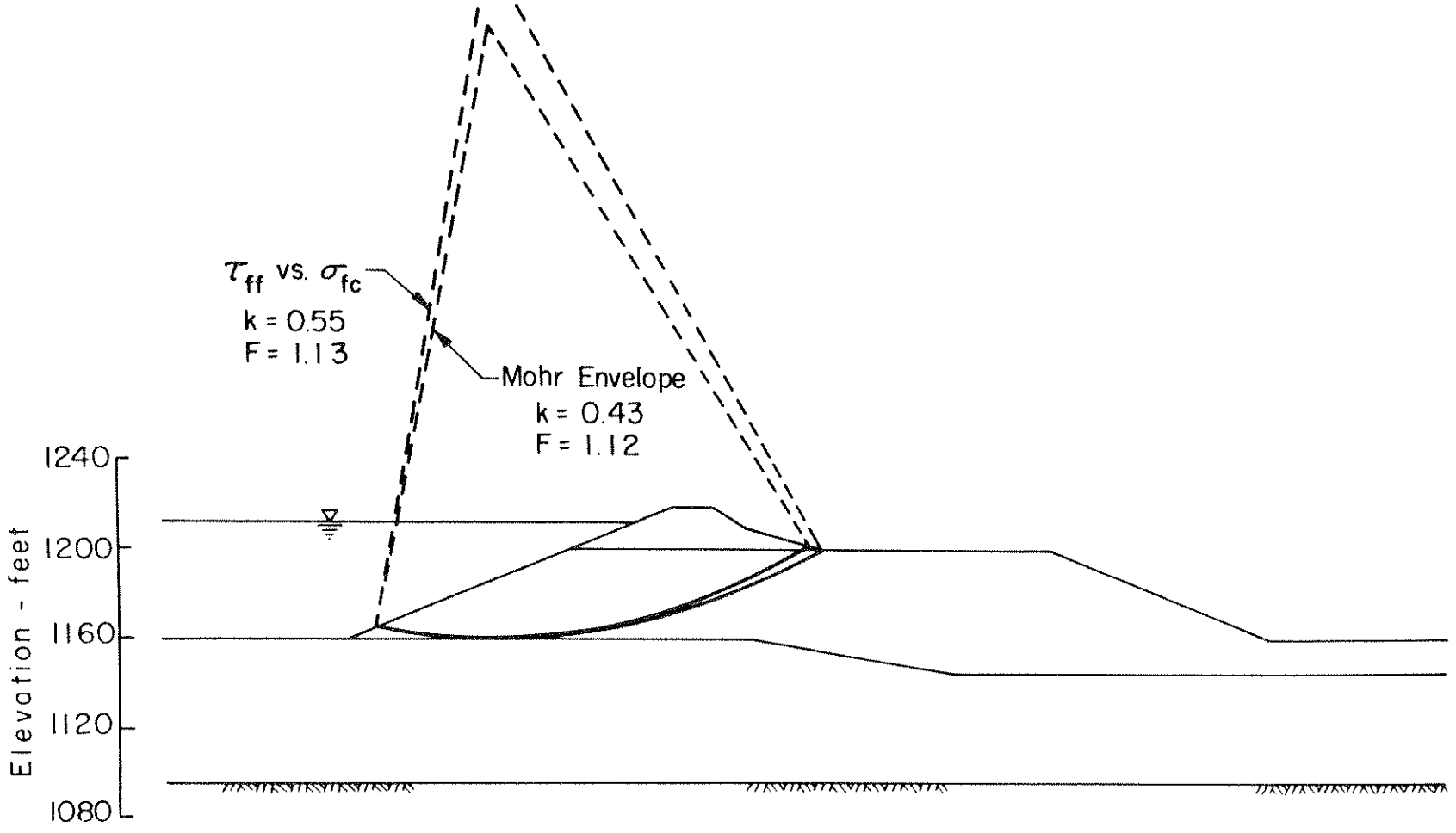

Fig. VII-4 RESULTS OF PSEUDO-STATIC ANALYSES OF STABILITY OF UPSTREAM SLOPE - UPPER SAN FERNANDO DAM.

Table VII-2

Results of Pseudo-Static Analyses of Stability of Upper San Fernando Dam

Embankment Strength Characteristics		Data form used in analysis	Factor of Safety for Seismic Coefficient k = 0.15	Seismic Coefficient for Factor of Safety = 1
c-psf	ϕ - degrees			
1100	24	Mohr envelope	2.03	k = 0.43
1400	28	τ_{ff} vs σ_{fc}	2.49	k = 0.55

In order to compute a factor of safety of 1.0 using the pseudo-static method of analysis, it would be necessary to use a seismic coefficient in the range 0.43 to 0.55 (Fig. VII-3), depending on how the consolidated-undrained test data is utilized in the computation procedure. These values are substantially higher than those currently used for seismic design but they are apparently necessary for the pseudo-static method of analysis to correctly indicate the performance of the Upper San Fernando Dam under the ground motion conditions which occurred in San Fernando in the 1971 earthquake.

It is interesting to note that the analysis correctly indicates a lower factor of safety for downstream sliding than for upstream slides. Using the seismic coefficient of 0.43 which indicates a factor of safety of 1.0 for downstream sliding, the computed factor of safety against an upstream slide was about 1.12 (Fig. VII-4).

Part VIII - Dynamic Analyses of the Stability of the Lower Dam During the San Fernando Earthquake

In view of the limitations of pseudo-static methods of analysis, procedures for dynamic analysis of embankment stability have been developed in recent years (Seed, 1966; Newmark, 1965). In dealing with saturated, cohesionless materials for which pore pressures may vary during an earthquake, it has been found most convenient to utilize the procedure proposed by Seed involving the following steps:

(1) Determine the initial stresses in the embankment before the earthquake.

(2) Determine the characteristics of the motions developed in rock underlying the embankment and its soil foundation during the earthquake.

(3) Evaluate the response of the embankment to the base rock excitation and compute the dynamic stresses induced in representative elements of the embankment.

(4) By subjecting representative samples of soil to the combinations of pre-earthquake stress conditions and superimposed dynamic stress applications, determine by test the effects of the earthquake-induced stresses on soil elements in the embankment. These effects will include any evidence of soil liquefaction and the magnitude of the deformations induced by the earthquake loading.

(5) From a knowledge of the deformations induced in individual soil elements in the embankment, evaluate the overall deformations and stability of the cross-section.

This procedure has been found to provide a satisfactory evaluation of the failure of the Sheffield Dam during the Santa Barbara earthquake of 1925 (Seed, et al, 1969) and it has been used for design studies of a number of other embankment dams. Accordingly it was adopted for analysis of the San Fernando dams in the 1971 earthquake. Details of the procedures followed in implementing the various steps in the analysis are described in the following pages.

Static Analysis

The dynamic test results summarized in Part V of this report clearly indicate that the effects of cyclic loading on the behavior of the embankment soils are considerably influenced by the stresses existing in the soil before the cyclic stresses are applied. Of particular importance are the initial normal stresses, σ_{fc}, and the ratio, τ_{fc}/σ_{fc}, along the potential failure plane (for which τ_{fc} is the initial shear stress). Therefore, in evaluating the effects of the San Fernando earthquake on the Lower Dam, the initial normal stresses, σ, and the initial shear stresses, τ, existing before the earthquake along potential failure planes throughout the dam must first be determined.

These initial stresses can be evaluated most conveniently by static finite element procedures. The use of these procedures for computing static stresses in soil structures is described in detail in several recent publications (e.g., Duncan and Chang, 1970; Kulhawy et al., 1971). The procedures permit the simulation of the appropriate construction sequence of the embankment and incorporate a non-linear representation of the stress-strain characteristics of the soils comprising the dam and its foundation. Appropriate non-linear stress-strain parameters for each soil type in the Lower Dam were established using the results of

consolidated-drained triaxial compression tests and published data for similar soils (e.g., Kulhawy, et al., 1971). The parameters used in the static analysis of the Lower Dam are summarized in Table VIII-1.

The initial static stresses were computed along several planes within the foundation layer and within the embankment. Typical values of initial effective normal stress, σ_o', initial shear stress, τ_o, and the ratio, τ_o/σ_o', along the base of the embankment are presented in Fig. VIII-6. Similar plots have been obtained for other parts of the embankment and foundation layer. These values, together with the cyclic test data presented in Figs. V-46 through V-51, were used to determine the stresses required to cause failure, as indicated by the development of excessive strain, in the hydraulic fill and the foundation soils.

Base Rock Motions

During the San Fernando earthquake of 1971, a good evaluation of the motions developed in the rock formations underlying the Lower Dam and the foundation alluvium is provided by the seismoscope record obtained on the abutment. The rock formation at the recording station is generally similar to that underlying the embankment and the motion characteristics should therefore be about the same. As previously discussed, the seismoscope record has been ingeniously interpreted by R. F. Scott to provide estimates of the time history of accelerations in directions normal and parallel to the axis of the dam. The resulting motions in a direction normal to the axis, as suggested by Scott, are shown in Fig. VIII-1a. This record of rock motions was used for evaluating the dynamic response of the embankment during the earthquake.

In view of the approximations required to obtain this record, however, and the fact that it contains some unusual low-frequency components

Table VIII-1

Soil Parameters used in Nonlinear Static Analysis

Lower San Fernando Dam

Soil Parameter	Symbol	Values used in Analysis					
		Rolled Fill	Ground Shale	Rolled Fill Berm	Hydraulic Fill	Clay Core	Foundation Layer
Dry Unit Weight	γ_d (pcf)	125	106	125	106	106	110
Buoyant Unit Weight	γ_b (pcf)	78	64	78	64	64	68
Cohesion	c (psf)	2600	0.0	2600	0.0	0.0	0.0
Friction Angle	ϕ	25°	37°	25°	37°	37°	38°
Modulus Number	K	300	510	300	510	510	330
Modulus Exponent	n	0.76	0.54	0.76	0.54	0.54	0.41
Failure Ratio	R_f	0.90	0.72	0.90	0.72	0.72	0.76
Poisson's Ratio Parameters	G	0.30	0.41	0.30	0.41	0.41	0.40
	F	0.10	0.23	0.10	0.23	0.23	0.16
	d	3.8	9.4	3.8	9.4	9.4	5.8

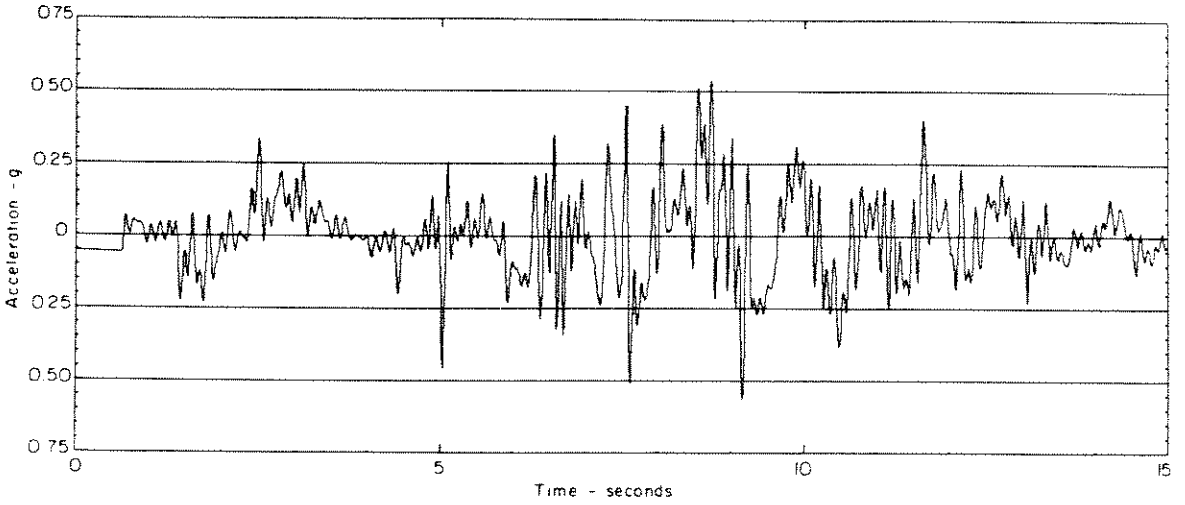

(a) Motions Determined from Seismoscope Record (after R. F. Scott).

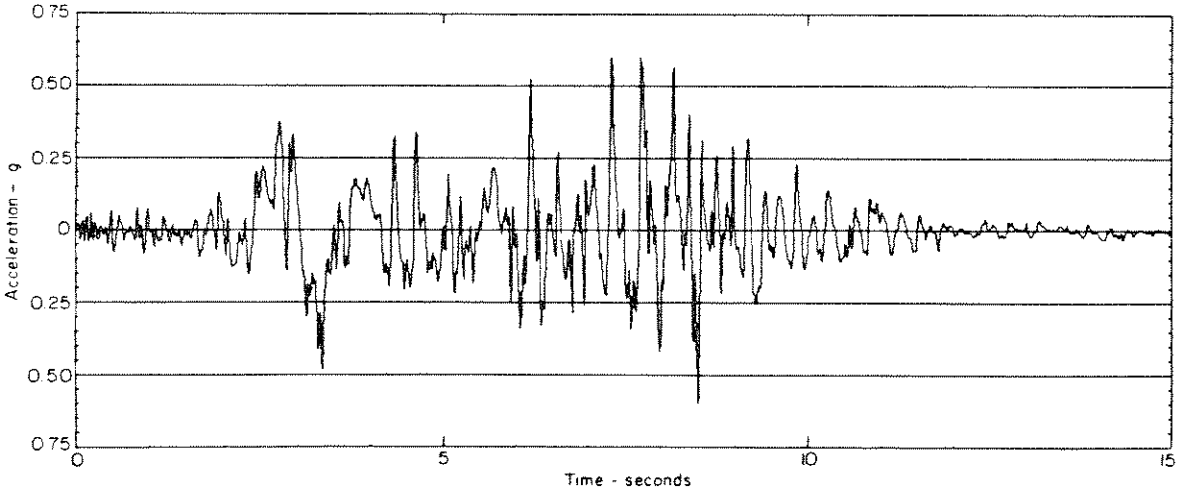

(b) Modified Pacoima Record.

Fig. VIII–1 TIME HISTORIES OF ACCELERATION IN BASE ROCK.

which have a strong effect on the embankment response, it was considered appropriate to use some other evaluation of rock motions, based on other rock records determined during the earthquake. Accordingly the record obtained at Pacoima Dam was modified to provide what is believed to be a reasonable estimate of the rock motions at the San Fernando Dam sites. The modifications involved the following:

(a) trimming off the record any acceleration pulses exceeding 0.9g to allow for the effects of topographic features of the Pacoima recording station,

(b) reducing all ordinates of the resulting record by a factor of 2/3 to provide a time history of rock motions having a maximum acceleration of 0.6g; this is in good accord with the peak acceleration indicated by the seismoscope record.

The resulting accelerogram is shown in Fig. VIII-1b.

Dynamic analyses were made for both of the rock motions discussed above after applying appropriate base line corrections as suggested by Berg and Housner (1961).

In analyzing the behavior of the dam, no consideration was given to the effects of vertical motions induced by the earthquake for several reasons:

(1) the shear stresses in a dam caused by vertical motions are much less than those due to horizontal motions,

(2) extensive laboratory tests have shown that the tendency for volume changes and associated pore pressure development caused by vertical vibrations is small compared with those resulting from shear deformations,

and (3) such pore pressures as may be introduced by vertical motions in the absence of shear stresses will be neutral pressures and

thereby will have no influence on the shear resistance of the soil.

Accordingly it seems reasonable to conclude that both the shear stresses and the shear strength are primarily determined by the horizontal shaking induced by an earthquake.

Dynamic Analysis

The next step in evaluating the performance of the embankment is to compute the response of the dam and underlying foundation during the earthquake (Seed et al., 1969). This computation can readily be made once the following parameters are known: (a) the base motions developed in rock underlying the dam, and (b) the dynamic material properties (modulus and damping) of the embankment and foundation soils. The results of this computation provide values of cyclic stresses which are likely to be induced in the soils during the earthquake.

The response of the embankment and foundation layer is most conveniently obtained using non-linear dynamic finite element procedures. The non-linear dynamic material properties are incoprorated in the analysis by using strain-dependent modulus and damping values as described below. The finite element representation used in evaluating the response of the Lower San Fernando Dam is shown in the upper part of Fig. VIII-2. Computer programs that permit the use of strain-dependent modulus and damping values for each element (Idriss, et al., 1973), were used in evaluating the response of this dam.

Recent investigations (e.g., Hardin and Drnevich, 1972; Seed and Idriss, 1970) indicate that the modulus of cohesionless soils varies with (a) the square root of the mean effective pressure, and (b) the strain level. This variation can be expressed by:

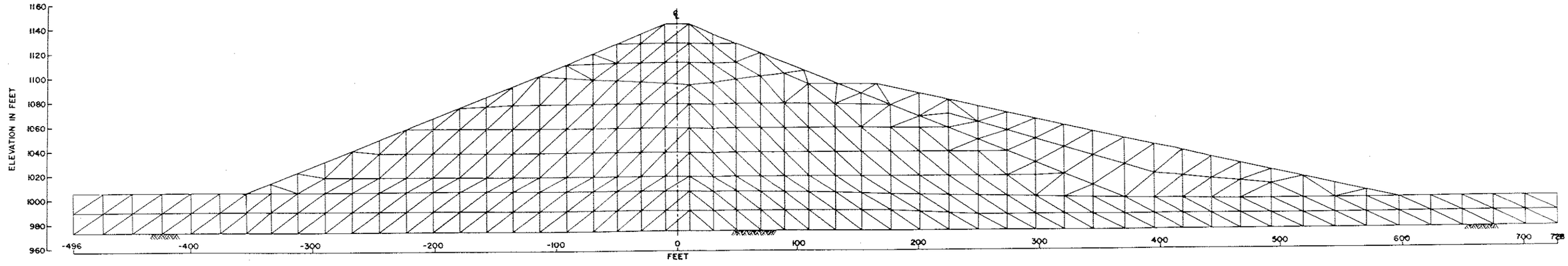

FINITE ELEMENT REPRESENTATION OF LOWER SAN FERNANDO DAM

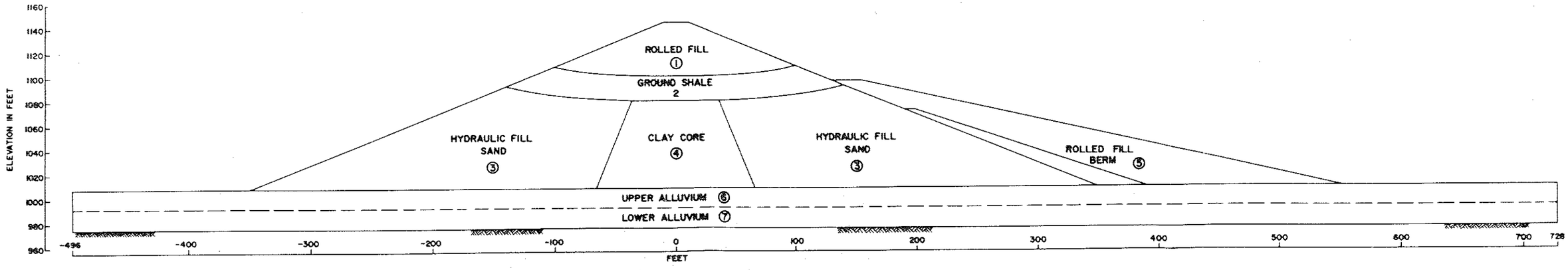

REPRESENTATIVE CROSS-SECTION THROUGH LOWER SAN FERNANDO DAM

Fig. VIII-2 CROSS-SECTION THROUGH LOWER SAN FERNANDO DAM USED FOR DYNAMIC ANALYSIS

$$G = 1000\ K_2 \sigma_m'^{1/2}$$

where G = shear modulus in psf;

σ_m' = mean effective pressure in psf; and

K_2 = a parameter relating G and σ_m'; this parameter is mainly a function of the type and relative density of the cohesionless soil and the strain.

At very low levels of strain, the maximum modulus value (and consequently the maximum value of K_2) is obtained. The maximum modulus values can be directly evaluated from measured shear wave velocities or from laboratory tests conducted at small strain levels.

It has been found (Seed and Idriss, 1970) that for a wide range of cohesionless soils, the decrease in value of K_2 with increase in strain and values of the damping ratio are typically represented by the relationships shown in Fig. VIII-3(a). These relationships were used in conjunction with appropriate values of $(K_2)_{max}$ to determine shear moduli and damping ratios for cohesionless soils in the embankment. For the hydraulic fill and alluvium, values of $(K_2)_{max}$ were determined from the measured values of shear wave velocity. For other soils in the cross-section, which have a lesser influence on the response, it was considered that estimates of $(K_2)_{max}$ based on previous test data for similar materials would provide a sufficient degree of accuracy.

Shear modulus values for saturated cohesive soils have been found to vary with the undrained shear strength and the strain level approximately as shown in Fig. VIII-3(b) (Seed and Idriss, 1970). Representative damping ratios for these soils are also shown in this figure. Shear moduli and damping ratios for the clay core of the Lower Dam were determined from the results shown in Fig. VIII-3(b), based on an average shear strength for the core material of 2000 psf.

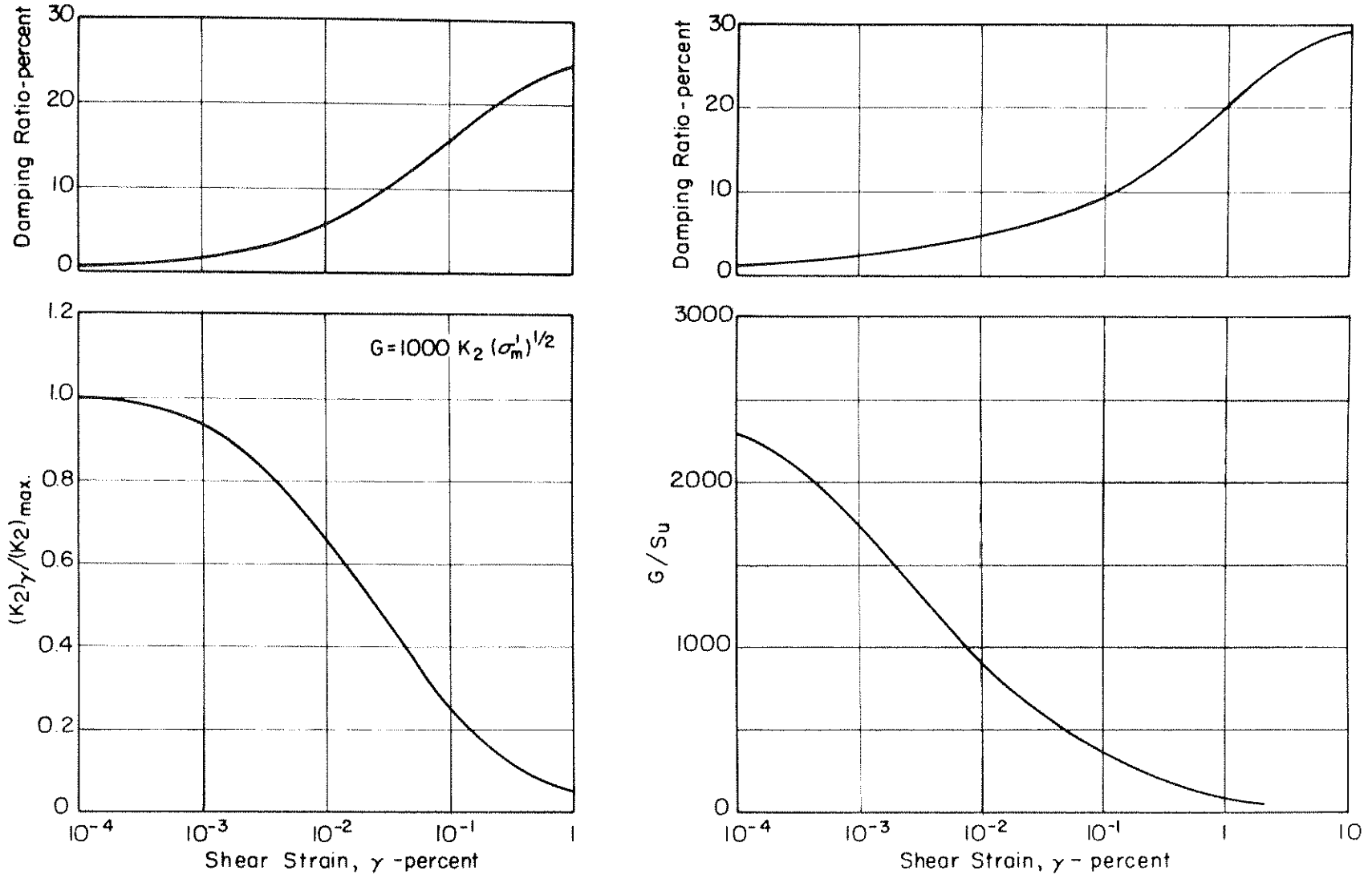

Fig. VIII–3 AVERAGE SHEAR MODULI AND DAMPING CHARACTERISTICS OF SOILS
(After Seed and Idriss, 1970)

Thus for dynamic analysis purposes, the cross-section of the Lower Dam was idealized to the form shown in the lower part of Fig. VIII-2 with dynamic properties for the soils in the various zones as shown in Table VIII-2. The finite element representation of this cross-section is shown in the upper part of Fig. VIII-2.

The computed response of this section to the rock motions determined from the seismoscope record is shown in Fig. VIII-4. Because the modulus and damping values are strain-dependent, these values are not known at the outset and an iterative procedure is required. The strain in each element is first estimated and the strain-dependent values of modulus and damping are obtained for that element. The analysis is then conducted and the values of strain are computed. Based on the computed strains, new values of modulus and damping are obtained and the analysis is repeated. Proceeding in this manner, the analysis is continued until the values of modulus and damping are compatible with the strain developed in each element.

The response evaluation provides time histories of acceleration at every node and shear stresses induced in each element during the earthquake. The computed time history of crest accelerations is shown in the upper part of Fig. VIII-4. As can be noted, the computed maximum crest acceleration of 0.6g is in reasonable agreement with the maximum acceleration indicated by the seismoscope record on the crest of the dam.

The time history of shear stresses at each location (see Fig. VIII-5 for typical examples) can readily be converted to an equivalent series of uniform cyclic stress applications. This conversion is accomplished by appropriate weighting of the ordinates of the stress time history based on the results of the laboratory cyclic test data (Lee and Chan, 1972).

Table VIII-2

Dynamic Properties of Soils in Lower Dam used for Response Analysis

Zone No. on Fig.	Soil	Soil Type for Dynamic Property Evaluation	$(K_2)_{max}$	Undrained Shear Strength
1	Rolled Fill	Cohesionless	55	--
2	Ground Shale	Cohesionless	52	--
3	Hydraulic Sand Fill	Cohesionless	43	--
4	Rolled Fill Berm	Cohesionless	48	--
5	Clay Core	Saturated Clay	--	2000 psf
6	Upper Alluvium	Cohesionless	52	--
7	Lower Alluvium	Cohesionless	105	--

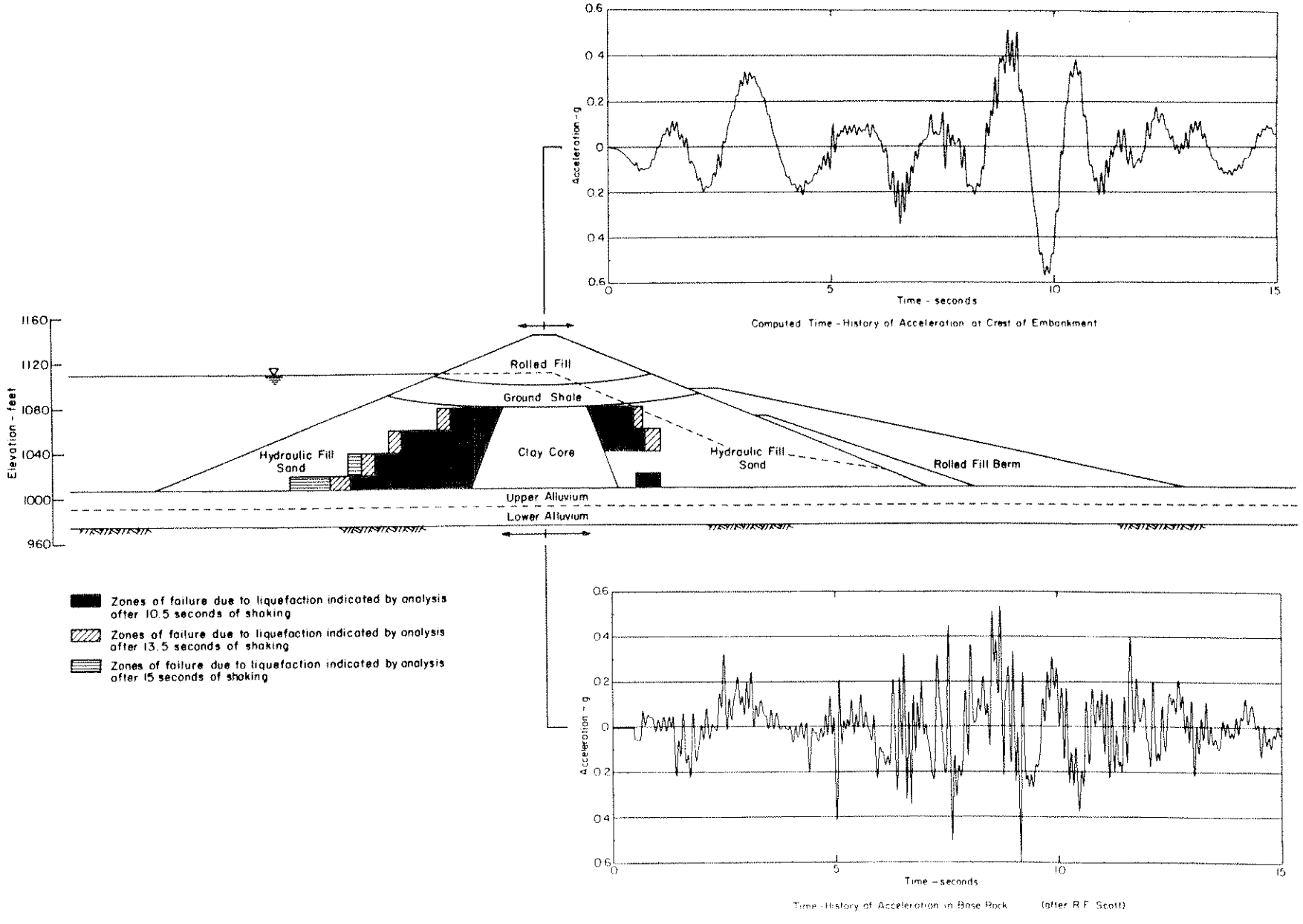

Fig. VIII-4 ANALYSIS OF RESPONSE OF LOWER DAM DURING SAN FERNANDO EARTHQUAKE TO BASE MOTIONS DETERMINED FROM SEISMOSCOPE RECORD.

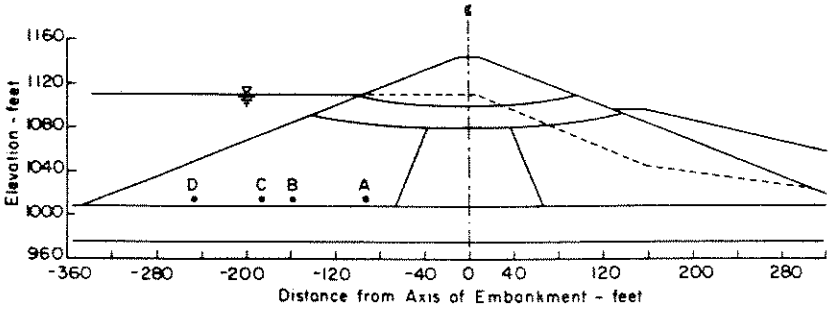

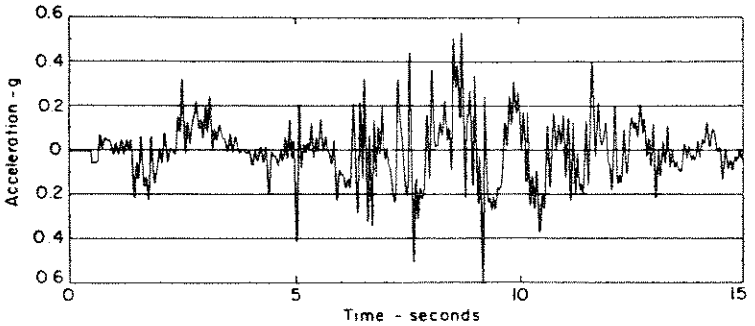

Time - History of Acceleration in Base Rock (after R.F. Scott)

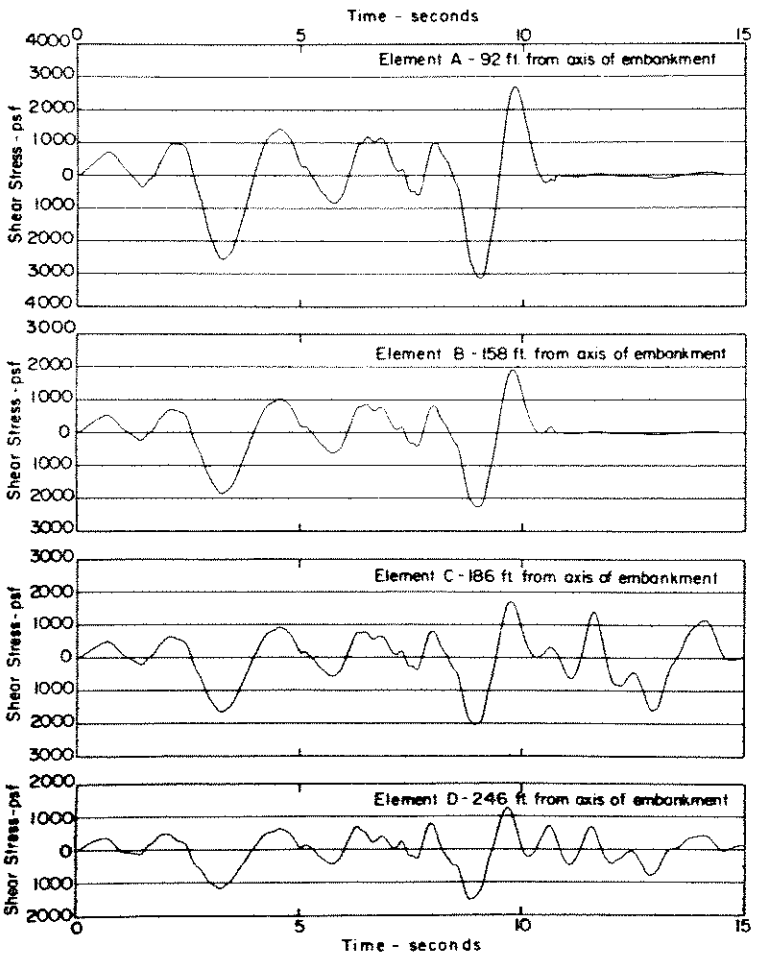

Fig. VIII-5 PROGRESSIVE LIQUEFACTION ANALYSIS OF LOWER SAN FERNANDO DAM: TIME HISTORIES OF SHEAR STRESSES DEVELOPED ALONG BASE OF EMBANKMENT.

The equivalent cyclic stress application can then be used in assessing the stability of the dam during the earthquake as summarized below.

Stability Analysis - Abutment Record

The stability of the embankment and underlying foundation is assessed by comparing the stresses induced by the earthquake (using the abutment record as input rock motion) and the stresses required to cause liquefaction and/or prescribed limits of strain. The locations in which the induced stresses exceed the stresses required to cause liquefaction or acceptable strain limits determine the extent of liquefaction or unacceptable performance.

Embankment

The stability of the embankment was evaluated by investigating the liquefaction and strain potential within four potential zones of failure located as follows:

1. A zone along the base of the embankment extending from Elevation 1008 to Elevation 1020; the stress conditions along the plane at Elevation 1014 (average elevation for the zone) were used for evaluating the liquefaction and strain potential in this zone.
2. A zone extending from Elevation 1020 to 1040; the stress conditions along the plane at Elevation 1030 were used for evaluating the liquefaction and strain potential in this zone.
3. A zone extending from Elevation 1040 to 1060; the stress conditions along the plane at Elevation 1050 were used for evaluating the liquefaction and strain potential in this zone.
4. A zone extending from Elevation 1060 to 1080; the stress conditions along the plane at Elevation 1070 were used for evaluating the liquefaction and strain potential in this zone.

The stability of the embankment during the San Fernando earthquake was assessed taking into consideration the tendency for liquefaction in the hydraulic fill to develop progressively. Previous studies (Seed, et al, 1969) have indicated that the progressive development of liquefaction, starting with elements near the center of an embankment and progressing toward the face of the dam, can markedly influence the potential behavior of embankments during earthquakes.

As can be noted from Fig. VIII-4, the peak accelerations (and therefore the peak stresses) occur approximately 10 or so seconds after the start of the motions. Accordingly, the liquefaction potential was initially investigated for the first 10.5 seconds of the motion. This evaluation along the base of the embankment is presented in Fig. VIII-6. The stresses induced in this section during the first 10.5 seconds of shaking were represented by 2 cycles of an equivalent uniform cyclic stress. The stresses required to cause liquefaction and 5 percent strain in 2 cycles were obtained from Fig. V-46, using the values of initial normal stress, σ_o', and the ratio, τ_o/σ_o', shown in the upper part of Fig. VIII-6. The stresses developed for 2 cycles in 10.5 seconds of shaking along the base of the embankment are compared to the stresses required to cause liquefaction in 2 cycles in the lower part of this figure. A very small zone of liquefaction (i.e., where the stresses developed during shaking exceed the stresses required to cause liquefaction) appears to develop in the downstream part of the dam. However an extensive zone of liquefaction, extending over a distance of approximately 100 ft, develops in the hydraulic fill upstream of the clay core.

Similar evaluations for other zones of the embankment with average depths at Elevation 1030, 1050 and 1070 are shown in Figs. VIII-7, VIII-8,

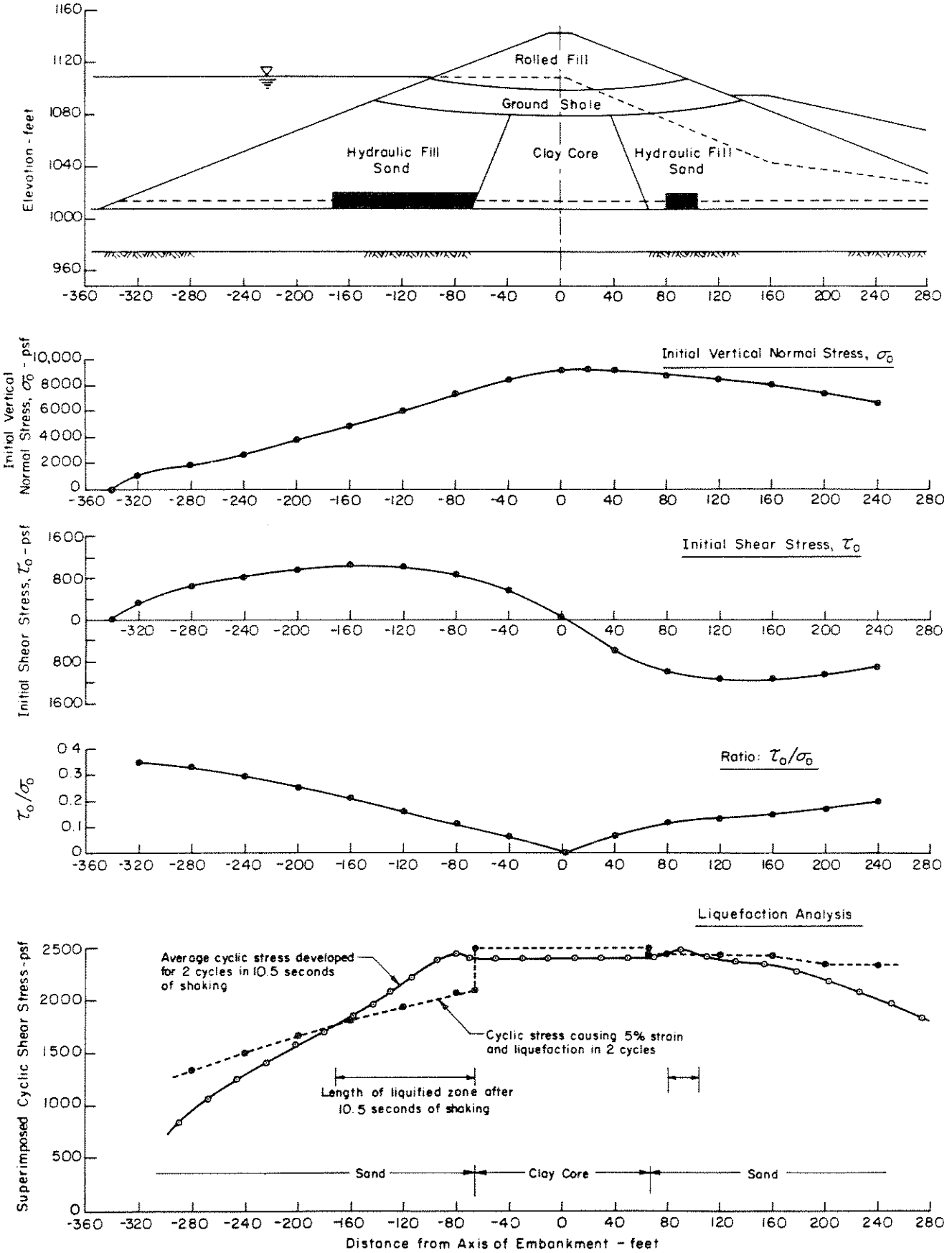

Fig. VIII-6 ANALYSIS OF SOIL STABILITY ALONG BASE OF EMBANKMENT (El. 1014') AFTER 10.5 SECONDS OF SHAKING, USING BASE MOTIONS DETERMINED FROM SEISMOSCOPE RECORD – LOWER SAN FERNANDO DAM.

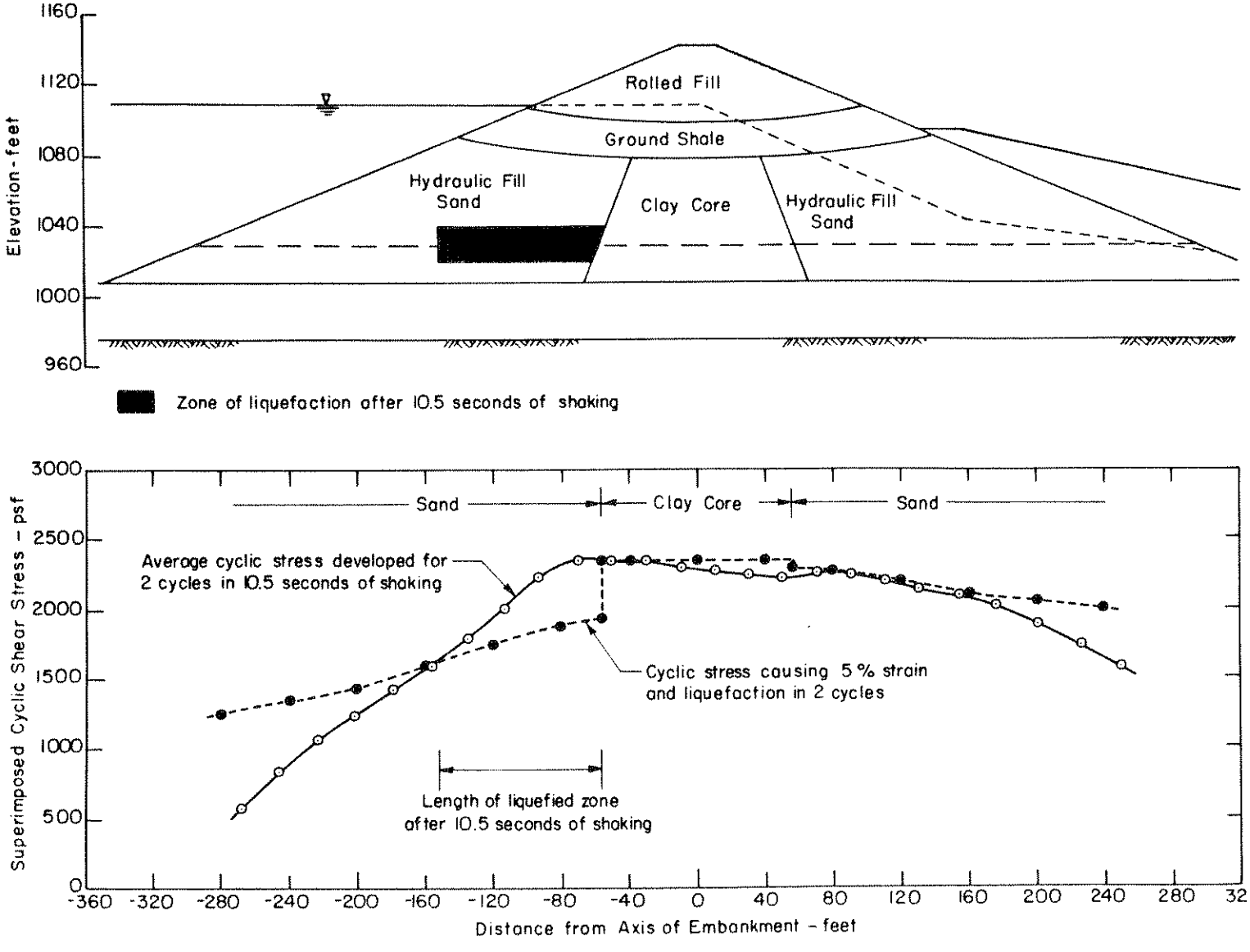

Fig. VIII–7 ANALYSIS OF SOIL STABILITY ALONG PLANE AT ELEVATION 1030 FT. AFTER 10.5 SECONDS OF SHAKING, USING BASE MOTIONS DETERMINED FROM SEISMOSCOPE RECORD – LOWER SAN FERNANDO DAM.

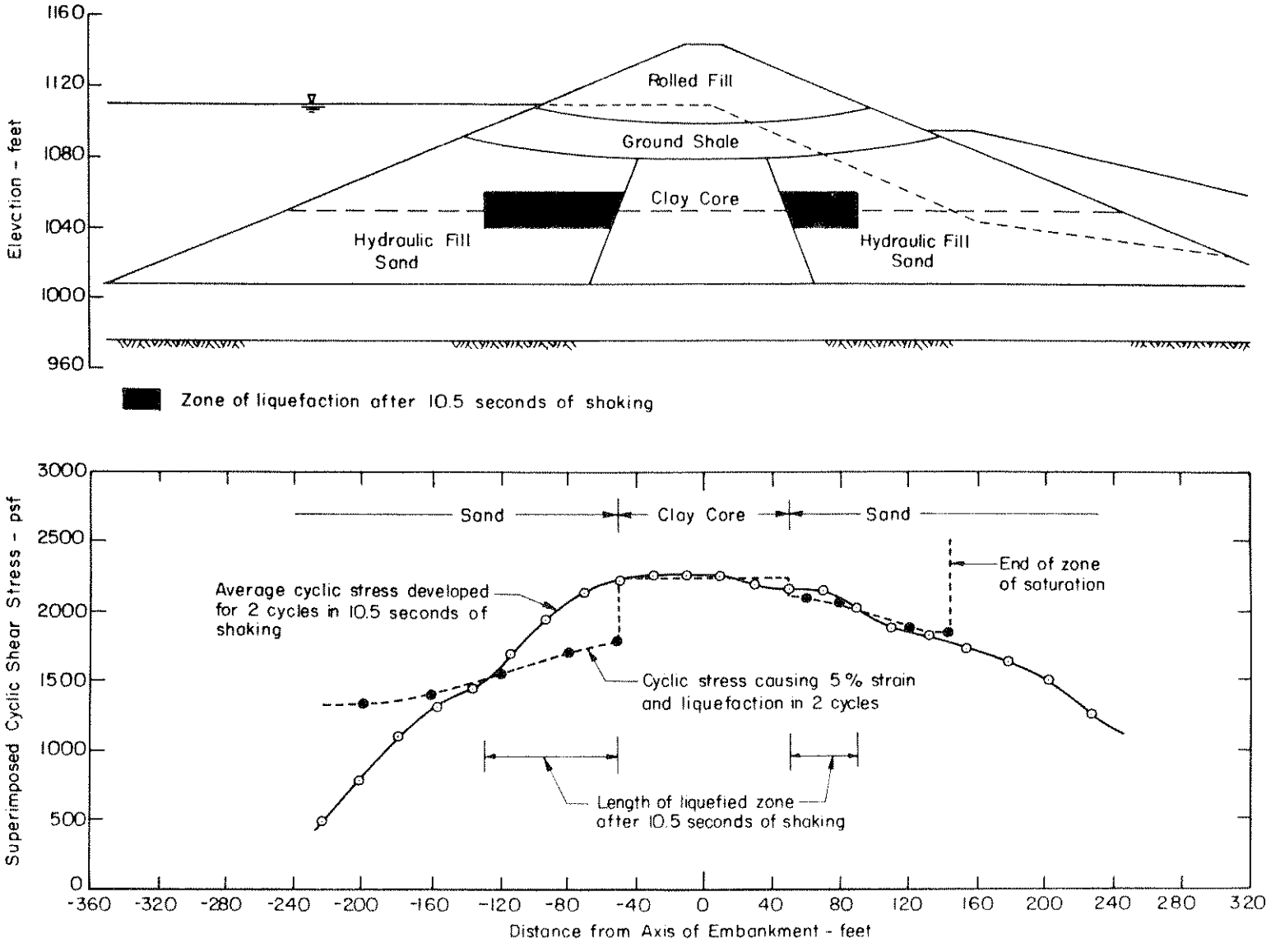

Fig. VIII–8 ANALYSIS OF SOIL STABILITY ALONG PLANE AT ELEVATION 1050 FT. AFTER 10.5 SECONDS OF SHAKING, USING BASE MOTIONS DETERMINED FROM SEISMOSCOPE RECORD – LOWER SAN FERNANDO DAM.

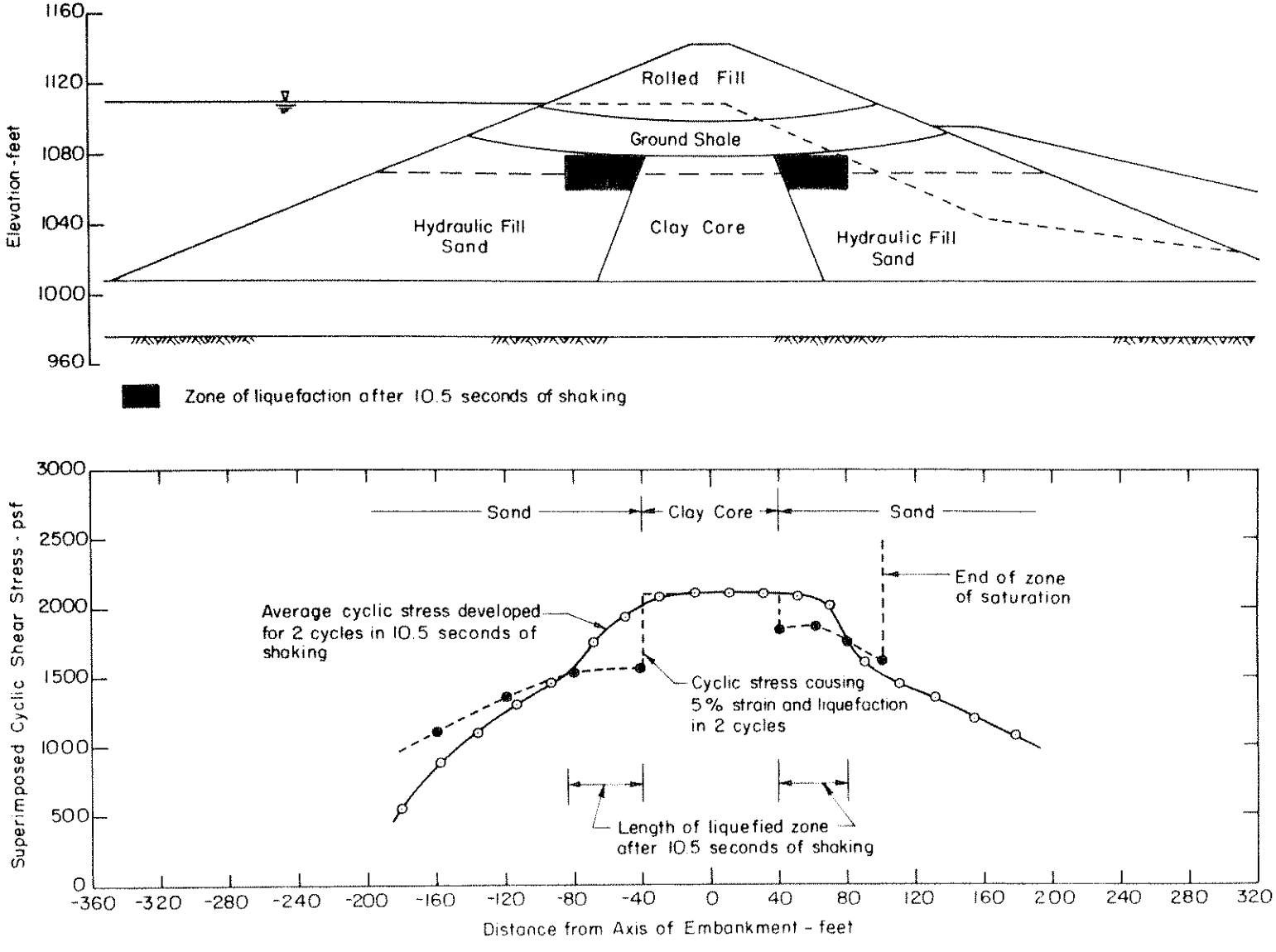

Fig. VIII-9 ANALYSIS OF SOIL STABILITY ALONG PLANE AT ELEVATION 1070 FT. AFTER 10.5 SECONDS OF SHAKING, USING BASE MOTIONS DETERMINED FROM SEISMOSCOPE RECORD – LOWER SAN FERNANDO DAM.

and VIII-9, respectively. The zones where liquefaction and strains exceeding 5 percent will develop within each zone are readily determined from the results presented in these figures.

The zones where liquefaction and strains exceeding 5 percent can be expected to develop within the embankment after 10.5 seconds of shaking in the upstream and downstream sections of the dam are summarized in Fig. VIII-4. As can be noted, liquefaction is indicated over a considerable part of the hydraulic fill upstream of the clay core; a much smaller zone of liquefaction is indicated in the hydraulic fill downstream of the clay core. However, the upstream extent of the liquefied zone does not appear to be sufficiently extensive at this stage to permit the upstream slide that took place during the earthquake.

The effects of additional shaking on the embankment can be studied by continuing the analysis beyond the first 10.5 seconds of shaking. Because a considerable part of the embankment has liquefied after 10.5 seconds, redistributions of both static and dynamic stresses in the adjacent nonliquefied elements would take place during the remainder of the earthquake. The redistribution of dynamic stresses can readily be taken into account by dropping the shear moduli in the liquefied zones close to zero for the ensuing period of shaking. The analysis is then continued with the previously computed response values after 10.5 seconds as initial values. It should be noted that the modulus and damping values for elements in the non-liquefied zone are established based on the strain developed in each element during the ensuing period of motion.

The increase in liquefaction potential in the hydraulic fill during the ensuing 3 seconds of motion (i.e., from 10.5 to 13.5 seconds) was evaluated in this way. The time histories of stresses developed in

elements along the base of the embankment after 13.5 seconds of shaking are shown in Fig. VIII-5. The time history of stresses in elements that had not liquefied after 10.5 seconds of shaking were converted to 3 equivalent uniform cycles using the procedures outlined earlier. The stresses developed for 3 cycles after 13.5 seconds of shaking along the base of the embankment are presented in Fig. VIII-10. These stresses are also compared to the stresses required to cause liquefaction in 3 cycles in the same figure. An additional zone of liquefaction extending approximately 25 feet upstream appears to develop after 13.5 seconds of shaking along the base of the embankment. No additional zone of liquefaction appears likely to develop in the downstream part.

Similar evaluations for the other parts of the embankments were made and the extent of liquefaction in the hydraulic fill after 13.5 seconds of shaking are summarized in Fig. VIII-4.

The procedure was repeated for the remainder of the motion (i.e., from 13.5 to 15 seconds). The analysis of the embankment was continued with the previous computed response values after 13.5 seconds as initial values, and the shear moduli in the liquefied zones assigned values close to zero. The time history of stresses in the elements that had not liquefied in 13.5 seconds of shaking, were converted to 4 cycles of equivalent cyclic stresses. The stresses developed along the base of the embankment for 4 cycles after 15 seconds of shaking and the stresses required to cause liquefaction in 4 cycles are compared in Fig. VIII-11. As can be noted, an additional zone of liquefaction extending approximately 50 feet upstream appears to develop along the base of the embankment after 15 seconds of shaking. Similar evaluations for the other parts of the embankment were made and the extent of liquefaction in the hydraulic

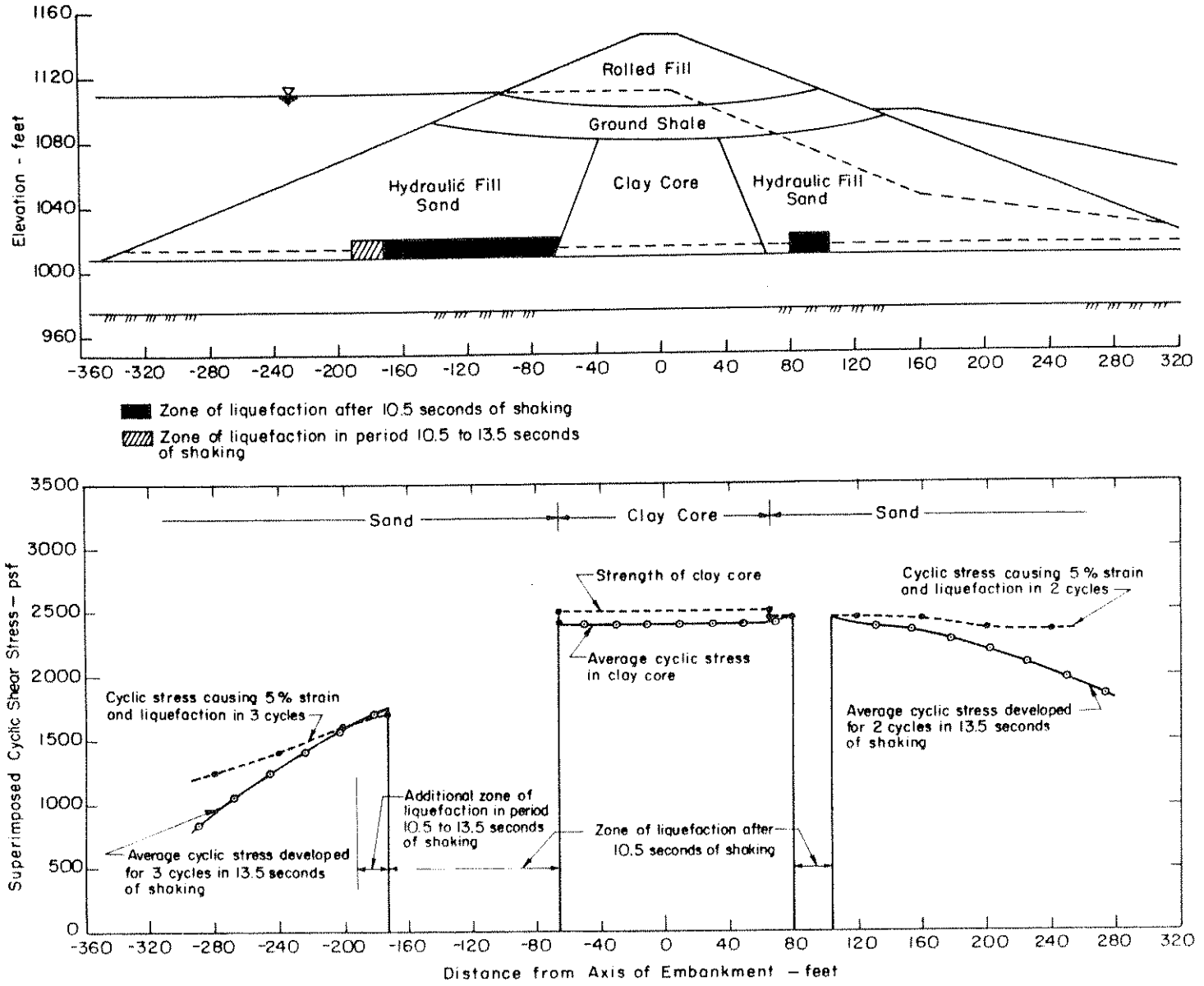

Fig. VIII-10 PROGRESSIVE LIQUEFACTION ANALYSIS ALONG BASE OF EMBANKMENT (El. 1014') AFTER 13.5 SECONDS OF SHAKING, USING BASE MOTIONS DETERMINED FROM SEISMOSCOPE RECORD – LOWER SAN FERNANDO DAM.

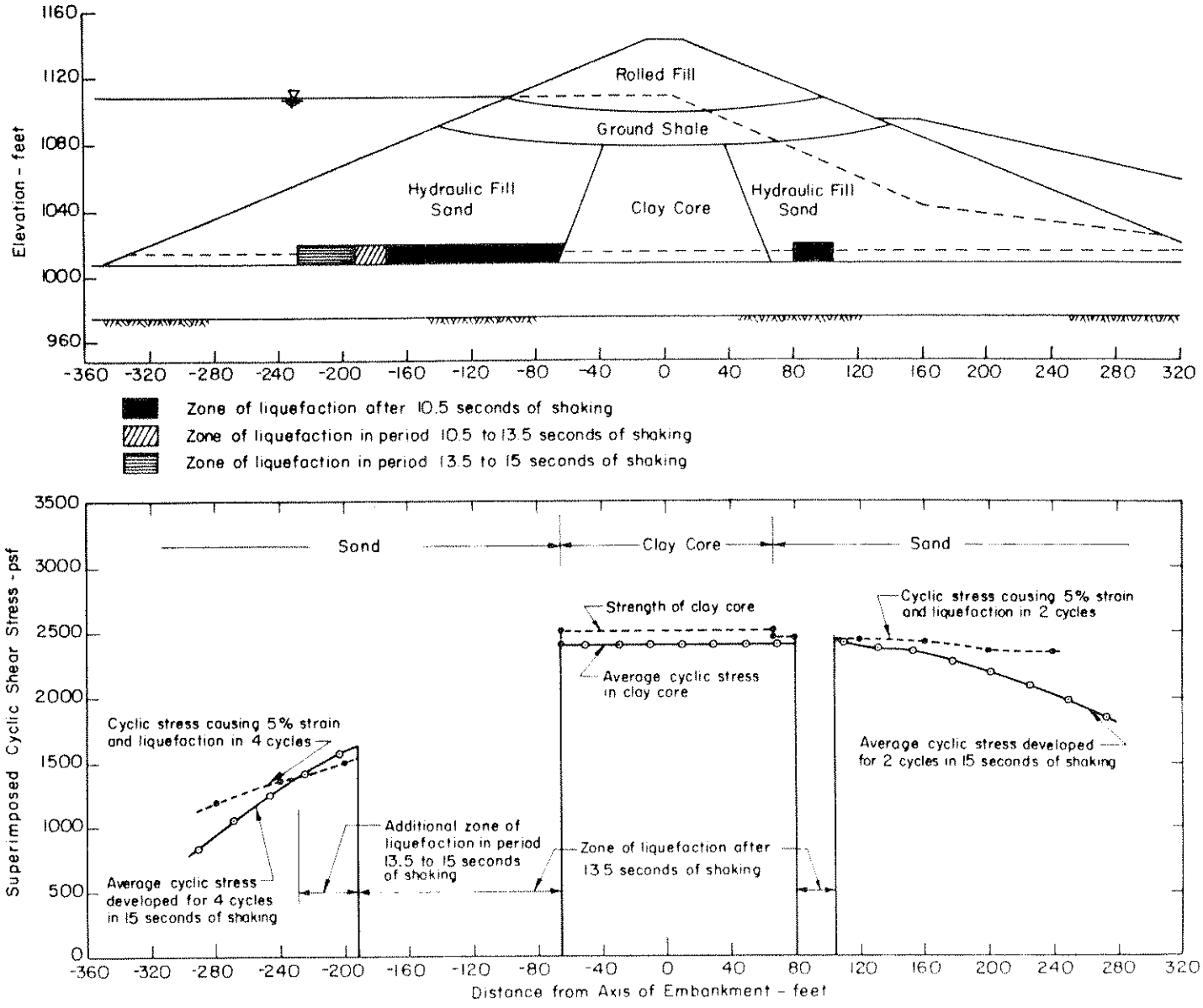

Fig. VIII-11 PROGRESSIVE LIQUEFACTION ANALYSIS ALONG BASE OF EMBANKMENT (El. 1014') AFTER 15 SECONDS OF SHAKING, USING BASE MOTIONS DETERMINED FROM SEISMOSCOPE RECORD – LOWER SAN FERNANDO DAM.

fill after 15 seconds of shaking was determined. The zones of liquefaction indicated by the analysis for the entire duration of motion are summarized in Fig. VIII-4. These zones are in reasonable agreement with the areas where liquefaction is indicated by the field observations and the reconstruction of the probable mechanism of sliding described in Part VI of this report.

The zone of liquefaction in the hydraulic fill upstream of the clay core, indicated by analysis after 15 seconds of shaking as shown in Fig. VIII-4, appears to be extensive enough to result in the upstream slide that took place during the earthquake. The extent of the zone of liquefaction downstream of the clay core, however, appears to be too small to result in any significant downstream movement during the earthquake.

Foundation Layer

The evaluation of liquefaction and strain potential in the foundation layer at Elevation 1000 (which represents the average depth within the upper alluvium) is illustrated in Fig. VIII-12. The stresses induced by the earthquake during the first 10.5 seconds of shaking are shown in the lower part of the figure. These stresses are expressed as the equivalent average cyclic stress developed in 2 cycles. The stresses required to cause liquefaction and 5 percent strain in 2 cycles are also shown in the lower part of the figure. The latter stresses were obtained from data similar to that presented in Fig. V-39 and using the values of initial normal stress, σ_o', and the ratio, τ_o/σ_o', computed by the static finite element analyses. As can be noted, the stresses induced by the earthquake after 10.5 seconds of shaking in the upper alluvium are considerably lower than the stresses required to cause liquefaction. Similar studies for the full duration of the earthquake show that no liquefaction would develop in the alluvium

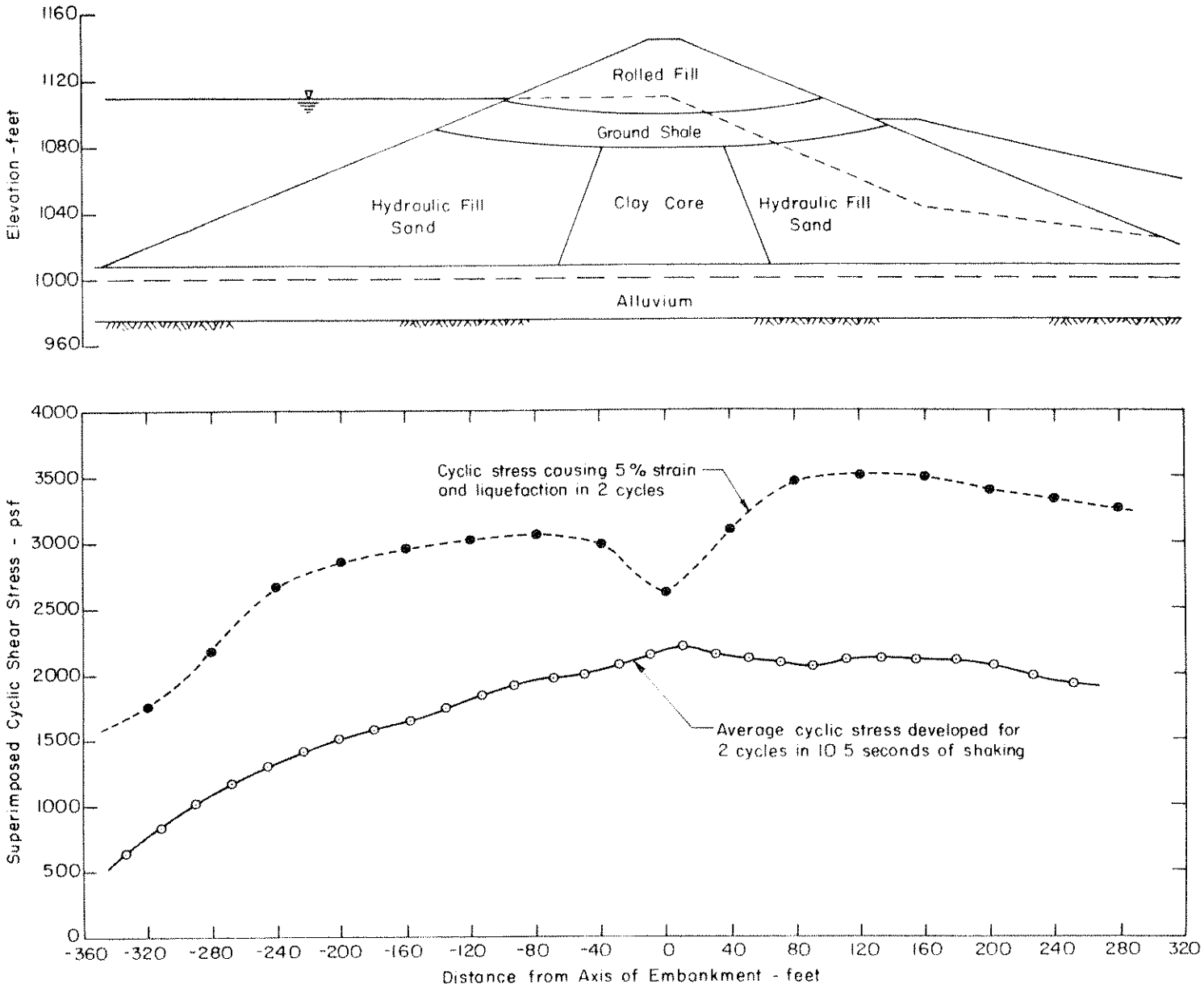

Fig. VIII-12 ANALYSIS OF STABILITY IN FOUNDATION SOIL (El. 1000') AFTER 10.5 SECONDS OF SHAKING, USING BASE MOTIONS DETERMINED FROM SEISMOSCOPE RECORD — LOWER SAN FERNANDO DAM

even after 15 seconds of shaking. The analysis would indicate therefore that there was ample margin of safety against development of liquefaction or 5 percent strain in the upper alluvium during the San Fernando earthquake. Since the lower alluvium is denser than the upper alluvium and has even higher cyclic strength characteristics, it would have an even higher margin of safety against deformation and failure during this earthquake.

The results of the analysis indicate no liquefaction or excessive strains in the foundation layer during the San Fernando earthquake. As described in Part III, there was no field evidence of failure in the alluvium. Thus the results of this part of the analysis also correlate well with the observed field performance.

In summary, the results of the analysis of the liquefaction and strain potential of the Lower Dam during the San Fernando earthquake, using the motions deduced from the abutment record as base excitation, indicate:

1. The zones of liquefaction and large strains determined by the analysis (Fig. VIII-4) are in reasonable agreement with the areas believed to have liquefied (as reconstructed in Part VI - see Plate 1).
2. The mechanics of failure in the upstream shell resulting from the liquefaction of the hydraulic fill are reasonably well constructed by the analysis. A considerable zone of hydraulic fill upstream of the clay core appears to have liquefied and undergone large strains during the earthquake. The movements in this extensive zone resulted in the upstream slide.
3. The zone of liquefaction in the downstream soil was not extensive enough to cause any significant downstream movements.
4. The foundation layer (consisting of the upper alluvium and the lower alluvium) did not liquefy during the San Fernando earthquake.

Stability Analyses - Pacoima Record

The stability of the Lower San Fernando Dam was also evaluated considering that the base motions developed in the rock underlying the dam were similar to the modified Pacoima record described previously, with a maximum acceleration of 0.6g.

The same procedures as those outlined in the previous section were used to compute the response and to evaluate the stability of the dam during this applied base motion. The time history of the base motion and the computed time history of acceleration at the crest of the embankment are shown in Fig. VIII-13.

Initially, the response of the embankment and underlying foundation was computed for 8 seconds of motion. The stresses computed along the base of the dam (at El. 1014) and along planes at Elevation 1030, 1050 and 1070 after 8 seconds of shaking were converted to 2 cycles of equivalent cyclic stress. The values of average cyclic stress developed for 2 cycles after 8 seconds of shaking along the base of the embankment are presented in Fig. VIII-14. The stresses required to cause liquefaction in 2 cycles (as determined from the test data in Fig. V-46 and using the applicable values of initial normal stress, σ_o', and the ratio τ_o/σ_o') along the base of the embankment are also shown in Fig. VIII-14. Similar plots for planes at Elevation 1030, 1050 and 1070 are presented in Figs. VIII-15, VIII-16 and VIII-17, respectively. Comparison of the values of developed stresses with the stresses required to cause liquefaction and 5 percent

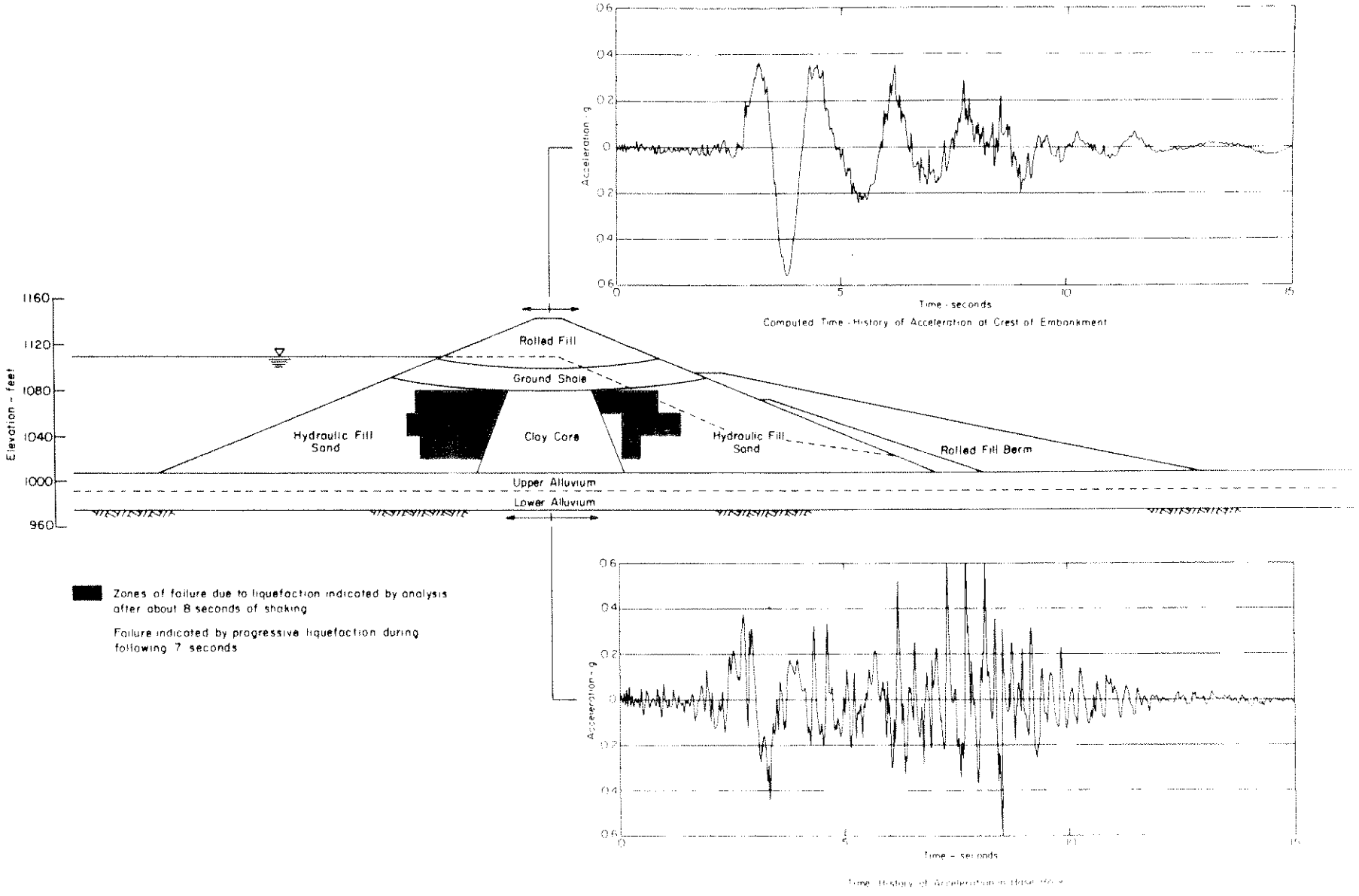

Fig. VIII–13 ANALYSIS OF RESPONSE OF LOWER DAM DURING SAN FERNANDO EARTHQUAKE TO BASE MOTIONS DETERMINED FROM MODIFIED PACOIMA RECORD.

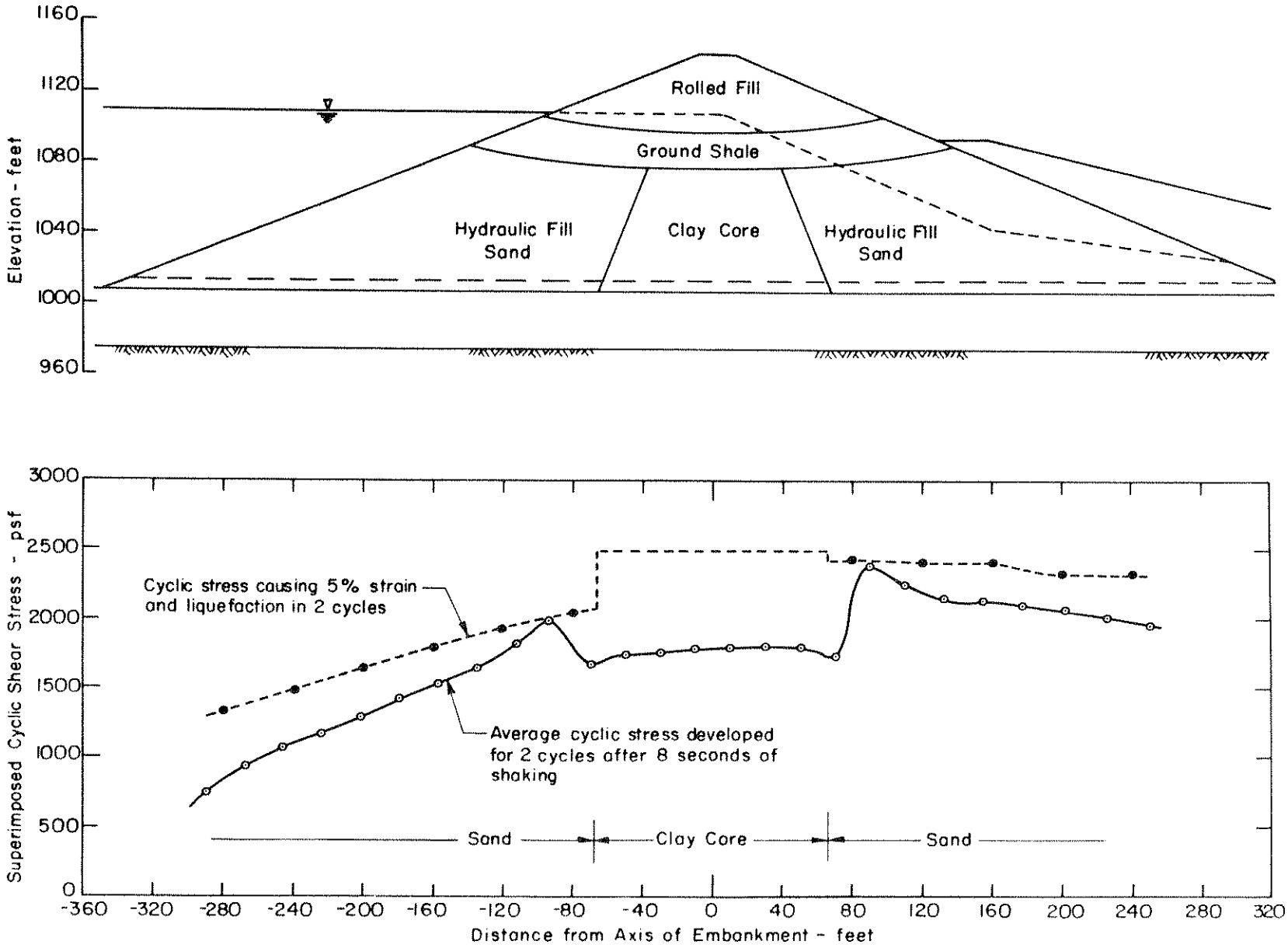

Fig. VIII-14 ANALYSIS OF SOIL STABILITY ALONG BASE OF EMBANKMENT (El. 1014') AFTER 8 SECONDS OF SHAKING, USING BASE MOTIONS DETERMINED

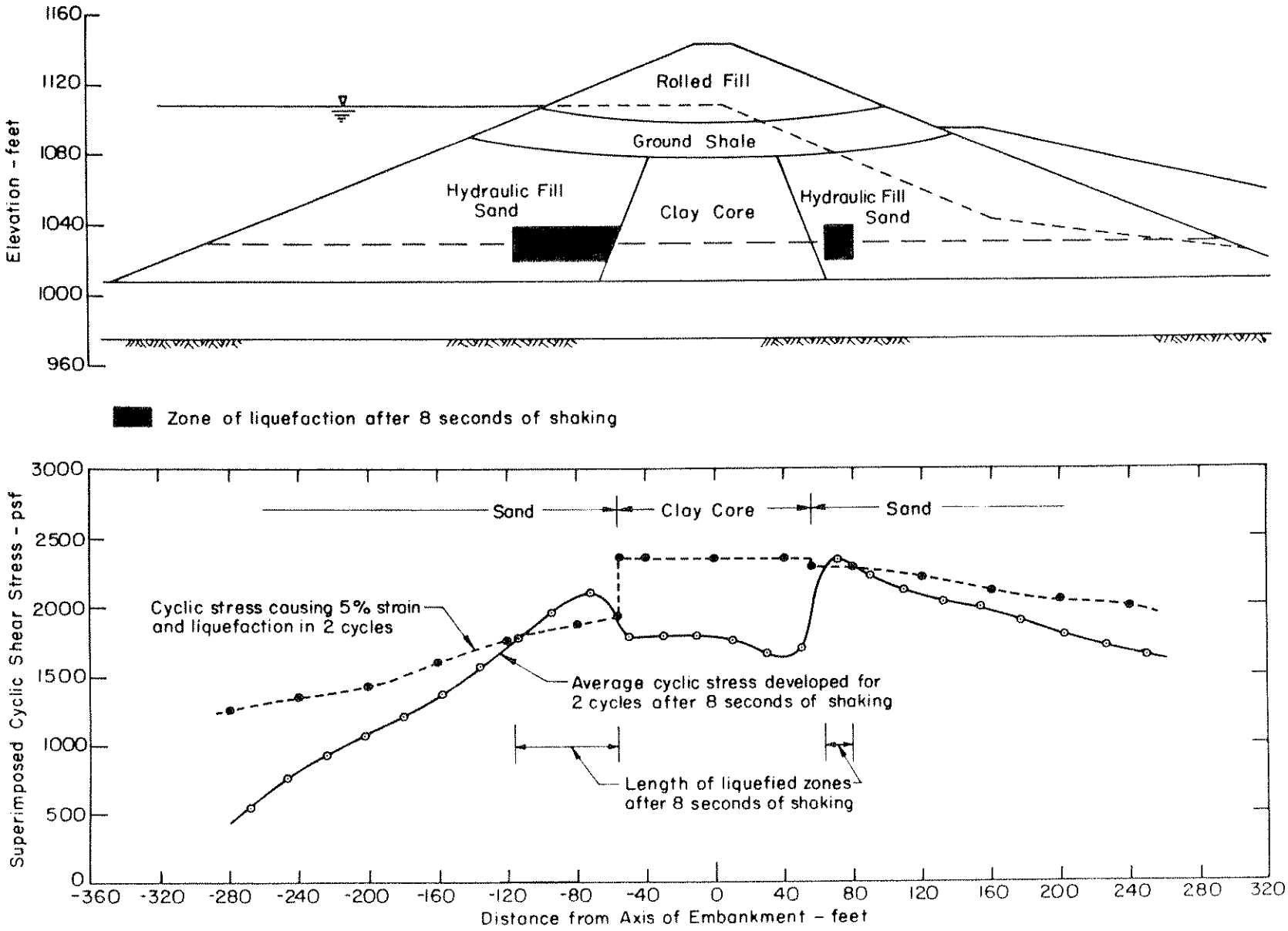

Fig. VIII-15 ANALYSIS OF SOIL STABILITY ALONG PLANE AT ELEVATION 1030 FT. AFTER 8 SECONDS OF SHAKING, USING BASE MOTIONS DETERMINED FROM MODIFIED PACOIMA RECORD – LOWER SAN FERNANDO DAM.

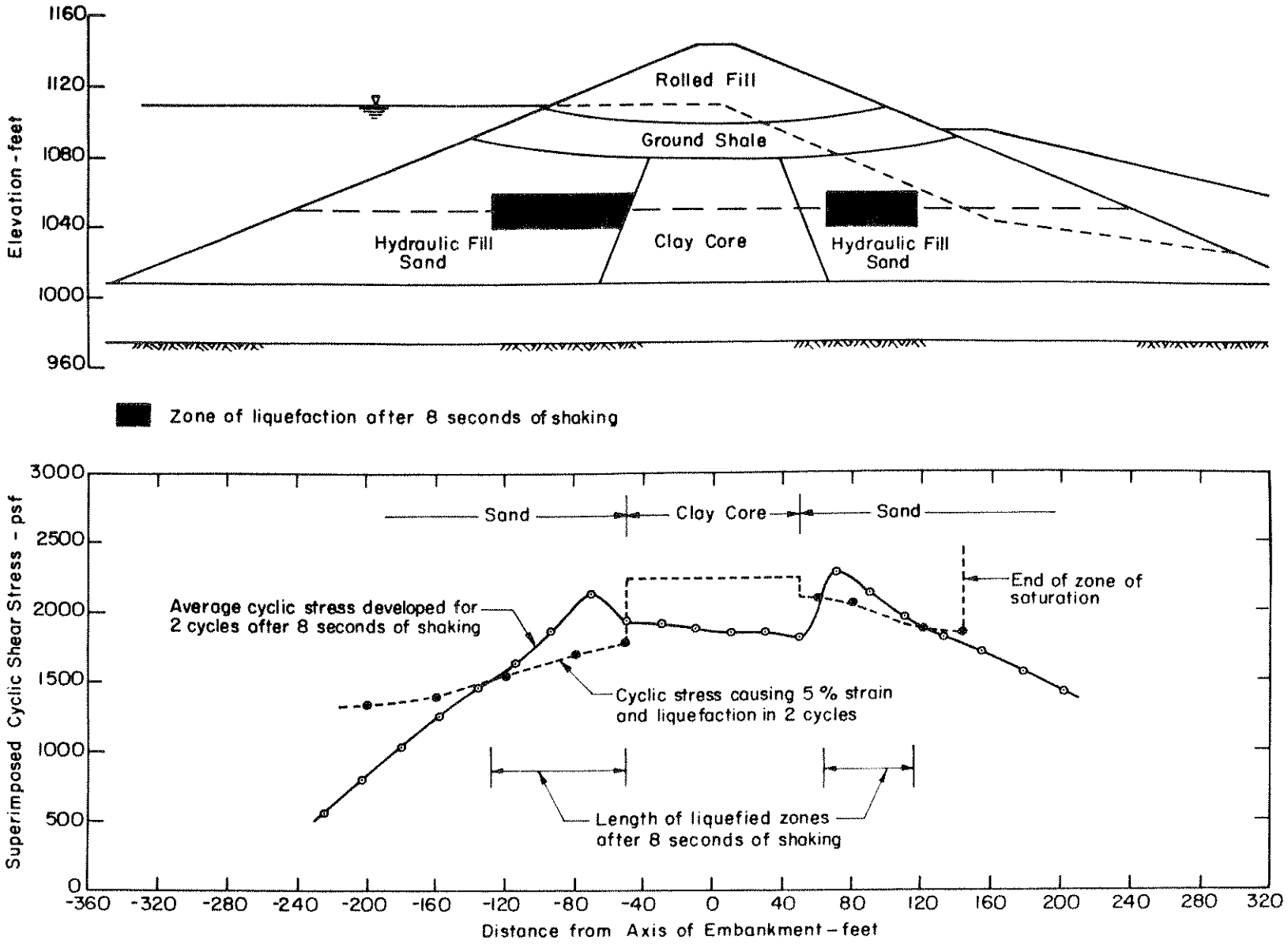

Fig. VIII-16 ANALYSIS OF SOIL STABILITY ALONG PLANE AT ELEVATION 1050 FT. AFTER 8 SECONDS OF SHAKING, USING BASE MOTIONS DETERMINED FROM MODIFIED PACOIMA RECORD - LOWER SAN FERNANDO DAM

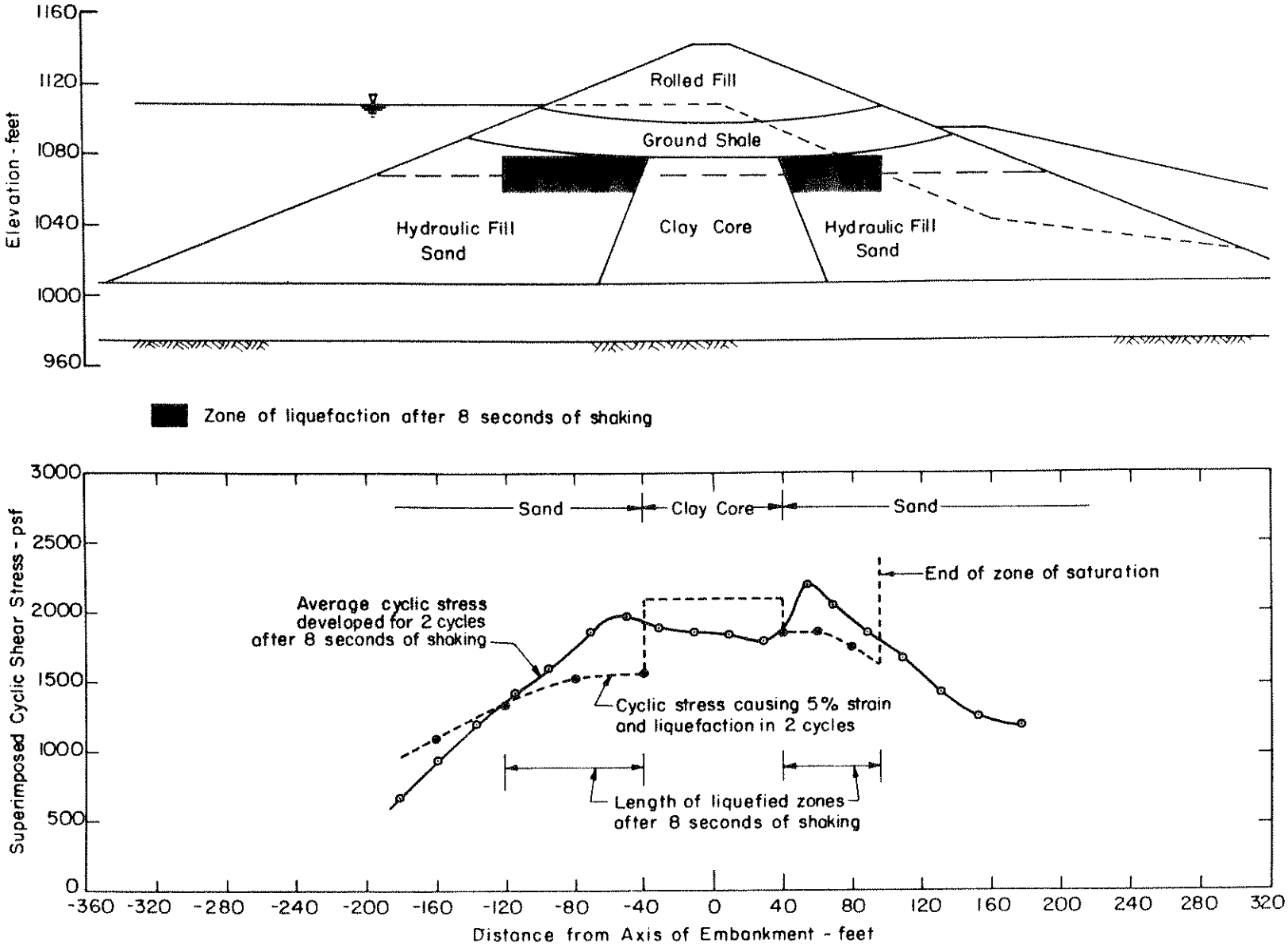

Fig. VIII-17 ANALYSIS OF SOIL STABILITY ALONG PLANE AT ELEVATION 1070 FT. AFTER 8 SECONDS OF SHAKING USING BASE MOTIONS DETERMINED FROM MODIFIED PACOIMA RECORD – LOWER SAN FERNANDO DAM.

strain along each plane provides the means for assessing the extent of liquefaction within each zone after 8 seconds of shaking. The extent of liquefaction for this duration of shaking is summarized in Fig. VIII-13.

The choice of 8 seconds for the initial duration of shaking was based on the facts that the peak acceleration in the input motion occurs at approximately 7.9 seconds, at least 2 major stress cycles had occurred by this time and it was apparent that a substantial zone of hydraulic fill would have liquefied, necessitating a redistribution of shear moduli for the remainder of the earthquake motions. The effects of the additional shaking (i.e. from 8 to 15 seconds) were studied by continuing the analysis in stages as described in the previous section. However it is apparent, by comparing the extent of the liquefied zones after 8 seconds with those shown in Fig. VIII-4 that they would be substantially enlarged by progressive failure effects. Again the extent of the liquefied zone appears to be sufficient to cause the upstream slide that took place during the San Fernando earthquake.

The zone of liquefaction downstream of the clay core indicated in the analysis using the Pacoima record is somewhat more extensive than that indicated using the abutment record. Nevertheless the extent of this zone downstream does not appear extensive enough to cause significant downstream movements.

Quantitative Evaluation of Slope Displacements

While the preceding analyses provide a qualitative evaluation of the embankment performance which is in good agreement with the observed behavior, quantitative assessments of the extent of slope movements will often be required. Preliminary assessments of the potential deformations

can be obtained by using the cyclic shear stresses computed by the dynamic response analyses in conjunction with the cyclic load test data to determine the potential compressive strains of individual elements of the embankment; that is, the compressive strain the element would develop if it were subjected to the dynamic stresses induced by the earthquake and were not constrained by the deformations in the surrounding soil. For example, for a soil element near the base of the embankment and just upstream from the core, the data in Fig. VIII-6 shows that the computed stresses considerably exceed those required to cause liquefaction and 5 percent strain. Using the results presented in Section V for the stresses required to cause larger strains than 5 percent, it can readily be estimated that after 10.5 seconds of shaking, elements of hydraulic fill in this zone of the embankment would develop a strain of the order of 20 to 30 percent if they were subjected to the computed stresses but were not constrained by the adjacent soil. This strain may be considered as the strain potential after 10.5 seconds of shaking for soil elements in this vicinity. It would, of course, be increased to some extent by further deformations occurring in the last five seconds of earthquake shaking.

Values of strain potential for all elements of hydraulic fill, as indicated by the computed stresses for the seismograph record of base motion and the test data presented in Section V, are shown in Fig. VIII-18. Contours of equal strain potential, based on these results are shown in Fig. VIII-19. It may be seen that very large strains, of the order of 20 to 50 percent tend to develop in zones of the embankment located in the upstream shell near the base and near the center of the embankment adjacent to the clay core. On the other hand the soil in the outer part of the upstream shell and in most of the downstream shell tends to develop relatively small potential strains ranging from 0 to 10 percent.

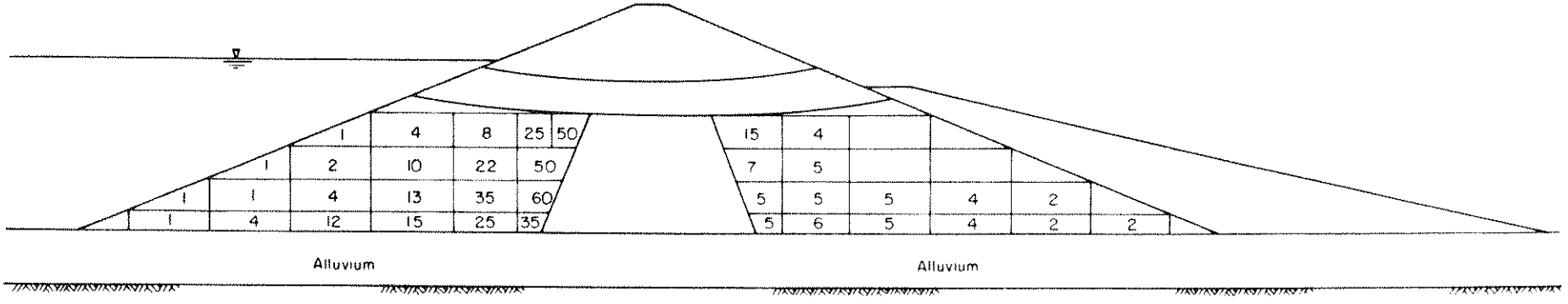

Fig. VIII–18 STRAIN POTENTIAL IN HYDRAULIC FILL – LOWER SAN FERNANDO DAM.

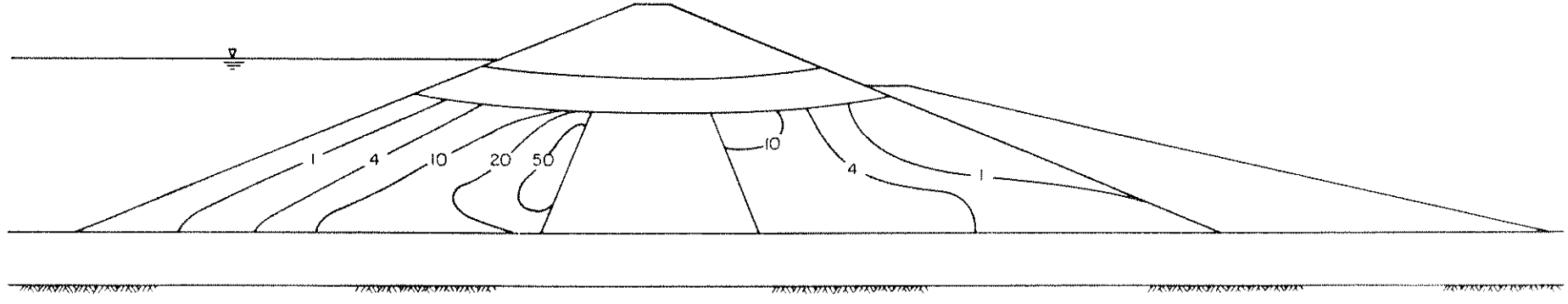

Fig. VIII–19 CONTOURS OF STRAIN POTENTIAL IN HYDRAULIC FILL – LOWER SAN FERNANDO DAM.

In reality the zones developing lower strains will restrain the movements of zones of higher strain potential so that the overall displacements in the embankment will be a representative average of the behavior of all the elements. Thus a first approximation to the overall movements might be obtained from the overall average shear strain for elements located on the upstream side of the clay core of the dam, as shown in Fig. VIII-20. In this figure values of shear strain potential are shown; these values were determined by multiplying the compression strains by 2, since for saturated soils deforming at constant volume, this is the approximate ratio of maximum shear strain to major principal strain under plane strain conditions.

For the hydraulic fill zone shown in Fig. VIII-20 with a depth of about 80 ft, the average shear strain is about 30% indicating a relative movement of about 24 ft between the top and bottom of the hydraulic fill zone. A movement of this magnitude would inevitably be accompanied by sloughing of the overlying soil, leading to substantial movements of the crest of the embankment.

This type of behavior is in general accord with the behavior of the embankment during the earthquake although the computed movements are clearly less than those which actually occurred. However the movements of the soil in the slide zone in this case could also be due in part to movements resulting from failure induced by the dead weight of the embankment after a zone of hydraulic fill adjacent to the core lost its shear resistance as a result of the earthquake shaking. Fig. VIII-21 shows the zone near the clay core where the shear strain potential is 20% or higher. If it is considered that the soil in this zone would provide no effective resistance to slide movements in the embankment (as a result of

Average shear strain in upstream hydraulic fill ≈ 30 %

Average depth of fill ≈ 72 ft.

Deformation at top of fill relative to base ≈ 0.3 × 72 ≈ 22 ft.

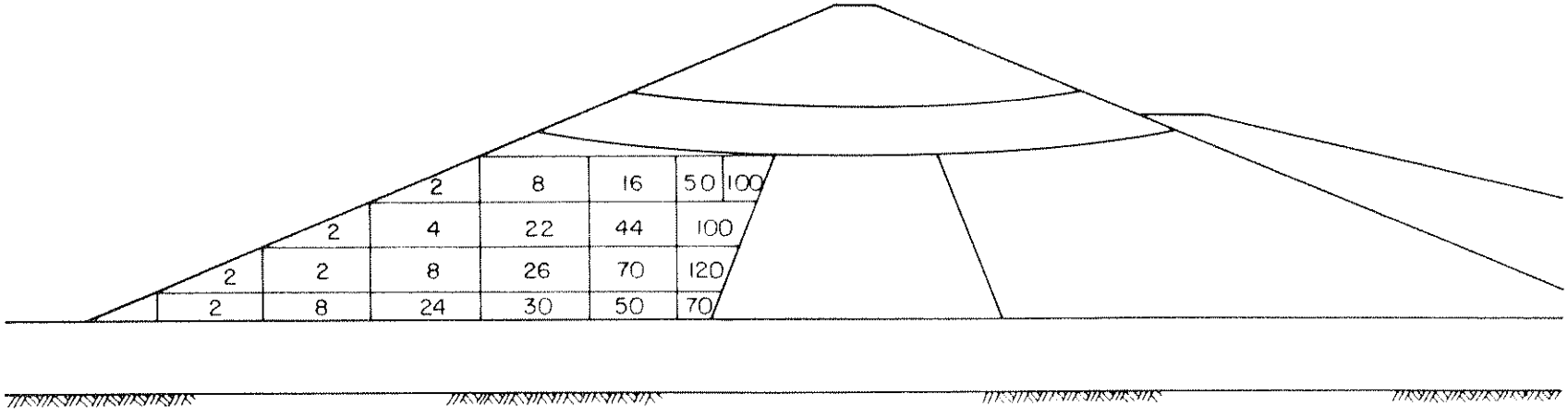

Fig. VIII–20 SHEAR STRAIN POTENTIAL FOR INDIVIDUAL ELEMENTS OF EMBANKMENT – – LOWER SAN FERNANDO DAM.

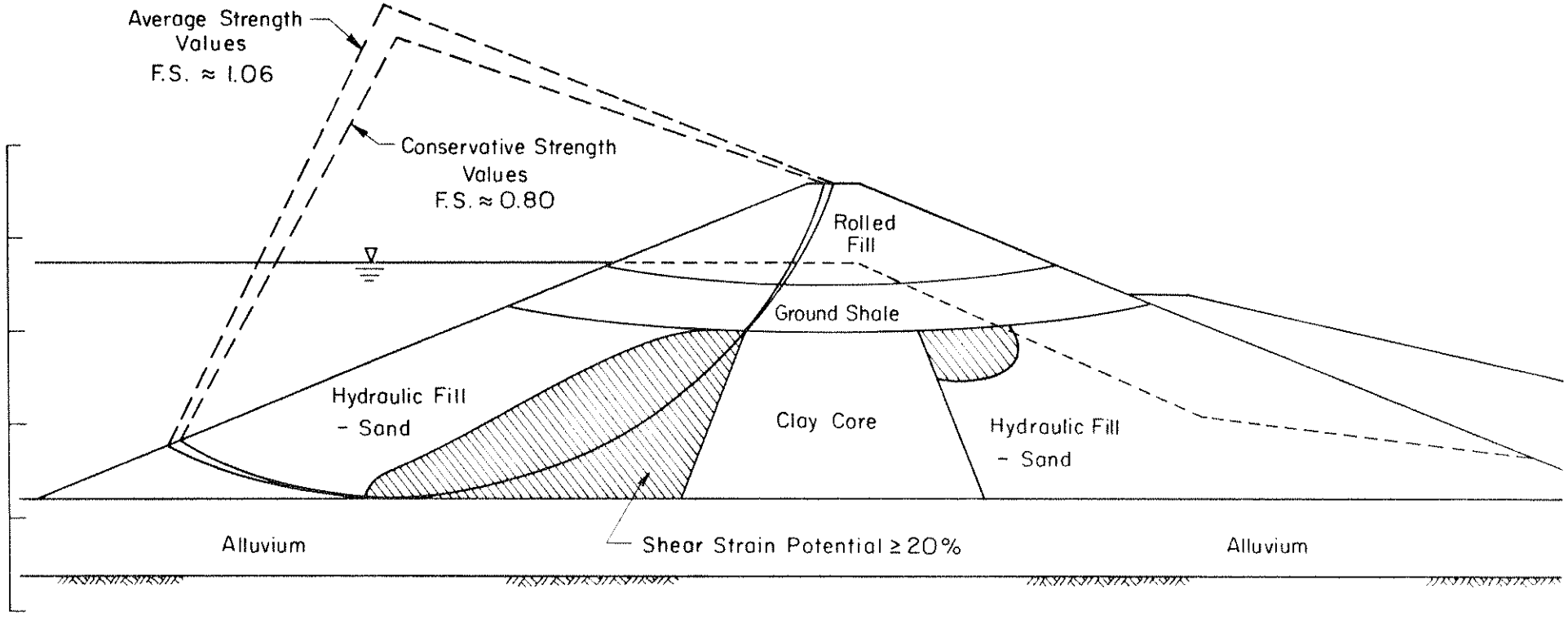

Fig. VIII-21 ANALYSIS OF STABILITY OF LOWER SAN FERNANDO DAM AFTER DEVELOPMENT OF ZONE OF HIGH STRAIN POTENTIAL

liquefaction and the development of high pore water pressures during the earthquake), a stability analysis can be made to assess the stability of the slope against static failure, as shown in Fig. VIII-21. Using average consolidated-undrained strength parameters because of the sudden change in stress distribution (see Fig. V-38b), the computed factor of safety along the critical sliding surface shown in Fig. VIII-21 is about 1.06; using conservative values of strength parameters (Fig. V-38a), the computed factor of safety is about 0.8.

These results would indicate that on completion of the ground motions or towards the end of the earthquake shaking, the upstream slope would be in a condition of incipient failure and might be expected to fail completely under the static weight of the embankment alone without the effect of inertia forces induced by the earthquake motions. Clearly the same failure could occur in the later stages of the earthquake shaking once the zone of liquefaction and strength loss had developed. The extensive lateral movements of the slide mass were no doubt due in large part to a failure of this type, probably accompanied by a further loss in strength of the soil once the peak strength had been exceeded and some pore pressure increase in the outer shell due to the earthquake shaking. Under these conditions the development of shear strains in the upper part of the hydraulic fill would be of relatively minor importance in determining the total movements of the slide mass.

An interesting aspect of this analysis is the fact that the computed margin by which complete instability is indicated is very low, suggesting that failure would only just occur in spite of the very strong motions to which the dam was subjected. This conclusion is supported by the fact that the slide apparently occurred in the very late stages of the earthquake

shaking (see Section III). Thus it would appear that if the shaking had been only a little less intense or the soil only a little stronger, the slope might well have retained its basic stability while undergoing large lateral displacements resulting in serious sloughing of the upstream slope of the dam. Thus it would appear that many hydraulic fill dams can be expected to withstand quite strong shaking of short duration without seriously detrimental effects or that earth dams constructed with soils having higher strengths than hydraulic sand fills, can withstand strong shaking similar to the type developed in the San Fernando area during the 1971 earthquake without hazardous consequences.

Part IX - Dynamic Analyses of the Stability of the Upper Dam During the San Fernando Earthquake

A dynamic analysis of the stability of the Upper San Fernando Dam during the earthquake of Feb. 9, 1971 was conducted using the same procedure as that described in Part VIII of this report. Based on the field investigations, the cross-section shown in the lower part of Fig. IX-1 was considered to be representative of the average conditions near the center of the embankment and all analyses were performed on this section.

Static Analysis

The procedures outlined in Part VIII for computing static stresses were also used for evaluating the stresses existing in the Upper Dam before the earthquake. The strength and deformation parameters for the embankment and foundation soils used in the analysis were those obtained from the laboratory test program and summarized in Table IX-1. The computed values of initial normal stress σ'_o, initial shear stress, τ_o, and the ratio, τ_o/σ'_o, along a horizontal plane at El. 1048.5 are shown in Fig. IX-4. Similar plots were obtained for other planes in the embankment and the foundation. These values of initial stresses together with the cyclic test data for samples obtained from this dam (see Figs. IV-35 and IV-36), were used to assess the stresses required to cause liquefaction and excessive strains in the embankment.

Dynamic Analysis

The response of the Upper Dam during the San Fernando earthquake was also evaluated using the dynamic-finite element method of analysis.

Table IX-1

Soil Parameters used in Nonlinear Static Analysis

Upper San Fernando Dam

Soil Parameter	Symbol	Values used in Analysis			
		Rolled Fill	Hydraulic Fill	Clay Core	Foundation Layer
Dry Unit Weight	γ_d(pcf)	125	100	100	107
Buoyant Unit Weight	γ_b(pcf)	78	60	60	67
Cohesion	c (psf)	2600	0	0	0
Friction Angle	ϕ	25°	37	37	37
Modulus Number	K	300	420	420	280
Modulus Exponent	n	0.76	0.52	0.52	0.80
Failure Ratio	R_f	0.90	0.78	0.78	0.66
Poisson's Ratio Parameters	G	0.30	0.33	0.33	0.32
	F	0.10	0.12	0.12	0.10
	d	3.8	10	10	9

The dam and underlying foundation were represented by the finite element mesh shown in the upper part of Fig. IX-1.

The modified Pacoima Dam record with a peak acceleration of 0.6g which indicated failure of the upstream slope of the Lower Dam, was used as input base rock motion for the analysis of the Upper Dam. The dynamic modulus values for the soils in the embankment and underlying foundation are summarized in Table IX-2. The choice of these values was based on measured shear wave velocities in the hydraulic fill and on the results of the field explorations and laboratory tests described in Part IV. Damping values and the variation of modulus values with strain were based on applicable published data for cohesionless soils and for saturated clays, Fig. VIII-3.

The response of the Upper Dam was then computed using the Modified Pacoima record as input base rock motion. The solution was repeated until strain-compatible modulus and damping values were obtained. Time histories of acceleration at every node and the shear stresses induced in each element during the earthquake were thus computed. The time history of accelerations at the crest and along the top of the berm, together with the time history of the input base rock motions, are shown in Figure IX-2. As can be noted, the computed maximum crest acceleration is approximately 0.6g and the acceleration along the berm is approximately 0.5g.

The computed time history of shear stresses in each element was converted to an equivalent series of average cyclic stress application. These equivalent stress applications were then used in assessing the stability of the dam during the San Fernando earthquake.

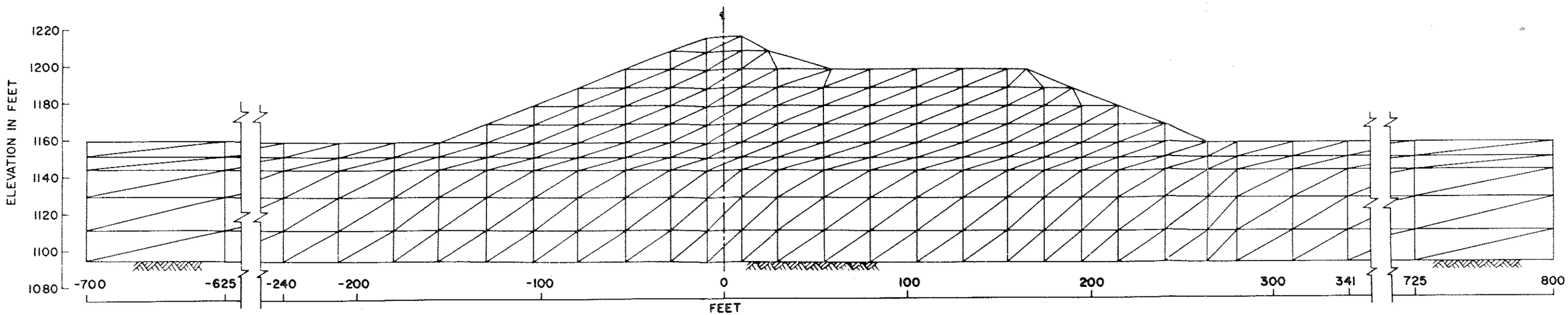

FINITE ELEMENT REPRESENTATION OF UPPER SAN FERNANDO DAM

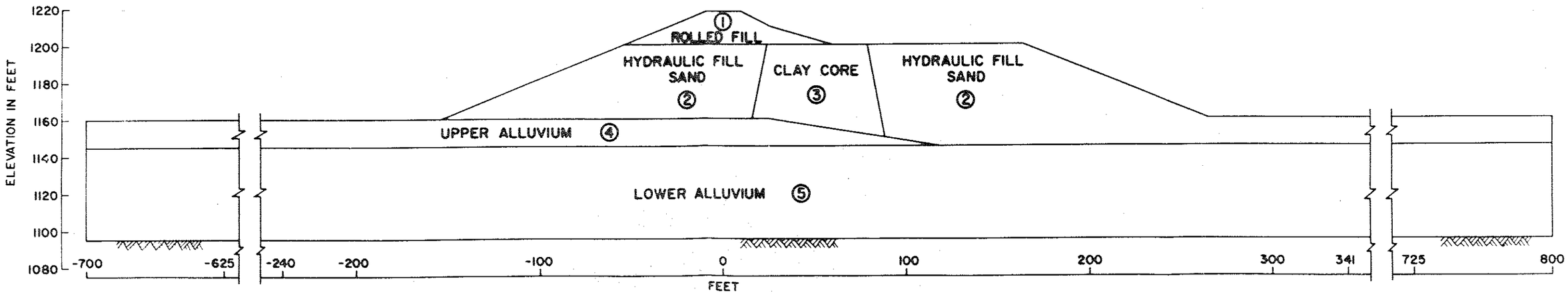

REPRESENTATIVE CROSS-SECTION THROUGH UPPER SAN FERNANDO DAM

Fig. IX-1 CROSS-SECTION THROUGH UPPER SAN FERNANDO DAM USED FOR DYNAMIC ANALYSIS

Table IX-2

Dynamic Properties of Soils in Upper Dam
used for Response Analyses

Zone No. on Fig.	Soil	Soil Type for Dynamic Property Evaluation	$(K_2)_{max}$	Undrained Shear Strength
1	Rolled Fill	Cohesionless	52	--
2	Hydraulic Sand Fill	Cohesionless	30	--
3	Clay Core	Saturated Clay	--	1200 psf
4	Upper Alluvium	Cohesionless	40	--
5	Lower Alluvium	Cohesionless	110	--

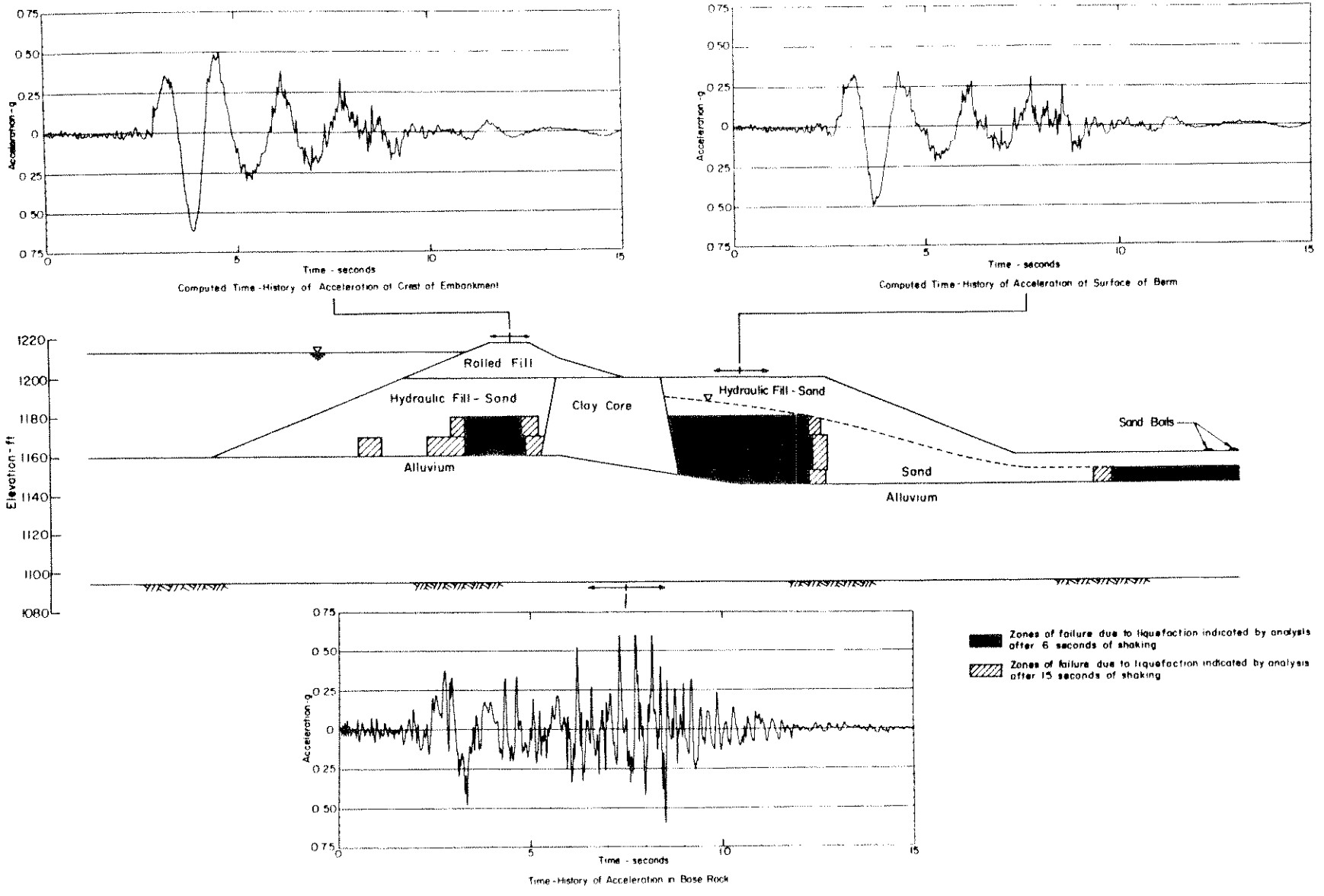

Fig. IX–2 ANALYSIS OF RESPONSE OF UPPER DAM DURING SAN FERNANDO EARTHQUAKE TO BASE MOTIONS DETERMINED FROM MODIFIED PACOIMA RECORD.

Stability Analysis

The stability in the embankment was evaluated by investigating the liquefaction and strain potential within four potential zones of failure, located as follows:

1. A zone along the base of the embankment extending from Elevation 1145 to Elevation 1152. The stress conditions along the plane at Elevation 1148-1/2 (average elevation for this zone) were used for evaluating the liquefaction and strain potential in this zone. As can be seen in the lower part of Fig. IX-1, this zone extends partly in the upper alluvium and partly in the hydraulic fill.
2. A zone extending from Elevation 1160 to 1170; the stress conditions along the plane at Elevation 1165 were used for evaluating the liquefaction and strain potential in this zone.
3. A zone extending from Elevation 1170 to 1180; the stress conditions along the plane at Elevation 1175 were used for evaluating the liquefaction and strain potential in this zone.
4. A zone extending from Elevation 1180 to 1190; the stress conditions along the plane at Elevation 1185 were used for evaluating the liquefaction and strain potential in this zone.

As in the case of the Lower Dam, the stability of the Upper Dam was evaluated taking into consideration the tendency for liquefaction in the hydraulic fill to develop progressively. The stability of the dam was therefore assessed in two steps; the behavior after 6 sec. of shaking was first evaluated and then the remainder of the motion (i.e. from 6 to 15 sec.) was applied. Typical time histories of stress at representative points in the embankment are shown in Fig. IX-3.

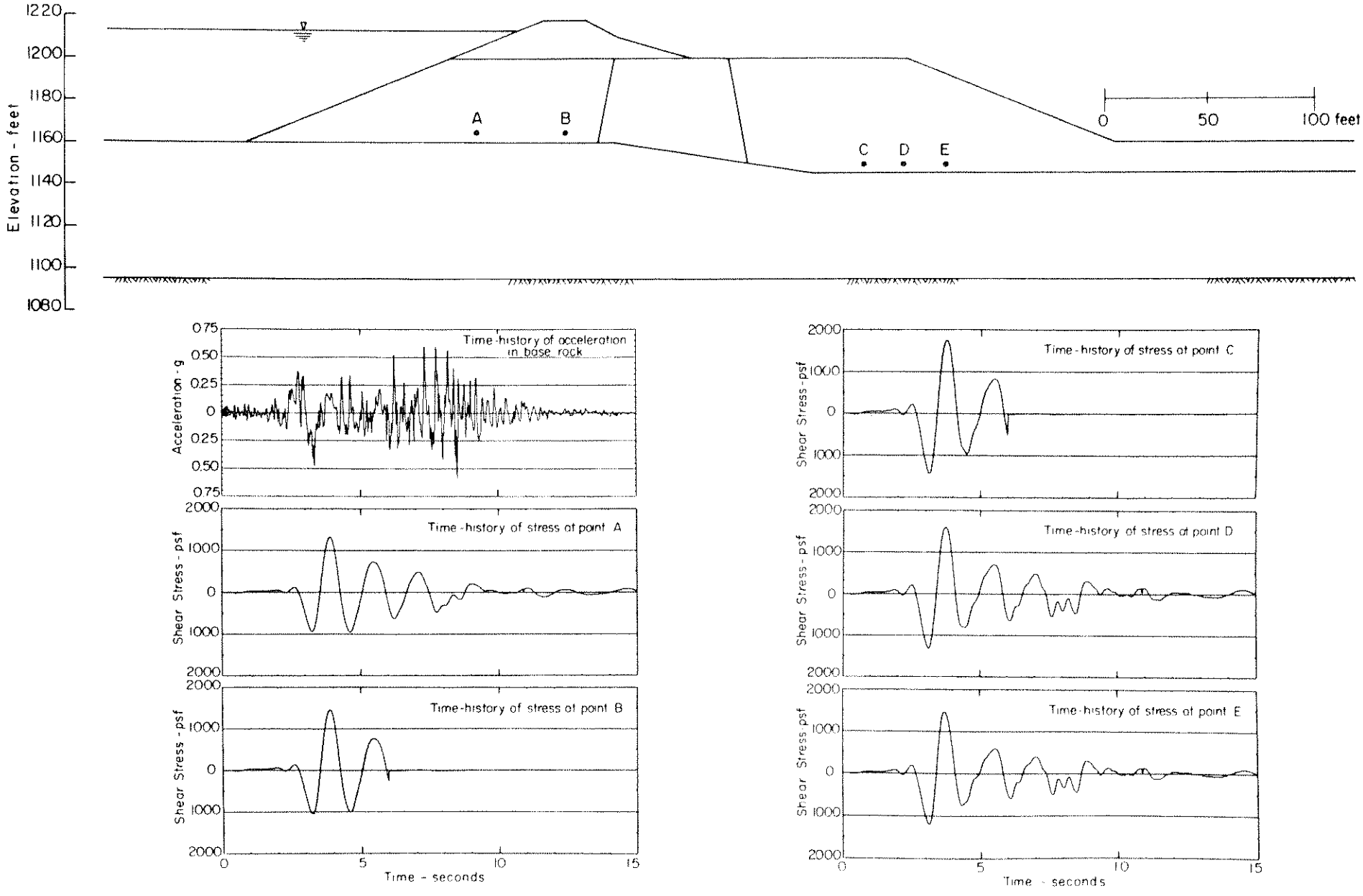

Fig. IX-3 PROGRESSIVE LIQUEFACTION ANALYSIS: TIME-HISTORIES OF SHEAR STRESSES DEVELOPED ALONG BASE OF EMBANKMENT - UPPER SAN FERNANDO DAM.

The stresses developed at different points in the embankment and its foundation during the first 6 seconds of shaking were judged to correspond to 2 cycles of equivalent uniform stress. The equivalent uniform stresses developed for 2 cycles after 6 sec. of shaking along the base of the embankment are presented in Fig. IX-4. The stresses required to cause liquefaction in 2 cycles (as determined from the test data in Fig. IV-35 in conjunction with the values of initial normal stress, σ_o', and the ratio, τ_o/σ_o', shown in the upper part of Fig. IX-4) along the base of the embankment are also shown in Fig. IX-4. As can be noted, an extensive zone of liquefaction, accompanied by strains exceeding 5 percent, develops in the hydraulic fill downstream of the core. No liquefaction appears likely in the alluvium upstream of the core.

Similar plots, to that shown in the Lower part of Fig. IX-4, for the planes at Elevation 1156, 1165, 1175 and 1185 are presented in Figs. IX-5, IX-6, IX-7 and IX-8, respectively. Comparison of the values of developed stresses with the stresses required to cause liquefaction and 5 percent strain along each plane provides the means for assessing the extent of liquefaction and excessive strain within each zone after 6 sec. of shaking. The extent of liquefaction for this duration of shaking is summarized in Fig. IX-2.

The effects of additional shaking (i.e. from 6 to 15 sec.) were studied by continuing the analysis with greatly reduced moduli of deformation in the liquefied zones and comparing the equivalent stresses after 15 seconds of shaking with the available resistance of the soil. The increase in the extent of liquefaction as a result of this additional shaking is summarized in Fig. IX-2.

In addition to the development of zones of liquefaction and significant strains within the embankment, the analysis also indicates

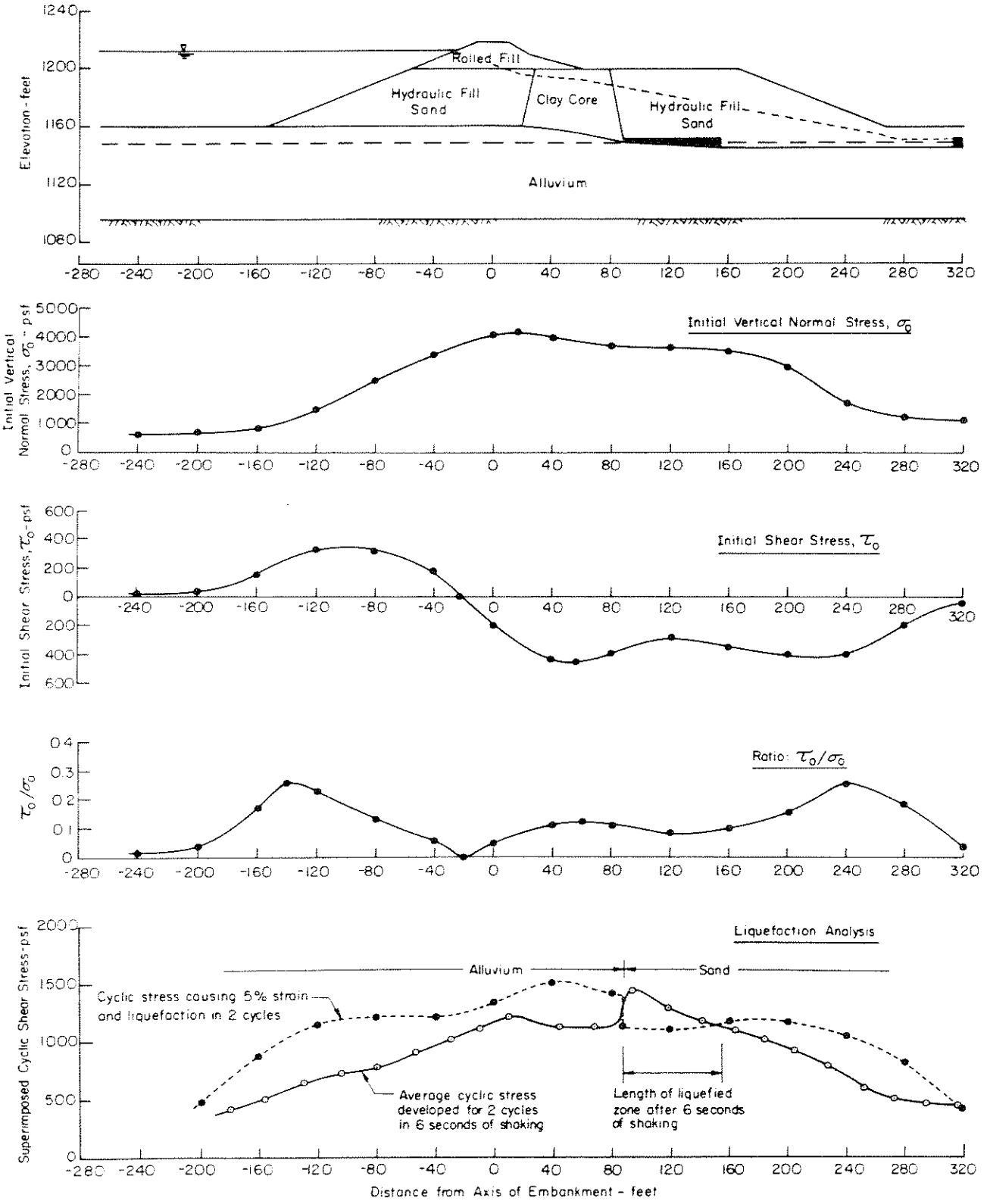

Fig. IX–4 ANALYSIS OF SOIL STABILITY ALONG PLANE AT ELEVATION 1148.5 FT. AFTER 6 SECONDS OF SHAKING, USING BASE MOTIONS DETERMINED FROM MODIFIED PACOIMA RECORD – UPPER SAN FERNANDO DAM.

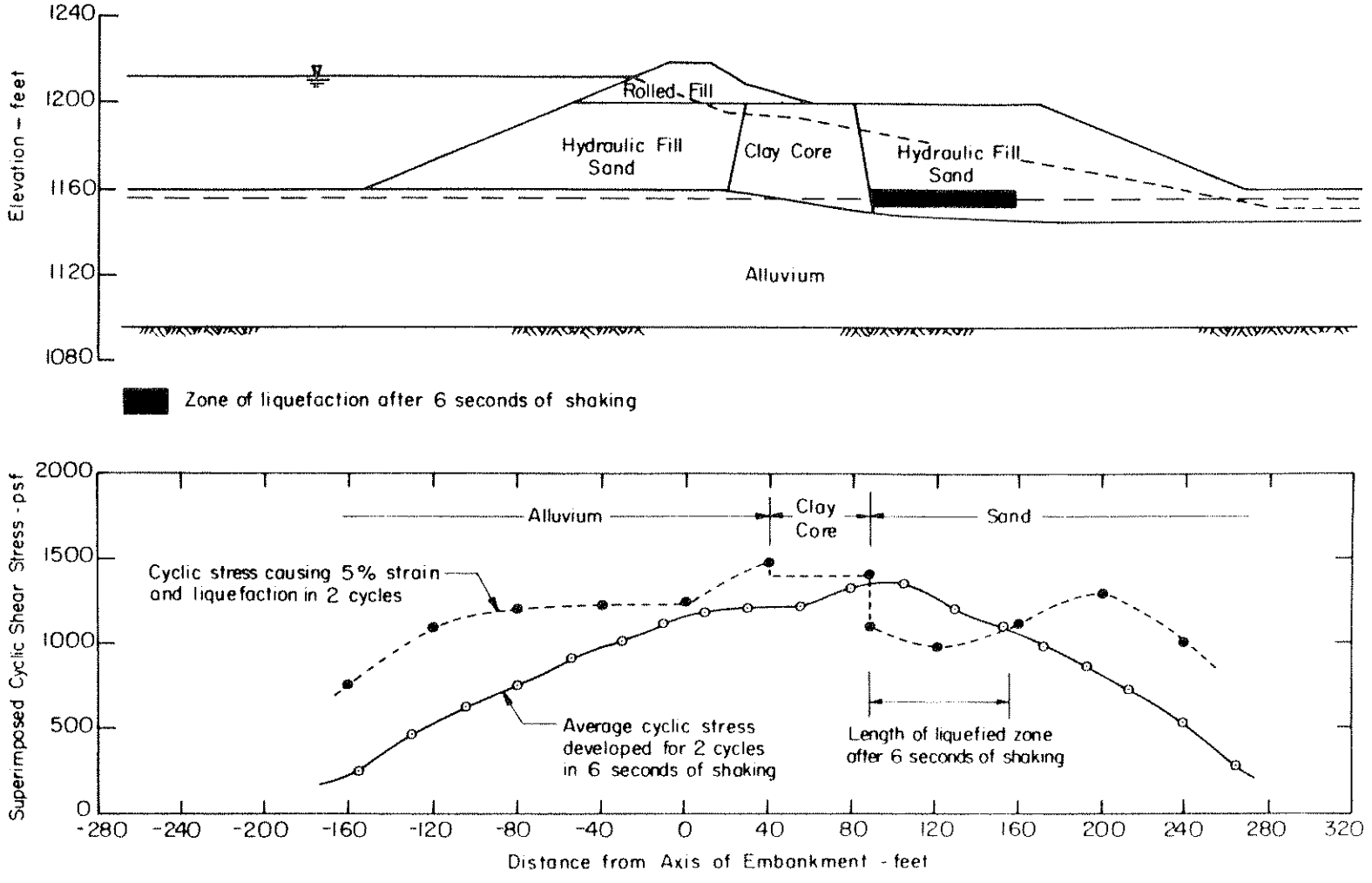

Fig. IX–5 ANALYSIS OF SOIL STABILITY ALONG PLANE AT ELEVATION 1156 FT. AFTER 6 SECONDS OF SHAKING, USING BASE MOTIONS DETERMINED FROM MODIFIED PACOIMA RECORD – UPPER SAN FERNANDO DAM.

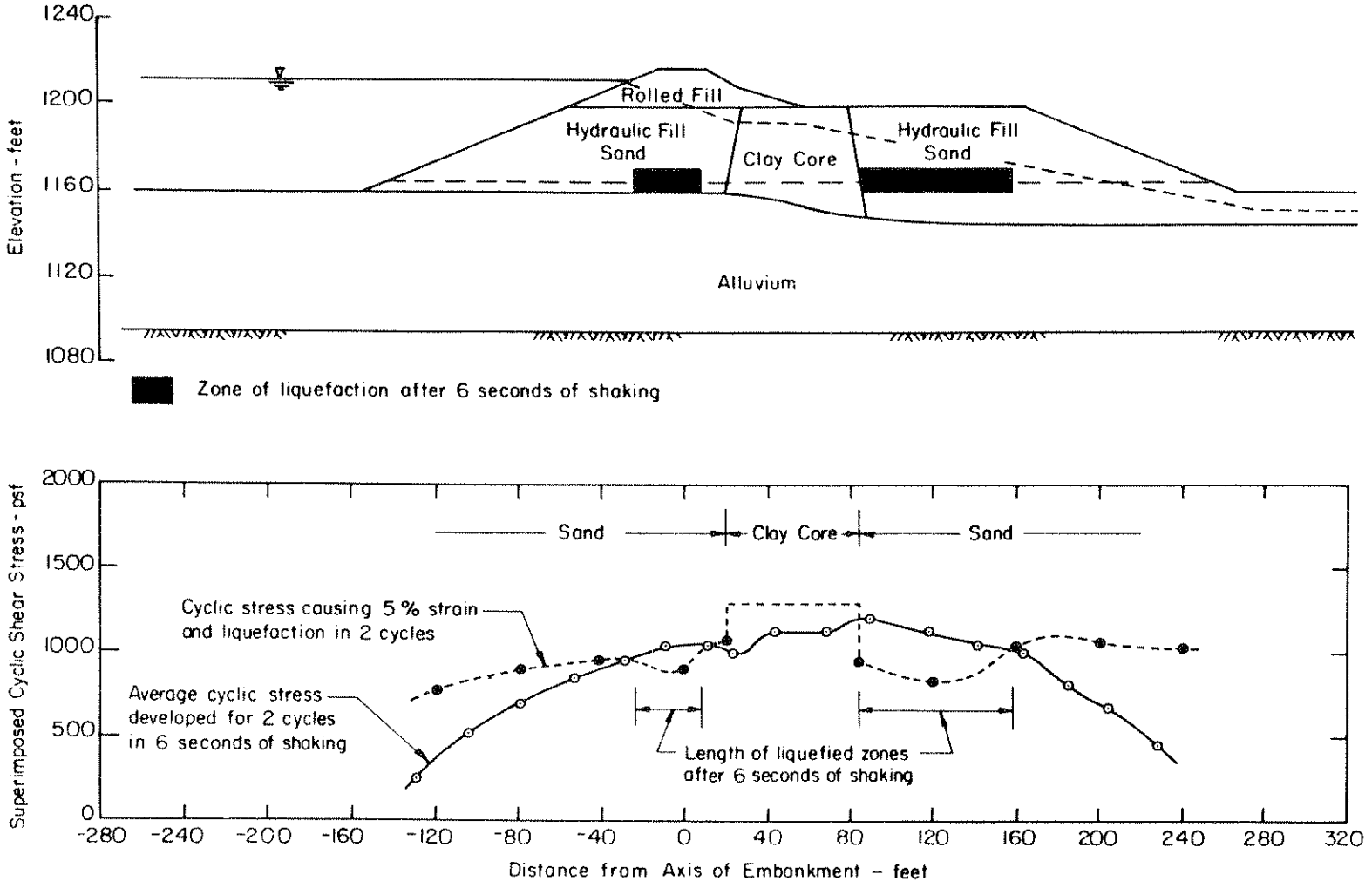

Fig. IX-6 ANALYSIS OF SOIL STABILITY ALONG PLANE AT ELEVATION 1165 FT. AFTER 6 SECONDS OF SHAKING, USING BASE MOTIONS DETERMINED FROM MODIFIED PAXOIMA RECORD – UPPER SAN FERNANDO DAM.

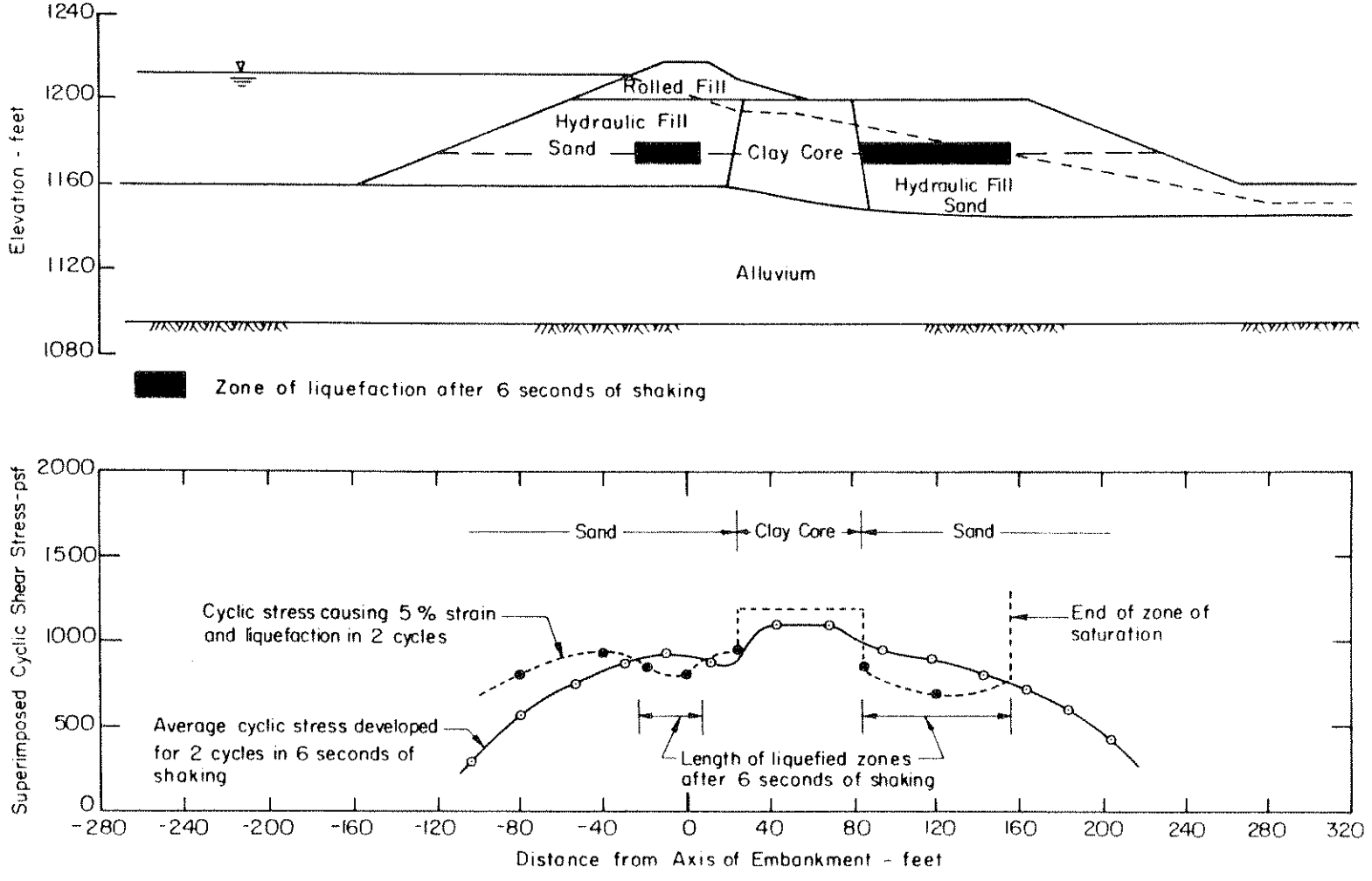

Fig. IX–7 ANALYSIS OF SOIL STABILITY ALONG PLANE AT ELEVATION 1175 FT. AFTER 6 SECONDS OF SHAKING, DUE TO BASE MOTIONS DETERMINED FROM MODIFIED PACOIMA RECORD – UPPER SAN FERNANDO DAM.

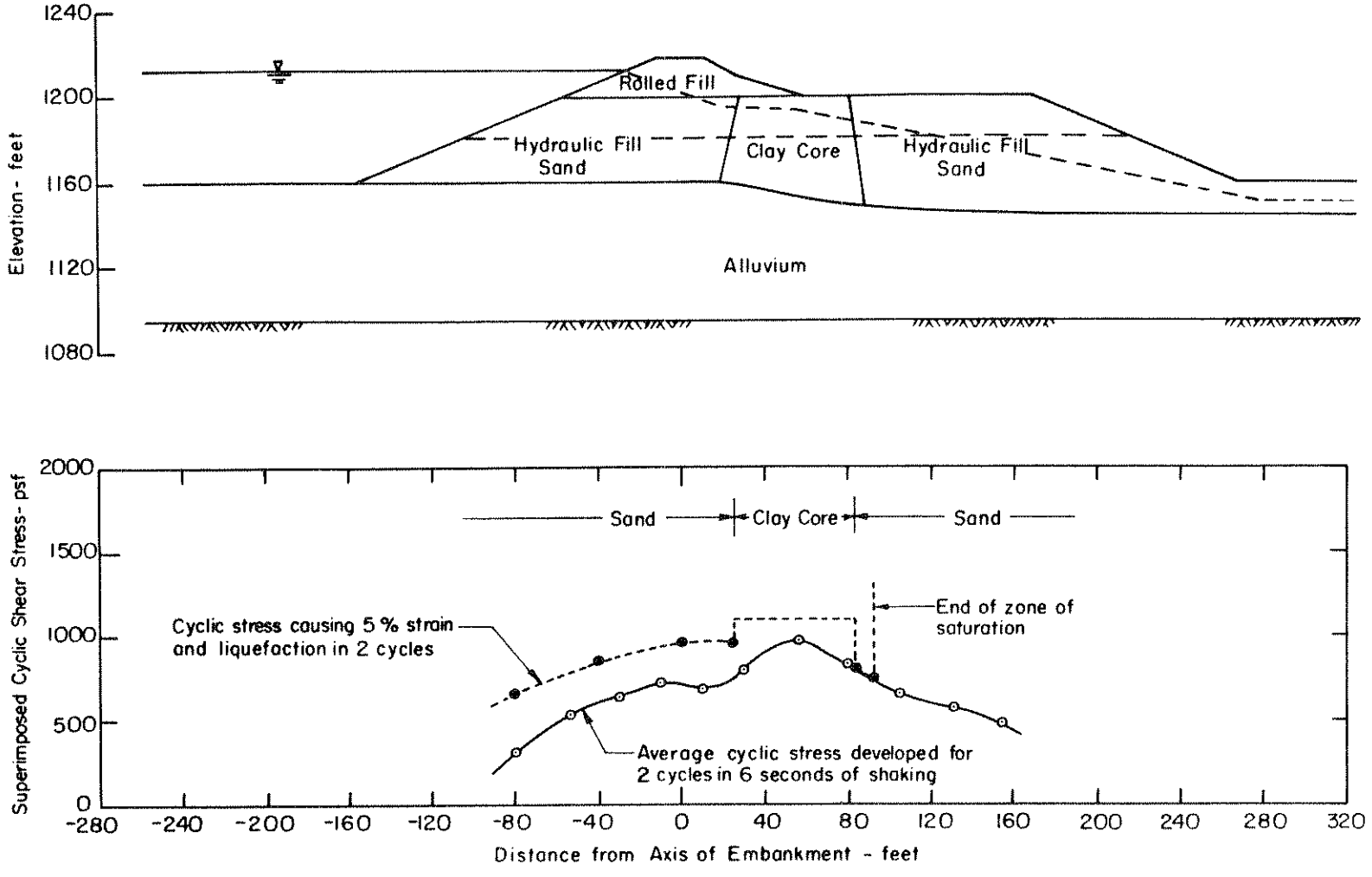

Fig. IX–8 ANALYSIS OF SOIL STABILITY ALONG PLANE AT ELEVATION 1085 FT. AFTER 6 SECONDS OF SHAKING, USING BASE MOTIONS DETERMINED FROM MODIFIED PACOIMA RECORD – UPPER SAN FERNANDO DAM.

an extensive zone of liquefaction in the depth range from El. 1145 to El. 1152 beyond the downstream toe of the embankment as shown in Fig. IX-2. It may be noted that several sand boils were found in this area after the earthquake.

However it may be seen from Fig. IX-2, that most of the upstream shell of the embankment and a substantial part of the downstream shell do not liquefy or tend to develop excessive strains. It was presumably the continued mobilization of high resistance to deformation in these zones which prevented a catastrophic failure of the embankment during the earthquake.

Furthermore, the locations and extent of the zones of liquefaction and high strain potential are indicative of the tendency of the embankment to undergo substantial movements in the downstream direction. Such movements would be anticipated simply from a loss of support at the downstream toe; the tendency would be strongly increased by a loss of resistance in a large part of the downstream shell and the central part of the upstream shell. The combined effects of movements through these zones would be likely to terminate near the upper part of the upstream slope. Thus in a qualitative sense, the results of the analysis are consistent with the behavior of the dam during the earthquake.

A more quantitative evaluation of the behavior of the embankment during the earthquake can be obtained by using the cyclic shear stresses computed by the dynamic response analyses in conjunction with the cyclic load test data to determine the potential compressive strains of individual elements of the embankment, as described in the previous section. These strains are shown in Fig. IX-9. Contours of equal potential strain, based on these results are shown in Fig. IX-10. It may be seen that the

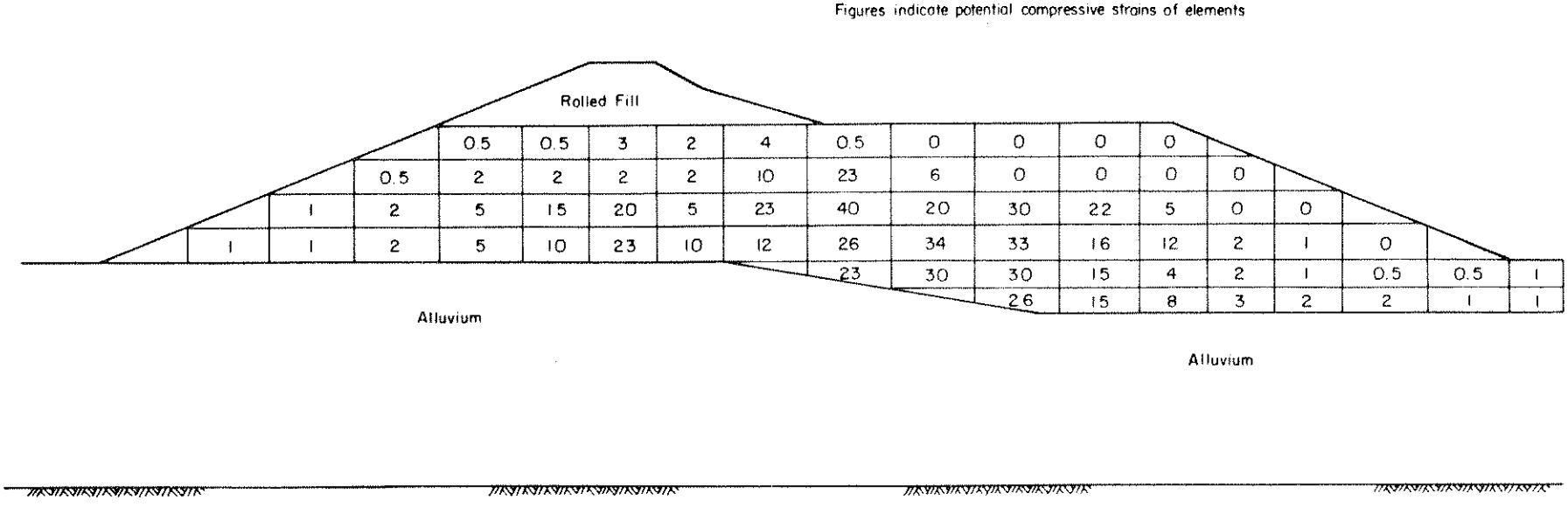

Fig. IX–9 STRAIN POTENTIAL IN HYDRAULIC FILL – UPPER SAN FERNANDO DAM.

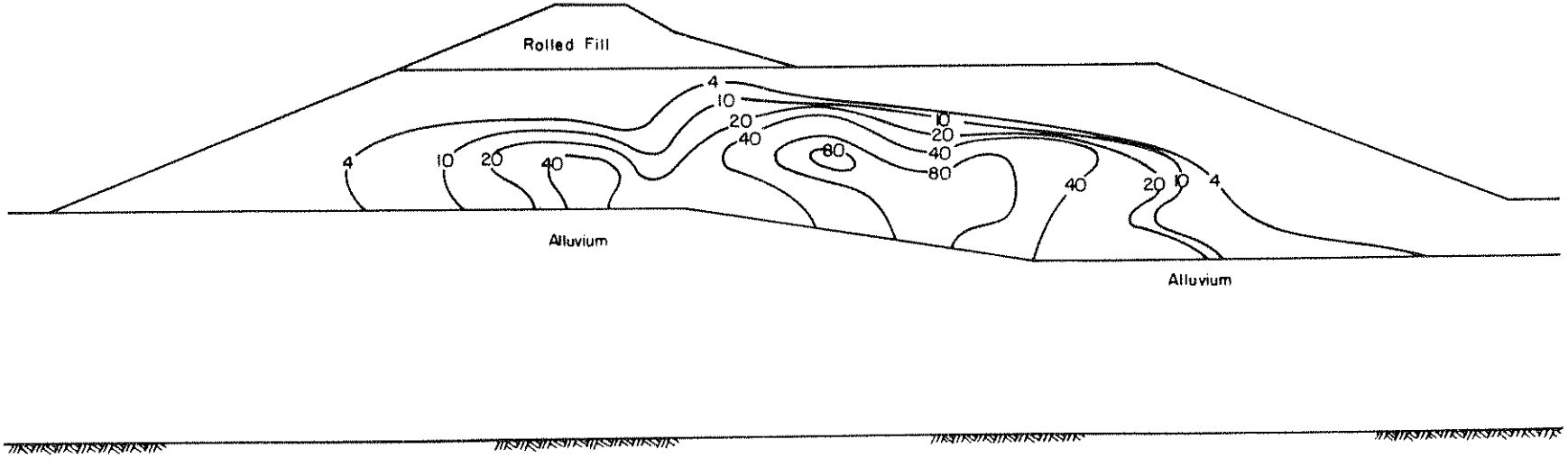

Fig. IX-10 CONTOURS OF SHEAR STRAIN POTENTIAL IN HYDRAULIC FILL – UPPER SAN FERNANDO DAM.

zones in the embankment which tend to develop the largest strains are near the base and near the center of the embankment and below the crest of the dam. On the other hand the soil in the shells tends to develop relatively small potential strains ranging from 0 to 7 percent.

An assessment of the overall stability of the embankment, in spite of the development of zones of high strain potential, can be made by considering that the soil in zones where the shear strain potential exceeds, say, 20 percent or the compressive strain potential exceeds about 10 percent, would provide no effective resistance to slide movements in the embankment. These zones are shown in Fig. IX-11, together with the results of an analysis to determine the minimum factor of safety against sliding in the downstream direction. For the sudden change in stress conditions, consolidated-undrained strength parameters were used in the analyses and seismic forces were neglected. The computed minimum factor of safety was 1.75 indicating that the embankment would easily be able to withstand the small inertia forces developed in the later stages of the earthquake, together with the static stresses, without development of a residual downstream instability condition.

On the other hand, the magnitude of the strains developed in the embankment would be expected to lead to substantial residual deformations. Values of the shear strain potential for individual elements of the embankment, obtained by multiplying the compressive strains by 2, are shown in Fig. IX-12. Since the zones developing lower strains will tend to restrain the movement of zones of higher strain potential, again a first approximation to the overall horizontal movements of the embankment might be obtained from the overall average shear strain for elements located on the downstream side of the axis of the dam, as shown in Fig. IX-12.

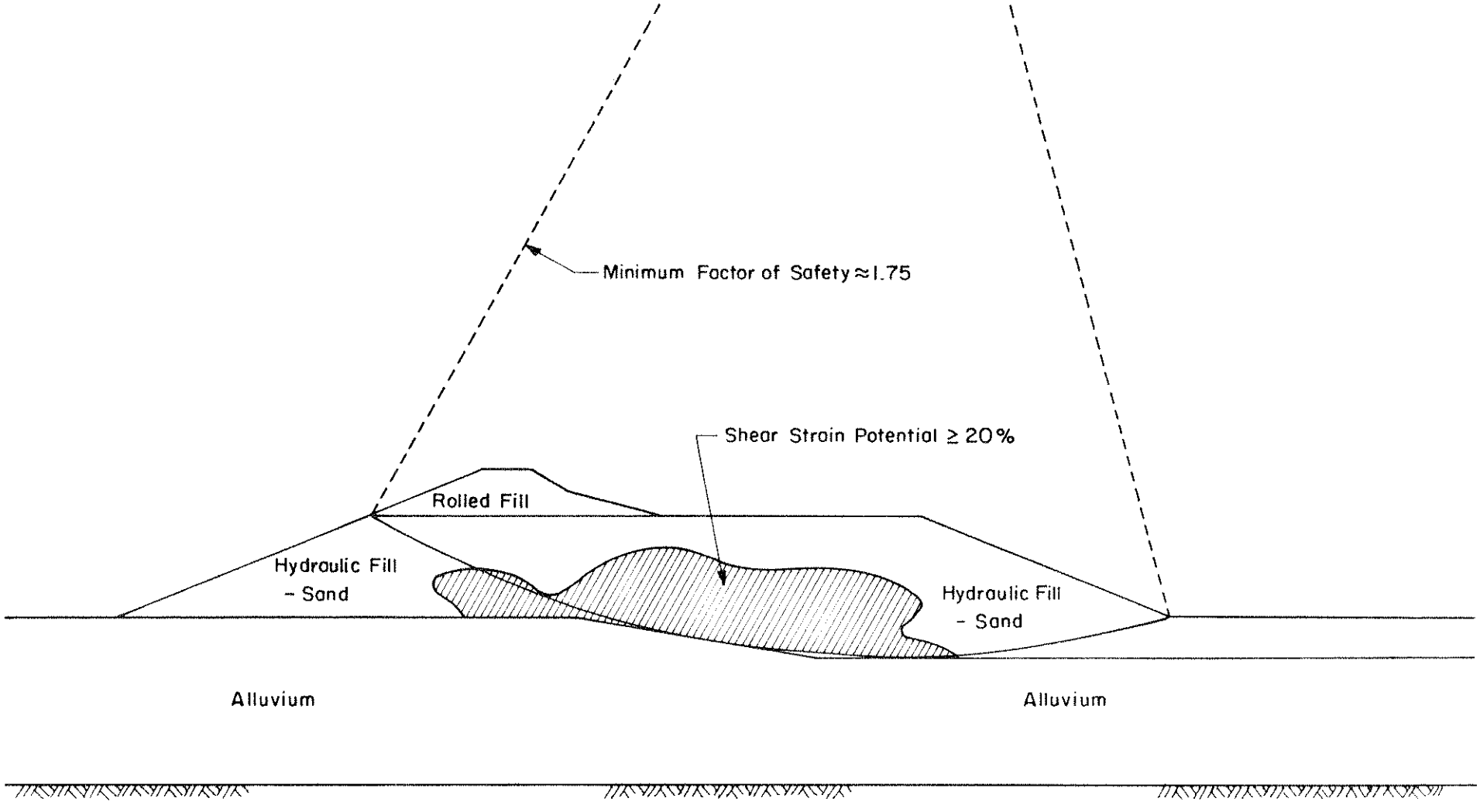

Fig. IX-11 ANALYSIS OF STABILITY OF UPPER SAN FERNANDO DAM AFTER DEVELOPMENT OF ZONE OF HIGH STRAIN POTENTIAL

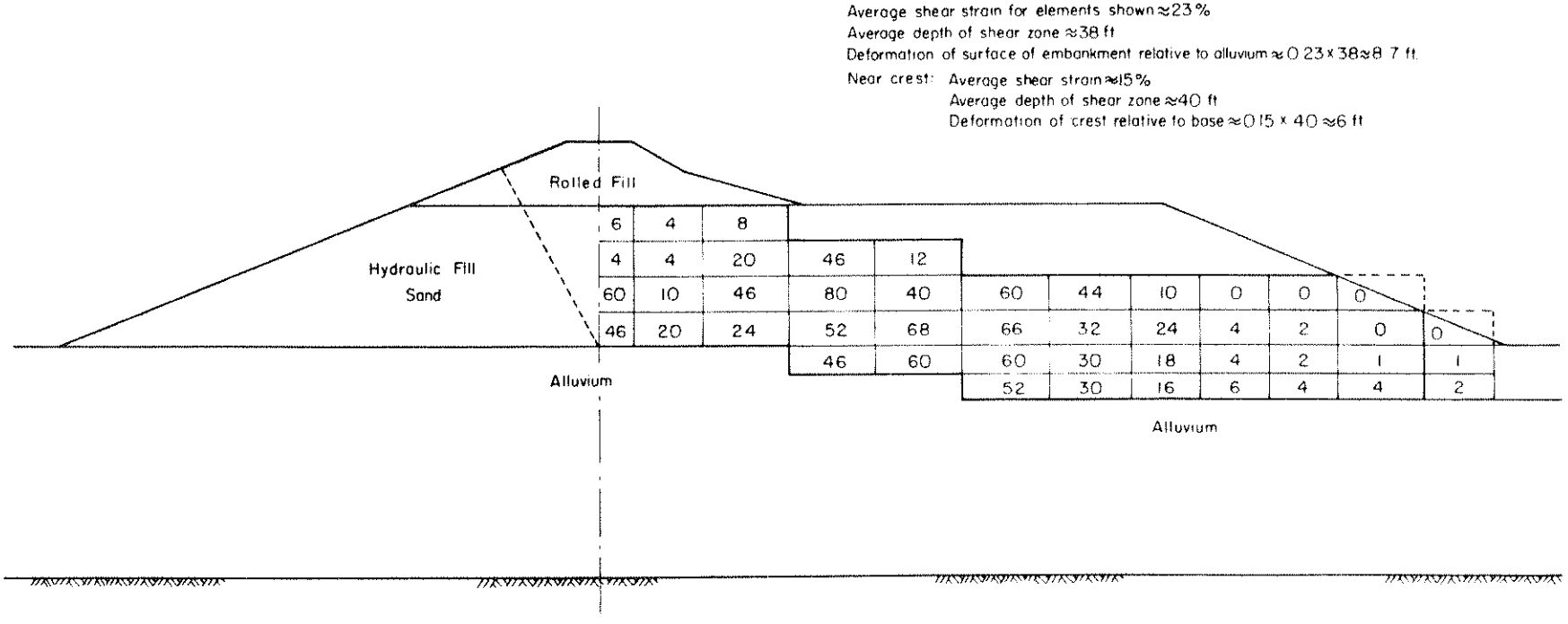

Fig. IX–12 SHEAR STRAIN POTENTIAL FOR INDIVIDUAL ELEMENTS OF EMBANKMENT – UPPER SAN FERNANDO DAM.

For the shear zone shown with a depth of about 38 ft, the average shear strain is about 22%. Thus the indicated relative movement of the surface of the embankment relative to the base is about 8.3 ft. A horizontal movement of this magnitude would be accompanied by sloughing of the triangular wedge of soil bounded by the dashed line in Fig. IX-12, producing slide scarps near the top of the upstream slope. In addition the movements near the base of the embankment would be relatively small.

It is interesting to note that the shear strains in the zone below the crest of the embankment are somewhat lower than those further downstream, indicating that the lateral movement of the crest would be somewhat less than that of the horizontal berm at El. 1200 approx. Such differential movements would be expected to lead to cracking near the downstream toe of the rolled fill, as was observed following the earthquake. Furthermore the average shear strain in the soil under the crest of the embankment is about 15 percent, indicating a crest displacement due to shear of about 6 ft, as shown in Fig. IX-12.

This type of behavior is in reasonable accord with the behavior of the embankment during the earthquake. More rigorous analyses of the deformations of an embankment resulting from different strain potentials in the various elements can be developed, taking into account the stress-strain properties of the soils and including evaluations of vertical movements. However the simplified approach discussed above appears to provide a simplistic concept of behavior which is adequate for many purposes.

Part X - Dynamic Analyses of Lower San Fernando Dam for Other Earthquakes

In addition to the earthquake which shook the San Fernando area on Feb. 9, 1971 the San Fernando Dams might well have been subjected to ground shaking from other earthquakes which might reasonably be expected to occur at some time in the Los Angeles area. For example, the Van Norman Lake Complex is located about 23 miles from the San Andreas fault which might generate earthquakes with any magnitude up to about 8.5. It was considered of interest therefore to evaluate the stability of the Lower Dam for shaking produced by earthquakes with magnitudes 8-1/4, 7-1/2 and 7 occurring on this fault.

Also in view of the presence of other faults cutting recent alluvium at the Lower San Fernando damsite, it is conceivable that the dam might possibly have been subjected to stronger motions than those which occurred at the site in 1971. Furthermore if the dam had been located several miles north of its present location it might possibly have been subjected to motions similar to those recorded near the Pacoima Dam. To determine whether a reasonably well-constructed earth dam could safely withstand such motions, it was considered of interest to evaluate the stability of the Lower San Fernando Dam if it were subjected to these motions but the relative density of the soils in the dam had been of the order of 75 to 80 percent.

The results of these studies are presented in the following pages. The analytical procedures used were similar to those described in detail in Part VIII and IX.

Stability for Magnitude 8-1/4 Earthquake on San Andreas Fault

The results of the analysis of the stability of the Lower Dam for a magnitude 8-1/4 earthquake occurring on the San Andreas fault at a distance of 23 miles from the damsite are shown in Fig. X-1. The motions in the rock underlying the dam produced by such an earthquake were considered to have a maximum acceleration of about 0.4g and a time-history similar to that proposed by Seed and Idriss (1969) for such events. The time-history of rock motions at the base of the embankment is shown in Fig. X-1.

The computed accelerations at the crest of the dam are also shown in the figure together with the zones of soil in the hydraulic fill which the analysis indicates would have failed by liquefaction after about 30 seconds of ground shaking. It may be seen that the extent of the zones is comparable to that shown in Fig. VIII-4 to have developed after about 10.5 seconds of the San Fernando earthquake. However since the total duration of shaking from a magnitude 8-1/4 earthquake is likely to be about 60 to 70 seconds, it is clear that further liquefaction in such an earthquake would rapidly occur by progressive failure and in fact, the dam would almost certainly have failed more extensively in such an earthquake than it did in the San Fernando event.

Clearly an earthquake of this magnitude would need to be considered in evaluating the safety of the dam, and depending on the possible magnitude of more local events, might be the controlling factor in determining an adequate design.

Stability for Magnitude 7-1/2 Earthquake on San Andreas Fault

The results of an analysis of the stability of the Lower Dam for a magnitude 7-1/2 earthquake occurring on the San Andreas fault are shown in Fig. X-2. The motions in the rock underlying the dam produced by such

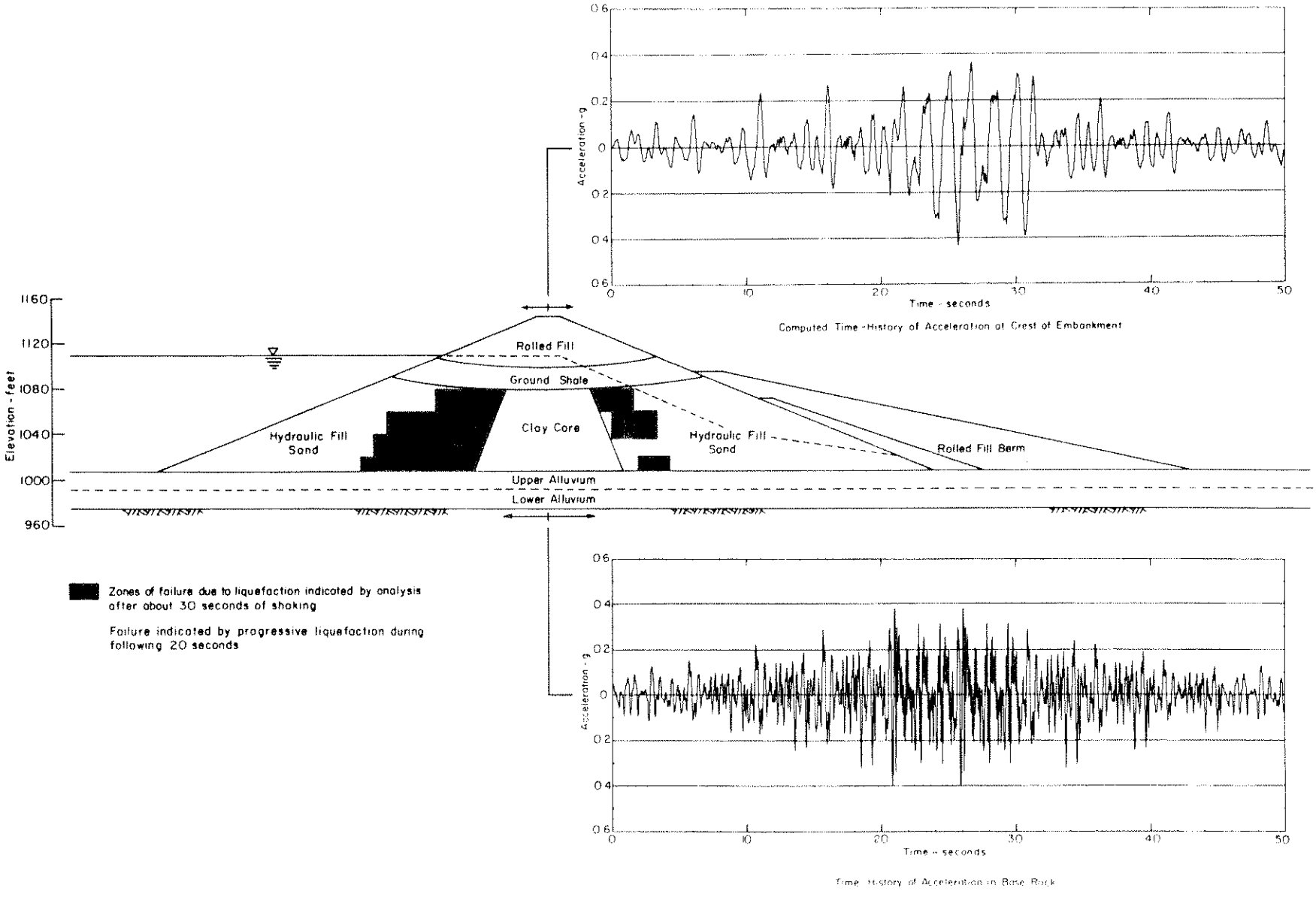

Fig. X-1 ANALYSIS OF RESPONSE OF LOWER DAM FOR MAGNITUDE 8 1/4 EARTHQUAKE ON SAN ANDREAS FAULT.

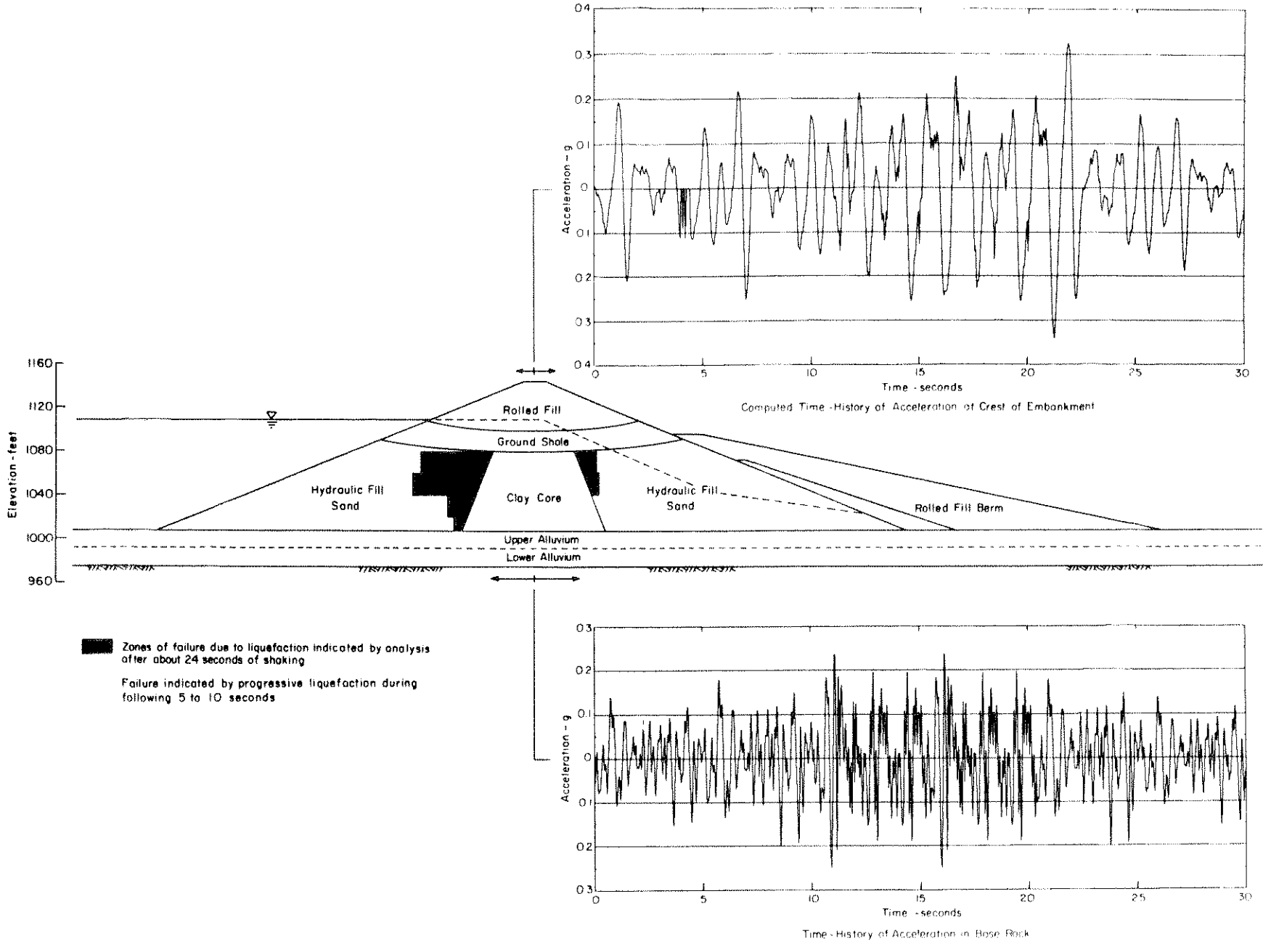

Fig. X–2 ANALYSIS OF RESPONSE OF LOWER DAM FOR MAGNITUDE 7 1/2 EARTHQUAKE ON SAN ANDREAS FAULT.

an earthquake were considered to be similar to those shown in Fig. X-1 but to have a maximum acceleration of 0.25g and a duration of strong shaking of about 35 to 40 seconds.

The computed accelerations at the crest of the dam for rock motions of this type are shown in Fig. X-2, together with the zones of failure in the hydraulic fill which the analysis indicates would have failed by liquefaction after about 24 seconds of ground shaking. While these zones are appreciably smaller in extent than those shown in Fig. X-1, they are never-the-less sufficiently comparable to those shown in Fig. VIII-4 to have developed after 10.5 seconds of shaking in the San Fernando earthquake that by analogy it seems highly probable that a similar slide in the upstream slope would occur by progressive failure in the subsequent 10 to 15 seconds of strong motion.

Thus an earthquake of magnitude 7-1/2 on the San Andreas fault might have been expected to cause sliding of a similar extent to that which occurred in 1971.

Stability for Magnitude 7 Earthquake on San Andreas Fault

The results of an analysis of the stability of the Lower Dam for a magnitude 7 earthquake occurring on the San Andreas fault are shown in Fig. X-3. The motions in the rock produced by such an earthquake were considered to have a maximum acceleration of about 0.2g, a duration of strong shaking of about 25 seconds and a time-history similar to that recorded at Taft in the Kern County earthquake of 1952. The resulting time history of such motions used in the analysis is shown in the lower part of Fig. X-3.

The computed accelerations at the crest of the dam are also shown in the figure but in this case, analysis of the stresses induced in the embankment did not indicate any zone where liquefaction would occur.

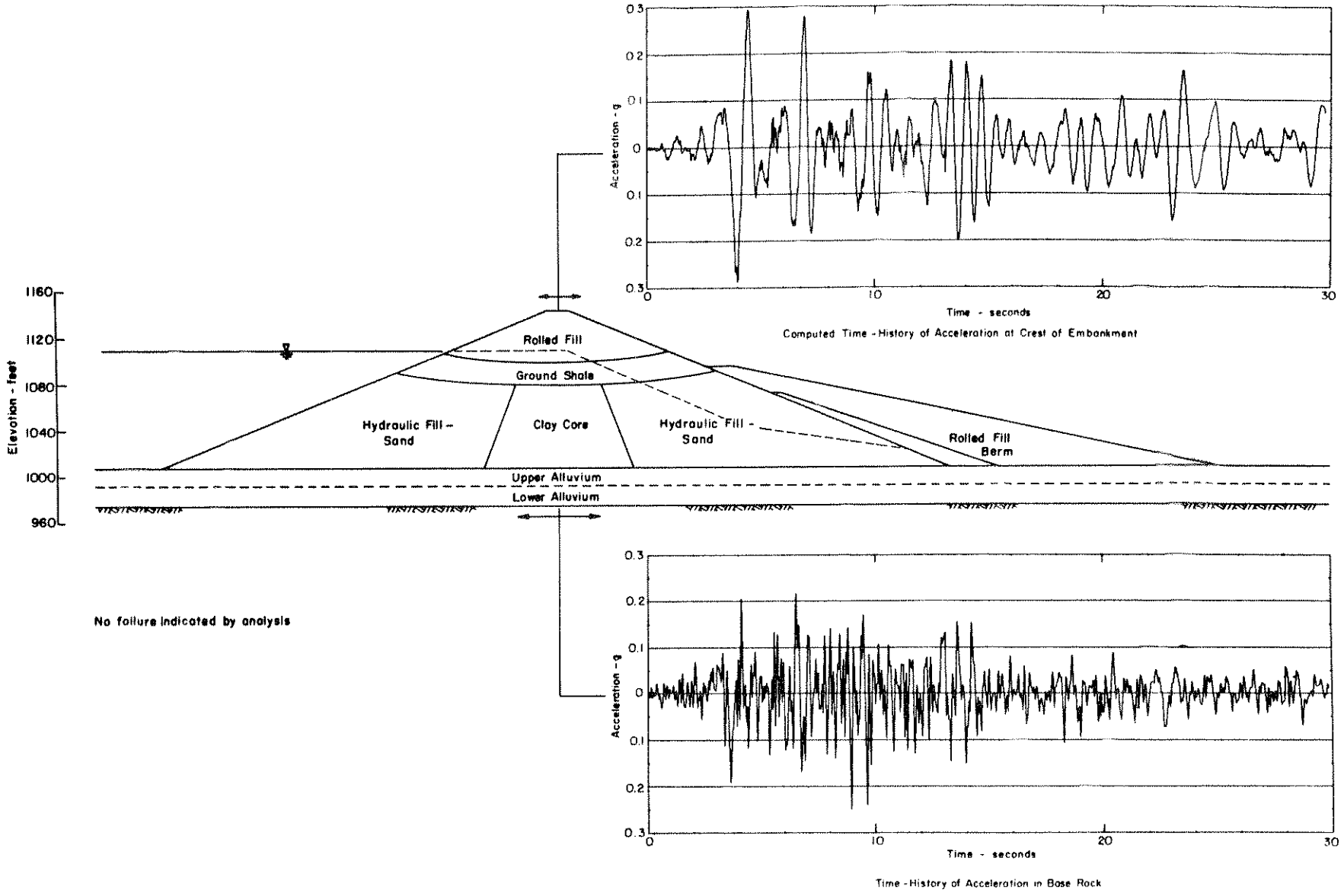

Fig. X–3 ANALYSIS OF RESPONSE OF LOWER DAM FOR MAGNITUDE 7 EARTHQUAKE ON SAN ANDREAS FAULT

Accordingly it is concluded that the Lower Dam would have been able to withstand the shaking produced by such an earthquake without any significant detrimental effects.

Stability of Embankment Dam Subjected to Pacoima Acceleration Record

In order to explore the possibility of a well-constructed embankment dam withstanding the intense shaking represented by the motions recorded near the Pacoima (concrete arch) Dam in the San Fernando earthquake, a hypothetical analysis was made for a dam having the same configuration as the Lower San Fernando Dam but composed of similar soils having a relative density of the order of 75 to 80 percent.

For a denser material of this type, the shear moduli would be appreciably higher than those in the actual dam and used in the analyses described previously. Typical values for such materials were selected from test data obtained in other studies (Seed and Idriss, 1970). Thus the embankment was considered to be constructed of sand having a maximum value of K_2 in the equation

$$G = 1000\ K_2(\sigma_m')^{1/2}$$

of about 62 at strains of the order of 10^{-3} percent. The proportionate reduction in moduli with increasing strain and the damping ratios at different strains were identical with those used for the preceding analyses.

In the absence of test data for the embankment sands at these higher densities, an estimate of the strength at a relative density of 80 percent was obtained by assuming that the proportionate increase in strength with increase in relative density would be similar to that found for Sacramento River sand (Lee and Seed, 1967). Thus the stresses required to cause 5%

strain and liquefaction at a relative density of 80 percent were considered to be about 60 percent higher than those for a relative density of 50 percent.

With these assumptions an analysis of embankment stability was made as before. The time history of accelerations in the base rock is shown in the lower part of Fig. X-4, and the computed time history of accelerations at the crest of the embankment in the upper part of the figure. It may be seen that although the base motions have a maximum acceleration of 1.25g, the maximum crest acceleration is only about 0.8g and furthermore the maximum crest acceleration occurs well before the maximum base rock acceleration is reached. Thus in fact, the maximum response in the embankment is independent of the maximum acceleration pulse in the base motion.

Analyzing the failure potential of different elements in the embankment as described in Part VIII leads to the zones of failure after 15 seconds shown in Fig. X-4. The extent of those zones is insufficient to cause any significant degree of progressive failure of the embankment and thus it seems likely that an embankment constructed primarily of sandy material with a relative density of about 80 percent would be able to withstand safely the strongest earthquake motion recorded to date. However the Pacoima Dam record is not necessarily the most damaging motion which would affect a dam and further studies for other motions are required before general conclusions concerning embankment dam stability during earthquakes can be drawn.

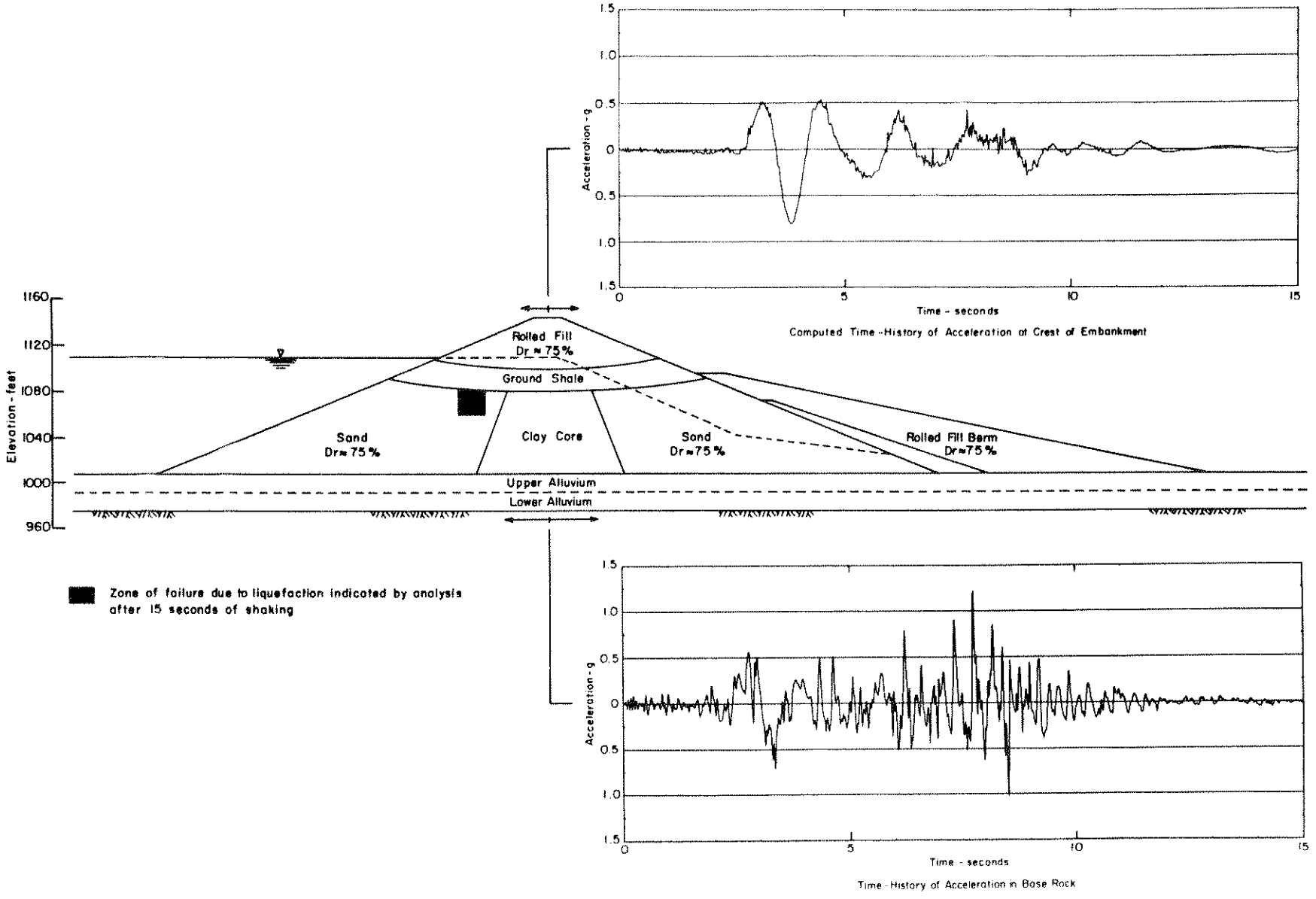

Fig. X–4 ANALYSIS OF RESPONSE OF DAM TO BASE MOTIONS DETERMINED FROM PACOIMA RECORD

Part XI - Dynamic Analyses of Lower San Fernando Dam for other Conditions

Stability with only 5 ft of Water in Reservoir

Although the upstream slope of the Lower San Fernando Dam proved to be unstable during the earthquake of Feb. 9, this condition was not determined solely by the characteristics of the soils comprising the embankment but also by such variable factors as the intensity and duration of the earthquake shaking and the water level in the reservoir. It has already been noted that the sliding probably occurred in the later stages of strong ground shaking and might not have occurred at all if the shaking had been a few seconds less in duration. Similarly if the water level in the reservoir had been very low, the condition of instability might never have developed. To explore this possibility an analysis of the embankment stability was made assuming a water level in the reservoir 5 ft above the base of the embankment. Thus the water level was sufficiently high to maintain a condition of saturation in the lower 5 ft of the embankment, thereby making this section vulnerable to strength loss and liquefaction as a result of earthquake shaking. However the liquefaction potential would be reduced significantly by the increase in effective pressures within the embankment.

The results of an analysis of embankment stability under these conditions, for the base rock motions represented by Scott's interpretation of the abutment seismoscope record are presented in Fig. XI-1. The maximum acceleration at the base of the embankment was about 0.6g and the computed maximum acceleration at the crest was about the same (see acceleration time histories in Fig. XI-1). However analysis of the stability of elements

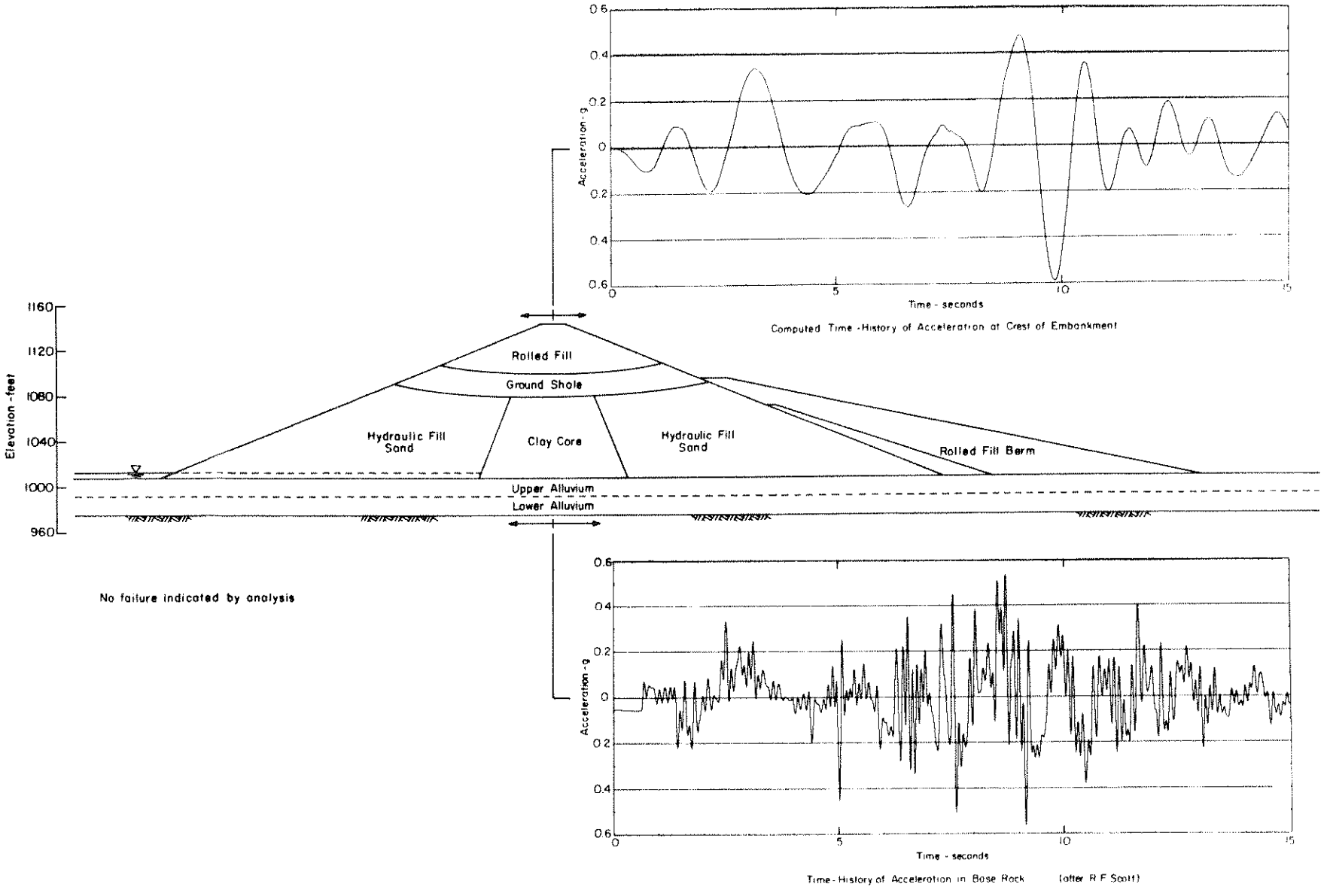

Fig. X1–1 ANALYSIS OF RESPONSE OF LOWER DAM WITH RESERVOIR ALMOST EMPTY TO BASE MOTIONS DETERMINED FROM SEISMOSCOPE RECORD.

within the embankment showed that none would reach a condition of 5 percent strain or liquefaction.

Thus the analysis indicates that the embankment would have been stable under these conditions, a conclusion confirmed to some extent by the performance of the Dry Canyon Dam in this earthquake. Dry Canyon Dam was located at about the same distance from the zone of energy release as the Lower San Fernando Dam. However it had no water in the reservoir and it suffered no significant damage, thereby demonstrating that hydraulic fills, per se, are not necessarily vulnerable to earthquake shaking; further it is the combination of the initial soil conditions, the pre-earthquake effective stress conditions and the dynamic stresses induced by the earthquake which determine the embankment stability. A significant change in any of these factors can materially affect the failure potential of an earth dam.

Stability Analysis Using Different Failure Criteria

In the stability analyses described in Parts VIII and IX, the stability of the embankment was first evaluated using the stresses required to cause 5% strain and liquefaction (pore pressure equal to effective confining pressure during cyclic loading) as a failure criterion. This strain criterion was chosen for several reasons including:

(1) If this strain level is not exceeded anywhere in an embankment, deformations of the embankment are likely to be well within acceptable limits.

(2) For the hydraulic sand fill complete failure of test specimens developed relatively rapidly once 5% strain had been reached; thus the development of this strain level in the embankment would be likely to be quickly followed by much larger strains and large movements.

and (3) It is an appropriate strain level at which progressive failure effects should be considered.

It has sometimes been suggested that higher strain levels of the order of 15 to 20 percent should be used for analysis purposes. The use of such higher strain criteria would tend to increase the apparent safety of an embankment by

1. Requiring higher stresses to cause the higher strain levels specified and
2. Eliminating the need for considerations of progressive failure in an embankment.

While such considerations may be appropriate for some types of soils, their use for soils which increase in strain relatively rapidly once initial liquefaction has occurred may lead to an over-estimate of the actual safety of an embankment dam.

To explore this possibility, an analysis of the stability of the Lower San Fernando Dam was made using a failure criterion of 20% in the cyclic triaxial compression tests. For this condition it was found from the test data that the stresses required to cause 20% strain were about 25 percent higher than those required to cause 5% strain. Thus the data shown in Figs. V-46 to V-51, increased by 25 percent, could be used for analysis purposes.

Using the modified Pacoima motion as a base excitation, the stress distribution in the embankment was determined and the values compared with those required to cause 20 percent strain. It was found that nowhere were the induced stresses high enough to cause a strain level of this mgnitude, leading to the conclusion that the embankment would adequately withstand base motions of this magnitude without excessive

deformation--a result in marked contrast to the actual behavior of the embankment during the earthquake.

In view of this result, a careful scrutiny was made of the cyclic load test data. It was noted that in many tests of this type, the magnitude of the cyclic stress applied to a test specimen drops off slightly once large strains are developed as a result of the inability of the load application system to keep pace with the deformations of the specimens. This was apparently the case in the test program for this investigation, and after correcting for this deficiency in the cyclic load test procedure, it was found that for constant stress applications, the stresses required to cause 20% strain were only about 15 percent higher than those causing initial liquefaction and 5% strain.

Accordingly a new analysis was made to compare the stresses induced in the embankment by the earthquake with those causing liquefaction and 20 percent strain determined in this way. The zones in which 20 percent strain would develop, as indicated by this analysis, are shown in Fig. XI-2. The limited extent of these zones might be considered indicative of adequate performance if the real behavior of the upstream slope had not been known.

Accordingly the use of higher strain criteria, without consideration of the possible effects of progressive failure, may lead to incorrect assessments of embankment performance under some conditions. In particular this study would seem to indicate the care required in interpreting the results of cyclic load tests for use in evaluations of embankment stability during earthquakes.

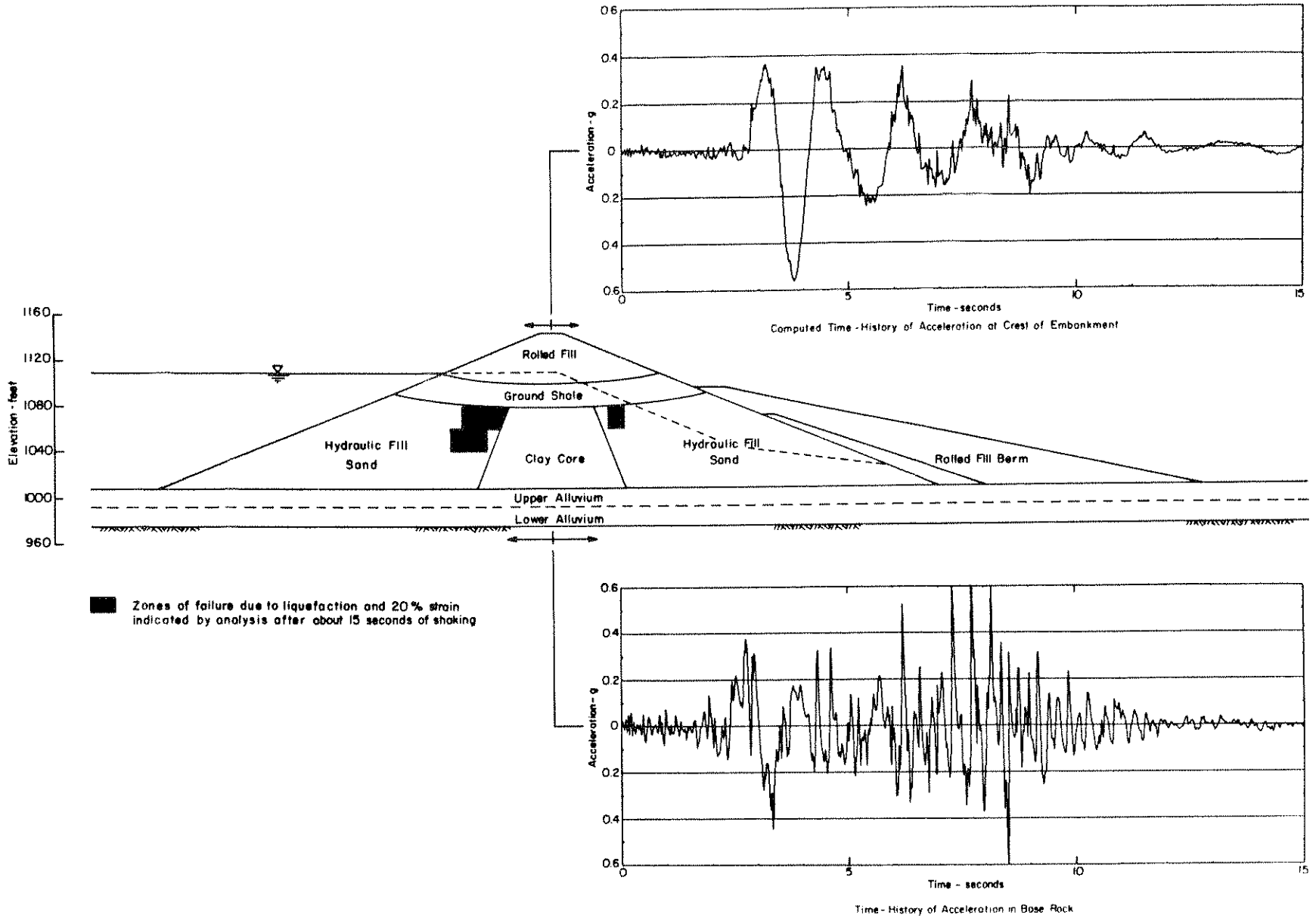

Fig. XI–2 ANALYSIS OF RESPONSE OF LOWER DAM DURING SAN FERNANDO EARTHQUAKE TO BASE MOTIONS DETERMINED FROM MODIFIED PACOIMA RECORD; FAILURE DEFINED BY LIQUEFACTION AND 20% STRAIN.

Part XII - Stability of Other Hydraulic Fill Dams in the San Fernando Earthquake

While this report is primarily concerned with the effects of the San Fernando earthquake on the Upper and Lower San Fernando Dams, it should also be noted that there were five other hydraulic fill dams located within about 20 miles of the epicentral region, and subjected to strong shaking during the earthquake. These dams are listed, together with the San Fernando Dams, in Table XII-1.

Dry Canyon Dam, located about the same distance from the epicentral region as the San Fernando Dams, had no water in the reservoir at the time of the earthquake and suffered no damage even though rock motions at the damsite are likely to have developed acceleration levels of the order of 0.5g. Clearly unsaturated hydraulic fills are not unstable even under conditions of extremely strong shaking.

Chatsworth Dam was under reconstruction at the time of the earthquake and thus no conclusions can be drawn from its behavior. However Fairmont, Lower Franklin and Silver Lake Dams, all storing water and located about 20 miles from the epicentral region where maximum rock accelerations were of the order of 0.2g, also suffered no significant damage. The behavior of these dams shows that hydraulic fill structures are capable of withstanding strong motions of this order of magnitude for 8 or 9 seconds without any detrimental effects; thus even saturated hydraulic fills will not become unstable unless the ground shaking becomes sufficiently intense, emphasizing that the liquefaction potential of a sandy soil during earthquakes is not determined simply by its void ratio or relative density but also by the magnitude and duration of the stresses to which it is subjected.

Table XII-1

Hydraulic Fill Dams within 25 Miles of Epicentral Region

Dam	Approx. Distance from Epicentral Region	Approx. Maximum Rock Accn.	Performance
Upper San Fernando	6	0.55g	Crest slid downstream 5 ft
Dry Canyon	$6\frac{1}{2}$	0.50g	Not in use - reservoir empty
Lower San Fernando	7	0.50g	Major slide upstream
Chatsworth	$14\frac{1}{2}$	--	Under reconstruction
Fairmont	20	0.20g	No significant damage
Lower Franklin	20	0.20g	No significant damage
Silver Lake	21	0.19g	No significant damage

It is interesting to note that the observed performance of all these dams is in accord with the behavior predicted by dynamic response analyses. Analysis of the lower San Fernando Dam with only 5 ft of water in the reservoir, as shown in Fig. XI-1, indicates no zones of failure or large deformation; similar results could readily have been obtained for the Dry Canyon Dam with low reservoir level.

Again, the analyses of the stability of the Lower San Fernando Dam show that it could safely withstand the effects of a magnitude 7 earthquake occurring about 22 miles from the damsite. Clearly then, no damage would be expected from a magnitude 6-1/2 earthquake at about the same distance, and similar results would be expected for other dams of similar construction; this was in fact borne out by the performance of the Fairmont, Lower Franklin and Silver Lake dams.

It is extremely important to note that both field performance and analytical studies show that the seismic stability of a hydraulic fill dam is not determined only by its composition and configuration, but also by the intensity of shaking to which it is subjected. Thus a dam which may be unsuitable for a highly seismic region may be entirely safe if it is located in a region of more moderate seismicity. In this respect the level of the water in the reservoir also has a major effect on the stability and increases in stability can be effected by limiting the reservoir level.

XIII - Conclusions

The events associated with the performance of the Upper and Lower San Fernando Dams during the earthquake of February 9, 1971 indicate that a major catastrophe was narrowly missed. Had any one of a number of possible conditions been slightly less favorable, such as the duration of shaking or the water level in the reservoir, the Lower Dam could have failed resulting in a sudden release of 10,000 acre-feet of water over a heavily populated urban residential area. The immediate recognition by responsible authorities that the margin of safety was unacceptably close led to the investigation described in the preceding pages. The study was specifically undertaken to determine whether the slide movements developed in the foundation or in the embankment soils, whether the mechanics of sliding was primarily due to liquefaction or more conventional slide mechanisms, whether existing analytical procedures are adequate to predict slide movements of this type and whether new criteria are required for evaluating the seismic stability of earth dams.

The main conclusions resulting from the study are summarized briefly below:

Field Conditions and Mechanism of Failure

1. Construction of the Lower and Upper San Fernando Dams was initiated in the years 1912 and 1921 respectively by hydraulic fill methods directly on the natural alluvial soils, with additional zones of compacted fill being added later.
2. The soil conditions at both dams were similar. The foundation alluvium consisted of a heterogeneous mixture of fairly well graded

clayey and sandy gravel with an average relative density of about 65 to 70 percent. The hydraulic fill forming the shells of the dam consisted of stratified layers of coarse to fine sand and clay, the degree of stratification tending to decrease from the outside toward a central clay core. The relative density of the hydraulic sand fill varied between about 40 and 70 percent but average characteristics were as follows:

	Upper Dam	Lower Dam
50 percent size, D50 - mm	0.05 to 0.8	0.05 to 1.0
Coefficient of uniformity	4 to 6	7 to 10
Dry unit weight - lb. per cu. ft.	90 to 115	95 to 110
Relative density - percent	51 to 58	51 to 54
Degree of compaction based on Standard AASHO test - percent	92 to 98	95 to 100
Degree of compaction based on Modified AASHO (1961) test - percent	83 to 92	88 to 93

3. The earthquake of February 9, 1971 produced about 15 seconds of strong shaking at the damsites with a peak acceleration of about 0.6g in the rock underlying the embankments.

4. As a result of this seismic shaking, the crest of the Upper Dam moved about 5 to 6 ft. downstream and settled about 3 ft. while the upstream part of the embankment of the Lower Dam, including the upper 30 ft. of the crest, moved some 70 ft. or more into the reservoir.

5. The slide movements in the upstream slope of the Lower Dam occurred as a result of an increase in pore water pressure in the embankment

soils resulting from the ground shaking and the resulting loss of strength and liquefaction of the hydraulic fill near the base of the embankment. Evidence supporting this conclusion includes:

(a) observed increases in pore water pressure in the soils comprising the downstream part of the embankment;

(b) the large horizontal displacements (about 75 ft) of the main parts of the slide mass;

(c) the spreading of embankment soil about 250 ft beyond the toe of the embankment;

(d) the formation of sand boils in the slide debris;

(e) the formation of cracks filled with liquefied sand in the slide mass;

(f) the complete distortion and intermixing of sand and clay layers in the slide zone;

(g) the mechanism of failure, as evidenced by the location of slide debris, was similar to that of other slides resulting from soil liquefaction;

(h) the positions of hydraulic sand fill in the slide debris in some areas could only have resulted from the soil being in a state of liquefaction or complete strength loss during the slide movements;

(i) reconstruction of the mechanics of sliding indicates an extensive zone of liquefaction near the base of the embankment;

(j) cyclic load tests on undisturbed samples consolidated to stress conditions equivalent to those existing in the dam prior to the earthquake and subjected to cyclic stresses

similar to those caused by the earthquake consistently produced failure by liquefaction where the pore water pressure reached values equal to the confining pressure and large deformations developed thereafter.

6. A review of all available evidence, including a reconstruction of the embankment section and the results of dynamic analyses of embankment stability, strongly suggests the following mechanism of failure of the upstream shell of the Lower San Fernando Dam: After about 12 seconds of strong shaking very high pore water pressures had developed in an extensive zone of hydraulic fill near the base of the embankment and upstream of the clay core so that much of this soil was in a liquefied condition. At this stage the shear resistance of the soil in the upstream shell could not withstand the dead load stresses caused by the weight of the embankment and slide movements developed. The slide mass moved outwards on the liquefied soil, breaking into blocks as the movement developed and removing support from the clay core, which was then extruded into the remaining part of the shell material by the pressure of the overlying portions of the embankment.

7. The horizontal movement of the Upper San Fernando Dam also resulted from increases in pore water pressure in the embankment soils leading to some loss of strength and complete liquefaction in some zones of the embankment; however since a significant body of the sand in the upstream and downstream shells retained considerable strength, complete failure could not occur and the movements were limited in extent.

8. There was no evidence of slide movements in the foundation alluvium for either dam; samples taken from the Lower Dam showed that the position of the original ground surface was unchanged by the slide movements immediately above, and careful examination of samples of alluvium at both damsites showed no evidence of disturbance. These observations are consistent with the laboratory and field determinations that the relative density of the alluvium at both sites was significantly higher than that of the hydraulic fill, and that the strength of the alluvium under cyclic loading conditions was significantly higher than that of the hydraulic fill under the same confining pressure conditions.

9. Three other hydraulic fill dams (Fairmont, Lower Franklin and Silver Lake) were subjected to base rock motions with maximum accelerations of the order of 0.2g during the earthquake without any detrimental effects, indicating that hydraulic fill dams are not inherently unstable structures but only become so when they are subjected to shaking of sufficient intensity and duration to initiate large increases in pore water pressure and accompanying loss of strength in the soil.

10. Another hydraulic fill dam (Dry Canyon), with no water in the reservoir, was subjected to shaking of comparable intensity to that at the Upper and Lower San Fernando damsites, without any detrimental effects, indicating that it is the presence of water pressure in the soils which leads to instability.

Pseudo-Static Analyses

1. Pseudo-static analyses of the seismic stability of the embankment of the Lower Dam made several years before the earthquake using conservative strength values and a seismic coefficient of 0.15, together with a partial drawdown, showed a factor of safety of about 1.05 for the upstream slope and led to the conclusion that the embankment would not fail due to anticipated earthquake ground motions; using average strength values for the embankment soil and discounting any effects of drawdown, the computed factor of safety for the same seismic coefficient would have been about 1.5. However the upstream slope failed completely during the San Fernando earthquake.

2. Pseudo-static analyses of the seismic stability of the embankment of the Upper Dam using average strength values for the embankment soil and a seismic coefficient of 0.15 show a computed factor of safety of about 2.0 to 2.5 depending on the method of data analysis. However the embankment moved 5 or 6 ft downstream and apparently approached a condition of failure during the earthquake.

3. While pseudo-static analyses using a seismic coefficient of 0.15 were inadequate for predicting the stability of the embankments during the San Fernando earthquake, they did serve to indicate the locations of the most critical sliding surfaces in the embankment sections.

4. In order to predict the conditions of instability of the San Fernando dams during the earthquake of February 9, 1971, using the pseudo static method of analysis, it would have been necessary to use a seismic coefficient of the order of 0.2 to 0.3 for the Lower Dam and about 0.5 for the Upper Dam.

5. The pseudo-static method of analysis with seismic coefficients of the order of 0.1 to 0.15 does not appear to provide an adequate basis for evaluating the seismic stability of dams which may fail as a result of increased pore water pressures and severe strength loss in the embankment or foundation soils, for the intensity of ground shaking developed in the San Fernando earthquake.

Dynamic Response Analyses

1. Dynamic analyses of the response of the San Fernando dams incorporating:
   (a) an analysis of the static stresses developed in individual elements of the embankment before the earthquake,
   (b) the use of a dynamic finite element analysis procedure, with strain-dependent properties to allow for non-linear stress-strain characteristics of the embankment and foundation soils, to determine the dynamic stresses developed in individual elements of the embankment,
   (c) the use of cyclic loading triaxial compression test data to determine the response of the soil elements to the induced stresses (i.e., whether liquefaction will occur and the magnitude of the strains developed),

and (d) consideration of progressive failure effects by determining the redistribution of dynamic stresses after liquefaction or 5 percent strain had developed in any soil element,

appears to provide a satisfactory basis for assessing the stability and deformations of the embankments during the earthquake. This type of analysis indicates the development of a zone of liquefaction along the base of the upstream shell of the Lower Dam, which would be sufficiently extensive near the end of the earthquake shaking to lead

to a condition of instability (factor of safety < 1). The same analysis procedure applied to the Upper Dam indicates that complete instability would not develop (factor of safety ≈ 2) but the development of large shear strains would lead to substantial deformations of the embankment section. The computed movements of the crest and berm of the embankment (6 to 8.5 ft) are in reasonable agreement with the observed downstream displacement of 5 ft at the crest of the dam.

2. If progressive failure effects were neglected and a failure criterion of 20 percent axial strain were used to determine the allowable dynamic stresses which could develop in the embankment without causing 'failure', the dynamic response analysis procedure described above would indicate the Lower San Fernando Dam to be 'stable' during the February 9 earthquake. Accordingly it is important to allow for progressive failure effects in soils where liquefaction and large strains develop rapidly once initial liquefaction has occurred.

3. Analysis of the stability of the Lower San Fernando Dam using the dynamic response analysis procedure for other earthquakes which might have affected the dam leads to the following results:

   (a) The dam, as it existed on February 9, 1971, would have been unstable for earthquakes with magnitudes 7-1/2 to 8-1/4 originating on the San Andreas fault some 23 miles away; however the dam would have been stable for a magnitude 7 earthquake occurring at such a distance. This latter result is in good accord with the observed performance of the Fairmont, Lower Franklin and Silver Lake dams during the February 9 earthquake.

(b) If the dam had been better constructed, with the same geometry and using the same materials, but with a relative density of the soils of about 80 percent, it would probably have been stable even if motions similar to those recorded at Pacoima Dam (maximum acceleration ≈ 1.25g) had developed in the underlying rock formations.

(c) If the reservoir had been almost empty so that the pre-earthquake effective pressures would have been due to the full weight of the embankment soils rather than their buoyant weights, the Lower San Fernando Dam would have withstood the shaking it received in the February 9 earthquake without seriously detrimental effects. The result is in general accord with the observed performance of the Dry Canyon Dam during the earthquake.

4. Both the analytical results and the field performance of hydraulic fill dams during the February 9 earthquake show that the seismic stability of hydraulic fills is not determined only by their void ratios or relative density, but also by the nature, intensity and duration of the seismic shaking.

5. The fact that the dynamic response analysis procedure used in the investigation gives reasonable evaluations of the performance of three different hydraulic fill dam conditions:

(1) Lower San Fernando Dam

(2) Upper San Fernando Dam

(3) Fairmont, Lower Franklin & Silver Lake dams

including some which developed large movements and some with no significant damage gives confidence in the ability of the method to

anticipate the performance of other structures subjected to different shaking intensities. Because of the analytical simplifications required, however, good engineering judgment must be exercised in the selection of soil characteristics for use in the analyses, in the detailed steps followed to conduct the analyses, and in the evaluation of the results obtained. Hopefully the degree of judgment required will be reduced as further developments in soil testing and analysis procedures are introduced. In the meantime, the detailed procedures used in this study should provide a useful guide for other evaluations. It is emphasized, however, that other procedures may well be applied and give acceptable results in many cases. It would seem desirable however that any analytical procedure used to evaluate the seismic stability of embankment dams should have the capability of correctly predicting the performance of hydraulic fill dams in the San Fernando earthquake.

Miscellaneous

1. In this investigation, the density determinations made on the undisturbed Shelby tube samples in the laboratory agreed well with those made in the field by the sand cone method.
2. Values of relative density determined from the measured field and limiting density data were in reasonably good agreement with the values determined from standard penetration test data using the correlation chart developed by Gibbs and Holtz.
3. Both field densities for the hydraulic fill and the limiting maximum and minimum densities decreased gradually with decreasing grain sizes in the soils; however the relative density of the undisturbed hydraulic fill was essentially independent of grain size.

4. In the Lower San Fernando Dam, the average relative density of the hydraulic fill was about 51 to 54 percent, the average degree of compaction based on the Standard AASHO test procedure was about 95 to 100 percent and the average degree of compaction based on the Modified AASHO (1961) test procedure was about 88 to 93 percent. Since this soil liquefied during the earthquake or lost sufficient strength to permit a major slide to develop - these values of relative density and degree of compaction are apparently insufficient to prevent failure of saturated sands in earth structures under the intensity of shaking developed in the San Fernando earthquake.
5. Even in their loosest possible states, the hydraulic fills in the San Fernando dams would have had a degree of compaction between 76 and 88 percent based on the Standard AASHO test or between 68 and 84 percent based on the Modified AASHO (1961) test. These results emphasize the necessity of developing high values of degree of compaction in the placement of dense sands in earth structures.

Part XIV - References

Berg, G. V. and Housner, G. W. "Integrated Velocity and Displacement of Strong Earthquake and Ground Motion," Bulletin Seism. Soc. Am., Vol. 51, 1961, pp. 175-189.

Duke, C. M., Johnson, K. E., Larson, L. E., and Egman, D. C. "Effects of Site Classification and Distance on Instrumental Indices in the San Fernando Earthquake," Report, UCLA Eng. 7247, School of Engineering, UCLA, 1972.

Duncan, James M. and Chang, Chin-Yung, "Nonlinear Analysis of Stress and Strain in Soils," Journal of the Soil Mechanics and Foundations Division, ASCE, Vol. 96, No. SM5, Proc. Paper 7513, September, 1970, pp. 1629-1653.

Felt, Earl J. "Laboratory Methods of Compacting Granular Soils," ASTM Special Technical Publication, No. 239, 1959, pp. 89-110.

Field Report on Addition to San Fernando Dam, 1929-30, City of Los Angeles, Department of Water and Power.

Finn, W. D. Liam, Bransby, Peter L., and Pickering, D. J. "Effects of Strain History on Liquefaction of Sand," JSMFD, ASCE, Vol. 96, No. SM6, Nov. 1970, pp. 1917-1939.

Finn, W. D. Liam "Soil Dynamics - Liquefaction of Sands," Proc. International Conf. on Microzonation, Seattle, Wash., Vol. I, Oct. 1972, pp. 87-111.

Geophysical Survey - Seismic Velocities, Embankment Materials of San Fernando Dams, State of California Department of Water Resources Office Report, Dec. 1971.

Gibbs, H. J. and Holtz, W. G. "Research on Determining the Density of Sand by Spoon Penetration Test," Proc. 4th Int. Conf. on Soil Mechanics and Foundation Engineering, Vol. I, 1957, pp. 35-39.

Hardin, B. O. and Drnevich, V. P. "Shear Modulus and Damping in Soils: I. "Measurement and Parameter Effects," JSMFD, ASCE, Vol. 98, No. SM6, June 1972, pp. 603-624. II. "Design Equations and Curves," JSMFD, ASCE, Vol. 98, No. SM7, July 1972, pp. 667-692.

Kelly, Allen "Construction of the Los Angeles Aqueduct, Final Report," Board of Public Commissioners of the City of Los Angeles, 1916.

Kolbuzewski, J. J. "An Experimental Study of Maximum and Minimum Porosity of Sand," Proc. 2nd Int. Conf. on Soil Mechanics and Foundation Engineering, Vol. I, 1948, pp. 158-165.

Kulhawy, F. H., Duncan, J. M., and Seed, H. Bolton "Finite Element Analyses of Stresses and Movements in Embankments During Construction," Geotechnical Engineering Report No. TE 69-9, Department of Civil Engineering, University of California, Berkeley, Nov. 1969.

Lee, K. L. and Seed, H. Bolton "Cyclic Stress Conditions Causing Liquefaction of Sand, JSMFD, ASCE, Vol. 93, No. SM1, Jan. 1967, pp. 47-70.

Lee, K. L. and Seed, H. Bolton "Dynamic Strength of Anisotropically Consolidated Sand," JSMFD, ASCE, Vol. 93, No. SM5, Sept. 1967, pp. 169-190.

Lee, K. L. and Fitton, J. A. "Factors Affecting the Cyclic Loading Strength of Soil," American Society for Testing and Materials, STP 450, 1969, pp. 71-95.

Lee, K. L. and Singh, Awtat "Relative Density and Relative Compaction," JSMFD, ASCE, Vol. 97, No. SM7, 1971, pp. 1049-1052.

Lee, K. L. and Chan, K. "Number of Equivalent Significant Cycles in Strong Motion Earthquakes," Proc. International Conf. on Microzonation, Seattle, Wash., Vol. II, Oct. 1972, pp. 609-627.

Morrill, B. J. "Seismoscope Resutls - San Fernando Earthquake of 9 February 1971," Chapter 3 of California Institute of Technology Report EERL 72-02, pp. 72-124.

Newmark, N. M. "Effects of Earthquakes on Dams and Embankments," Geotechnique, 15, 2, June, 1965.

Oakeshott, Gordon "Geology and Mineral Deposits of San Fernando Quadrangle, L. A. County, California," Division of Mines, Bull. 172, 1958.

Proposed enlargement of the Lower San Fernando Dam, August 1, 1929, Los Angeles Department of Water and Power.

Report of Soils Testing of Lower San Fernando Dam, State of California Department of Water Resources, Jan. 1972.

Report of Soils Testing of Upper San Fernando Dam, State of California Department of Water Resources, Nov. 1971.

Scott, Ronald F. "The Calculation of Horizontal Accelerations from Seismoscope Records," Paper presented at a Seismological Society of America Conference in Hawaii, 1972.

Seed, H. Bolton "A Method for Earthquake Resistant Design of Earth Dams," JSMFD, ASCE, Vol. 92, No. SM1, Jan. 1966, pp. 13-41.

Seed, H. Bolton and Chan, C. K. "Clay Strength Under Earthquake Loading Conditions," JSMFD, ASCE, Vol. 92, No. SM2, March 1966, pp. 53-78.

Seed, H. Bolton and Idriss, I. M. "Rock Motion Accelerograms for High Magnitude Earthquakes," EERC Report 67-7, College of Engineering, University of California, Berkeley, April 1969.

Seed, H. Bolton and Idriss, I. M. "Soil Moduli and Damping Factors for Dynamic Response Analyses," EERC Report 70-10, College of Engineering, University of California, Berkeley, Dec. 1970.

Seed, H. Bolton and Idriss, I. M. "A Simplified Procedure for Evaluating Soil Liquefaction Potential," JSMFD, ASCE, Vol. 97, No. SM9, Sept. 1971, pp. 249-1274.

Seed, H. Bolton and Lee, K. L. "Liquefaction of Saturated Sands During Cyclic Loading," JSMFD, ASCE, Vol. 92, No. SM6, Nov. 1966, pp. 105-134.

Seed, H. Bolton and Lee, K. L. "Pore-Water Pressures in Earth Slopes Under Seismic Loading Conditions," Proceedings, 4th World Conference on Earthquake Engineering, Santiago, Jan. 1969, Session A5.

Seed, H. Bolton, Lee, K. L. and Idriss, I. M. "Analysis of Sheffield Dam Failure," JSMFD, ASCE, Vol. 95, No. SM6, Nov. 1969, pp. 1453-1490.

Seed, H. Bolton and Peacock, W. H. "Procedures for Measuring Soil Liquefaction Characteristics," JSMFD, ASCE, Vol. 97, No. SM8, Aug. 1971, pp. 1099-1119.

Seed, H. Bolton and Wilson, S. D. "The Turnagain Heights Landslide, Anchorage, Alaska," JSMFD, ASCE, Vol. 93, No. SM4, July 1967, pp. 325-353.

Terzaghi, K. and Peck, R. B. "Soil Mechanics In Engineering Practice," 2nd Edition, Wiley 1967, p. 117.

Turnbull, Willard, S. "Compaction of Hydraulically Placed Fills," Reprint, No. 1802, ASCE Annual National Meeting, Houston, Texas, Oct. 1972, p. 30.

Whitman, Robert V. "Hydraulic Fills to Support Structural Loads," JSMFD, ASCE, Vol. 96, No. SM1, Jan. 1970, pp. 23-47.

EARTHQUAKE ENGINEERING RESEARCH CENTER REPORTS

EERC 67-1 "Feasibility Study Large-Scale Earthquake Simulator Facility," by J. Penzien, J. G. Bouwkamp, R. W. Clough and D. Rea - 1967 (PB 187 905)

EERC 68-1 Unassigned

EERC 68-2 "Inelastic Behavior of Beam-to-Column Subassemblages Under Repeated Loading," by V. V. Bertero - 1968 (PB 184 888)

EERC 68-3 "A Graphical Method for Solving the Wave Reflection-Refraction Problem," by H. D. McNiven and Y. Mengi - 1968 (PB 187 902)

EERC 68-4 "Dynamic Properties of McKinley School Buildings," by D. Rea, J. G. Bouwkamp and R. W. Clough - 1968 (PB 187 902)

EERC 68-5 "Characteristics of Rock Motions During Earthquakes," by H. B. Seed, I. M. Idriss and F. W. Kiefer - 1968 (PB 188 338)

EERC 69-1 "Earthquake Engineering Research at Berkeley," - 1969 (PB 187 906)

EERC 69-2 "Nonlinear Seismic Response of Earth Structures," by M. Dibaj and J. Penzien - 1969 (PB 187 904)

EERC 69-3 "Probabilistic Study of the Behavior of Structures During Earthquakes," by P. Ruiz and J. Penzien - 1969 (PB 187 886)

EERC 69-4 "Numerical Solution of Boundary Value Problems in Structural Mechanics by Reduction to an Initial Value Formulation," by N. Distefano and J. Schujman - 1969 (PB 187 942)

EERC 69-5 "Dynamic Programming and the Solution of the Biharmonic Equation," by N. Distefano - 1969 (PB 187 941)

EERC 69-6 "Stochastic Analysis of Offshore Tower Structures," by A. K. Malhotra and J. Penzien - 1969 (PB 187 903)

EERC 69-7 "Rock Motion Accelerograms for High Magnitude Earthquakes," by H. B. Seed and I. M. Idriss - 1969 (PB 187 940)

EERC 69-8 "Structural Dynamics Testing Facilities at the University of California, Berkeley," by R. M. Stephen, J. G. Bouwkamp, R. W. Clough and J. Penzien - 1969 (PB 189 111)

Note: Numbers in parentheses are Accession Numbers assigned by the National Technical Information Service. Copies of these reports may be ordered from the National Technical Information Service, Springfield, Virginia, 22151. Accession Numbers should be quoted on orders for the reports.

EERC 69-9 "Seismic Response of Soil Deposits Underlain by Sloping Rock Boundaries," by H. Dezfulian and H. B. Seed - 1969 (PB 189 114)

EERC 69-10 "Dynamic Stress Analysis of Axisymmetric Structures Under Arbitrary Loading," by S. Ghosh and E. L. Wilson - 1969 (PB 189 026)

EERC 69-11 "Seismic Behavior of Multistory Frames Designed by Different Philosophies," by J. C. Anderson and V. V. Bertero - 1969 (PB 190 662)

EERC 69-12 "Stiffness Degradation of Reinforcing Concrete Structures Subjected to Reversed Actions," by V. V. Bertero, B. Bresler and H. Ming Liao - 1969 (PB 202 942)

EERC 69-13 "Response of Non-Uniform Soil Deposits to Travel Seismic Waves," by H. Dezfulian and H. B. Seed - 1969 (PB 191 023)

EERC 69-14 "Damping Capacity of a Model Steel Structure," by D. Rea, R. W. Clough and J. G. Bouwkamp - 1969 (PB 190 663)

EERC 69-15 "Influence of Local Soil Conditions on Building Damage Potential During Earthquakes," by H. B. Seed and I. M. Idriss - 1969 (PB 191 036)

EERC 69-16 "The Behavior of Sands Under Seismic Loading Conditions," by M. L. Silver and H. B. Seed - 1969 (AD 714 982)

EERC 70-1 "Earthquake Response of Concrete Gravity Dams," by A. K. Chopra - 1970 (AD 709 640)

EERC 70-2 "Relationships between Soil Conditions and Building Damage in the Caracas Earthquake of July 29, 1967," by H. G. Seed, I. M. Idriss and H. Dezfulian - 1970 (PB 195 762)

EERC 70-3 "Cyclic Loading of Full Size Steel Connections," by E. P. Popov and R. M. Stephen - 1970 (PB 213 545)

EERC 70-4 "Seismic Analysis of the Charaima Building, Caraballeda, Venezuela," by Subcommittee of the SEAONC Research Committee, V. V. Bertero, P. F. Fratessa, S. A. Mahin, J. H. Sexton, A. C. Scordelis, E. L. Wilson, L. A. Wyllie, H. B. Seed, and J. Penzien, Chairman - 1970 (PB 201 455)

EERC 70-5 "A Computer Program for Earthquake Analysis of Dams," by A. K. Chopra and P. Chakrabarti - 1970 (AD 723 994)

EERC 70-6 "The Propagation of Love Waves Across Non-Horizontally Layered Structures," by J. Lysmer and L. A. Drake - 1970 (PB 197 896)

EERC 70-7 "Influence of Base Rock Characteristics on Ground Response," by J. Lysmer, H. B. Seed and P. B. Schnabel - 1970 (PB 197 897)

EERC 70-8 "Applicability of Laboratory Test Procedures for Measuring Soil Liquefaction Characteristics Under Cyclic Loading," by H. B. Seed and W H. Peacock - 1970 (PB 198 016)

EERC 70-9 "A Simplified Procedure for Evaluating Soil Liquefaction Potential," by H. B. Seed and I. M. Idriss - 1970 (PB 198 009)

EERC 70-10 "Soil Moduli and Damping Factors for Dynamic Response Analysis," by H. B. Seed and I. M. Idriss - 1970 (PB 197 869)

EERC 71-1 "Koyna Earthquake and the Performance of Koyna Dam," by A. K. Chopra and P. Chakrabarti - 1971 (AD 731 496)

EERC 71-2 "Preliminary In-Situ Measurements of Anelastic Absorption in Soils Using a Prototype Earthquake Simulator," by R. D. Borcherdt and P. W. Rodgers - 1971 (PB 201 454)

EERC 71-3 "Static and Dynamic Analysis of Inelastic Frame Structures," by F. L. Porter and G. H. Powell - 1971 (PB 210 135)

EERC 71-4 "Research Needs in Limit Design of Reinforced Concrete Structures," by V. V. Bertero - 1971 (PB 202 943)

EERC 71-5 "Dynamic Behavior of a High-Rise Diagonally Braced Steel Building," by D Rea, A. A. Shah and J. G. Bouwkamp - 1971 (PB 203 584)

EERC 71-6 "Dynamic Stress Analysis of Porous Elastic Solids Saturated with Compressible Fluids," by J. Ghaboussi and E. L. Wilson - 1971 (PB 211 396)

EERC 71-7 "Inelastic Behavior of Steel Beam-to-Column Subassemblages," by H. Krawinkler, V. V. Bertero and E. P. Popov - 1971 (PB 211 335)

EERC 71-8 "Modification of Seismograph Records for Effects of Local Soil Conditions," by P. Schnabel, H. B. Seed and J. Lysmer - 1971 (PB 214 450)

EERC 72-1 "Static and Earthquake Analysis of Three Dimensional Frame and Shear Wall Buildings," by E. L. Wilson and H. H. Dovey - (PB 212 589)

EERC 72-2 "Accelerations in Rock for Earthquakes in the Western United States," by P. B. Schnabel and H. B. Seed - 1972 (PB 213 100)

EERC 72-3 "Elastic-Plastic Earthquake Response of Soil-Building Systems," by T. Minami and J. Penzien - 1972 (PB 214 868)

EERC 72-4 "Stochastic Inelastic Response of Offshore Towers to Strong Motion Earthquakes," by M. K. Kaul and J. Penzien - 1972.

EERC 72-5 "Cyclic Behavior of Three Reinforced Concrete Flexural Members with High Shear," by E. P. Popov, V. V. Bertero and H. Krawinkler - 1972 (PB 214 555)

EERC 72-6 "Earthquake Response of Gravity Dams Including Reservoir Interaction Effects," by P. Chakrabarti and A. K. Chopra - 1972

EERC 72-7 "Dynamic Properties of Pine Flat Dam," by D. Rea, C. Y. Liaw and A. K. Chopra - 1972

EERC 72-8 "Three Dimensional Analysis of Building Systems," by E. L. Wilson and H. H. Dovey - 1972

EERC 72-9 "Rate of Loading Effects on Uncracked and Repaired Reinforced Concrete Members," by V. V. Bertero, D. Rea, S. Mahin and M. Atalay - 1973

EERC 72-10 "Computer Program for Static and Dynamic Analysis of Linear Structural Systems," by E. L. Wilson, K. J. Bathe, J. E. Peterson and H. H. Dovey - 1972

EERC 72-11 "Literature Survey - Seismic Effects on Highway Bridges," by T. Iwasaki, J. Penzien and R. Clough - 1972

EERC 73-1 "Optimal Seismic Design of Multistory Frames," by V. V. Bertero and H. Kamil - 1973

EERC 73-2 "Analysis of Slides in the San Fernando Dams During the Earthquake of February 9, 1971," by H. B. Seed, K. L. Lee, I. M. Idriss and F. Makdisi - 1973